UNIVERSITY OF SOUTHAMPTON

FACULTY OF PHYSICAL AND APPLIED SCIENCES

Electronics and Computer Science

Intensive intervention delivery in autism and early prediction of cognitive outcomes in children using computerised game and wireless EEG in naturalistic setting

by

Valentina Bono

Thesis for the degree of Doctor of Philosophy

March 2017

UNIVERSITY OF SOUTHAMPTON

ABSTRACT

FACULTY OF PHYSICAL AND APPLIED SCIENCES
Electronics and Computer Science

Doctor of Philosophy

INTENSIVE INTERVENTION DELIVERY IN AUTISM AND EARLY PREDICTION OF COGNITIVE OUTCOMES IN CHILDREN USING COMPUTERISED GAME AND WIRELESS EEG IN NATURALISTIC SETTING

by Valentina Bono

Neuro-developmental disorders, like Autism Spectrum Disorder, are common in youths and their incidence is increasing over the last decades. Although these disorders are attributed to disrupted brain functioning, there is no agreed biological marker for their diagnosis and treatment, thus they are based on behavioural analysis. Combating autism relies in three particular strands: early diagnosis, intensive personalised intervention (25 hours/week), and effective monitoring strategy of the children to tailor the therapy depending upon evolution of their developmental trajectories.

In this dissertation we contribute to each of these aspects as follows: We develop a multi-player game platform (GOLIAH) that enables delivering intensive intervention, not only in clinical, but also at-home settings. It implements the most recent ESDM intervention protocol targeting two "pivotal" skills that promote the learning process. In addition, it automatically generates behavioural measures when the child goes through the intervention process (playing the game). The operational procedure of GOLIAH was validated in a 3-month open trial conducted at Pitié-Salpêtrière Hospital and Stella Maris Foundation. We develop a combined developmental and neuro-biological marker strategy for monitoring the trajectory of the children during the intervention.

The behavioural parameters for monitoring are based on the performance parameters of the child while playing GOLIAH. For the neurological markers we used wireless EEG-derived functional connectivity networks and its associated parameters. However, since the EEG recorded in mobile environment is corrupted by artefacts, as a first step for EEG processing, we develop two novel artefact reduction algorithms, WPTEMD and WPTICA. Through detailed analysis of semi-simulated and real EEG data and comparison with state-of-the-art algorithms, we establish that WPTEMD works best for wireless EEG data in naturalistic settings.

We explore the possibility of using functional brain connectivity networks for early detection of cognitive disabilities in an at-risk population (neonates with HIE). Our analysis shows that two years cognitive outcomes could be predicted from EEG recorded within two weeks of life with 87.5% of accuracy. We expect that over the first few months of life, a periodic monitoring of the functional brain connectivity networks and its parameters could help in improving the final outcome prediction.

Contents

List of Figures

List of Tables

Declaration of Authorship

I, Valentina Bono , declare that the thesis entitled *Intensive intervention delivery in autism and early prediction of cognitive outcomes in children using computerised game and wireless EEG in naturalistic setting* and the work presented in the thesis are both my own, and have been generated by me as the result of my own original research. I confirm that:

- this work was done wholly or mainly while in candidature for a research degree at this University;
- where any part of this thesis has previously been submitted for a degree or any other qualification at this University or any other institution, this has been clearly stated;
- where I have consulted the published work of others, this is always clearly attributed;
- where I have quoted from the work of others, the source is always given. With the exception of such quotations, this thesis is entirely my own work;
- I have acknowledged all main sources of help;
- where the thesis is based on work done by myself jointly with others, I have made clear exactly what was done by others and what I have contributed myself;
- parts of this work have been published as: (Bono et al., 2014), (Bono et al., 2016a) and (Bono et al., 2016b)

Signed:.....

Date:.....

Acknowledgements

I would like to take this opportunity to thank Dr. Kouhsik Maharatna for his continuous support and guidance throughout the duration of my research. I am grateful to Dr. Srinandan Dasmahapatra for his technical advices and suggestions.

I also thank my co-authors and all colleagues in the research group Saptarshi, Dwaipayan, Wasifa, Sanmitra, Evangelos, Shre and Taihai for their co-operation, support and cultural exchange that I would have not experienced without.

I am very grateful to my parents Rosaria and Calogero, my brother Danilo and the rest of my big family for their continuos support and for being an example of honesty that has inspired me throughout my life and research. To them I dedicate my thesis.

Finally, I would like to thank Matteo for his support, criticism and motivation that have contributed to my growth and wider vision towards the future. Thanks also go to my near and far friends Amy, Francesca, Lucia, Pasquale, Francesco, Supuni, Maria Chiara, Enrica and Stefano for sharing joyful moments, discussions about life and visiting beautiful places around the world through these years.

Nomenclature

d_j^p	Node of the WPT tree in level j and p nodes on its left
$h_d[2k]$	High pass filters of WPT
$g_d[2k]$	Low pass filters of WPT
$< \cdot >$	Inner product
ψ_{j+1}^{2p}	Wavelet packet orthogonal basis
x	Input variable
s	Independent component of x
a	Mixing coefficient of ICA
A	Mixing matrix of ICA
W	Unmixing matrix of ICA
S	Source matrix of ICA
$G(\cdot)$	Contrast function of ICA
$E\cdot$	Expectation operator
ν	Zero-mean, unit variance Gaussian random variable
$J(\cdot)$	Approximation of negentropy
w	Single column of the unmixing matrix
$h_i(t)$	Intrinsic mode function of EMD
$r(t)$	Residual of EMD
$\zeta(t)$	Evaluation function of EMD
ξ_1, ξ_2	Stopping criteria of EMD
EGY	Energy
σ	Standard deviation
J	Criterion for artefact identification in WPTEMD
S	Entropy
IMF	Intrinsic Mode Function
$RMSE$	Root Mean Squared Error
ASR	Artefact to Signal Ratio
P	Power of a signal
λ	Level of artefact contamination
ϕ	Instantaneous phase
x_{an}	Analytical signal
$x_H(t)$	Hilbert transform

ρ	Synchronisation measure
τ	Time delay
R	Euclidian distance
$S(\cdot\|\cdot)$	Synchronisation measure
$H(\cdot\|\cdot)$	Synchronisation measure
$N(\cdot\|\cdot)$	Synchronisation measure
$L(\cdot\|\cdot)$	Synchronisation measure
$M(\cdot\|\cdot)$	Synchronisation measure
$\Theta(\cdot)$	Step function
SL	Synchronisation Likelihood
k_i	Degree of a node in a network
P_{ij}	Length of an edge in a network
d_{ij}	Shortest path length of two nodes in a network
T	Transitivity of a network
Q	Modularity of a network
CPL	Characteristic Path Length of a network
E_{Glob}	Global Efficiency of a network
ecc_i	Eccentricity of a node in a network
R	Radius of a network
D	Diameter of a network
$\epsilon^2(w)$	Squared error

Chapter 1

Introduction

Mental disorders are common among youths affecting 13.4% (241 million) of children and adolescents worldwide (Polanczyk et al., 2015). Although these diseases, like disruptive behaviour and depressive disorders, have similar incidence as obesity and asthma, they constitute health priorities compared to the latter, especially because of their more severe life-long consequences. Oxygen deprivation at birth, like Hypoxic-Ischemic Encephalopathy (HIE) can result in such disabilities, like Cerebral Palsy (CP), Autism Spectrum Disorder (ASD), Attention Deficit Hyperactivity Disorder (ADHD), seizures, behavioural and cognitive impairments. Autism Spectrum Disorder (ASD) is one of the most common mental disorders. It is a type of neurobiological disorder characterised by atypical functioning in social interaction, communication and behaviour, manifested before the age of three (World Health Organization, 2011).

The prevalence of ASD has been found to differ across countries and ethnicities. This is mostly due to methodological factors which may influence the detection and analysis of the disorder (Zaroff and Uhm, 2012), the case definition and case-finding procedures (Elsabbagh et al., 2012). The first epidemiological study in the UK showed the prevalence of autism to be 4.1 every 10000 individuals (Lotter, 1966). In the last two decades, the global prevalence of autism has been increased and is estimated to affect 1 in 150 persons with a female to male ratio of $1:4$ (Fombonne, 2009). A higher prevalence is found in the United States (Baoi, 2014) and Europe (Elsabbagh et al., 2012) where it is estimated to be 1 in 68 children. However, the improved awareness and recognition as well as changes in the diagnostic process may contribute to this estimates increase.

ASD is a life-long developmental disorder and it has several consequences to the health and quality of life of individuals with this disorder and to their families. This results in a high economic cost for the families and society. The cost of supporting an individual with ASD during their lifespan is estimated to be £1.4 million and $0.92 million in UK and US respectively. This cost increases to £1.5 million and $2.4 million when considering an individual with intellectual disabilities in UK and US respectively. This

cost covers different areas in public sector expenditure such as education, housing, social care, health and it is mostly due to accommodation, direct medical costs and loss of productivity (Buescher et al., 2014). The support of individuals with ASD may vary with age: special education is the main contribution to the high cost in childhood, whereas residential accommodation, productivity losses and medical care are the main factors for the cost in adults.

The main characteristic of the ASD is the heterogeneity of its symptoms. Children with autism fail to interact with others, use eye gazing and make facial expressions appropriate to the situation. They are unable to share their interests, emotions and activities in peer relationships. Furthermore, these children show repetitive and stereotyped behaviours in their body movements. More than 70% of individuals affected by ASD are commonly characterised by co-morbidity: they show concurrent medical, psychiatric or developmental conditions (Lai et al., 2014). Among the co-occurring conditions, like anxiety and hyperactivity (McPheeters et al., 2011), 32% of individuals with autism present regression (Barger et al., 2013) and 45% have intellectual disabilities (Fombonne, 2009). Delay or lack of language development, often accompanied by echolalia is also one of the co-occurring conditions (Boucher, 2012). Individuals with ASD are also subjected to difficulties in cognitive processes involved in planning, initiating, motor actions, mental flexibility and working memory (Funahashi, 2001; Elliott, 2003; Hill and Frith, 2003).

Despite the wide research on ASD in different areas, from genetics to behavioural and neuroimaging, ASD cannot be uniquely identified by a single or group of biomarkers (Lai et al., 2014). There has been several attempts to study the neurobiological basis of the ASD behavioural phenotype. The behavioural traits of autism are the result of an underlying altered brain connectivity, with difficulties in the integration and segregation of the information. More importantly, unlike the behavioural symptoms, the altered brain connectivity seems to be present much earlier than the first (in the first six months of life) (Jones and Lord, 2013). Despite these important findings, a biomarker that can be used for an efficient clinical diagnosis, monitoring of the disease evolution and the intervention efficacy is still to be found. Because of the absence of such a biomarker, the diagnosis and intervention are based uniquely on behavioural observations, rendering them available only later in life (the behavioural symptoms are manifested in the second year) and less efficient (because of the heterogeneity of the symptoms). On the other hand, early diagnosis is critical to begin the treatment before the syndrome is manifested fully and in a stage of life characterised by maximal brain plasticity (Altemeier and Altemeier, 2009).

Several research studies targeting biomarkers for early detection analyse behavioural and neurological measures in population at-risk of developing ASD (Sacrey et al., 2015). Examples of populations at-risk are siblings of children with ASD and subjects with a pathological condition that presents elevated rates of developing ASD later in life. HIE is a condition occurring at birth that causes a high risk of brain injury and development of

Cerebral Palsy (CP), severe neuromotor, cognitive impairments and ASD (Schreglmann et al., 2016).

In this context, this work would like to answer the following questions:
"Is there an early intervention that can be delivered intensively and monitored with a combination of behavioural and neurological markers? Can these neurological markers be used for outcome prediction in a population at-risk?"

To answer these questions, various challenges need to be addressed at both behavioural and neuro-developmental levels. More details on the motivations that prompted us to ask these questions are given in the next sections, highlighting both behavioural (see Section 1.1) and neuro-developmental (see Section 1.2) shortcomings.

1.1 Diagnosis and intervention of ASD

The screening and diagnosis of ASD is based only on behavioural analysis and cannot rely on the existence of biological markers (Lai et al., 2014). The diagnosis of ASD is mainly based on the use of interview administered by clinicians to the parents to retrieve historical and current information about the social and communicative behaviour of the child. Since it is totally based on observable developmental and behavioural markers, the efficacy of the diagnosis of ASD depends on experienced clinicians for the identification of its features. The heterogeneity of ASD symptoms, the highly variable behaviours and severity (Hall, 2012) and the high frequency of co-morbidity extensively hamper the diagnosis and are its main limitations. Despite the availability of the screening and diagnostic instruments, on average children with ASD receive a diagnosis when they are at school age (Mandell et al., 2002). For the United Kingdom, only 10% of children with ASD are diagnosed within the first three years of life (Buescher et al., 2014).

An early diagnosis is crucial to ensure that the child can be eligible for accessing services, school and community-based intervention. In essence, the outcomes of the subsequent intervention is related to the time of the diagnosis. The earlier the diagnosis, the sooner the child can benefit from the intervention. The benefits of early identification and interventions have already been recognised by parents and professionals (Dawson and Osterling, 1997; Lord, 2000; Rogers, 1996).

Although ASD remains a devastating disorder with a poor outcome in adult life (Howlin et al., 2013; Roux et al., 2013), various therapeutic approaches have been developed and showed improvements in the condition. Some programs are highly structured and delivered in one-to-one settings, others are delivered in group settings including typically developing children and are based on behavioural intervention (Bush et al., 2015). Some other therapies, like speech and occupational therapies, are delivered in outpatient hospitals (Bush et al., 2015).

The psychologist community recently proposed alternative interventions named Naturalistic Developmental Behavioural Interventions (NDBIs) (Schreibman et al., 2015), which combine both behavioural and developmental treatments. These interventions are early intensive, delivered in naturalistic settings and involve the parent in the delivery of the treatment. Such early, intensive and specialised interventions, like the Early Start Denver Model (ESDM) protocol (Dawson et al., 2010), may alter the course of early behavioural and brain development (Dawson, 2008). They are applied in a critical stage when the brain's plasticity is maximal and environmental influences may interfere with neural connections (Altemeier and Altemeier, 2009). Intensive and specialised treatments are crucial to enhance developmental outcomes in terms of encouraging achievements in language and cognitive skills as well as social functioning (Dawson et al., 2010; Landa, 2008; National Academy of Sciences-National Research Council, 2001; Reichow and Wolery, 2009; Stone and Yoder, 2001; Szatmari et al., 2003). They also help in reducing anxiety and aggression (Lai et al., 2014). Early intervention is beneficial especially for children with milder autism who are more likely than others to achieve the "optimal outcome" when treated at an earlier age (Fein et al., 2013). Nonetheless, treatments early in life are crucial to considerably reduce the high individual, family and societal expenditures because they are likely to change the trajectory of the disorder (Barbaro and Halder, 2016).

The disadvantage of such treatments is due to the high cost required for the training of professionals and parents, rendering them inaccessible to a wide population of children. The main requirements to deliver effective early intensive intervention are the following:

- *Intensive intervention.* A weekly time delivery of at least 25 hours/week is essential (Remington et al., 2007).
- *Individualised intervention* (Maglione et al., 2012; Pilling et al., 2012). Appropriate characterisation of the child undergoing the treatment is required due to the significant inter-child variability. Adapting the intervention to the child's skills will maximise the treatment outcomes.
- *Naturalistic settings.* The treatment needs to be delivered in an interactive social context, like playing and daily routines, to facilitate and empower the generalisation of the improved skills in a real-life setting (Schreibman et al., 2015).
- *Parent-mediated intervention* (Maglione et al., 2012; Pilling et al., 2012). Active involvement of the parents is essential to increase parent's confidence in approaching their child's difficulties and facilitating the transfer of the intervention to naturalistic setting (Schreibman et al., 2015).

Telemedicine and Information and Communications Technologies (ICT) foster the use of technology to monitor the treatments in a semi-automated way and enhance their efficacy. Along this line, several computer-based interventions such as telehealth methods

and serious games (Whyte et al., 2015; Lofland, 2016) have been designed and used to aid the delivery of such treatments. Specifically, these applications may lead to a vast array of advantages, highlighted here:

- *Cost effective.* A computer-based intervention can be accessed remotely from home and in low resource settings and developing countries (Barbaro and Halder, 2016).
- *Reduce the amount of training and coaching of professionals.* The effective implementation of an intervention requires not only manuals detailing the cores of such treatments, but also therapists and parents training and coaching (Schreibman et al., 2015).
- *Fidelity of implementation.* It is essential for obtaining results that can be replicated across studies to draw conclusions on the effects of an intervention (Ploog et al., 2013).
- *Data collection.* A computer-based approach might help in collecting several measures in a systematic way to monitor child's response across trials and child's progress across sessions (Schreibman et al., 2015). This will facilitate the identification of those objective and behavioural measures that can describe the developmental trajectory of the child along the intervention.

In addition to the above mentioned advantages, due to the increased popularity of computers or tablets, computer-based interventions may enable the treatment to be deployed to a wider population.

The main drawback of the existing computer-based interventions relies on the individuality of the designed platforms. They are, in fact, single-user platforms which renders them less effective for children with ASD. Indeed, a game platform should be designed to foster the interactions with others, which is the fundamental process underlying learning (Schreibman et al., 2015). Nonetheless, the computer games designed for neurodevelopmental disorders target specific abilities, instead of treating "pivotal" skills that facilitate the learning of a vast array of abilities.

The next section will describe the shortcomings that motivated us to research into the neurological possible biomarkers for intervention monitoring and neurological outcome prediction.

1.2 Brain Connectivity

As mentioned above, due to the lack of a biomarker, comprehending the nature of ASD necessitates an investigation at different levels of analysis, such as genetic, biochemical, psychological and physiological. In particular, the early behavioural anomalies of autism

are related to neuropathological alterations that occur in early development and are the results of atypical brain connectivity (Belmonte et al., 2004; Frith, 2003; Courchesne and Pierce, 2005b,a). Cognitive neuroscientists focus on the analysis of the brain dynamics linked to cognitive processes to identify neurological traits of ASD and investigate their relation with behavioural symptoms. For instance, neuroimaging studies in infants at high risk of autism[1] found different neural signatures between typically developing children and infants at high risks that later were negative to ASD diagnosis (Belmonte et al., 2010).

Neuroimaging studies on autism mainly focus on: (a) anatomical connection and (b) functional connection between different brain areas. The first describes the physical connection and the structure of the brain using Magnetic Resonance Imaging (MRI), the latter represents the synchronisation of spatially distributed groups of neurones when they interact with each other. Essentially, these neuroimaging studies attempt to understand the information flow among brain regions, which is crucial to pinpoint the brain dynamics underlying the atypical behavioural characteristics of autism.

Numerous studies carried out on the anatomical brain connectivity in autism show a larger growth rate of the autistic brain compared to the brain of a control subject (Courchesne et al., 2003, 2001; Lainhart et al., 1997). Results from MRI and DTI recordings suggest that the overgrowth of the brain seems to affect more the frontal and temporal lobes than the parietal and occipital ones. Particularly, the enhancement of frontal white matter results in frontal hyper-connectivity (Coben et al., 2014). In addition, this altered brain development seems to have effects also at a system level, leading to long distance (from back to front) anatomical hypo-connectivity (Barnea-Goraly et al., 2004; Courchesne and Pierce, 2005b). Functional connectivity analysed with functional MRI (fMRI) is consistent with the findings at the anatomical level. In an fMRI based study autistic individuals showed overall functional under-connectivity compared to control subjects (Just et al., 2004). Another study based on fMRI during facial expression tasks indicated local functional hyper-connectivity in autistic brains (Welchew et al., 2005). These outcomes are in line with the weak central coherence theory (Happé and Frith, 2006) which describes the propensity of autistic subjects to focus on processing the input information locally disregarding the global view (Moseley et al., 2015).

Electroencephalography (EEG) is another tool extensively used to acquire and analyse brain signals for clinical and research purposes. Although fMRI is used for studying functional connectivity, EEG with its higher temporal resolution is the tool able to capture the reorganisations of local neuronal clusters which occur within a millisecond timescale (Bressler and Kelso, 2001). EEG is also a widely available, less invasive, compact and cost-effective tool (Wolpaw et al., 2002) and the only one that allows to record in naturalistic settings. Traditional EEG research on ASD is based on absolute

[1] Siblings of children with ASD are considered infants at high risk of autism.

and relative power and coherence (Heunis et al., 2016). But recently, EEG studies are moving towards the analysis of *functional connectivity networks* which combines functional connectivity and graph theory. EEG functional connectivity networks allow to understand the brain dynamics in terms of whole-brain with features that can have meaningful biological interpretation (Sporns, 2011). They may give deeper insights into the complex interactions between large-scale brain networks in ASD (Heunis et al., 2016). Preliminary findings showed long-range hypo-connectivity and local hyper-connectivity (Barttfeld et al., 2011), in accordance to the results from fMRI (Welchew et al., 2005). In essence, the functional connectivity networks can be used first to identify and quantify the local and global aspects of brain connectivity, and then to investigate how they change along with the intervention in a longitudinal study.

Among the EEG devices commercially available, various EEG systems are used in research for recording resting-state or task-dependent EEG, from high (128 channels) to low density (19 channels). Recently, wireless EEG became popular as they use dry contact electrodes which do not require conductive gel and skin preparation (Chi et al., 2010) resulting in reduced setup time for data acquisition. Since it allows studying the brain waves in unconstrained settings (Hu et al., 2011), wireless EEG may consent the assessment of cognitive functionalities of a subject (Sanei and Chambers, 2008) during tasks performed in daily life. But such potential is hindered by a wide variety of motion artefacts (like head and hand movement, talking, chewing, etc.) introduced in the recorded EEG by the higher degrees of freedom of body movement. In practice, these movements strongly affect the recordings such that the underlying EEG signal may not be recognisable. The biggest problem is that these artefacts are radically different from the traditional EEG literature (with high inter-trial variability) and being of random natures no a-priori knowledge exists about their characteristics, based on which they could be separated from EEG using traditional artefact removal techniques.

Combining neurological instruments, like EEG, with the behavioural clinical diagnosis could provide tools to predict a more reliable diagnosis of ASD and the identification of its subgroups. Genetic and neurological instruments could offer more objective information to detect a biomarker or a set of biomarkers (Jones and Lord, 2013). Understanding the interplay between these three factors (behavioural, genetic and neuro-developmental) will be beneficial not only for improving the reliability of the screening and diagnostic processes but also for understanding the trajectories of subject's functioning during the development and intervention.

One attempt was done in this direction by (Dawson et al., 2012): EEG coherence was used to assess the outcomes of the Early Start Denver Model (ESDM) intervention in a randomised control trial of children with ASD. Results showed increased cortical coherence during face processing and concurrent enhanced social behaviour. However, the relation between EEG networks and behaviour is still a challenge and an open research question. The reduced capacity of integration between brain areas might explain

the low level of socialisation and task performances, while the greater local connectivity is indicative of the repetitive behaviours (Matlis et al., 2015).

The shortcomings described above motivated us to set our objectives in order to answer the questions given at the beginning of the chapter. The next section details these objectives.

1.3 Monitoring and intervention delivery: a behavioural-neuro-developmental approach

In view of the shortcomings described in the previous sections, we here propose a new approach for delivering intensive intervention that allows monitoring behavioural and neuro-developmental progresses of children with ASD recruited in a longitudinal study. Particularly, this work aims at exploring behavioural correlates with EEG functional connectivity networks in autistic children, by taking into account the advantages of both behavioural and neurological concepts described in the previous sections. Moreover, we exploit those brain network features to investigate whether they can provide outcome prediction in a population at-risk of developing ASD. The generalised view of the proposed intervention for ASD and its behavioural and neuro-developmental monitoring in naturalistic settings is illustrated in Figure 1.1.

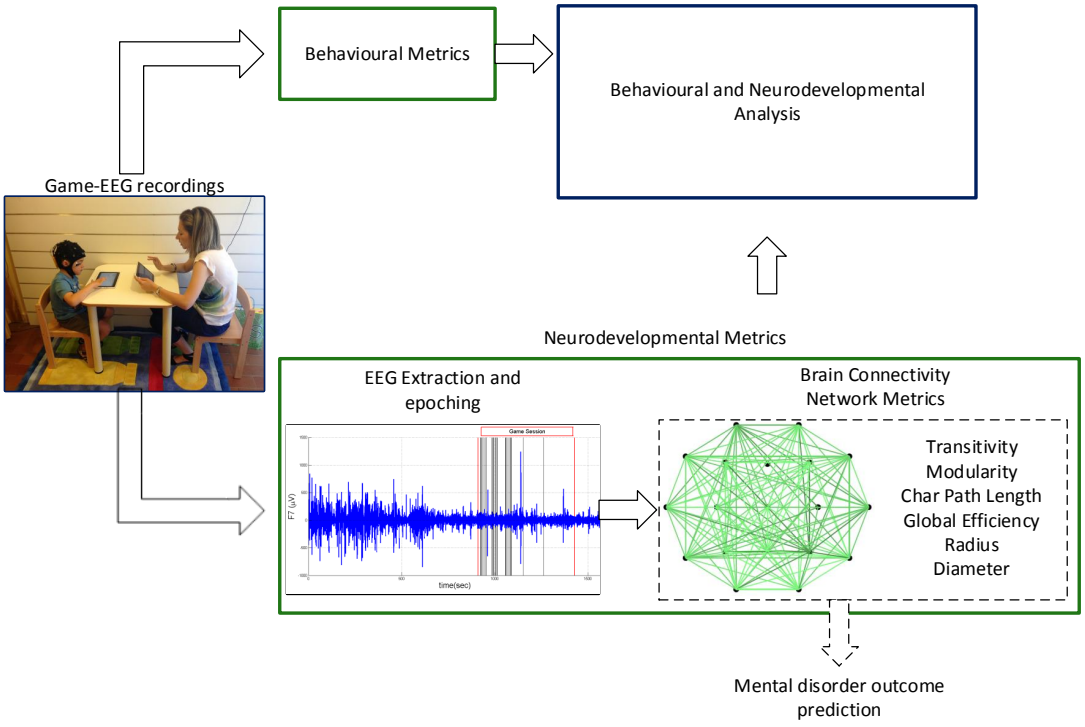

Figure 1.1: The flowchart shows the core issues of the behavioural and neuro-developmental approach proposed in this work.

To fulfil the proposed approach, we identified the following four main objectives.

1. **Computer-based intervention:** The adaptation of one of the most recent ESDM intervention into a computer game-based treatment can be achieved by implementing the games traditionally played during the intervention session between the child and the therapist. The game platform designed for the delivery of the intervention should provide behavioural measures that allow to monitor the progress of the patients.

2. **Wireless EEG, artefact reduction and brain networks:** A *wireless EEG* system is employed during the computer-based intervention where the therapist and the child interact via the designed game platform. Wireless EEG device allows to record neurological data in a naturalistic setting while the child is engaged in the cognitive tasks solicited by the game platform. As mentioned in the previous section, wireless EEG requires novel techniques to suppress the motion and physiological artefacts affecting the EEG recordings, since the existing methods require *a-priori* knowledge of the artefact. The *artefact suppression* is crucial for the subsequent analysis of possible neurological biomarkers to monitor the proposed intervention. In particular, we aim at extracting functional connectivity network measures (functional connectivity and its graph theoretic measures) from the EEG recorded during the early intensive intervention and investigate their potential for treatment monitoring.

3. **Behavioural and neurological markers:** The behavioural (from the game) and neurological (from the wireless EEG) metrics are explored to understand how the game-based intervention can be monitored in terms of behavioural and neurological markers. A systematic exploration of the available functional connectivity measures and related complex networks is needed for the identification of the most meaningful neurological metrics.

4. **Neurological markers for outcome prediction:** We want to explore if the neurological markers identified in the previous step can be used for outcome prediction of mental disorders. For this purpose, EEG recordings from a population at-risk are used for the analysis of the brain networks.

It is worth mentioning that the game platform has beneficial impacts on the EEG recordings, in addition to its advantages on the interventional perspectives. In fact, experimental paradigms used to collect behavioural brain signals are data centred; since their goal is to acquire as many trials as possible, they are not motivating or engagement. The subjects are required to repeatedly perform a specific behavioural task like finger tapping (Darvas et al., 2010), attention (Vuilleumier et al., 2001) and mental imagery (Porro et al., 1996) which are demanding but not motivating or engaging. Individual cooperation might decrease over time because of boredom or frustration, especially for

subjects with difficulty in focusing for extended time periods. Design of user-centred experimental paradigms with more motivating tasks may increase the task-compliance and produce more distinctive brain activation patterns (Yoder and Belmonte, 2010). For instance, a game can increase the engaging with motivating behavioural tasks and allow the related brain mapping (Eisenberger et al., 2003; Yoder and Compton, 2004).

1.4 Challenges

The primary challenges towards fulfilling the research objectives can be summarised as follows:

- *Game platform: design, implementation and behavioural monitoring.* Implementing games planned in a traditional treatment into a game platform is not an easy process. The game has to be the mean for fostering the interaction between subjects and avoid the user's alienation. Moreover, a multi-language game platform allows to reach a multi-cultural population, which implies that the games need to be adapted to language and cultural differences (Barbaro and Halder, 2016). When describing the behavioural progress of a child, appropriate behavioural markers are required to describe the child's skills during the cognitive tasks.

- *Automated artefact reduction algorithm.* Because the most efficacious interventions are realised in naturalistic settings, the wireless EEG system is the only tool that fulfils this requirement. However, an apposite artefact reduction algorithm must be designed to clean the data and render them available for further neurological marker extraction.

- *Exploration of functional connectivity networks.* Various functional connectivity measures and complex network features are available in literature (Wang et al., 2014). However, there is no single functional connectivity measure generally recognised to be the best one, but each measure has its advantages and disadvantages (Sakkalis, 2011). It is difficult to select the most suitable to the purpose of the study and it is preferred to use various methods to identify the most appropriate (Fallani et al., 2014).

- *Behavioural and neurological monitoring.* Monitoring of behavioural and neurological measures requires their extraction from the two systems, the game platform and the EEG device. Data recorded from the two platforms during a longitudinal study must be extracted and combined along the clinical sessions of the intervention. This allows the monitoring of the early intensive intervention from behavioural and neurological perspectives.

- *Neurological markers for atypical cognitive development.* A population at-risk has to be identified to extract the functional connectivity networks from the EEG

data. Neurological markers used for the intervention monitoring need to be used in combination with clinical outcomes in a follow-up to investigate their capability of detecting the development of cognitive impairments like ASD later in life.

1.5 Contributions

In this work, the focus lies on exploring the effects of a computer-based intervention in children with ASD by means of both behavioural and neuro-developmental metrics extracted during a longitudinal study. In view of this, the primary contributions of this research work can be outlined as follows.

1. **Game-platform for computer-based intervention (Chapter 3):** The design and development of a multi-player gaming platform called Gaming Open Library Intervention for Autism at-Home (GOLIAH) for diagnostic behavioural characterisation and treatment of autistic children. The multi-player gaming platform contains various games which map different stimuli utilised in the ESDM protocol. The GOLIAH emulates the interactive games played between a child and a therapist or a parent during the therapeutic sessions. The availability of various games using different stimuli and of various levels of difficulty allows the therapist to customise the treatment according to the early state cognitive skills of the child. GOLIAH game allows intensive intervention in naturalistic settings and parent-mediated intervention without requiring high demanding training for therapists and parents.

2. **Behavioural performances analysis (Chapter 3):** The GOLIAH game is employed in a 3-month open trial on 10 autistic children. The cognitive skills of the children are assessed by extracting and analysing their behavioural performances across the different sessions during the longitudinal study.

3. **Artefact reduction algorithms (Chapter 4):** We designed and implemented two hybrid algorithms, Wavelet Packet Transform-Empirical Mode Decomposition (WPTEMD) and Wavelet Packet Transform-Independent Component Analysis (WPTICA), to suppress the artefacts contaminating the EEG data recorded with a wireless EEG device. Two EEG datasets were constructed containing several artefacts to explore the algorithms' performances in semi-simulated and real EEG data. These EEG datasets were essential to assess the feasibility of such a pervasive EEG system for brain network analysis. The performance of the two algorithms is assessed in comparison with two state-of-the-art methods.

4. **Functional connectivity network analysis (Chapter 5):** The EEG recorded during the game sessions is used to extract neuro-developmental measures in terms

of functional connectivity networks. For this purpose, several functional connectivity measures are employed to estimate the synchronisation between the EEG recordings in different brain sites at the scalp level. Following, graph theory is applied to express the functional connectivity in terms of a complex network, to explore changes in brain integration and segregation while performing the game-related cognitive tasks.

5. **Atypical cognitive development prediction (Chapter 6):** The functional connectivity networks mentioned above can also be used at an earlier stage of life, like the early postnatal period. This would allow to analyse the neuro-cognitive functions in newborns at-risk of developing neurological pathologies at an older age. With this in mind, we use employ these functional connectivity networks to predict two years outcome in newborns affected by HIE at birth, selected as a population at-risk of developing ASD, neuro-cognitive and neuro-motor impairments. Two classification algorithms are employed to predict the neonates that later will show cognitive disabilities.

1.6 Research Constraints

This research work was part of the European Seventh Framework Programme under the project name Michelangelo: New technology to help children with Autism[2]. The project intends to develop a patient-centric and home-based intervention with the use of ICT. Data acquisition from children with ASD was performed at the Department of Child Neuropsychiatry of Stella Maris Foundation (Pisa), and at the Department of Child and Adolescent Psychiatry of Pitié-Salpêtrière Hospital (Paris), two clinical partners of the project. The EEG and the game related data were recorded from 10 children who were available within the stipulated time at hospital. Each parent gave informed written consent before inclusion for participation and for publication of the individual clinical data. This is an open study to assess the feasibility of the intervention inclusive of ICT and EEG. However, the study is limited by the unavailability of an age-matched group. Additional data from 16 neonates was recorded at the University Hospital Southampton, Department of Clinical Neurophysiology. The newborns were affected by HIE at birth and were selected as a population at-risk of developing cognitive diseases. The newborns were subject to EEG data recorded during the first two weeks of life and to clinical examinations in a two-year follow-up.

The primary focus of this work lies in developing an intervention tool comprising of both behavioural and neurological data, in order to better characterise and monitor the improvement of a child during the intervention period. We also aim at using the neurological data for disease prediction in a population at risk. However, this work has

[2] http://www.michelangelo-project.eu/en/

been partly constrained by the availability of more autistic children for data acquisition and evaluation of the developed framework on a wide population and on a longitudinal scale.

1.7 Thesis Outline

The rest of the thesis is organised as follows: in Chapter 2 we discuss the relevant state-of-the-art diagnostic and intervention protocols for ASD. In particular, various examples of application for realising computer-based intervention are described along with their drawbacks. Besides the behavioural interventions, various state-of-the-art techniques for brain network analysis are detailed together with a deeper description of the approaches based on EEG analysis. Chapter 3 describes the game platform implemented for delivering computer-based intervention, together with the results obtained from its engagement during the 3-month open trial. Chapter 4 gives a detailed description of the two automated artefact reduction algorithms designed to suppress the artefact acquired during body movements, typically occurring in naturalistic settings. In Chapter 5, the various approaches for extracting functional connectivity networks from the EEG recordings are described. Specifically, we show the changes in such networks during the 3-month open trial. In Chapter 6, we describe the classification used for outcome prediction by extracting the functional connectivity networks from EEG data recorded in newborns affected by HIE. The conclusions along with the highlights of the possible future work that can follow this research are detailed in Chapter 7.

1.8 Publications

The work presented in this thesis has appeared in the following publications.

1.8.1 Journal Papers

Bono, Valentina, et al. "GOLIAH: A Gaming Platform for Home-Based Intervention in Autism-Principles and Design." *Frontiers in psychiatry* 7 (2016).

Bono, Valentina, et al. "Hybrid wavelet and EMD/ICA approach for artefact suppression in pervasive EEG." *Journal of neuroscience methods* 267 (2016): 89-107.

1.8.2 Conference Papers

Bono, Valentina, et al. "Artefact reduction in multichannel pervasive EEG using hybrid WPT-ICA and WPT-EMD signal decomposition techniques." *2014 IEEE International Conference on Acoustics, Speech and Signal Processing (ICASSP)*. IEEE, 2014.

Chapter 2

Background and Literature Review

In this chapter, we review the key background research and clinical applications related to ASD diagnosis, characterisation and interventions defined in Chapter 1. This background will provide the theoretical basis for the frameworks (game platform, EEG processing algorithms and neurological measures for intervention monitoring and atypical cognitive development prediction) presented in the following chapters. This chapter begins with an overview of the ASD, its diagnosis (Section 2.1), the traditional (Section 2.2) and the most recent computer-based interventions (Section 2.3). In the second part, we will give an overview of the different tools employed for the analysis of the neurological mechanisms underlying the atypical behaviour of ASD (Section 2.4). In particular, we will focus on the state-of-the-art methodologies for artefact reduction of EEG recordings (Section 2.5). Subsequently, we survey research approaches related to the brain network analysis, in terms of functional connectivity and complex networks and their application on ASD (Section 2.6). Section 2.7 describes the state-of-the-art EEG approaches for the outcome prediction of newborns with HIE who are an at-risk population to develop neuro-developmental disorders later in life.

2.1 Autism Spectrum Disorder (ASD)

The term autism originates from the Greek word *autos*, which means *self*. In the past 70 years, there has been an exponential increase of studies aiming at understanding autism, as shown in Figure 2.1. The definition of autism has developed over time since the first one adopted in the mid-20th century, describing autism as a form of childhood psychosis. The latest definition is given in the fifth edition of the Diagnostic and Statistical Manual of Mental Disorders (DSM-5) (American Psychiatric Association, 2013): it introduces the umbrella term *autism spectrum disorder* characterised by (1) difficulties

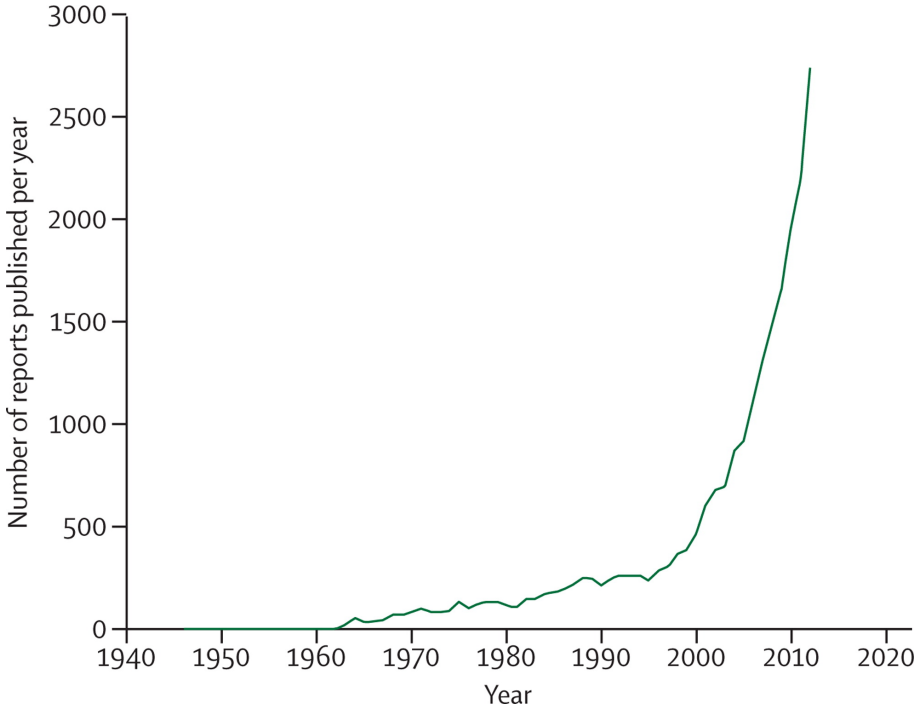

Figure 2.1: The increase of autism research since the first study (Lai et al., 2014)

in social communication and social interaction; and (2) restricted and repetitive behaviour, interests, or activities. These impairments are typically manifested before the age of three (World Health Organization, 2011). The American Academy of Paediatrics guidelines suggest screening all children in the age between 18 and 24-30 months for possible ASD. The parental report Modified Checklist for Autism in Toddlers Revised Form (Robins et al., 2014) is the most widely used tool for screening the ASD symptoms. Early indicators used in these screening tests are: deficits or delays in the emergence of joint attention, decreased imitation, deficits in reciprocal affective behaviour, decreased response to own name and motor delay. Based on the preliminary results obtained from the screening, healthcare providers can refer those children identified at risk of ASD for expert diagnostic evaluations.

Various concerns have been raised about the appropriateness of such screening for all children for ASD. The major issue of these screening tools pertains the trade-off between higher specificity (lower number of false negative) or higher sensitivity (lower number of false positive) (Zwaigenbaum et al., 2013). The false negative subjects will have a late diagnosis, whereas the false positives will require an extensive time-consuming specialised assessment which was not essential (Costanzo et al., 2015). Due to the need of early intervention (addressed later in the chapter), cut offs for these screening tests are developed to ensure a low number of false negatives (higher specificity). Therefore, the high false positives will traverse the unnecessary diagnostic process, thus impacting on the limited available resources for ASD diagnosis. However, some of these false positive

children might be affected by other developmental disorders which could be recognised by the diagnostic evaluation (García-Primo et al., 2014). Feasibility of these instruments to be used across the world is another reason that limits their standardisation worldwide. In fact, a rigorous approach for early identification of ASD worldwide would require a common screening instrument that investigates ASD symptoms by adapting a common tool to language and culture of each country (Barbaro and Halder, 2016).

2.1.1 Clinical diagnosis

The diagnostic process is determined by a multidisciplinary team of clinicians consisting of a psychologist, a physician (developmental paediatrician, psychiatrist or a child neurologist) and additionally a speech language pathologist (Ozonoff et al., 2005). All professionals involved in the diagnostic process have clinical experience and specialised training (Manning-Courtney et al., 2013). The diagnostic process involves the following steps:

1. A *developmental paediatric evaluation* helps in identifying possible risk factors for ASD and associated medical conditions (Manning-Courtney et al., 2013). It comprises of a detailed description of birth, developmental, medical and family history, neurological and physical check-up and developmental observation (Johnson et al., 2016).

2. *Additional medical tests* may be necessary to confirm or exclude conditions identified during the paediatric evaluation: DNA analysis for Fragile X Syndrome is one of these.

3. *ASD-specific diagnostic instruments*, like the gold standard parent report measure Autism Diagnostic Interview-Revised (ADI-R) (Lord et al., 1994) and the diagnostic observation measure Autism Diagnostic Observation Schedule (ADOS) (Lord et al., 2012). The ADI-R is a semi-structured interview administered with caregivers or parents to retrieve historical and current information of the subject. The ADOS is a standardised instrument to observe social and communicative behaviours relevant to ASD. This test is based upon observations of spontaneous behaviours elicited by planned social interactions and communication instances during a structured session with an experienced clinician. The main advantage of these two diagnostic tools relies on the fact that they have separate scores to assess social communication (including non-verbal and verbal communication) and repetitive behaviours. However, they do not analyse other ASD criteria, like behaviours in peer interactions and relationships with others.

4. A *comprehensive psychological evaluation* assesses the cognitive, like intelligence quotient (IQ), social, emotional, behavioural, current developmental and adaptive

functioning of the subject. The current developmental functioning is crucial to compare the subject's social and communication skills to his current developmental age rather than his chronological age. The adaptive functioning, instead, is essential for intervention planning (Klinger et al., 2009).

2.1.2 Limitations of clinical diagnosis

The efficacy of the diagnostic tools is hampered by the heterogeneity of ASD symptoms. The ASD phenotype can be characterised by a constellation of different behaviours and depends on several other factors like developmental level, IQ and language ability. As a result, children affected by ASD can present symptoms that are not identical. Nevertheless, the ASD symptomatology and functioning is highly variable over a lifetime (Blumberg et al., 2015), which makes even more difficult to list the behaviours and their lifetime appearances for the clinical diagnosis.

Early diagnosis is positively associated with symptoms severity, socioeconomic status and parental concern (Costanzo et al., 2015). In fact, late diagnosis has been encountered particularly in high functioning subjects, especially females (Lai et al., 2014). Gender difference influences the diagnosis: females need more severe symptoms than males to be diagnosed (Dworzynski et al., 2012).

In the long term, between 3% and 25% of children diagnosed with ASD lose their diagnosis: they achieve social and communicative functioning that is within the normal limits of typically developing children (Helt et al., 2008; Fein et al., 2013). The subjects' functioning could be affected positively from early intensive intervention, but over diagnosis and misdiagnosis seem to be the main reasons of lost diagnosis. In both cases, a wrong diagnosis is likely to be caused by the difficulty in differentiating behavioural symptoms belonging to ASD and other developmental conditions (Blumberg et al., 2015).

2.2 Intervention in Autism Spectrum Disorder

Once diagnosed, children with ASD require a treatment that should be individualised and across multiple disciplines and dimensions (Lai et al., 2014). The intervention would span across behavioural, rehabilitative, educational and mental health areas (Bush et al., 2015). The treatment mainly aims at improving the quality of life, functional independence, social skills and communication of the subjects, reducing their disability and comobordity and providing support to their families (Lai et al., 2014). Among the various approaches, we here provide a survey of two main categories of interventions and a widely used comprehensive protocol along with their limitations.

2.2.1 Non hybrid interventions

Traditionally, interventions in autism could be divided into two categories: developmental and behavioural. The treatments based on a *behavioural* model are the most common interventions; they are considered the most effective for individuals with ASD, leading a degree of improvement (National Academy of Sciences-National Research Council, 2001). These models try to teach a child cognitive and behavioural skills that are considered essential for independent living in the long run and a significant number of such techniques have been developed over the years. The Early Intensive Behavioural Interventions (EIBI) are high intensity intervention programs focused on teaching skills to the child through repeated precise instructions. Several studies have shown notable improvements and significant decrease of autism symptoms in autistic children receiving early intensive interventions (Dawson et al., 2010; Howard et al., 2005; National Academy of Sciences-National Research Council, 2001; Sallows and Graupner, 2005).

Instead, *developmental* interventions, like the Floortime (Greenspan and Wieder, 2009) and the Relationship Development Intervention (RDI) (Gutstein and Sheely, 2002), originate from research on typical infant and child development. They focus on learning and integrating skills from social, language and cognitive areas to target the core difficulties of autism. In the developmental approach, the subject has an active role in the process of learning being engaged in a continuous exchange with the therapist.

2.2.2 Hybrid interventions

The literature on interventions in ASD has become quite extensive, with increasing convergence between behavioural and developmental methods (Narzisi et al., 2013; Ospina et al., 2008). These combined approaches are recently referred as Naturalistic Developmental Behavioural Interventions (NDBIs) (Schreibman et al., 2015). As the name suggests, they merge the behavioural and developmental approaches and are employed in naturalistic and interactive settings, such as during a game with a therapist. The main characteristics of such interventions are the followings:

- *Child's active learning engagement*: the child is actively engaged in the learning process, rather than receiving repeated instructions passively.
- *Parent-mediated intervention*: families are included in the intervention, they can actively participate in the learning process.
- An *initial developmental profile of the child* is assessed in order to identify an individualised set of goals that the child has to achieve.
- A *constructive sequential approach* is used for the learning process: at the beginning of the intervention instructions are simple and adapted to the initial skill level of the child, the instructions become more complex as the child improves.

- A *systematic selection of the skills* is employed to foster the generalisation and the contextualisation of the learned skills: for example, learning the word "ball" and use it when playing football with a peer.
- *Manuals of the intervention* are available to facilitate the implementation of the treatment among professionals, researchers and families.
- *Precursors of specific abilities* are identified and used as target skills. For example, most of the interventions focus on enhancing imitation and joint attention skills, which are the precursors of language and high-level abilities.

These features are in accordance with clinical and research guidelines recommending that interventions for children with ASD should be individualised, implemented soon after the diagnosis and engage the families (Maglione et al., 2012; Pilling et al., 2012). A well-known NDBI treatment targeting imitation and joint attention is the Early Start Denver Model, used in this work to implement a game-based intervention.

2.2.3 Early Start Denver Model (ESDM)

The Early Start Denver Model (ESDM) is a comprehensive behavioural early intervention protocol for autistic children (Dawson et al., 2010) and recently categorised as a NDBI intervention (Schreibman et al., 2015). The ESDM is defined as a comprehensive treatment because it focuses on enhancing a vast array of abilities such as cognitive and communication functioning, adaptive and motor behaviours. ESDM uses a combination of developmental and behavioural techniques in both therapist and parent-implemented early intervention model. It is an intervention for infants with autism aged 12-36 months that combines Applied Behaviour Analysis (ABA) with developmental and relationship-based approaches. The treatment is provided by trained therapists and parents in several settings, such as group programs, individual therapy sessions and natural environments, like home. Each child's treatment program includes models based on development, functional profile, relational patterns and modification of behaviours. The curriculum includes systematic activities on receptive and expressive communication, social, play, cognitive, self-care and fine and gross motor skills. Particular attention is devoted to specific tasks regarding "pivotal" abilities, such as Imitation (gestural, facial, vocal and with toys) and Joint Attention (JA) (sharing, showing and pointing).

Lack of Imitation and JA are the main problems when interacting with children with ASD. While playing a game or conducting other activities with a social partner, these children tend to not concentrate on what others are actually doing, switching to repetitive and stereotypical behaviours that are of interest for the child but that usually have no or few relations with the actual social context. Young children with autism are not very imitative. This deficiency of imitation may drastically reduce their learning opportunities, and if it continues, it can be a huge impediment for learning from teachers,

parents, therapists, and other children. Because of its important role in social and language learning, building imitation skills in children with autism is a critical component of the ESDM intervention. In addition, children with ASD can display concerted attention to toys or objects that they like, but they have difficulties in sharing attention or interests with others (Rogers and Dawson, 2009). For example, maintaining eye contact with the caregiver is especially complicated (Saint-Georges et al., 2010) and the scarcity of JA is the consequence (Dominey and Dodane, 2004).

Although several definitions of Imitation exists, there is no universal agreement. The three main definitions are described here. (1) Thorndike (1898) offered a definition based on visual aspects: "learning to do an action by watching someone doing it", although the multi-sensory aspect should be considered. (2) Wallon (1942) defined imitation as a learning technique without reward (or reinforcement). (3) Whiten and Ham (1992) defined imitation as the process by which the imitator learns some behavioural characteristics of the model. Imitation fulfils two essential functions for adaptation: it is used for learning and it serves to communicate without words (Nadel, 2006). Two children involved in imitation coordinate two roles: the model and the imitator. They are temporally synchronised because they are engaging in the same activity at the same time; they respond to the perception of movements or actions to produce a similar behaviour. There are several levels of Imitation that constitute a continuum, from simple to complex and from familiar to new. All these levels have in common a response to the perception of movements or actions, finalised by the production of a similar behaviour.

Compared to Imitation, JA introduces a third partner during interaction. Emery (2000) defined JA as a triadic interaction that showed that both agents focus on a single object. Agent 1 detects that the gaze of agent 2 is not directed at him/her and, therefore, follows the direction of the gaze to look at the object of attention of agent 2. This definition highlights a unidirectional process, unlike shared attention which appears to be a coupling between mutual attention and JA. Tomasello (1995) have argued that JA implies viewing the behaviour of other agents as intentionally driven. In that sense, JA is much more than gaze following or simultaneous looking (Carpenter et al., 1998).

As mentioned above, the ESDM is delivered in highly engaging and naturalistic environment. The interactive learning takes place in systematic sessions both at home and hospital, with parents and therapists. During the one to one session, different *imitative tasks* may be proposed to the children: (a) imitation of actions on objects, (b) imitation of gestures, (c) vocal imitation of sounds and words. Children are asked to imitate conventional or unconventional actions with and/or without objects. They are also involved in vocal tasks through the imitation of words pronounced by the interlocutor. During a *JA activity* two subjects are engaged with each other in the same cooperative activity, attending the same objects or playing or working together on a common activity. A JA task in the ESDM protocol involves four phases. (1) The *opening or set-up phase* involves the acts that precede the establishment of the first shared play activity based

on the theme of the play. (2) The child and adult are engaged in a definable *play activity*, either object centred, like building blocks, pouring water, marking with crayons, or involving a social game like singing a song, dancing to music or playing hide and seek. (3) The *elaboration phase* involves variation on the theme to keep it interesting or to highlight different aspects of the activity. This preserves the play from becoming repetitious and allows more skill areas to be addressed. Variation and elaboration allow the adult to extend the child's attention, promote flexibility, develop creativity, and address a number of skill areas. (4) The *closing phase* takes place when attention is waning or the teaching value of the activity is all used up.

2.2.4 Limitations of interventions

Despite the efficacy of behavioural intensive interventions, researchers pointed to the inadequacy of one single treatment approach for all areas of learning for children with ASD (National Academy of Sciences-National Research Council, 2001; Schreibman, 2000) and, there is now a consensus that there is no "one-size-fits-all" treatment for this population. Two main problems are associated with these programmes: (a) the time requirement of at least 25 hours/week of intervention (Remington et al., 2007), and (b) the need of individualised intervention protocol specific for the developmental level of the subject. ASD is a broad spectrum with significant inter-child variability and it has already been established that tailor-made personalised intervention may be more effective compared to any generic type of treatment (Picard and Goodwin, 2008). A tailor-made personalised intervention accounts for the actual difficulties and strengths of a child and needs to be designed to achieve maximal effects.

Very little is known about how to individualise treatment protocols or how to best determine a priori which intervention is most likely to benefit individual children (Schreibman, 2000; Sherer and Schreibman, 2005; Yoder and Compton, 2004). One way to individualise the intervention could be to implement combined treatments with a systematic approach (Iovannone et al., 2003; Rogers and Vismara, 2008; Schreibman, 2000). Combined intervention is crucial since the exclusive use of one treatment method may ignore important aspects of social, emotional, communicative or pre-academic development.

Repeatability is an essential requirement to apply an intervention in a systematic way. It also allows avoiding subjective biases that might happen during the traditional behavioural assessment of the child done by trained therapists in clinical settings. To avoid such biases, one needs to employ a set of stimuli multiple times ensuring their repeatability and then extracting a set of objective measures for characterising the outcomes. Repeatability is an essential criterion in this case so that an average performance measure in a stimulus-specific way could be obtained reflecting the child's actual ability for responding to the stimuli in question. Such repeatability in a strict sense is difficult and costly to achieve even by a trained therapist in a real-life scenario. A computer-based

approach could be the solution to systematically apply repeatable tasks for characterisation and treatment of children with ASD.

On the other hand, the intensive intervention, owing to the significant number of hours required per week, is also difficult to achieve. Firstly, it needs a trained therapist and, given the prevalence of ASD, the workload of a therapist could be enormous making the effective implementation of this strategy impractical. Secondly, the overall economic cost is also significant and therefore may hamper its sustainability. One way of reducing these problems is to involve parents/carers in the intervention protocol and thereby carry out a significant part of the intervention in home settings. The role of parents as co-therapist can improve their confidence in approaching the atypical behaviour characteristics of autistic children. Though, this requires parent training and regular monitoring to check whether the parents implement the intervention protocol adhering to that outlined by the therapist properly. Again the economic implication of such process is quite significant. Computer-based intervention could again help in delivering parent-mediated intervention at home settings. The next section provides a survey of the technology based intervention proposed in literature.

2.3 Technology - assisted intervention

Thanks to the rise of internet, mental health researchers have increased their interest to employ technology in the treatment of mental diseases. Smartphones, tablets and mobile computer devices are now integrated in our everyday life and might be used for supporting interventions in subjects with ASD. Both adults and children, typical and atypical, have increased their use and knowledge of technology which allows the involvement of mobile devices in educational and communicational routines. Specifically, children with ASD dedicate almost the double of the time playing video games than typically developing youths (Mazurek and Engelhardt, 2013).

Traditional methods which usually involve human intervention may be subjective, inconsistent and thus less reliable. Computer-based treatments may be preferred to the traditional programs because they decrease the variability and increase the precision due to the repeatability of the instructions presented to the children. Employing computers in educational and treatment programs of patients with ASD helps in increasing motivation and maintaining treatment fidelity (Ploog et al., 2013).

A computer-based intervention, considering the ample presence of computers in families, can be more accessible and affordable and, consequently, it increases the chance of involving more patients. The computer is not thought as a replacement of the professionals involved in the therapy, but it is intended as a helpful tool to minimise the time spent by the therapist to treat the children or to foster the childrens' engagement. Moreover, computer-based interventions reduce the chance of having external stimuli

from the environment, which can distract the child (Moore, 1998). The use of computers in the early intervention programs enables treatment of the child in his/her natural setting which is considered relevant for the child's behavioural improvements.

In a comparative study between traditional behavioural and computer-based programs, children showed higher motivation and learned a wider vocabulary when computers were included in the treatment (Moore and Calvert, 2000). Children with autism accomplish the given task better when they receive feedback from the computer compared to the one from a human examiner (Pascualvaca et al., 1998). Computer games are also developed to enhance the social interaction of children with ASD within a work group. Working in pairs in a computer-based intervention system improves the learning process, compared to the children who work alone (Mevarech et al., 1991).

Information Communication Technology (ICT) and computer-based intervention in autism research has started almost two decades ago. Technology has been applied in various areas to improve social skills of the children, like face-object distinction and face recognition (Tanaka et al., 2005), language and social skills to help them to behave in everyday situations. ICT educational and intervention programs in ASD can be delivered in a wide range of applications, like interactive and virtual environments, serious games and cognitive training methodologies. They typically focus on the enhancement of a specific target skill in language (vocabulary and reading), face-processing (emotion recognition and face recognition) and social skills related to social behaviour. The next sections give an overview of the most relevant ICT-aided interventions.

2.3.1 Language

iCAN (Chien et al., 2015) is a computer-based intervention that implements the conventional Picture Exchange Communication System (PECS) into a tablet. PECS is a pedagogic approach to enhance the communication skills of children with ASD. It uses picture cards containing the name and a description of the object or action in the card. iCAN shows the cards with their labels, it reduces the preparation time for the cards and fosters the increase of the number of cards. iCAN was used for four weeks on 11 children who showed increased enthusiasm in learning and interacting with others.

Macpherson et al. (2015) used an iPad® for video modelling intervention in children with ASD to foster their verbal compliment behaviour. For this purpose, they recruited five children with ASD for athletic group play with peers and adults. Children were required to kick a ball and watch videos of a familiar adult playing the same game while saying three different verbal compliment accompanied by a related gesture. The game sessions were recorded to be later scored by independent therapists to assess the behaviour of the children during the kickball game. Participants increased their use of verbal compliments after the intervention.

ECHOES (Bernardini et al., 2014) is a serious game on a multi-touch display integrated with an eye-tracking device. It is designed to promote social communication in children with ASD at schools and home. ECHOES is based on interactive learning activities based on JA between a child and a 3D intelligent virtual agent. The agent can be seen as a peer or a tutor and it is controlled using artificial intelligence algorithms. This character lives in a garden containing magic elements, like flowers, that are transformed into other objects when are touched by either the agent or the child. Some learning activities are goal oriented and individual while others require the cooperation between the child and the agent. This platform was employed in five schools during a six weeks period with children aged between 4 and 14 years. Results from 19 children with ASD showed increased occasions of initiated interactions between the child and the virtual character and the career during the intervention.

2.3.2 Emotion

Je stimule (Serret et al., 2014) is an individual serious game developed for children with ASD to foster social cognition, particularly the recognition of facial expression, emotional situations and emotional gestures. The game was deployed to 33 children for two sessions (one hour/session) over a four weeks period. It is composed by static and animated avatars with different facial expressions indicating anger, happiness, fear, pain and other emotional states. The trial confirmed the usability and efficiency of the game: children increased their emotion recognition skills in various tasks.

Let's Face it! (Tanaka et al., 2010) is an individual computer-based game to train and reinforce face processing skills, like recognition of face and emotional expression, of children with ASD. The game comprises seven games targeting the enhancement of facial processing strategies and attention to details associated with it, like eye-gaze. The game was played at home by 42 children with ASD recruited in a 4-month randomised control trial. Results showed increased facial recognition skills of children belonging to the face training group.

2.3.3 Social behaviour

Several applications use tabletops to enhance cooperative skills in children with ASD. Piper et al. (2006) realised a cooperative multiuser tabletop game to motivate and practice social and group work skills. The game involves a group of children playing to achieve a common goal and thus supports social group therapy activities.

Battocchi et al. (2009) designed a Collaborative Puzzle Game (CPG) in a multiplayer touch-screen, capable of detecting simultaneous actions of each player in a small group, to encourage the cooperation in children with ASD. The game is characterised by a set

of rules, defined as Enforced Collaboration (EC), that force the users to simultaneously touch, drag and release a piece into the solution area. The use of the EC while playing the game facilitates the teaching of typical behaviours of social engagement and interaction in pair.

Cheng et al. (2003) designed and developed KidTalk, an online chat room involving a group of children and an online therapist. The application aims at teaching children how to behave in everyday situations, like a birthday party.

Hourcade et al. (2012) realised a multi-touch tablet game for control and autistic children, where they have the opportunity to play alone or with others. The main purpose of the game was to explore the engagement of children with ASD when playing a game that required collaboration, creativeness and emotion understanding. The authors concluded that the use of technologies is beneficial for understanding how the information is processed by a child with ASD compared to a typically developing child.

Pico's adventure (Malinverni et al., 2016) is a full-body Kinect-based game designed to enhance social initiation skills of children with ASD. The character of this game is the alien Pico who has just arrived in the earth and try to socialise with the child by asking him help for various tasks, like repairing his spaceship, discover the environment or looking for food. The child can play alone or with peers to assist Pico in succeeding in various missions with increasing the difficulty. The game was played by 10 children with high functioning autism aged between four and six years during four weeks (one session/week). This exploratory study showed promising results in terms of usability of the game and increased social initiation events.

2.3.4 Imitation training to parent

A hybrid tele-health program is used in (Wainer and Ingersoll, 2015) to involve parents in an imitation-based intervention program. The platform relies on the Reciprocal Imitation Training (RIT) intervention, a naturalistic behaviour approach targeting spontaneous imitation skills in young children with ASD. This tele-health program is an internet-based learning program consisting of audio lectures and video examples of the RIT program and remote coaching sessions that can be accessed by parent from their home computers. Parents assessed positively the usability of this program, while children showed increased spontaneous imitation skills.

2.3.5 Comprehensive

Unlike the technology assisted examples given above, a comprehensive intervention targets abilities from various areas, like communication, motor, cognitive and adaptive behaviour. We describe three ICT-based comprehensive interventions in autism.

TechTown Basics (Jones et al., 2016) is an educational computer-based intervention based on ABA designed for children with ASD aged between two and seven years. It contains more than 500 computer lessons with the focus of enhancing various skills: language, arts, mathematics, adaptive, cognitive, social and emotional. It is an individual program with lessons that are self-adapted based on the student's success. This software was assessed on different schools on children with ASD; they improved their cognitive and language skills during a 3-month trial.

TOBY Playpad (Venkatesh et al., 2013) is a computer-based intervention based on ABA to empower parents to mediate the early intervention of children with ASD at home settings. The software contains different tasks to enhance sensory, imitation, and social and language skills. It requires the parents to select the tasks that the children will play during the game. It is an individual game, where the child has to achieve the selected goal. Parents positively assessed the usability of TOBY and were inspired by new activities that could be done at home to facilitate the child's learning.

Vismara et al. (2013) proposed a tele-health program for children with ASD based on ESDM intervention. It aims at promoting parent-therapist communication, engage and train parents on the intervention at home. It consists of a self-guide website containing activity tools and live video conferences between the family at home and the therapist. The video conference sessions were conducted on a weekly basis for 12 weeks on eight children with ASD. During a single session, the parent plays an activity with the child and discusses with the therapist on the events occurred in the past week, the activities performed during the present session and their overall experience on the intervention, behaviour of the child and their respective learning goals. Parents could implement activities preserving the fidelity of the intervention and children increased their social communicative behaviours.

The sections above gave an overview of the start-of-the-art on the behavioural analysis in the field of atypical behaviours in ASD. The next sections will focus on the available tools to study the neurological mechanisms underlying those typical behaviours.

2.4 Brain studies

Behavioural diagnosis and characterisation of children with ASD is the most reliable and currently used clinical approach. Concurrent research is focusing to find a neural, genetic or biological marker that can objectively identify the presence of ASD. Neuroimaging methods and electroencephalography (EEG) are currently used to complement the behavioural analysis to find a biological marker of ASD. Behavioural symptoms of ASD which can be identified after the 18^{th} month of life might be anticipated by neural abnormalities and atypical brain development in the first 12 months (Sacrey et al., 2015).

Studying the brain from a neurological perspective can give insights to foster the understanding of behavioural and developmental trajectories of children with ASD in relation to the correspondent brain activity. The following sections give insights on the human brain and the clinical tools to study its anatomical and functional structure.

2.4.1 Methods of studying the human brain

The brain structure and functions, as well as the physiology behind it, have been investigated through the application of several techniques, like Magnetic Resonance Imaging (MRI), Computerised Tomography (CT), Positron Emission Tomography (PET), Single Photon Emission Tomography (SPECT), functional Magnetic Resonance Imaging (f-MRI), Magnetoencephalography (MEG) and Electroencephalography (EEG). The first two methodologies have been applied to investigate the anatomy of the brain, the others are useful to explore the brain activity.

CT is an invasive technique, which combines an X-Ray technique with image reconstruction to produce horizontal sliced images of the brain (Kak and Slaney, 2001). The distinction among different brain tissues is made thanks to their different X-Ray absorption properties. CT is widely employed to investigate several brain diseases, such as tumours and lesions caused by strokes.

MRI is a non-invasive technique: it provides 3D representations of the brain to measure the size and the shape of different brain regions (Haacke et al., 1999). It combines the use of a strong magnetic field, the hydrogen nuclei in the brain and radio waves. The hydrogen nuclei within the brain align to the applied strong magnetic field. When they return to their initial condition, these nuclei emit different radio waves (depending on the property of the tissue) which will be detected by the surrounding receivers. Images of the brain are obtained through the application of image reconstruction techniques.

PET combines CT technology with radioisotope imaging to investigate the functional activity of the brain (Bailey et al., 2005). The radioisotope is a compound of water, oxygen, or glucose bounded with an isotope, like O^{15} or F^{18}, which emits positrons. Once in the body, the compound concentrates in the most active brain areas: neurons in these regions raise their need of oxygen and glucose, thus the compound concentration is directly proportional to the cerebral blood flow and volume, glucose metabolism and oxygen extraction. The radioisotope emits positrons which collide with electrons, producing γ rays recorded by the detectors surrounding the patient. This detection is processed to evaluate the physiological activity of various regions within each slice of the brain. PET is used while the patient is performing a specific task in order to identify the corresponding active cerebral regions. It is also applied to investigate the neurotransmitter pathways in patients with degenerative diseases like Alzheimer and Parkinson. The large cost of the radioisotope production is one of the disadvantages

related to this technique. PET is also characterised by a time resolution of minutes which is very low compared to the fraction of seconds in which a cognitive task happens. SPECT is similar to PET and analyses the brain activity in terms of cerebral blood flow within and between the cortical regions (Bushberg and Boone, 2011), widely used to localise damaged cerebral regions of interest in epilepsy.

As in PET, the flow, oxygenation and volume of the blood in the brain can be measured by the fMRI (Huettel et al., 2004). This technique exploits different magnetic properties of two types of haemoglobin flowing during brain activity. In fact, as a consequence of oxygen requirement in neurons in high active regions, oxyhemoglobin is converted into deoxyhemoglobin. Water molecules produce different radio waves, depending on the type of haemoglobin present in the region. This phenomenon allows the brain images to be obtained with a temporal resolution of approximately one second. To investigate the activity changes in brain regions during cognitive processes with finer temporal resolution, MEG and EEG are more suitable.

MEG provides a measurement of the magnetic fields originated from the electrical currents of neurons (Babiloni et al., 2009). Its technology consists of superconducting antenna coils installed in a captor surrounding the patient's head. Although it provides high temporal resolution, MEG is an expensive tool and thus, the use of EEG technique is more preferable.

Most of the techniques above are expensive and require sedation or use of radioactive material to the subjects. Given the age and atypical behaviour of the children with ASD, the EEG with its ability of analysing brain dysfunction is the most clinically available technique used in this population.

2.4.2 Electroencephalography (EEG)

EEG is an inexpensive and non-invasive system able to capture electrical brain signals produced by the neurons' activity. The first EEG in humans was recorded by the German physician Hans Berger in 1924 (Niedermeyer and da Silva, 2005). The interest in EEG started to grow ten years later, when Adrian and Mathews (1934) demonstrated that the alpha rhythm was likely generated in the occipital lobes (Adrian and Matthews, 1934). Since then, several works have been carried out on spontaneous and electrical stimulation in animals, in epileptic manifestations and during human sleep. Nowadays, EEG technique is widely used for clinical and research purposes to investigate neurobiological and physiological abnormalities of the brain.

EEG signals are recorded by electrodes placed on the scalp: they measure the coherent electrical activity of pyramidal neurons when activated with a certain degree of synchrony. These pyramidal neurons are located in the cortex with the apical dendrites aligned perpendicularly to the cortical surface (Da Silva, 2009).

Electric activity of neurons occurs by generation of (a) action potential and (b) postsynaptic potential. The *action potential* consists of a rapid change (around 1 ms) in membrane potential that jumps from negative to positive and returns to the resting intracellular negativity. It is generated when the electrical excitation of the membrane exceeds a threshold and it is mediated by the sodium and potassium voltage-dependent ionic conductances. Once triggered, the impulse travels along the axon toward its terminal where it signals other neurons. When the action potential reaches the synapse (the junction between the axon of a neuron and the dendrite of the next neuron), the neuron releases a transmitter into the synaptic space that binds to the receptors of a postsynaptic neuron and causes a change in the permeability of the postsynaptic membrane. Depending on the type of neurotransmitter and ionic currents, the *postsynaptic potentials* can be excitatory (EPSPs) or inhibitory (IPSPs). Postsynaptic potentials are slower than the action potentials and span between 10 and 50 msec. In order to fire, the amplitudes of many postsynaptic potentials have to be superimposed in the soma of the postsynaptic neuron. This neuronal electrical activity described above generates currents along the cell membrane in the intra- and extracellular spaces, and produces an electric field similar to that of a dipole. In order to be measurable, a large number of these dipoles have to be (1) synchronised and (2) oriented in parallel (Nunez and Srinivasan, 2006). The EPSPs (with their relatively long duration) and the pyramidal cells of the cortex (with their orientation) fulfil the criteria to generate measurable electric activity. Indeed, the EEG derives from the summation of synchronously generated postsynaptic potentials of pyramidal neurons.

Although the potentials in neurons are characterised by an amplitude of several mV, EEG amplitude is commonly within the range 10–100 μV. In fact, the electrical signal is attenuated by various tissues, like dura, matter, galea, cerebrospinal fluid, bone and scalp.

EEG signals are characterised by five major brain rhythms characterised by different frequency ranges, listed in Table 2.1. Four of these brain waves are shown in Figure 2.2. Each rhythm changes its characteristic with age and mental state, like sleeping and alertness. Abnormal presence of these brain rhythms can be related to a disease.

In addition to the rhythms mentioned above, other brain waveforms may be observed in EEG signals, such as the breach rhythm, similar to the α rhythm and mainly found in the temporal region and due to a cranial bone defect (Cobb et al., 1979). Mu rhythm is an α-like rhythm related to the motor cortex; it may be suppressed when the subject performs or imagines a motor action. It has also been investigated for feedback training for various purposes like treatment of epileptic seizure disease (Sterman et al., 1974).

EEG signals are recorded by electrodes placed on the scalp according to the conventional electrode settings, called 10–20 System in Figure 2.3. The location of the scalp electrodes is related to the underlying areas of the cerebral cortex. Two reference points are used

EEG band	**Frequency range**	**Description**
δ **band**	$0.5 - 4Hz$	Mainly associated with deep sleep and may appear in the waking state.
θ **band**	$4 - 8Hz$	Typical in: young children, drowsiness and deep meditation. Its presence is abnormal in awake adults EEG and may be caused by various pathologies.
α **band**	$8 - 13Hz$	Typical during rest and eyes closed. May be suppressed when a subject opens the eyes, hears unfamiliar sounds or is anxious. Its origin and physiological meaning are still unknown (Niedermeyer, 2005).
β **band**	$13 - 30Hz$	Usually observed in normal adults during active thinking or solving problems; may be present in a panic state.
γ **band**	$> 30Hz$	Their presence may confirm the presence of certain brain diseases.

Table 2.1: Typical EEG brain rhythms.

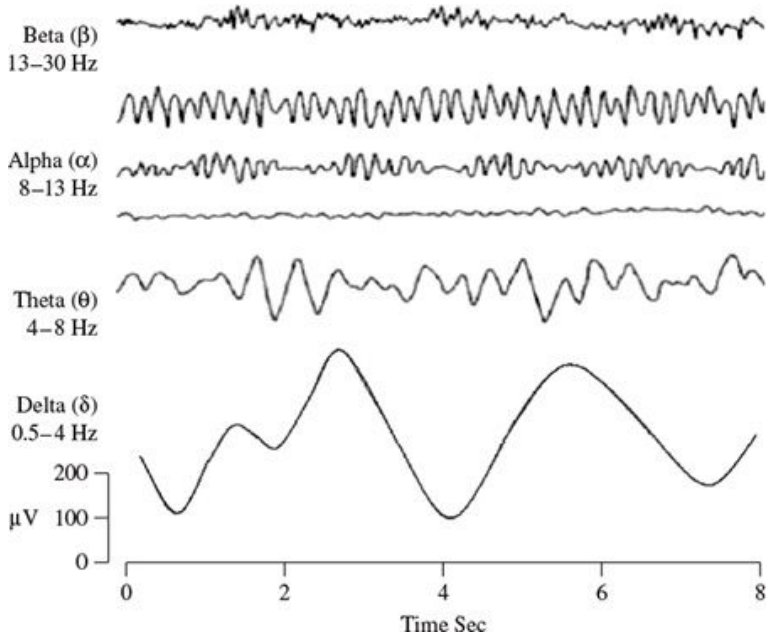

Figure 2.2: Different brain rhythms in EEG signals (Sanei and Chambers, 2008).

to locate the electrodes: the nasion, on the nose at the level of the eyes, and the inion, at the base of the skull at the back of the head on the midline. The distance between nasion and inion is considered the front-back distance of the skull and each pair of the electrodes is located 10% or 20% of the distance between these two points. Since the 10–20 system is based on fixed distances of each electrode from the nasion, inion and the preauricolar points, it takes into account the variability of the head size (Herwig et al., 2003). EEG is usually visually inspected and analysed by clinicians; a description of EEG in normal awake adults has been provided in (Rutkove and Blum, 2007; Niedermeyer,

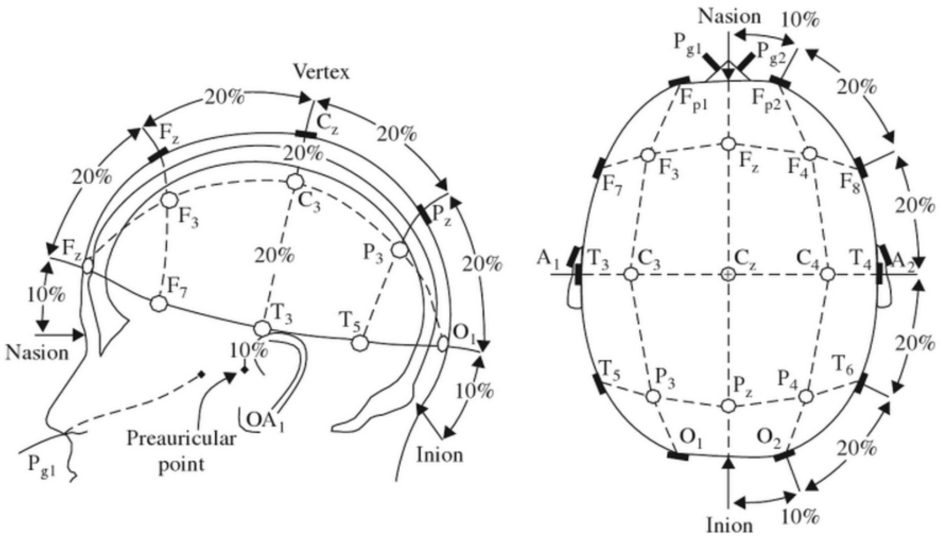

Figure 2.3: 10-20 Electrode placement system (Sanei and Chambers, 2008).

2005). However, the literature lacks a translation of such visual descriptions into analytic metrics of EEG. The EEG systems vary according to different characteristics: they can be wired or wireless, with dry or wet electrodes and with a variable number of electrodes (from one to 256).

2.4.3 Wireless EEG systems

Wireless EEG is crucial in facilitating the monitoring of a patient, preserving his/her comfort in an everyday environment. Clinical EEG systems transmit the EEG data through a wired serial port interface. EEG recording in a standard clinical environment is a tedious procedure requiring extensive setup time, skin preparation and gel-electrode application or the immersion of the cap into a saline solution.

Recent advances in technology have led to the development of portable, wireless and battery operated EEG systems that are suitable for experimental studies (Grummett et al., 2015) in naturalistic settings. Typical EEG experiments require the subjects to perform cognitive tasks in a controlled position without body movement. These experimental conditions limit the range of cognitive assignments that can be performed for monitoring the brainwave behaviour. A better understanding of the patient's cognitive functions needs unobtrusive EEG systems (Hu et al., 2011) which allow the subject to perform cognitive tasks in a more natural environment.

In this study, EEG data are recorded with the Enobio system[1], a wireless and portable EEG monitoring device. It consists of an elastic cap with dry electrodes and an embedded portable recording unit placed on the back of the head transmitting the recordings

[1] http://www.neuroelectrics.com/products/enobio/enobio-20/

via Bluetooth. Compared to other wireless devices commercially available, like Emotiv®, Enobio presents higher spatial resolution with its 20 electrodes. The dry electrodes provide the advantage to avoid the use of gel and skin preparation; they showed high test-retest reliability of brain recordings (Collado-Mateo et al., 2015) and data recording comparable to the EEG acquired with conventional EEG systems (Wyckoff et al., 2015).

Wireless EEG systems are widely used for Brain Computer Interface; recently they were used for health applications, such as diagnosis of Alzheimer Disease (AD), epileptic seizure detection and Event Related Potential (ERP). Handayani et al. (2016) used Emotiv Epoc 14 channels to identify differences in the power spectral, brain mapping and chaos properties of EEG data recorded in AD and control subjects. The same EEG system was used to assess its ability of recording face-sensitive N170 Event Related Potentials (ERP) (de Lissa et al., 2015) and compared it with a traditional clinical EEG system. Results showed that such wireless devices can be used for the analysis of the face-sensitive ERP, useful for understanding the neural processing occurring during face perception in children and adults with cognitive impairments, like ASD. Menshawy et al. (2015) employed the Emotiv 14 electrodes in combination with a mobile app to detect epileptic seizures during the EEG recordings.

As introduced in Chapter 1, EEG data can be corrupted by artefacts. In the next section, a survey of the start-of-the-art techniques for their suppression is given along with their limitations.

2.5 Signal Processing on artefact removal

EEG is an inexpensive and non-invasive tool which allows monitoring of brain signals and assessment of cognitive functionalities of a subject (Sanei and Chambers, 2008; Sörnmo and Laguna, 2005). However, EEG data are prone to be corrupted by artefacts which render the acquired data unusable.

An artefact is defined as any unwanted modification in the measured signal caused by external sources. Biomedical signals can be affected by three different types of artefact: environmental, experimental and physiological (Huppert et al., 2009). (a) The *environmental artefacts* are mostly caused by the mains power leads and their coupling with the measurement cables and other devices. (b) The *experimental errors* are related to the experimental setup, human errors and subject movements during the signal acquisition. (c) The *physiological artefacts* are related to other physiological processes, like respiration, eye-blinks, cardiac and myogenic activity. The last two types of artefacts are the most difficult to deal with, due to the overlap of their frequency band with the

physiological measurements. For instance, muscle activity is characterised by high amplitude, wide spectral distribution and variable topographical distribution (McMenamin et al., 2011).

Clinical EEG data affected by artefacts are typically discarded and not considered for further analysis. The possible body movements performed by the subject during the wireless EEG acquisition introduce new severe artefacts that cannot be removed by the conventional techniques. In fact, most of the existing methods of artefact separation from clinical EEG systems need *a-priori* information of the source of artefacts or use simulated artefacts which are morphologically different from the experimentally acquired data. Since wireless EEG allows natural body movement of the subjects, it is not feasible to assume *a-priori* information of the artefacts characteristics. Therefore, pervasive EEG requires a fundamentally new approach to suppress such artefacts. Several algorithms have been proposed for artefact removal from EEG following three main approaches: (a) linear methods, (b) Blind Source Separation (BSS) techniques and (c) hybrid semi-automatic techniques, described in the next sections.

2.5.1 Linear methods

Linear filtering and linear regression (Narasimhan and Dutt, 1996) can separate an artefact from a corrupted signal if the source of the artefact is known: Electrooculogram (EOG) data is used to remove eye-blinking, Electrocardiogram (ECG) for heart-beat related artefacts and Electromyogram (EMG) for muscle artefacts (Sanei and Chambers, 2008; Sörnmo and Laguna, 2005).

Adaptive filtering techniques require that the artefact is uncorrelated from the desired signal. These methods like Least-Mean-Square (LMS) and Wiener filter in Finite/Infinite Impulse Response (FIR/IIR) structure (Sweeney et al., 2012b; Sörnmo and Laguna, 2005) are able to remove the artefacts when their statistics or model is known. The LMS algorithm has a complexity of $O(L)$ (L is the filter length), it estimates the desired signal through the adaptation of the filter coefficients; however, it requires an additional sensor to capture the artefact source. The Wiener filtering operates under the assumption that the signal and the artefact are stationary linear stochastic processes with known spectral characteristics. Therefore, calibration prior to usage is required for their estimation.

2.5.2 Blind Source Separation based methods

BSS techniques, like Independent Component Analysis (ICA) (Crespo-Garcia et al., 2008; Joyce et al., 2004; Ting et al., 2006) and Canonical Correlation Analysis (CCA) (De Clercq et al., 2006; Hallez et al., 2009; Vergult et al., 2007), have been applied on artefacts caused by unknown sources. ICA is based on three assumptions: (1) EEG

data originates from a spatial mixture of temporally independent brain and artifactual sources, (2) the propagation delays from the sources to the electrodes are negligible, (3) the signal at the electrodes is a linear summation of the potentials arising from several sources (brain, scalp and body). However, the small propagation delay of physiological signals might alter the instantaneous mixing of the sources (Zou et al., 2013). Unlike ICA, CCA takes into account the temporal correlation of the sources and produces the same results when repeatedly applied on a given dataset. However, like ICA, CCA is able to extract component of artefacts with stereotyped scalp topographies, like eye-blink.

In a pervasive EEG scenario, brain signals may be affected by a large amount of undetermined artefacts (Vialatte et al., 2008) which may be caused from a distributed or multiple sources, rendering ICA and CCA less reliable for extracting the artefact components from EEG data.

2.5.3 Hybrid semi-automatic techniques

When dealing with artefacts like muscle activity and body motion, with non-stereotyped artefacts, a combination of techniques based on different approaches may help (Urigüen and Garcia-Zapirain, 2015). New hybrid techniques have been proposed to suppress EEG eye-blinking and simulated artefacts: wavelet enhanced ICA (Akhtar et al., 2012; Castellanos and Makarov, 2006; Zima et al., 2012; Zou et al., 2013), EMD-ICA (Mijovic et al., 2010), ensemble EMD (EEMD)-ICA (Sweeney et al., 2012a), EEMD-CCA (Sweeney et al., 2013).

Castellanos and Makarov (2006) designed a wavelet enhanced ICA (wICA) for removing ocular activity and heart beat corrupted EEG which was shown to perform better than ICA. Discrete Wavelet Transform (DWT) is applied on the independent components extracted by the ICA; the wavelet coefficients exceeding a fixed threshold are recognised as artefacts and thus rejected. Results showed that the algorithm is capable of removing only the artefacts with stereotyped scalp topography, like eye-blink. However, the selection of a threshold is an essential constituent of the algorithm, which needs tuning according to the peculiarities of the artefacts to remove.

A similar approach was proposed in (Akhtar et al., 2012; Zou et al., 2013), although the wavelet thresholding in these cases was applied only on the independent components identified as artefact sources. Akhtar et al. (2012) proposed an algorithm based on Spatially Constrained ICA (SCICA) and wavelet denoising and applied it on 19-Channel real EEG data corrupted by simulated eye-blink artefacts. The authors first apply SCICA (Hesse and James, 2006) to identify the artifactual independent components on which they later use the Stationary Wavelet Transform (SWT) to remove any leaked EEG activity and obtain only artifactual components. They then reconstruct the EEG data by subtracting the identified artefact-only signals. The algorithm was capable

of recovering the neural activity within and outside the artefact episodes. However, it is a semi-automatic approach because it requires prior knowledge about the spatial topography characteristic of the sources generating the artefact.

Zima et al. (2012) designed a Robust Artefact Removal (RAR) method based on wICA to identify and remove short duration and high amplitude artefacts from long neonatal 8-Channel EEG, mainly caused by movement activity. They segment the EEG for three times by following different rules and then apply wICA on each of the three partitions. Instead of applying DWT on all the ICA components, they use a fixed threshold on the sparsity value of each component to identify the one containing the artefact which will be then decomposed with the wavelet and thresholded again as in wICA (Castellanos and Makarov, 2006). Later, they average the results from the three partitions and obtain the final artefact free EEG. Results showed that the method performs better than wICA. However, fine-tuning of the sparsity and wavelet thresholds is necessary to apply the RAR method to other types of EEG recordings. In this regard, Zima et al. (2012) investigated the effect of different thresholds in wICA on the results and found that the default threshold is too aggressive and it removes part of the EEG signal.

Most of the above literature have been applied on simulated well-behaved artefacts which differ highly from the experimental ones. Safieddine et al. (2012) compared two stochastic approaches (ICA and CCA) and two deterministic approaches (EMD and WT) in removing muscle artefacts in epileptic signals. Results showed that the performance of each method depends on the level of EEG contamination. When data is highly corrupted by the myogenic artefacts, EMD outperforms the other methods, while for less corrupted data ICA and WT give similar and better performances. BSS methods did show weak performances in case of low SNR data, mostly due to the low number of electrodes (32 channels): the number of sources is probably greater than the number of channels, leading to a wrong estimation of the sources. The main drawback of these approaches is that they rely on the use of several thresholds for: (a) the wavelet coefficients, (b) the Intrinsic Mode Functions (IMFs) for EMD and (c) the autocorrelation of the independent components to identify the artifactual component for ICA and CCA.

Sweeney et al. (2013) combined the Ensemble Empirical Mode Decomposition with Canonical Correlation Analysis (EEMD-CCA) as a single channel technique to remove motion artefacts. They compare results obtained from two techniques employing wavelet (Robertson et al., 2010) and EEMD-ICA (Mijovic et al., 2010) using two recordings of single channel EEGs and functional near-infrared spectroscopy (fNRIS) data. fNRIS is a measure of the concentration levels of oxygenated (oxy-Hb) and deoxygenated (deoxy-Hb) haemoglobin which are related to brain activity (Bunce et al., 2006). To determine the artefact component they induce the motion artefact in one channel only, keeping the other channel as the "ground truth" signal. In this way, they could identify the artefact component as the one which, when removed, increased the correlation between the clean signal and the ground truth. Both EEMD-ICA and EEMD-CCA work as follows: firstly

the single channel is decomposed by EEMD, several IMFs are then used as input for CCA and ICA to determine and remove the artefact components. Finally, the single channel is reconstructed. Apart from the high cost of fNIRS systems, this approach is not employable in a naturalistic environment since it is not possible to record any ground truth signal but it was proved to be useful in comparing the algorithms.

Nolan et al. (2010) developed a Fully Automated Statistical Thresholding for EEG artefact Rejection (FASTER) and tested it on 128, 64 and 32-Channel EEG ERP data collected during a visual oddball paradigm. The FASTER algorithm uses a subset of statistical thresholds on both EEG data and independent components obtained from ICA for the detection and rejection of channels and epochs affected by the artefacts. However, FASTER is based on the assumption that clean EEG parameters should be distributed normally and this could be violated in the case of a low numbers of data points. In fact, results showed that the algorithm can work effectively on all datasets, including the 32-Channel EEG, but the sensitivity of the algorithm decreases dramatically in case of low density EEG.

The main limitation of the described approaches is the use of fixed thresholds to recognise the component underlying the artefact. Some methods, like wICA and SCICA, are advantageous when applied on artefacts with well localised scalp topography, but the feasibility of their application on other types of artefacts has not been investigated.

Since in this work, we use a wireless system in a naturalistic environment, the recorded EEG data may be caused from several sources that have unknown scalp topographies and no *a-priori* information. In this work, two artefact removal methods are designed and described in Chapter 4 which do not require *a-priori* information and do not use any threshold for the artefact suppression.

Once the artefact corrupting the EEG recordings are suppressed, they can be used for estimating the brain connectivity underlying a resting-state or a cognitive task using various methodologies that are described in the following section.

2.6 Brain connectivity

Brain connectivity is crucial for understanding how the information is processed by neurons and neural networks. The information exchange between different brain areas is regulated by the synchronised activation of local neuronal groups at different brain sites (Womelsdorf et al., 2007). Changes in the strength, frequency and pattern of oscillatory synchrony of these groups can be the way in which the brain dynamically coordinate the information flow (Bastos and Schoffelen, 2015). The synchronous oscillations of cortical regions in different frequency bands are related to various motor and cognitive states and can also be related to brain diseases (Fallani et al., 2014). For example,

EEG recordings show increase in α band during mental calculation and reduction in β activity during motor acts. These local and long-range synchronisation of brain regions are critical mechanisms for information exchange in the brain (Schnitzler and Gross, 2005; Varela et al., 2001). Brain connectivity quantifies the synchronisation between various physiological signals recorded in task-specific experiments or at resting state to complement the conventional EEG analysis.

Connectivity refers to different aspects of brain organisation (Horwitz, 2003). It can be categorised as anatomical, functional or effective connectivity (Friston, 1994).

- *Anatomical or structural connectivity* describes the anatomical links between neurons and their synaptic strength, commonly referred to as fibre pathways spreading across different brain regions (Sakkalis, 2011). It is stable for short time scale (seconds to minutes), but it is likely to be affected by plasticity and morphological changes at longer time scales (hours to days). These fibre pathways or white matter tracts are measured by MRI and especially Diffusion Tensor Imaging (DTI).
- *Functional Connectivity (FC)* investigates statistical dependencies between distributed neuronal populations regardless of whether they are directly anatomically connected. Unlike anatomical connectivity, the FC patterns can fluctuate and change over milliseconds order timescale. FC can be assessed on signals measured by EEG, MEG, PET and fMRI (Sakkalis, 2011).
- *Effective connectivity* is useful to study causal and dynamic interactions between brain regions. It can be estimated through data-driven (directly from the signals) or model-based (specifying the links between structural and FC) technique (Sakkalis, 2011). It is usually estimated from EEG or MEG signals.

In this work we focus on the analysis of functional brain connectivity from EEG data. Functional connectivity is based on two principles: segregation and integration (Tononi et al., 1994). *Segregation* indicates the organisation of specialised neurons into separate neuronal populations which locally process separate features like the colour and the motion of an object. *Integration* refers to the coordinated activation of different neuronal populations from various brain areas to lead the brain into different cognitive states. The segregation (local connectivity within a cortical area) and integration phenomena (global connectivity between cortical areas) are known as synchronisation in time scale (Roelfsema et al., 1997). The following section provides more details on the various measures of functional connectivity from EEG.

2.6.1 Functional brain connectivity

Various approaches can be used to assess FC and they can be categorised as linear or non linear methods, as in time or frequency domain (see Table 2.2), and as providing directed or non directed synchronisation information. Since we are interested in functional connectivity, we provide details of the non directed measures. We refer the interested readers to Pereda et al. (2005) for details on directed measures of synchronisation, like Granger Causality (GC) or Partial Directed Coherence (PDC).

FC measures	**Time domain**	**Frequency domain**	**Linear**	**Non linear**
Cross-Correlation	√		√	
Coherence		√	√	
Phase Synchronisation		√		√
Generalised Synchronisation	√			√

Table 2.2: Functional connectivity measures

The *cross-correlation* is a linear method in time domain that measures the linear temporal synchronisation between two signals x and y as a function of their delay time: higher synchronisation is explained by higher correlation. If the two signals are linearly related, the delay time that maximises their cross-correlation is considered as an estimation of the delay between them. However, this time delay cannot be considered as a measure of the propagation time of the electrical signals within the cerebral cortex (Pereda et al., 2005).

The *coherence*, also termed as magnitude squared coherence, is the equivalent of the cross-correlation measure in the frequency domain. The coherence between two signals is their cross-spectral density function normalised by their individual auto-spectral density functions. Since the signals' spectrum is derived via Fast Fourier transform, its estimation requires the signals to be short enough to satisfy the condition of stationarity and long enough to provide good frequency resolution. The coherence is preferred to the cross-correlation if the synchronisation occurs in specified bands (Quiroga et al., 2002).

Both coherence and cross-correlation detect a mixture of amplitude and phase information; this makes them inadequate to measure the relationship between the phases of the signals which is important for the analysis of cognitive integration of multi-sensory attributes.

Phase synchronisation is a class of non linear functional connectivity measures in frequency domain. Phase synchronisation occurs when the phases of two coupled nonlinear oscillators synchronise even when their amplitudes remain uncorrelated (Pikovsky

et al., 2003). This concept is applied in neurophysiology to analyse the synchronization between pairs of EEG signals to test the hypothesis that neural communication is regulated by changes in synchronisation (Bastos and Schoffelen, 2015). Phase synchronisation is commonly found in γ band on EEG recorded during cognitive tasks or in subjects affected by epilepsy (Sakkalis, 2011) and mild cognitive impairment (Wen et al., 2015). The analysis of phase synchronisation requires the calculation of the instantaneous phase of each EEG signal through the application of non-parametric methods, like the Fourier decomposition, wavelet analysis, or Hilbert transformation (Bastos and Schoffelen, 2015). These phase based methods (Lachaux et al., 1999) include the Phase Locking Value (PLV), Phase Lag Index (PLI) and Rho; they analyse the relative phase difference between the signals recorded at two different brain sites. *PLV* is a measure of how the relative phase is distributed over the unit circle (Lachaux et al., 1999). *PLI* (Stam et al., 2007) measures the asymmetry of the distribution of the relative phase difference which is robust against field spread. Vinck et al. (2011) proposed a modified version of PLI, called weighted PLI (*wPLI*), which is even more robust against volume conduction, noise and sample size. *Rho* is another measure of synchronisation between the EEG recorded at two scalp sites: it is based on the Shannon entropy of the relative phase difference between these two sites (Tass et al., 1998). It is robust against sporadic jumps of the relative phase difference. More details on these phase synchronisation measures are given in Section 5.1.1.

Various measures under the name of *Generalised Synchronisation* (i.e Synchronisation Likelihood, S, H and N) have been recently proposed and are derived for the study of chaotic dynamical systems. These methods are based on a state space reconstruction: they analyse the interdependence between the amplitudes of the signals in the reconstructed state spaces to analyse reveal the presence of synchronisation between the two signals. Neurons are highly nonlinear devices, not (low-dimensionally) chaotic (Lehnertz et al., 2000), even though in some cases show chaotic behaviour (Matsumoto and Tsuda, 1988). In spite of that, representing the EEG signals in the phase space may reveal nonlinear structures hidden to the above mentioned approaches. These generalised synchronisation measures try to identify the case in which the states of a dynamical system x are a function of the states of another dynamical system y. The different indexes of generalised synchronisation, like the S, H and N, quantify how neighborhoods in one attractor of the state space maps into the other. More details on how to build the state space and on these generalised synchronisation measures are given in Section 5.1.2.

2.6.2 Complex network analyses on Functional Connectivity

While FC measures describe the pairwise relationships between electrodes (or brain regions), graph theory may identify the complex network associated to those pairwise measures. The application of graph theory aims to quantify the overall organisation of

the brain networks with a reduced number of features that are easy to compute and may have a neurobiological interpretation (Rubinov and Sporns, 2010). These features are useful to describe the integration and segregation phenomena responsible for the information exchange within the brain. Through the quantification of local and global network attributes, it is possible to determine differences in the network topographies between healthy/diseased subjects or between task/resting conditions (Fallani et al., 2014), to detect changes across developmental stages and to identify the brain capacity to functionally rearrange after a lesion (Carter et al., 2012).

Once the FC is extracted from the EEG recordings, there are two types of graph network that can be built: *binary networks* obtained by applying a fixed threshold on the FC values and *weighted networks* obtained by retaining those FC values (Bassett et al., 2011). The selection of a threshold and the discretisation of the FC values constitute the main disadvantage of the binary networks (Bassett et al., 2011) and make them inadequate to describe the complexity of real systems (Boccaletti et al., 2006). Weighted networks overcome these problems: several network features are proposed by Sporns (2011) for such graphs to exploit the whole available information.

Wu et al. (2012) used this approach to study the effect of music on large-scale structure of functional brain networks. Results of the high clustering coefficient and the short path length show that background music increases the local cooperative efficiency and the music condition promotes global interactions. Graph analysis applied on several brain diseases showed significant alterations of the integration and segregation phenomena occurring in schizophrenia (Wang et al., 2010a), stroke (Wang et al., 2010b) and Alzheimer disease (Supekar et al., 2008).

2.6.3 Brain connectivity in ASD

ASD is a mental disorder characterised by impaired socio-emotional processing, which depends on various intellectual skills, like memory, language, mentalisation (understanding the others' actions) and emotion. The socio-emotional and the problem solving processing are based on three main components connected by various white matter tracts (Sinha et al., 2015) in the front-temporal areas:

- The *limbic system* (fronto-temporal area) with its central role in memory and emotion (Catani et al., 2013).
- The *facial processing system* consisting of amygdala, fusiform gyrus and the superior temporal sulcus. It mediates components of social cognition like the eye gaze, facial recognition and expression (Ameis and Catani, 2015).

- The *mirror neuron system* (temporo-parietal area); it is involved in mentalising processes (Assaf et al., 2010) and in imitation abilities (Iacoboni and Dapretto, 2006).

Several studies on structural and functional brain networks have shown altered connectivity of these networks and their relative white matter tracts (Sinha et al., 2015). Various studies on structural brain networks have found two main patterns of connectivity in ASD: frontal and local hyper-connectivity (Li et al., 2014) and long distance hypo-connectivity, between anterior to posterior hemispheres and during visual evoked potentials (Coben et al., 2014). Frontal over-connectivity is most likely to be caused by an increase in frontal white matter tracts resulting in brain overgrowth in the first two years of life, which interferes with typical developmental trajectory (Coben et al., 2014). Decreased connectivity among cortical networks, instead, may explain why autistic subjects focus more on details instead of a global picture (Pellicano et al., 2006).

Several studies, listed in Table 2.3, have applied structural and functional connectivity on data recorded from various tools, from fMRI to EEG, to investigate short and long range connectivity across different tasks, age and ASD condition. Only few studies have applied network analysis on EEG recordings in subjects with ASD. FC was calculated with the *PLI* in α band in high and low risk infants (12-17 months) while attending to videos (Orekhova et al., 2014). Hyper-connectivity in frontal regions was higher in infants at high risk and strongly correlated with symptoms severity.

Barttfeld et al. (2011) used EEG *Synchonisation Likelihood* and graph networks to measure FC in the δ band and analyse long-range cortico-cortical connections in autistic subjects (16-38 years). Results showed short range connections in lateral and frontal areas. Compared to brain networks of controls, subjects with ASD are characterised by lower Clustering coefficient, higher Characteristic Path Length and Modularity. The combination of these parameters represents a less efficient network (Latora and Marchiori, 2001). They also found that local coherence and long distance coherence are positively and negatively correlated to ASD severity, respectively.

Increased path length and reduced clustering were also found in FC networks extracted from EEG signals in toddlers with ASD (mean age 3.5 years) during visual stimuli. These results suggest that global communication is already impaired during early development (Boersma et al., 2013). Matlis et al. (2015) built FC networks in the α band in children with ASD (4-8 years) from EEG recorded at resting-state. Overall connectivity was significantly lower compared to control subjects. Peters et al. (2013) calculated FC networks from *Coherence* in 128 channel-EEG recorded in children and adults with ASD (1-25.6 years). Results showed decreased long-over short range coherence and increased network resilience in ASD subjects.

Despite the wide consensus on the two main patterns of local hyper-connectivity and long-distance hypo-connectivity, results from other studies contrast these two patterns.

Study	**Results**	**Task**	**Tool**
Youths (Li et al., 2014)	Greater local connectivity and shorter path length in left superior parietal lobule, the precuneus and angular gyrus, and the right supra marginal gyrus	None	DTI
Adolescent (Moseley et al., 2015)	Reduced correlation between brain regions, greater number of high-strength nodes in visual systems	Visual stimuli, resting-state	fMRI, Correlation, network
Youths, adults (Alaerts et al., 2015)	Significant lower network efficiency and higher shortest path lengths and centrality	Resting-state	fMRI, FC, network
High and low risk (Righi et al., 2014)	Lower FC between frontal and parietal sites	Auditory stimuli	EEG, Coherence γ band
Adults (Mathewson et al., 2012)	Preferential attention to detail associated with lower coherence in posterior regions	Resting-state	EEG, Coherence α band
Children (Khosrowabadi et al., 2015)	Front-parietal and temporo-parietal (long-range) functional underconnectivity	Facial emotion pictures	EEG, FC
Children (Isler et al., 2010)	Less inter-hemispheric synchrony between early visual areas of ASD than controls	Visual evoked potential	EEG, Coherence

Table 2.3: Brain connectivity (structural and functional) studies on subjects with ASD.

Léveillé et al. (2010) showed pattern of increased EEG coherence with extra-striate areas in both short-range and long-range connections in adults with ASD (17.1-25.1 years) during REM sleep. Rudie et al. (2013) found pattern of decreased local and long-range connectivity in adolescents with ASD (9.3-17.9 years) at resting-state. Analysis of the fMRI networks revealed lower Modularity and Clustering resulting in reduced local efficiency and shorter characteristic path length indicating greater global efficiency.

Several factors may bias the results and potentially contribute to these inconsistent findings (Moseley et al., 2015): the heterogeneity of participants (in terms of age, IQ and gender), the experimental paradigm used (different task states during the recordings and their duration, the EEG frequency band of interest and the FC measure selected, as well as the EEG reference electrode. These inconsistent findings highlight the need of further investigations on the network organisation of brain processing in autistic and at-risk populations both in resting-state and in task-related analysis as well as with matched age, gender and IQ participants.

The previous sections focused on EEG studies in autism. As mentioned in Chapter 1, the analysis of behavioural and neurological measures in population at-risk of developing ASD can help in understanding this neurological disorder. The next section describes the Hypoxic-ischemic encephalopathy, the related risk of developing cognitive impairments as well as the current EEG studies for outcome prediction.

2.7 Hypoxic-ischemic encephalopathy (HIE)

Hypoxic-ischemic encephalopathy (HIE) is a common type of brain damage caused by Peripartum asphyxia, which is due to oxygen loss and reduced blood supply to the brain in the peripartum period (Berger and Garnier, 1999). It affects 1.3 to 1.7 per 1000 term newborns (Kurinczuk et al., 2010) and 23% of the neonatal deaths are caused by HIE (Lawn et al., 2010). Newborns with HIE are at high risk of brain injury and, consequently, of various developmental problems. Depending on the severity of the HIE, these subjects can be affected by Cerebral Palsy (CP) or severe neuromotor, cognitive and behavioural impairments (van Schie et al., 2015). Evidence suggests that at school age, even the subjects who did not develop CP, are at high risk of developing learning disabilities (van Schie et al., 2015). Higher incidence of delayed cognitive and language developments as well as attention problems was found in two-year old children who were affected by HIE at birth and did not develop severe neuromotor impairment (Schreglmann et al., 2016).

Because of the devastating effects that mild and severe cognitive disabilities can have on families and society (Lai and Yang, 2010), predicting the HIE outcomes at an early stage can help in accessing to neurorestorative therapies.

Due to its cost-effective, temporal resolution and non-invasiveness, EEG is commonly used for prediction outcome, early diagnosis of HIE and classification of its severity (Walsh et al., 2011). Typically, these studies employ either single, dual or multiple electrodes EEG. They rely on the visual calculation of amplitude integrated EEG (aEEG) and background features (Awal et al., 2016). This approach is mainly hampered by the absence of a standardised definition of abnormal patterns. Abnormal EEG features include flat trace EEG, burst suppression, abnormal phase or frequency. There is no common consensus on the voltage levels used to define the presence of an abnormal pattern. In addition, the time of the EEG recordings (like six hours or one week after birth) as well as the duration of the EEG analysed for the feature extraction differs across studies (Awal et al., 2016).

A computerised analysis based on functional brain connectivity and related network topographies can give insights on the brain dynamics underlying the long-term outcomes through the detection of features that are not observable by visual inspection. An

example of such approach is used in (Omidvarnia et al., 2015) where EEG at resting-state is recorded in newborns. Network brain connectivity analysis is applied on the EEG recordings to predict two years outcomes of newborns affected by intraventricular haemorrhage, which can cause neurocognitive impairments as in the case of HIE. The neuro-developmental outcome at two years were negatively correlated with the clustering coefficient and weight dispersion of the connectivity network.

Similar to the previous study, connectivity networks were built from DTI recordings of newborns with neonatal encephalopathy (Ziv et al., 2013). Results suggest that clustering coefficient and transitivity would differ between healthy and non-healthy subjects, with clustering coefficient being anti-correlated with a neuromotor score (Tymofiyeva et al., 2012).

2.8 Summary

In this chapter we introduced the key notions within the literature for characterising and treat children with ASD. Specifically, we began by discussing various approaches employed in clinical environment to diagnose and characterise children with ASD. We highlighted that all these approaches are based solely on behavioural analysis. Like the diagnosis, current intervention procedures are based on behavioural and developmental intervention in naturalistic settings. However, the heterogeneity of the ASD symptoms and the need of intensive treatments constitute the main limitations of the current methodologies. One way to mitigate these drawbacks is identified in the use of computer-based interventions in the treatment of ASD. In this regard, we described different computer applications proposed in literature implemented to enhance a single target impaired skill specific to socio-behavioural symptoms. Despite their demonstrated feasibility and efficacy, the individuality (i.e. single-user games) of such applications does not fulfil the criterion for which a computer-based intervention should be a mean for enhancing a social skills with a partner. In addition to this deficiency, the current computer applications restrict the vast array of impaired skill to a single target skill. To overcome this problems, we designed a multi-user computer platform based on a current NDBI treatment which will be described in Chapter 3.

Despite the effort of researchers in understanding the complex and heterogenous autism disease, the identification of a biomarker remains a great challenge. For this purpose, we then discuss various tools that have been employed to date for studying the brain connectivity underlying the atypical behaviours of ASD. Among the available devices, we favoured the Electroencephalogram as the main instrument for capturing the fundamental neurological abnormalities of ASD. Particularly, we focused on the use of a wireless EEG system, thanks to its usability, low cost as well as its high temporal resolution. However, such a system is sensitive to artefact corruption caused mainly by

environmental, physiological and motion related sources. A variety of methodologies to suppress the artefacts are described: they are mainly based on *a-priori* knowledge of the artefact which allows the selection of appropriate thresholds for artefact detection and suppression. In addition, these methods are mainly applied on well characterised artefacts, which differ from the artefact generated in naturalistic environment. Therefore, two new methodologies will be proposed and described in Chapter 4 that address these limitations and are suitable for EEG recorded in naturalistic environment.

Following the description of artefact removal methods, we describe the different types of brain connectivity that can be extracted from neurological devices. In particular, we focus on the vast array of FC measures that can be extracted from EEG data and the differences between them. We then highlight the additional and meaningful information that can be extracted from these FC measures when they are modelled as complex networks. FC is widely used to address the brain connectivity dysfunction in ASD. Despite the wide research employing FC analysis, only few attempts have combined it with complex network theory. In view of the additional information that such an approach can give, we identified the complex FC networks as a possible technique to analyse the relation between the behavioural symptoms and cognitive skills and the underlying neurological processes in intervention of ASD. This approach will be described in Chapter 5, where it will be used to investigate how the children progress during the computer-based intervention employing the game platform described in Chapter 3.

The identified framework of combined FC and complex networks can be also used on the analysis of other neuro-developmental disorders and in healthy subjects. In this work, this approach is applied for the first time on newborns affected by HIE. We discuss the previous research works on prediction outcomes using EEG data and their limitations. These methods rely solely on feature extraction from EEG data, which lack a meaningful clinical interpretation. As in the case of ASD, functional complex network analysis can give insights on the brain connectivity in children affected by HIE and who later develop neuro-developmental disorder. The use of this framework for prediction of two years outcome is explained in Chapter 6.

Chapter 3

GOLIAH: Gaming Open Library Intervention for Autism at-Home

As per the objectives outlined in Chapter 1, we wish to build a framework for monitoring behavioural and neuro-developmental trajectories in children with ASD during early intensive intervention. In this chapter, we focus on the first challenge: we develop an effective intervention framework that can be delivered at home and allows behavioural monitoring. In Chapter 1 and 2, we described the difficulties encountered when comparing different behavioural treatments to determine the most effective intervention. Since a systematic delivery of the interventions may help this comparison, we recognise that a computerised game platform based on an established treatment protocol could be an efficient way to perform a systematic intervention.

We propose a novel multi-player gaming platform, Gaming Open Library Intervention for Autism at-Home (GOLIAH), implementing the ESDM protocol for early intervention in ASD children. GOLIAH is not intended to replace the ESDM intervention but to supplement it for achieving its maximal benefit. The main goal of GOLIAH is to allow: (a) delivering of intensive intervention in *nomadic environments* (clinical and home setting), (b) *tailoring* the intervention based on the characterisation of the child's skills, and (c) achieving the *required intervention hours* without incurring in significant delivery costs and parents' specialised training.

Compared to the contemporary approaches, GOLIAH targets a vast array of imitation and joint attention skills rather than focusing on a single ability, as in the current ASD targeted games. Since imitation and joint attention are precursors of language and high-level abilities, they are considered essential to enable the learning process. GOLIAH ensures the repeatability of the instructions and the involvement of parents in the intervention. It is implemented in a multi-player form, thus avoiding the risk of isolation typical of the state-of-the-art computer-based intervention.

GOLIAH is validated across two datasets of children with ASD at two different hospitals for a 3-month open trial to assess: (a) the seamless operation of the game at-home settings and (b) the feasibility of the game in treating ASD children.

The remainder of this chapter is structured as follows. In Section 3.1 we describe the use of GOLIAH as a closed-loop system for delivering parent-mediated intervention at-home and hospital. Section 3.2 describes the software design. In Section 3.3, we describe the stimuli selected from the widely used ESDM protocol and implemented in the proposed gaming library, along with the GOLIAH game. In Section 3.4 we present the results obtained during the open trial of GOLIAH on two groups of children with ASD. Finally, Section 3.5 concludes the chapter with a summary of the results.

3.1 Conceptual system for closed-loop intervention system and its advantages

GOLIAH can be thought at the centre of a closed-loop system that may enable effective intervention at-home and in clinical settings as shown in Figure 3.1. This closed-loop operation of the game provides various advantages: (a) maximal intervention hours (b) in nomadic settings, (c) repeatability of the stimuli, (d) tailored intervention and (e) automated data generation to monitor the child's progress.

GOLIAH consists of a set of games created by mapping the desired intervention stimuli (from ESDM) into the games. In theory, the library could be divided in two parts, *characterisation* and *therapeutic* games, although they could be used interchangeably without loss of any generality. (1) At first, during the *characterisation* phase, the child will be asked to play a set of games carefully selected from the library by the therapist for characterising the child's difficulties/strengths. Since a particular type of stimulus could be mapped in different ways and multiple games, various games can be used to ascertain the child's difficulties/strengths pertaining to a type of stimulus in a repeatable way without inflicting boredom on the child and, thereby, obtaining a much more precise average characterisation of the child. (2) Once characterised, during the *therapeutic* phase, the therapist defines a tailored protocol by selecting appropriate games that the child needs to play at his/her home setting on a regular basis. The aim here is to enhance the cognitive performances of the child by playing these games at-home so that the effective intervention hours could be increased.

GOLIAH embeds an automated evaluation process that produces a set of quantitative evaluation metrics: they characterise the child's performance within each game and provide the temporal evolution of the child's performance. This set of quantitative evaluation metrics is based on automated and manual scores that can be checked by the therapist to investigate how the child is improving and whether the parents are adhering

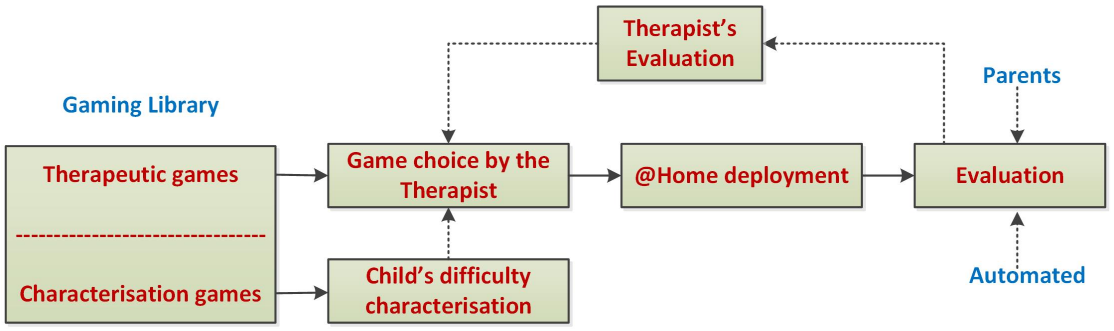

Figure 3.1: Closed-loop intervention of GOLIAH system.

to the prescribed protocol truthfully. (3) Once the child achieves a target outcome, the therapist may choose a more difficult game level or different games within GOLIAH and the whole process may continue. The next section details the software development to create the GOLIAH platform.

3.2 Software Design and development

The game software runs on any standard Internet-connected Windows device. It was developed in Microsoft Visual Studio 10 Platform in C# language. The platform game has as many classes as the number of included mini-games; thus, creation of new games will not alter the existing ones. Real-time communication between two devices is performed through a multi-threading process consisting of (a) a *Game flow thread*, where all the game tasks are performed (including sending objects to the other user), and (b) a *Receiving thread*, where the objects from the other user are received and fire the semaphore in the other thread. A server acts as a bridge between the devices of the two players. The objects exchange occurs through a Socket connection based on TCP/IP protocol, which ensures that the information exchange will not be lost during the transmission.

The next section details the skills targeted by the game and the correspondent mini-games.

3.3 Gaming platform: mapping the ESDM stimuli

The GOLIAH gaming platform consists of 11 games, based on two main categories: Imitation and JA skills. These are two pivotal skills critical for enabling the social and language learning and addressed in the well established ESDM treatment (see Section 2.2.3). In fact, learning is mainly based on activities that require the interaction between partners, like attending and imitating others, and sharing emotions through JA, participate with others in coordinated activities and communicate with gestures and words (Schreibman et al., 2015).

A list of the mini-games, a brief description and the related ESDM stimuli is given in Table 3.1. The seven Imitation-based mini-games comprise of tasks which involve the imitation of drawing, speech, sounds and building actions in order to complete the game. The other four games are based on JA stimuli, including the identification of objects such as fruits, home furniture, and vehicles. A more detailed description of each game is given in the following sections.

Game type	**Description**	**ESDM stimuli**
Imitate free drawing	Imitation of a drawing – Open stimuli	(lev.4) FM 4
Imitate step by step drawing	Imitation of a drawing (three difficulties) – Open stimuli	(lev.4) FM 4
Imitate Speech	Imitation of words or phrases (three difficulties) – Stimuli library	(lev.2) IM 3, 9
Imitate sounds	Imitation of sounds (four difficulties and two categories of stimuli) – Stimuli library	(lev.2) IM 2
Imitate actions	Imitation of actions with balls (three difficulties and two types of task) – Open stimuli	(lev.2) IM 6
Imitate actions and build	Imitation of actions with cubes (three difficulties and two types of task) – Open stimuli	(lev.3) FM 3
Guess the instrument	Identification of musical instruments (two difficulties) – Stimuli library	(lev.1, 2) IM
Follow the therapist's pointing	Identification of the object indicated (verbally, visually or pointed) on a video (six difficulties and eight categories of stimuli) – Stimuli library	(lev.1) RC 1, 4 (lev.2) JA 2, 4, 6
Cooperative drawing-connect dots	The therapist and the child cooperatively connect dots to complete a figure (two difficulties and four categories of stimuli) – Stimuli library	JA subset
Bake a cake	The child cooks a recipe by clicking and dragging into a bowl ingredients (11 categories of stimuli) – Stimuli library	JA subset
Receptive communication	Identification of objects verbally described (three difficulties and five categories of stimuli) – Stimuli library	(lev.2) RC 5, (lev.1) RC 6, (lev.1) RC 4

Table 3.1: GOLIAH games and mapped ESDM stimuli. Some games contain various levels of difficulties and several tasks. The stimuli included can be from a Stimuli library or it can be created by the master (Open stimuli). Details of the fine motor (FM), Imitation (IM), JA, Receptive Communication (RC) skills and the respective levels are described in (Rogers and Dawson, 2009).

GOLIAH is a multiplayer game with two main users: the therapist or parent acting as the *master* and the child designated as the *player*. The choice of the language, goal setting and the game to play (according to the desired ESDM stimuli) is made by the master. The role of the player is to achieve the goal set by the master at the end of

the game. Currently the platform is implemented in three different languages (Italian, English and French) for providing instructions to the child although it has the flexibility of recording the instructions in any other language. In developing the games, special attention has been devoted to their realistic resemblance to the real-life scenario, more importantly emulating human-human interactions during the game playing phase.

The stimuli presented to the children during a game can be either from a pre-developed library, *Stimuli library*, or it can be generated by the master, *Open stimuli*. In the first case, the master selects appropriate stimuli from the *Stimuli library*: the player is required to respond to the stimuli following the automated instructions embedded within the game. This allows the parent to choose the stimuli scheduled by the therapist and extends the possibility to present the same stimuli to the player repeatedly, in order to evaluate the improvement of the child over time. Furthermore, a list of stimuli can be played with different children in order to make an evaluation of the response of different children to the given stimuli. When using the *Open stimuli*, the master has an active role and the flexibility to create new ones. All the games have different levels of difficulty allowing the therapist to adjust the intervention according to the cognitive skills of the child during the characterisation and the intervention phases.

The performance of the player is assessed in different ways: it can be evaluated in terms of correct responses or through more articulate metrics. The following section details the various measures generated by the GOLIAH platform to evaluate the player's performances.

3.3.1 Performance Evaluation

The evaluation of the player's performance takes place in two different ways, depending on the game: some game requires a manual evaluation of the master, others automatically generate a score. The manual evaluation uses a scoring system of 0 to 2 where 0 means that the player did not achieve the goal, 1 for partial achievement and 2 for successfully satisfying the goal. The automated evaluation generates a +1 for each correct response to the given stimulus within a game. In addition to this score, the gaming platform provides a large number of quantitative measures for each session that will help to characterise the child's performance in terms of time. For each task accomplished by the child, such as clicking on an object or drawing, an event is generated detailing the time of the response and the related outcome, if successful or not. Table 3.2 provides the objective measurements generated by the game along with their definitions. This set of metrics allows the therapist to analyse quantitatively the performance of the player in a stimulus-specific way not only at a particular time point but also the progression of the child's performance over a time window (hours, days, months, etc.) giving a holistic picture of the child's development. It also supports the therapist to ascertain the appropriateness of the parents' scoring and their adherence to the prescribed protocol. Such

Metric	Description
Name of stimulus (A)	Name of the object the player has to click/drag/draw
Time of stimulus (A)	Difference $\Delta T_s = T_{ss} - T_{es}$; it is the time window during which the stimulus is shown on the child's device
Time of response (A)	Difference $\Delta T_r = T_{sr} - T_{er}$; it is the time window during which the child's responds to the stimulus
Type of response (A)	Whether the child performs the action as intended by the master (only Correct/Incorrect)
Score of response (A)	It can be (1/0); depending on the type of response
Image of stimulus and response (A)	Screenshot of the player's device at the end of the imitation drawing and action games
Sound recording (A)	Audio response of the player recorded during the sound and speech imitation games
Master evaluation (M)	Defined as Complete/Partially complete/Incomplete response of the child according to the master judgment
Manual score (M)	It can be 0/1/2 depending on the master evaluation

Table 3.2: Objective metrics extracted from the gaming platform. The (A) indicates automated metrics, while the (M) signifies manual metrics. T_{ss} and T_{es} indicate the start and end time of the appearing of a stimulus respectively. T_{sr} and T_{er} signify the start and end time of the response of the player to a stimulus.

analysis could be done both online and offline by the therapist as the metrics are stored at each game session. The therapist can inspect the changes in reaction time, scores obtained and number of failures over the period in which the child is being treated to examine any trends or improvements. The data acquired can also help in comparing the child's performance at the hospital and at-home, in order to determine the place where the child is more confident. The player's score might change depending on who is acting as the master, whether is the parent or the therapist.

GOLIAH provides a positive reinforcement to the child at the end of each game: it consists of a smiley face and it is used as positive feedback to the player simulating the reward-based intervention. This feedback is programmable and an appropriate reward could be set by the therapist according to the player's motivation factors, like playing music that the child likes.

3.3.2 GOLIAH: the games

The game software runs on any standard Internet-connected Windows PC or Tablet. At the start of the game, the main windows, in Figure 3.2, will appear in the master's device. He will first choose the language in which the stimuli and instructions will be played. Thereafter, the master selects the desired game which will automatically be launched on both devices. In this Section, we provide a description of all the available games together

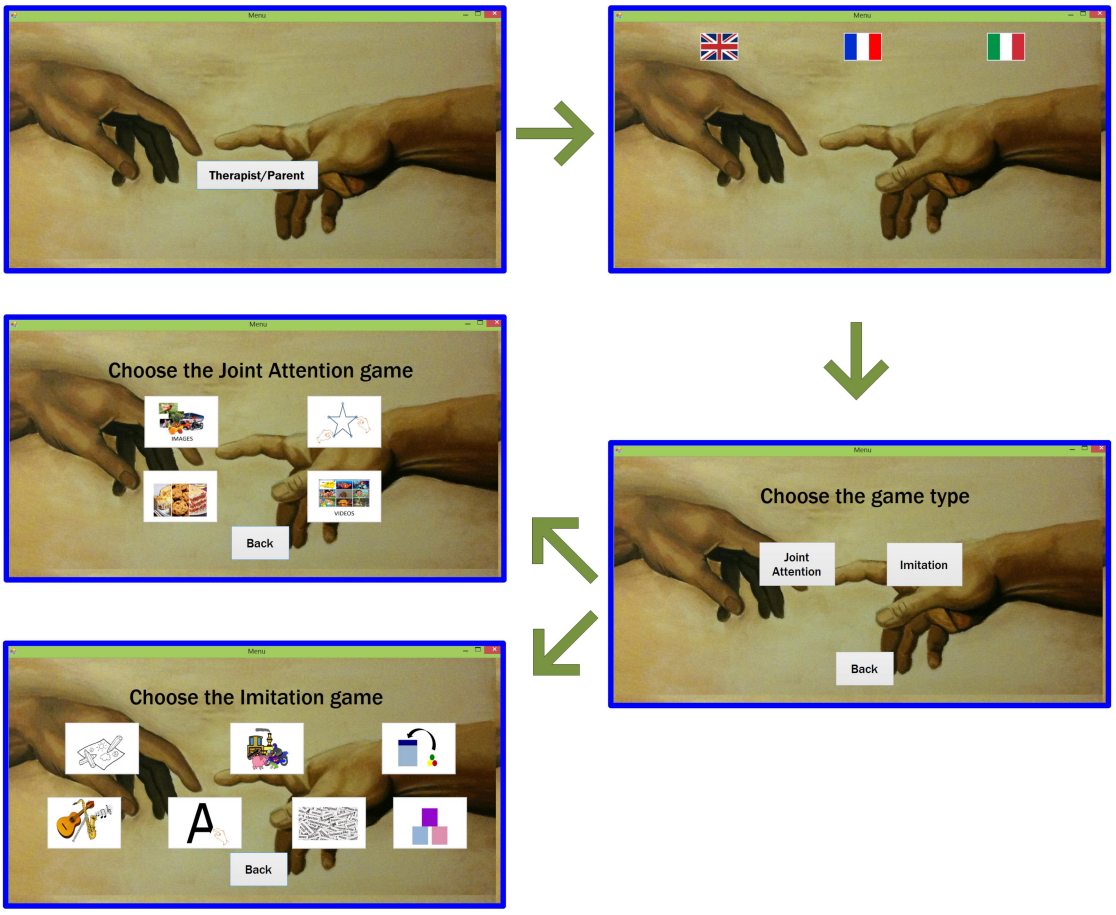

Figure 3.2: GOLIAH: main windows of the master during the beginning of the game.

with the representative steps required to the master and player to complete each game. The colour of the window indicates the correspondent player: the blue corresponds to the master's device and the red to the child's device.

Imitation game 1 and 2: Free drawing and Imitate step by step drawing
This imitation game is intended for examining the player's ability to imitate several objects drawn by the master, starting from very basic drawings, such as scribbles and dots, to very complicated, like letters and numbers. The whole process of the two imitation games is shown in Figure 3.3: a window appears on both master and player's devices with clearly marked separate drawing panels. (1) The master can draw any object of any shape in the panel dedicated to him on the right. Once completed, (2) the master's drawing appears on the player's device: he needs to imitate it by drawing on the left panel (his dedicated panel). (3) The live outline of the player's drawing will appear on the master's device. Depending on whether the drawing is correct or not, (4) the master can decide to finish the game, by clicking on the tick button, or encourage the player to have another try, by clicking on the cross button. (5) The quality of the imitation will be evaluated by the master among three possibilities: correct, incorrect

or partially correct. Regardless the master judgement, a smiley face will appear on the player's device .

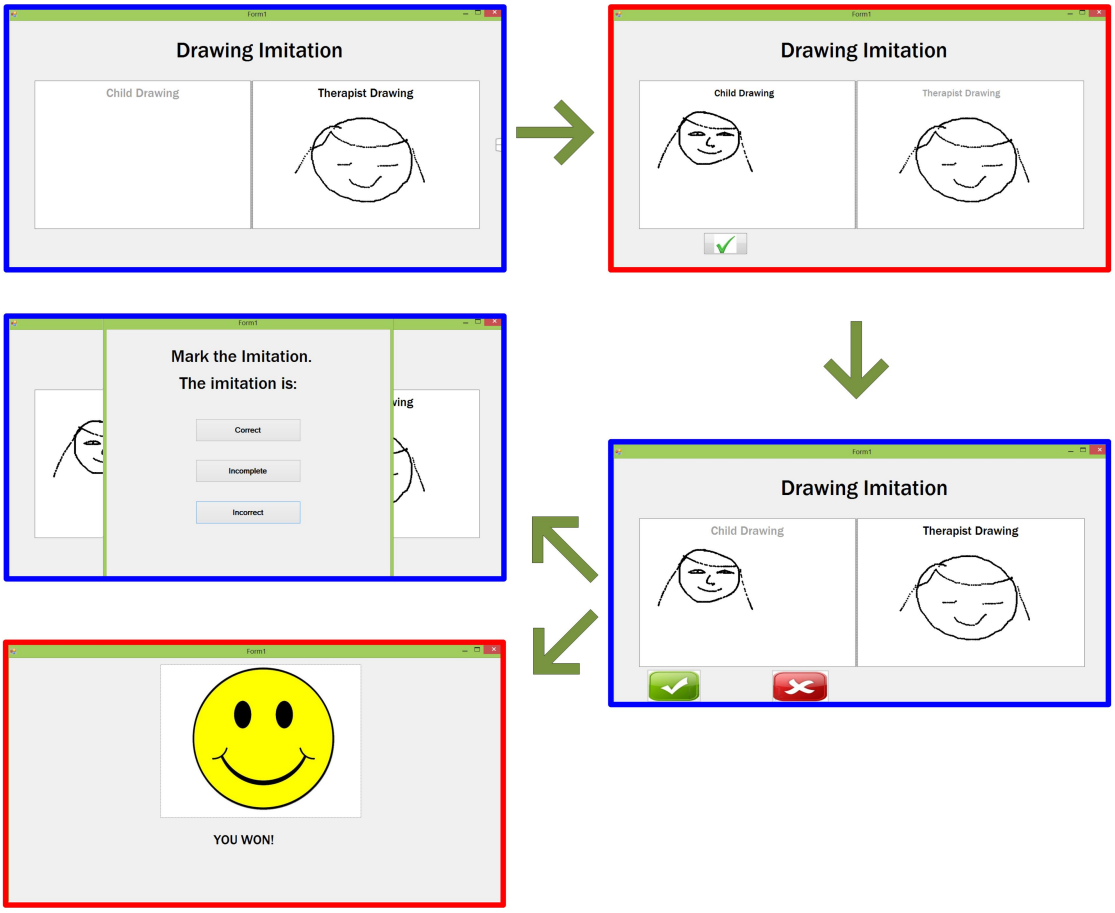

Figure 3.3: GOLIAH: flow of the Imitation game 1 - Free drawing.

The Imitation game 2 is similar to the first, but it has three difficulty levels.

- *Step by step difficulty*: the master would draw an object in several steps. For instance, a house could be sketched by drawing, first a square, then adding a triangle on the top, and so on. At every step, the player will copy the masters sketch. The master may draw more complicated shapes at each step after seeing the imitation ability of the player in the previous drawing.
- *End-step by step* and *Snapshot at the end*: the master first draws all the steps required to complete the drawings. The player will imitate the sketch after the appearance of the sequence of steps (end-step by step) or the complete drawing (snapshot at the end).

In all the difficulty options mentioned above, the master can accept the player's drawing or can encourage him to give another try at any intermittent step.

Imitation game 3: Imitate Speech

This game is based on the imitation of sound of recognisable single words or phrases. The player has to first hear and then repeat the sound of the words or sentences selected by the master from the standardised library. The whole process of this game is shown in Figure 3.4. (1-2) The master can select the stimuli among three levels of difficulty: *words* ("mother"), *simple phrases* with few words ("I want") or more *complicated phrases* ("my mother is at-home"), by selecting the appropriate option from a drop-down menu in his device. (3) The selected words or phrases will be played on the player's device who, after each sound, (4) will imitate the word or the phrase. The player's imitation is

Figure 3.4: GOLIAH: flow of the Imitation game 3 - Imitate Speech.

recorded automatically and played back to the master for the evaluation. The response will be stored in the player's device to allow the therapist to investigate offline the parent's evaluation when the game is played between the child and the parent. As in the previous games, the assessment of the imitation's quality is performed by the master among the three available choices as shown in Figure 3.3.

Imitation game 4: Imitate Sound

This sound imitation game allows the analysis of the player's skills in the imitation of sounds of *everyday objects* or *animals*. The sounds can be reproduced with four levels of difficulty: *human imitation and picture* (the sounds imitated by a third person will be reproduced together with the picture of the chosen item), *true sound and picture* (the picture is associated with the real sound of the stimulus), *true sound* (the sound is played without any picture), *picture* (the picture is shown without any sound). The game flow is shown in Figure 3.5: (1) after the difficulty, (2) the master selects the appropriate category of stimuli by clicking either on the animal icon or the object icon in his window. As shown in Figure 3.5, (3) this will open the available stimuli already

stored in a pre-defined library. Currently the two libraries for the everyday objects and animals include the sounds of train, scooter, donkey, pig, etc. (4) Following the presentation of each selected stimulus, the player will imitate the sound. The recordings acquired on the player's device will then be played on the master's device to score the imitation, similarly to the previous games. As with the Imitation game 3, the responses are recorded in the player's device to allow the therapist to investigate the parent's evaluation offline at a later stage.

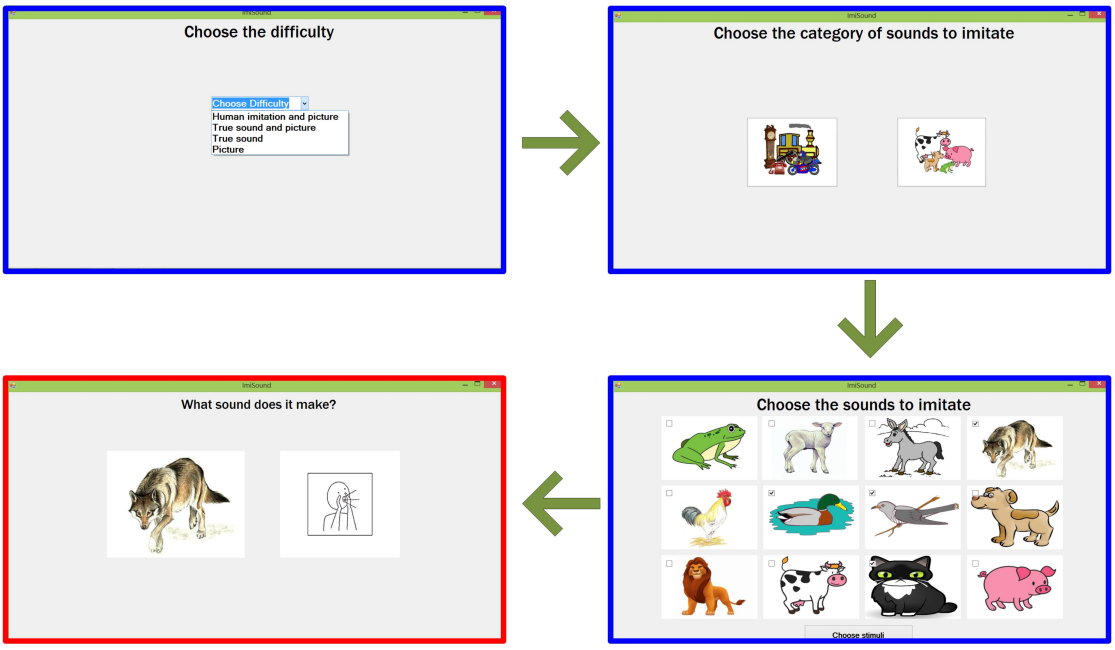

Figure 3.5: GOLIAH: flow of the Imitation game 4 - Imitate Sound.

Imitation game 5: Imitate Actions

The goal of this game is to imitate the actions initiated by the master with an object in multiple steps. As shown in Figure 3.6, (1) the master can select among three difficulty levels, depending on the number of balls to move during the actions; they can put into a box *one*, *two* or *three* balls. (2) The child can imitate the actions performed by the master according to two types of imitation: at each step (*each step imitation*), or after seeing all the steps (*full action imitation*). The game involves a minimum of three action steps: (3-4) the master and the player have to open a box by moving a lid to a dedicated space on their respective panels, put one or more balls into the box and close the box with the lid. Both the master and the player visualise the opponent actions on the right panel of their device. The game requires manual scoring (Section 4.3.3); the final image with master and player's actions is saved for further analysis by the therapist.

Imitation game 6: Imitate Actions and Build

The purpose of this game is to imitate and build objects by moving the cubes inside the apposite panel, as shown in Figure 3.7. Similarly to the previous game, the player's imitation skills can be analysed by following two different procedures: the player can

Figure 3.6: GOLIAH: flow of the Imitation game 5 - Imitate Actions.

emulate the action at each step (*each step imitation*), or after the master has finished moving all the cubes (*full action imitation*). (1) The master can build different objects by using *three*, *four* or *10 cubes*, according to the selected difficulty. (2-3) A single or all the steps are displayed in the player's device, (4) who will imitate the actions performed by the master. As in the previous game, the master will evaluate the player's performance after the imitated actions are displayed on his device. The final image showing both the master and the player's actions will be saved for further checking.

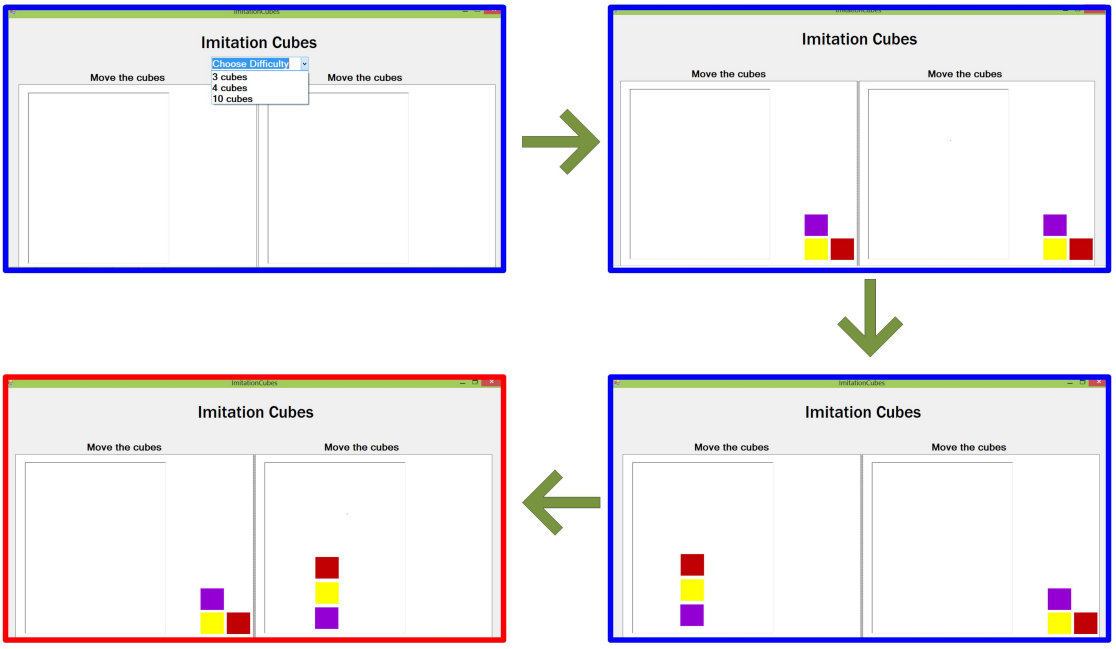

Figure 3.7: GOLIAH: flow of the Imitation game 6 - Imitate Actions and Build.

Imitation game 7: Guess the musical instrument

This game is based on the imitation of a sequence of musical sounds selected by the master: (1) he can select the number of musical instruments to show, *three musical instruments* or *six musical instruments*, as in Figure 3.8. According to the initial skills of the player, (2) the master may select a sequence of one to six musical instruments. (3) The selected music is then played on the player's device; (4) he needs to identify and click on the corresponding instruments. In this case, the evaluation of the player's skills is automated: each correct answer will produce an event labelled with a unit score. In case the player has difficulties in guessing the instrument, the sound could be played back once again by clicking the Play button. The number of errors and replays will be saved, allowing further analysis to monitor the player's improvements over time.

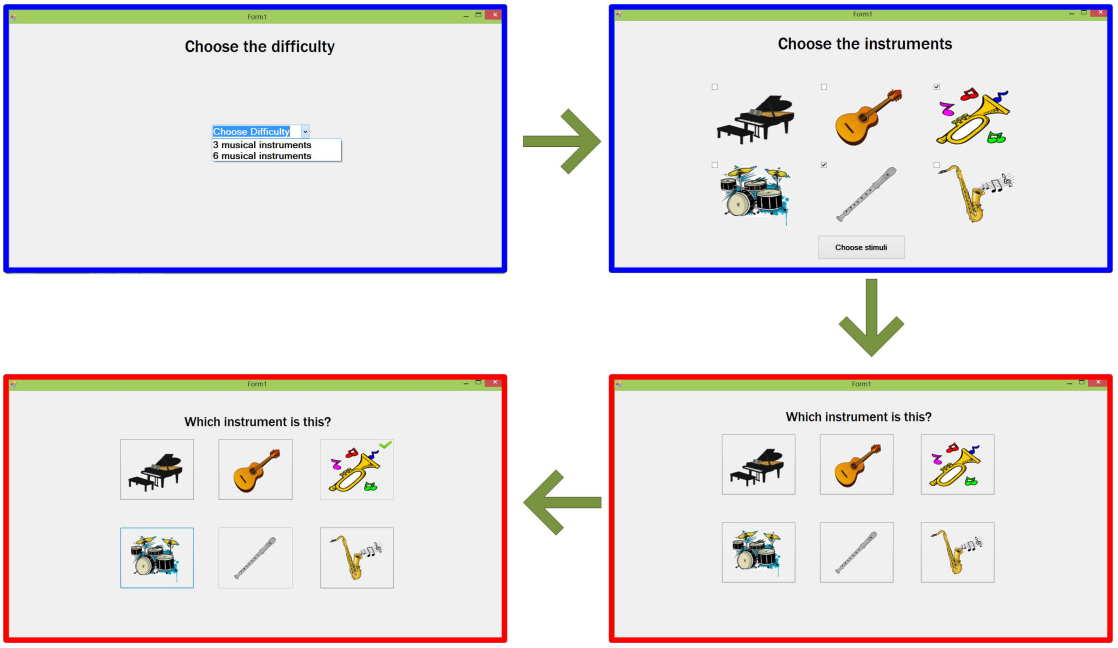

Figure 3.8: GOLIAH: flow of the Imitation game 7 - Guess the musical instrument.

Joint attention 1: Follow the therapist's pointing (both audio and visual)

This game is based on different JA stimuli from the ESDM such as looking at a picture indicated verbally, pointed with a finger or with a gaze shift. As shown in Figure 3.9, the game consists of a library of pre-recorded videos in which a person indicates an object with different difficulties: *point only*, *speak and look*, *speak only*, *point and look*, *look only* or look but in the meanwhile point at the opposite direction (*inconsistent condition*). At first, (1-2) the master selects the following criteria: the type and number of pointed objects and the indication procedure. The master can opt to play with two, four, six or eight objects which can be squares, cartoons, superheroes, food, cars, etc. Next, the master selects one item at a time. For each item, (3) the corresponding video from the pre-recorded library is played on the player's device: it consists of a person pointing to the item, like the yellow rectangle at the top of the window. This approach mimics

Figure 3.9: GOLIAH: flow of the Joint Attention game 1 - Follow pointing (both audio and visual).

human-human interaction to some extent giving the impression to the player that he is interacting with a person and not with a mere machine. After watching this video, the player will have to click on the pointed item. In case of failure, the player clicking on the wrong item, the video is played again to help him to respond correctly. An automated event for each correct or wrong answer is created, respectively with a positive or negative score.

Joint attention 2: Cooperative drawing – connect dots

In this game, the master and the player create a figure or shape by cooperatively connecting the dots on its edges, as shown in Figure 3.10. At first, the master selects (1) the difficulty (*easy* or *hard*) and (2) the figure to draw from a library. This figure can be a *letter of the alphabet*, an *object* like a tree, a *geometric shape* or a *number*. In the master and player's devices, (3) the window is divided in two panels: the right side shows the final figure, while on the left side the dots and lines will appear in real time each time one clicks and/or connects two dots. After the first dot, (4) the master and the player alternatively put a new dot next to the previous one in order to connect them and complete the final figure shown on the right. An event with a positive or negative score will be produced each time the child attempts to put a new dot and, therefore, connect a new line. The evaluation of the player's skills is automatically produced at the end of the game with a final score.

Joint attention 3: Bake a recipe

This game is targeted to cook a recipe by mixing six ingredients in a bowl, as shown in Figure 3.11. (1) The master selects the recipe to cook among 11 dishes from a standardised library, which includes pizza, tiramisu, lasagne, omelette, roasted chicken,

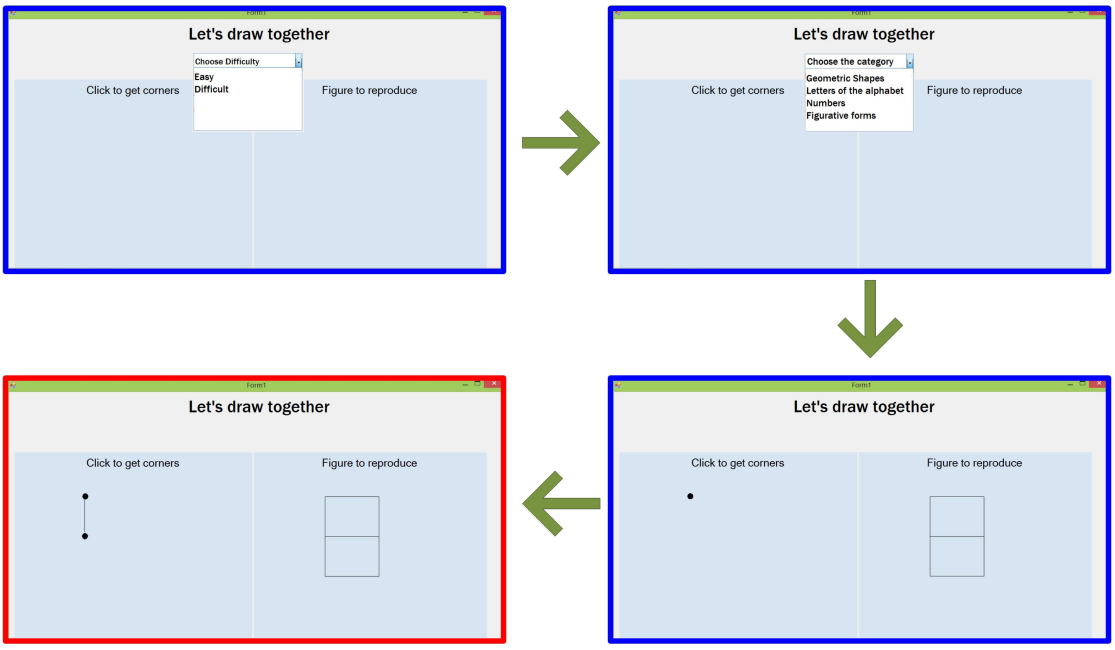

Figure 3.10: GOLIAH: flow of the Joint Attention game 2 - Cooperative drawing – connect dots.

pasta, etc. For each of the six ingredients, (2) as soon as the master clicks on it, (3) an arrow connecting this ingredient to the bowl will appear on the child's device. Next, the player has to drag the ingredients into the bowl. When all the ingredients are in the bowl, the child has to click on the Mix button and, finally, (4) he has to choose the recipe they cooked among seven dishes shown in the window. As for the previous game,

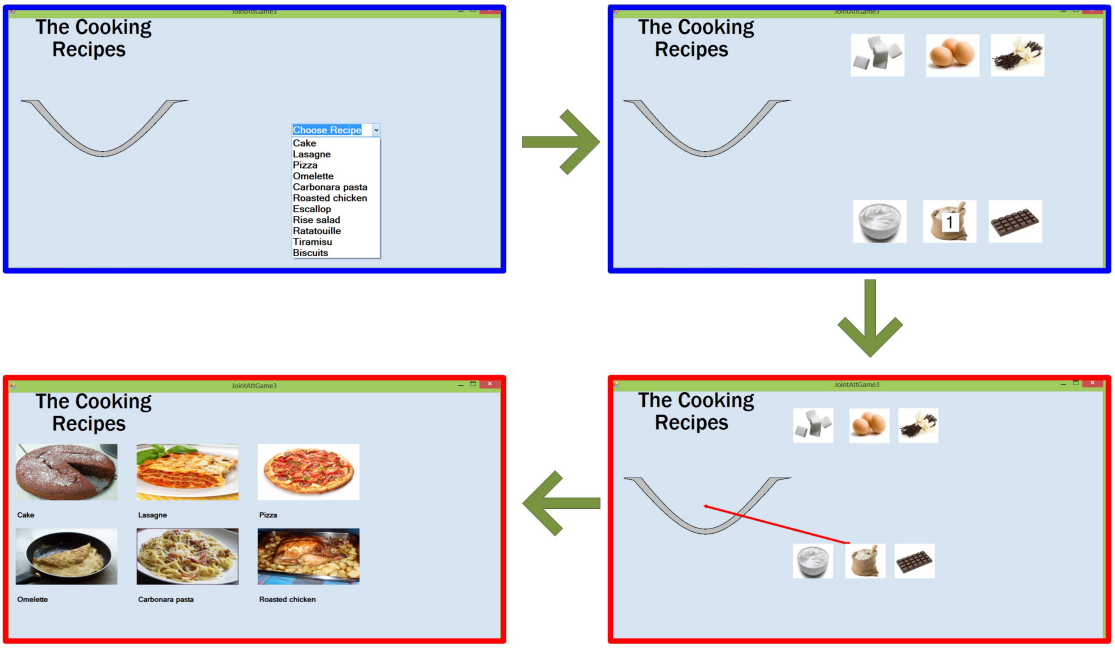

Figure 3.11: GOLIAH: flow of the Joint Attention game 3 - Bake a recipe.

an event with positive or negative score is generated each time the player clicks on an

ingredient and drags it into the bowl, as well as when the correct recipe is recognised.

Joint attention 4: Receptive communication

This game is based on various JA ESDM stimuli, including the identification of a named picture. As shown in Figure 3.12, the difficulty options of this game are based on the number of pictures shown on the player's device (Step 1): the player has to identify and click the object described by the master. This is illustrated among (1) *three*, (2) *five* and (3) *eight* objects. The master selects the item from the library which consists of five categories of pictures (Step 2): (1) *animals*, (2) *furniture*, (3) *vehicles*, (4) *fruits* and (5) *vegetables*. Once the master has picked all the pictures to be described (Step 3), the player sees those figures on his/her device and has to identify and click on them (Step 4). For each item, the event related to the correct or incorrect answer will be produced with the related positive or negative score.

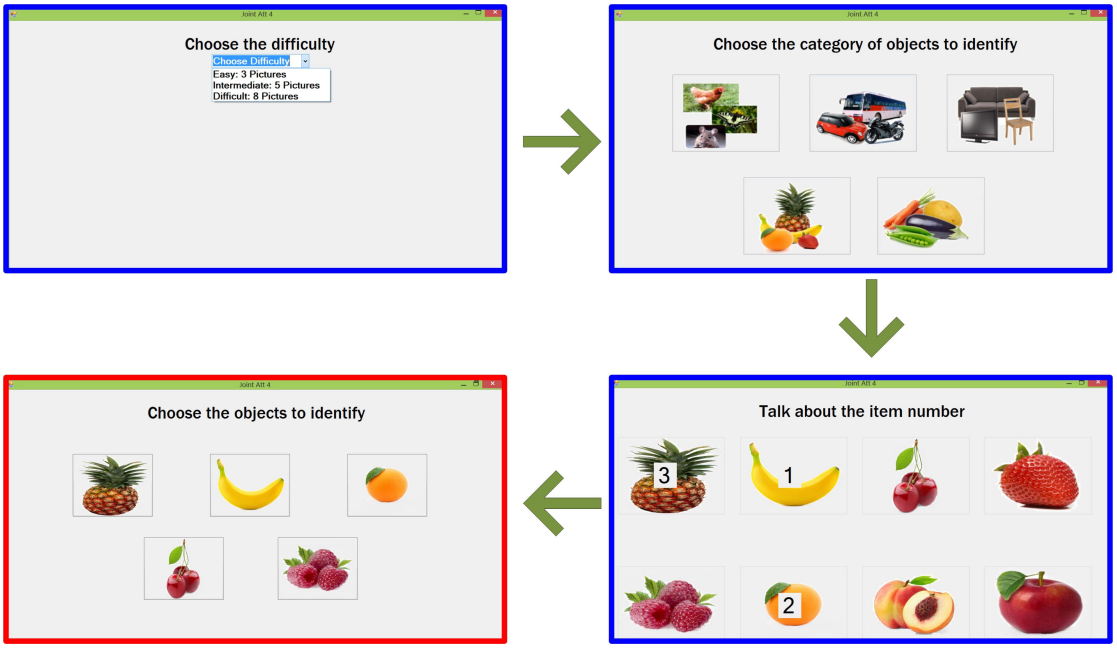

Figure 3.12: GOLIAH: flow of the Joint Attention game 4 - Receptive communication.

3.4 Open trial and Results

GOLIAH was tested in a 3-month open trial with children with ASD at two hospitals and at-home. This open-trial aimed at assessing (a) the usefulness of the gaming platform with children-therapist and with children-parents interactions, (b) whether tailored intervention was compatible with at-home use and parents and (c) whether children performed as expected when using the different Imitation and JA games. To do so, we used both the objective GOLIAH metrics (Section 4.3.3) and the clinical annotations from the therapists. (d) Finally, subjective views from users were also explored.

3.4.1 Participants and sessions

Ten children with ASD (all boys, aged 5 to 9 years) were recruited in the Department of Child and Adolescent Psychiatry, Pitié-Salpêtrière Hospital, Paris and in the Department of Child Neuropsychiatry, Stella Maris Institute, Pisa. The intervention protocol consisted of six GOLIAH-based sessions (20 minutes) per week: the children played GOLIAH five sessions at-home with the parents (mother or father) and one session at the hospital with the therapist.

To assess in detail the usability of the gaming platform, we planned a systematic recording of the games played in each session for all the children during the 3-month study period. Table 3.3 lists the number of sessions the children played a specific game during the intervention: all the mini-games were exploited but not all their variants, due the ample number of difficulty levels, tasks and stimuli. Given the diversity of the games and the heterogeneity of children profile and skills, the number of sessions dedicated to each game varied across children. All games were well tolerated and followed by the children, therapists and parents. Children engaged in activities that they previously refused to execute in the non-computerised version, even showing enjoyment. One family initially had troubles in using the two tablets system related to Wi-Fi connecting problems that could be easily corrected. Tailoring treatment during the hospital session and data transfer from home was easily achieved.

Child	**1**	**2**	**3**	**4**	**5**	**6**	**7**	**8**	**9**	**10**
IMITATION GAMES										
Imitate free drawing	11	4	4	6	3	19	16	19	15	16
Imitate step by step draw	17	13	24	10	5	20	11	18	13	9
Imitate speech	17	13	15	9	11	15	11	19	12	6
Imitate sounds	2	19	10	13	11	10	17	9	11	8
Imitate actions	15	23	7	6	10	14	11	14	4	16
Imitate actions and build	12	11	19	13	12	12	14	11	12	13
Guess the instrument	4	3	11	10	9	2	1	7	6	5
JA GAMES										
Follow therapist's pointing	15	19	20	17	12	14	13	16	21	12
Cooperative drawing	2	19	15	11	13	9	11	11	18	18
Bake a cake	10	13	16	14	11	12	12	12	12	16
Receptive communication	21	25	31	20	17	16	15	25	9	12

Table 3.3: Number of sessions per game and per child during the 3-month study period.

3.4.2 Children performance through sessions and games

The children's performances across sessions are described in relation to the imitation and JA based games, by using either quantitative or qualitative scoring. The goal here is to verify the appropriateness of the GOLIAH scores extracted from each game session to monitor the child's progress.

3.4.2.1 Bake a recipe (JA game 3 – quantitative scoring)

The Bake a recipe game is one of the most played games. The performance of the children is analysed in terms of number of errors committed and time employed to complete the game. Figure 3.13 represents the evolution of the time utilised to complete a task for the JA game 3. Since the game is played multiple times during a session, the completion time T_i for session i is averaged across the multiple run. For all children, the task completion time decreases during the intervention indicating that the children become faster to achieve the task. The dotted curve represents the logarithm of the task completion time averaged for all children across the sessions. The average completion time logarithmically decreases with a coefficient of determination of $R^2 = 0.7824$.

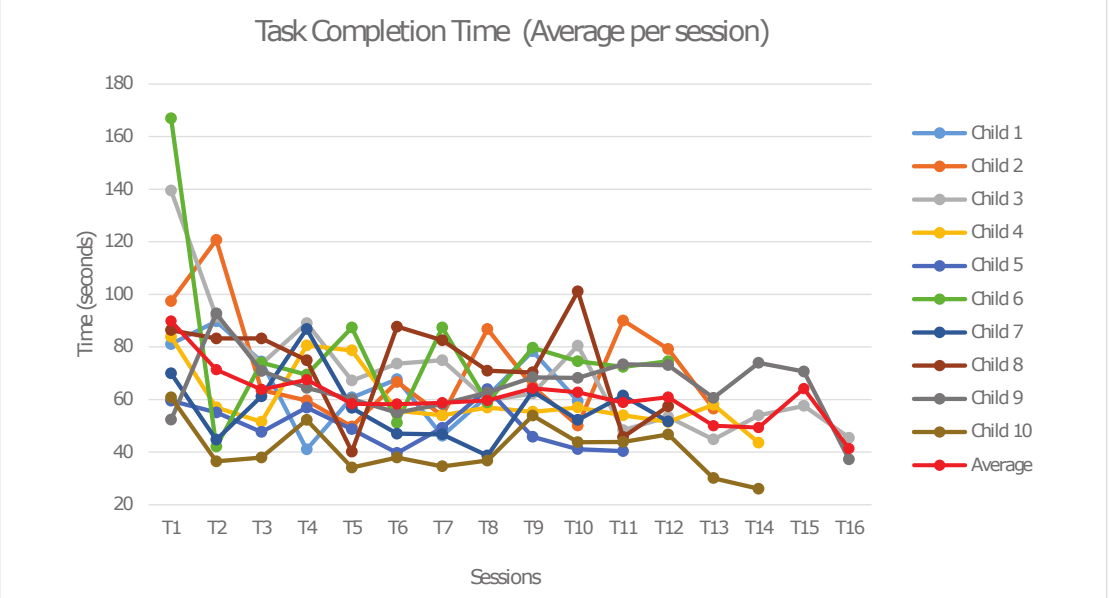

Figure 3.13: Evolution of the time (in seconds) to complete the task for the JA game 3 - Bake a recipe.

Figure 3.14 shows the variation of the number of errors committed while playing the Bake a recipe game. The mistakes considered here are of two types: during the first phase of the game when the child selects one or several wrong ingredients before or after selecting the correct one, and during the second phase when the child selects the wrong recipe. For reasons of readability of the box plot type graph, the sessions are grouped

into four periods consisting of four sessions each. According to our data, the children who had already good performances at the beginning (Period 1) kept their performances constant all along. But there is an important decrease of the number of errors per child across the four periods, particularly for the children who committed several mistakes initially. At the end (Period 4), the number of mistakes is decreased for all children.

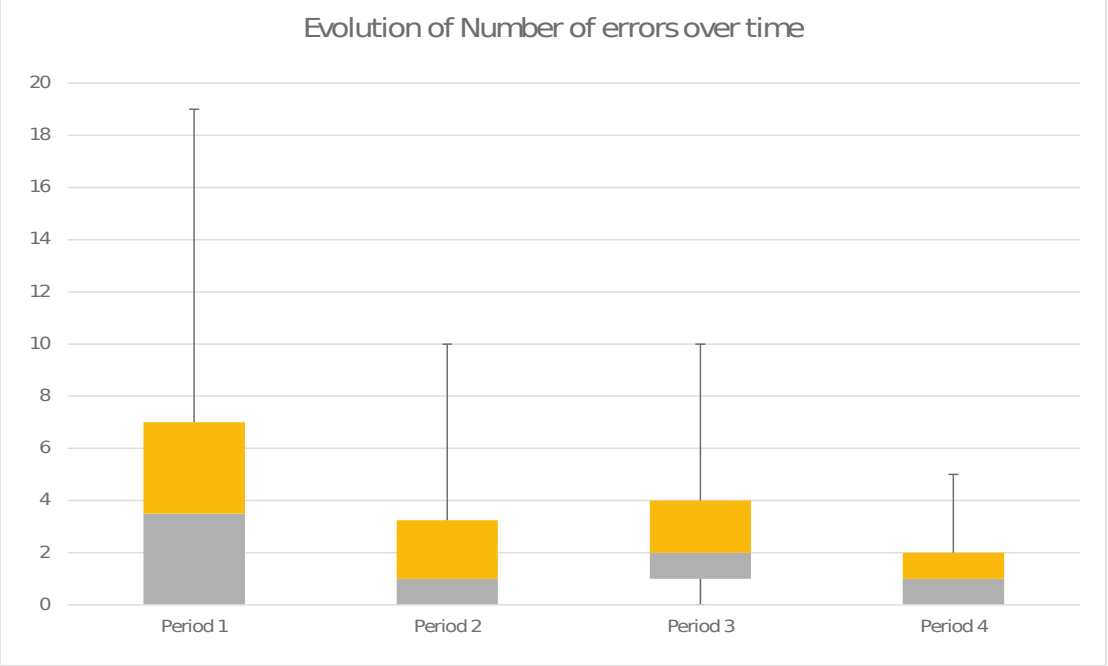

Figure 3.14: Number of errors performed to complete the task for the Joint attention game 3 during different periods.

3.4.2.2 Free drawing: qualitative scoring

The Free drawing imitation game consists of open stimuli that can be created by the master (parent or therapist). The imitation skills of the children for this games are manually evaluated by the therapist based on the quality of the child's drawing, as described in Table 3.2. A comparison of the drawings across children is difficult to perform due to the complexity of pictures, differences in drawing time and in fine motor skills. For this open trial, we show the evolution of the performances in one subjects in terms of manual score of the imitation. The quality of imitation is improved, as shown by the evolution of the imitation scores (given by the master) in Figure 3.15. The average score ($av = 1.7$) during the third period ($T_7 - T_9$) is closer to the maximum score (score 2) and different from the initial scores for the periods $T_1 - T_3$ ($av = 1.1$) and $T_4 - T_6$ ($av = 1.1$). In addition, the child needs fewer trials to reproduce the master's drawing.

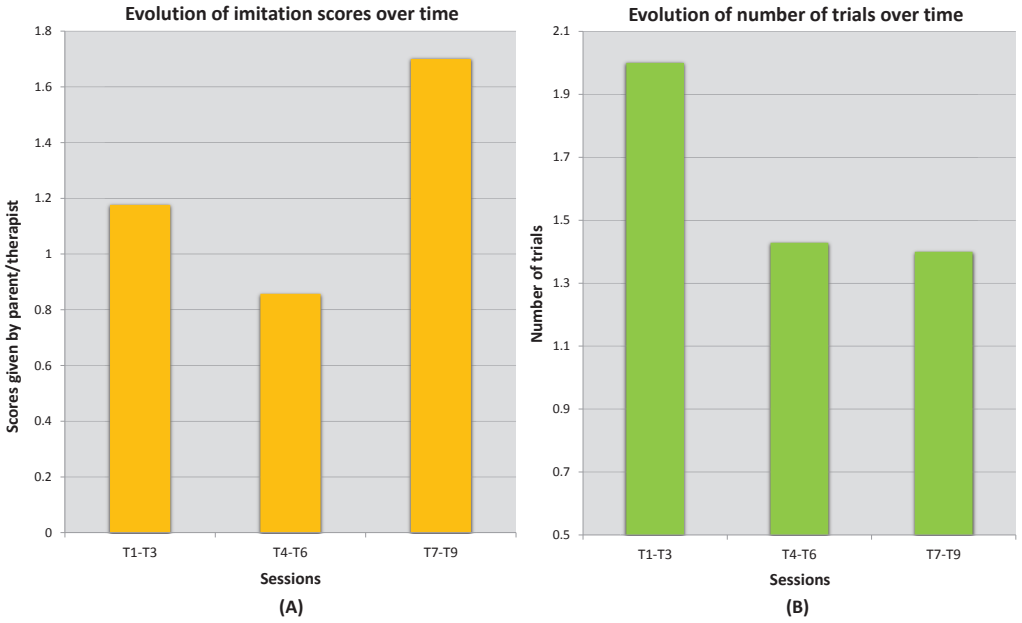

Figure 3.15: Evolution of the performances of one child during the Imitation game 1 - Free drawing.

As an illustration, Figure 3.16 represents the evolution of child's imitation skills in drawing across the 3 periods. The right panel shows the master's drawing and the left the correspondent child's drawing.

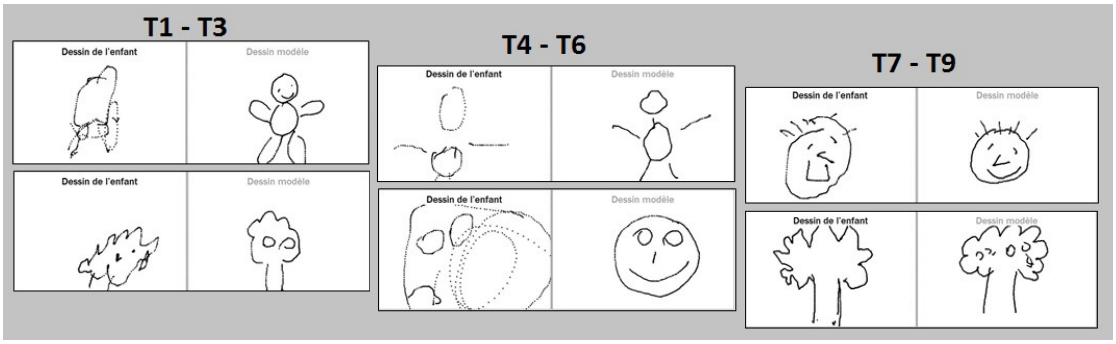

Figure 3.16: Evolution of the imitation skills of a child across three periods of the intervention.

3.4.3 Parents experience and view

At the end of the 3-month open trial, parents were interviewed from the therapists to discuss about their experience with GOLIAH. Parents positively assessed the use of the serious game as a treatment. They did not observe a decrease in the child's motivation to work on the tablets. Various skills not directly trained by the games strongly evolved during the course of this open trial: child's self-esteem, concentration and flexibility, as well as an improvement of the quality of parents-child relationship.

We provide here some comments given by the parents of the children enrolled in the open trial after the three months.

"*This is a tool that enables me for the first time to objectively interact with my son*".

"*My son used to be extremely nervous and agitated when faced unfamiliar situations. After these 3 months of using GOLIAH I can see that he has a changed attitude to a similar situation; he stays calm and tries to understand the situation and act accordingly often in correct way*".

"*We observed significant change in attention and problem solving capability of our son after the trial period of 3 months*".

A demo of a GOLIAH based session was shown to four reviewers of the European commission. One of the reviewers commented: "*The proposed system could represent a significant step forward for ASD patients, especially in the field of rehabilitation and training*"".

3.4.4 Discussion

The results described in above sections are promising and show children amelioration and high acceptance of the platform from the therapists, children and parents. However, the present study has several limitations that prevent us from drawing any significant conclusion. These are mainly related to the lack of a control group and the restricted sample size.

First, a control group with age-matched children would have lead to a comparison of amelioration of children with ASD versus a typical population.

Second, even without a control group, the number of subjects recruited in the three months are not sufficient to draw significant conclusions for the results presented in this chapter.

Third, specific methodology would be required to externally evaluate the Imitation and JA progression outside the game and in this way, compare the automated scores of the game with the scores given by professionals.

Fourth, the game has the potential to monitor the efficacy of the intervention in a systematic procedure: each skill can be monitored by analysing the results of each game on multiple sessions and multiple children. However, it is well known that the ASD is a spectrum consisting of children characterised from very low disabilities to high cognitive impairments. In order to monitor the efficacy of each game, the subjects dataset has to contain various sub-groups of children belonging to a narrow range of the spectrum. In this way, the efficacy of each game could be tested on various spectrum band. Surely, this

problem affects the traditional intervention protocols as well, but this computer-based intervention may overcome this problem due to its cost effective advantage.

3.5 Summary

In this chapter, we described a gaming platform for home-based intervention in ASD. Within the context of a pilot open trial, we showed the seamless operation and feasibility of the intervention. We found that (a) the gaming platform was useful during both child-therapist interaction at hospital as well as child-parent interaction at-home, (b) tailored intervention was compatible with at-home use and non-professional therapist/parents, (c) children performed as expected when using the different Imitation and JA games and no game appeared inaccurate, (d) data computed from the platform and clinical annotations produced by parents and therapists allowed session-to-session monitoring and helped therapists to dynamically reconfigure treatment, and (5) subjective views from users (mainly parents here) were overall positive. From the clinical point of view, the most important benefits of this novel method of intervention for children with autism are: (1) the rapid performance amelioration on tasks based on Imitation and JA that are considered pivotal for children with autism; and (2) to create a scenario where the spontaneous, and usually lone, activity with video games is easily pushed to become a shared activity. However, the issues presented in **??** prevent us from drawing significant results. Further trials addressing those limitations would be beneficial to obtain significant results.

Chapter 4

EEG Artefact Removal

In the previous chapter, we addressed the first challenge encountered to deploy a system for behavioural and neuro-developmental monitoring during early intensive intervention. In particular, we implemented a widely used treatment protocol on a game platform. The GOLIAH game automatically allows the automatic recording of behavioural outcomes and, simultaneously, the recording of EEG signals. The latter are of particular interest for monitoring the neuro-cognitive abilities during the intervention. Since we aim at monitoring the intervention in naturalistic settings, we target the use of wireless EEG. However, wireless EEG data can be corrupted by unknown and severe artefacts (due to body movement, like head-shaking, jaw and hand movement) in addition to the typical physiological artefacts characterised by stereotyped scalp topographies (eye-blinks, eye-ball movement, respiration and cardiac activity). The presence of these artefacts restricts the use of raw EEG data: the amplitude of the artefacts is much higher than that of the neural signal, thus artefact suppression is crucial for the subsequent EEG brain connectivity analysis.

In this chapter, we propose two hybrid artefact removal algorithms: Wavelet packet transform-Independent Component Analysis (WPTICA) and Wavelet Packet Transform-Empirical Mode Decomposition (WPTEMD) in pervasive EEG scenario, assuming existence of no *a-priori* knowledge about the artefacts. The two proposed techniques are first compared with two state-of-the-art algorithms using semi-simulated signals and then validated on real 19-channel EEG data recorded with a wireless EEG device. EEG data were recorded on ten healthy adults while performing various body movements, which led to eight types of artefacts.

Typically, clinicians visually inspect the EEG data and manually select the artifactual epochs to discard; this leads to a substantial decrease of the data available for the consequent analysis. To address this issue, various artefact suppression techniques are proposed in literature. They require *a-priori* knowledge about the source of the artefact affecting the EEG data, as in the case of SCICA (Hesse and James, 2006), or rely on the

use of fixed thresholds that need to be tuned according to the different type of artefact's sources, like FASTER (Nolan et al., 2010) and wICA (Castellanos and Makarov, 2006). In a wireless scenario, the corruption might be caused by a combination of artefact sources, which highlights the need of a generic artefact suppression algorithm.

The remainder of this chapter is structured as follows. We first describe the constituents of the proposed techniques in Section 4.1 and, next the hybrid algorithms WPTEMD and WPTICA in Section 4.2. Later in Section 4.3 we describe the semi-simulated and real EEG data experimentally generated to evaluate the performance accuracy of the algorithms together with the performance evaluation metrics adopted. In Section 3.4 we present our empirical results obtained by applying the suppression algorithms on the two EEG datasets. Finally, we summarise our conclusions in Section 4.5.

4.1 Decomposition techniques

In this section, we give a brief description of the main constituents (WPT, ICA and EMD) used in the two hybrid artefact suppression algorithms. In essence, the three techniques decompose a signal into subcomponents: limited frequency components (WPT), statistically independent sources (ICA) and spectrally independent oscillatory modes (EMD). ICA is applied at all electrodes, whilst WPT and EMD are applied on EEG single channels. While WPT uses predefined linear time-invariant filters to decompose the data, EMD is data-driven technique. More details are given in the following subsections.

4.1.1 Wavelet Packet Transform Analysis (WPT)

WPT allows to analyse a signal in time and frequency domain by decomposing it into a tree, as shown in Figure 4.1. Wavelet Transform uses short windows at high frequencies and wide windows at low frequencies to obtain a multi-resolution analysis with balanced resolution in time and frequency. This is accomplished by passing the signal through low and high pass filter banks: the first corresponds to an averaging operation and provides the approximation coefficients, the latter to a differencing operation and results in detail coefficients. WPT decomposes the detail and approximation coefficients iteratively, generating the full tree (Walczak and Massart, 1997). Each set of coefficients in the tree is called a node; for N decomposition levels the tree contains $2N$ nodes: N detail coefficients d_{j+1}^{2p+1} and N approximation coefficients d_{j+1}^{2p}, defined as follows.

$$\begin{cases} d_{j+1}^{2p}[k] = d_j^p * h_d[2k] \\ d_{j+1}^{2p+1}[k] = d_j^p * g_d[2k] \end{cases} \tag{4.1}$$

where d_j^p is the node at the previous decomposition level, k is the number of samples, (j, p) is the location of the node in the tree, j indicates the decomposition level, and p

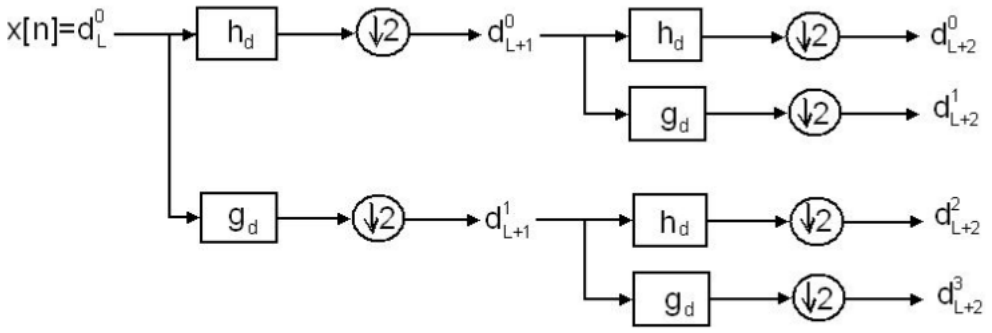

Figure 4.1: Wavelet Packet Tree: the signal is decomposed through the application of low pass and high pass filters on both approximation d_{j+1}^{2p} and detail d_{j+1}^{2p+1} coefficients. A decimation step is applied at each decomposition (Adam, 2010).

indicates the number of nodes on its left. The high and low pass filters $h_d[2k]$ and $g_d[2k]$ are defined as follows:

$$\begin{cases} h_d[k] = \langle \psi_{j+1}^{2p}(u), \psi_j^p(u - 2^j k) \rangle \\ g_d[k] = \langle \psi_{j+1}^{2p+1}(u), \psi_j^p(u - 2^j k) \rangle \end{cases} \tag{4.2}$$

where $< . >$ is the inner product, ψ_{j+1}^{2p} and ψ_{j+1}^{2p+1} are the wavelet packet orthogonal bases at the nodes, and $\psi_j^p(u - 2^j k)$ is an orthonormal basis. To obtain the bases, the mother wavelet $\psi^p(u)$ is dilated by j and shifted by k. Once decomposed, the signal can be reconstructed by the following equation:

$$d_j^p[k] = d_{j+1}^{2p} * h[k] + d_{j+1}^{2p+1} * g[k] \tag{4.3}$$

The wavelet decomposition and reconstruction allow to decompose a signal to analyse its characteristics in coarser or finer resolution for various purposes, from the analysis of EEG records in epileptic seizure (Adeli et al., 2003) to denoising. In the last case, one or more nodes can be identified as artifactual component, rejected and the signal reconstructed.

4.1.2 Independent Component Analysis (ICA)

ICA is another technique for signal decomposition. It applies the principle of statistical independence to a set of multivariate data to find a representation in which its components are independent. Let us consider N random variables $x_1, x_2, \ldots, x_N$ that are linear combinations of n sources $s_1, s_2, \ldots, s_N$ called independent components:

$$x_i = a_{i1}s_1 + a_{i2}s_2 + \cdots + a_{in}s_N, \ i = 1, \ldots, N \tag{4.4}$$

where the a_{in} are the mixing coefficients. The sources are statistically independent if their joint probability density function is equal to the product of their probabilities: $f(s_1, s_2, \ldots, s_N) = f(s_1)f(s_2)\ldots f(s_N)$. Both sources s_i and mixing coefficients a_{ij} are unknown and will be determined by using only the multivariate data.

In matrix form, Equation 4.4 becomes $X = AS$, where the source matrix is given by $S = [s_1, s_2, \ldots, s_N]^T$. The aim of ICA is to identify an unmixing matrix $W = A^{-1}$ to calculate the independent components as:

$$S = WX \tag{4.5}$$

To accomplish it, there are various implementations of ICA, among which we will use Fast-ICA (Hyvarinen, 1999). (1) At first the observed data X are whitened, which results in a zero-mean, unit variance vector $Z = VX$ of uncorrelated data, with the whitening matrix V obtained from the covariance matrix of the data. (2) Next, ICA uses an approximation of negentropy to maximise the non-gaussianity of the estimated sources. This step is necessary because ICA uses higher order statistics which are null for Gaussian distributions and, according to the central limit theorem, the distribution of a linear combination of independent variables tends to be gaussian. The approximation of negentropy of a random variable y for a non-quadratic function G (i.e. contrast function), and zero-mean, unit variance Gaussian random variable ν is defined as:

$$J(y) \approx [E\{G(y)\} - E\{G(\nu)\}]^2 \tag{4.6}$$

(3) The final step is the maximisation of negentropy: it returns the unmixing matrix W to obtain the independent components (Equation 4.5). In Fast-ICA, it is implemented with a fixed-point iteration scheme:

$$w \leftarrow E\{zg(w^T z)\} - E\{g'(w^T z)\}w \tag{4.7}$$

where w is a single column of the unmixing matrix W, z is the whitened and centred data, g and g' are the first and second derivatives of G respectively.

ICA has been traditionally used to identify the sources of the artefacts contaminating EEG data, like eye-blink artefact corrupting the frontal lobe electrodes (Li et al., 2006). Typically, the clinicians visually inspect the independent components to manually identify the artefact; once identified, this artifactual component is rejected and the signal is reconstructed, according to Equation 4.4.

4.1.3 Empirical Mode Decomposition (EMD)

EMD is a data driven decomposition technique for nonlinear and non-stationary signals. Given a signal $x(t)$, it can be decomposed as a linear combination of a finite number N

of Intrinsic Mode Functions (IMFs) $h_i(t)$ and a residual $r(t)$, as follows:

$$x(t) = \sum_{i=1}^{N} h_i(t) + r(t) \tag{4.8}$$

The IMFs should satisfy two conditions: (a) the number of extrema and the number of zero-crossings must either be equal or differ at most by one; (b) at any point the mean value of the envelope of the local maxima and minima should be zero (Huang et al., 1998).

A *sifting* process is applied recursively to obtain each IMF. First, (1) a smooth upper $u(t)$ and lower $l(t)$ envelope of the signal $x(t)$ are calculated from the extrema through cubic spline interpolation. Then, (1) the mean envelope $m(t)$ is calculated as $m(t) = \frac{u(t)+l(t)}{2}$ which is then subtracted from the original signal, i.e. $h(t) = x(t) - m(t)$. (3) At this point, if $h(t)$ satisfies the two conditions above or a given stopping criterion, the $h(t)$ is identified as the first IMF $h_1(t)$, it is subtracted from the signal $x(t)$ and the sifting restarts for the next IMFs until the residual will be reached. The stopping criterion used in the WPTEMD algorithm is based on two thresholds ξ_1 and ξ_2 to guarantee the presence of small global fluctuations (EEG) and large local excursions in the mean (artefact) (Rilling et al., 2003). The stopping criterion here is based on the evaluation function $\zeta(t) = |2m(t)/[u(t) - l(t)]|$ and the following conditions:

$$\begin{cases} \zeta(t) < \xi_1, & \text{for } (1-\alpha) \text{ fraction of the signal length} \\ \zeta(t) < \xi_2, & \text{for the remaining fraction} \end{cases} \tag{4.9}$$

where $\alpha \approx 0.05$, $\xi_1 \approx 0.05$ and $\xi_2 \approx 10\xi_1$ (Rilling et al., 2003). The decomposition achieved with EMD enables identifying the basic irregular components of the corrupted signal: the artefacts in the EEG can be identified as IMF and hence can be rejected to clean the signal. The following section describes how the techniques described above are integrated within the two hybrid algorithms.

4.2 Hybrid Artefact Suppression Algorithms: WPTEMD and WPTICA

Artefact reduction of EEG data is crucial for monitoring the neurological trajectories of the subjects undergoing the early intensive intervention. To address this issue, we formulate a generalised framework for automatic artefact removal in pervasive EEG recorded during natural body movements. We propose two hybrid artefact removal algorithms, WPTICA and WPTEMD, that combine the techniques described in the previous section. Figure 4.2 shows the two algorithms and the criteria formulated to automatically identify the artifactual component corrupting the EEG data. The WPTEMD algorithm

consists of the combination of WPT (step 2-3) and the consequent EMD decomposition (step 4a-5a). WPTICA, instead, consists of the WPT (step 2-3) and the consequent ICA decomposition (step 4b-5b). WPT decomposition and reconstruction are performed equivalently in both methods.

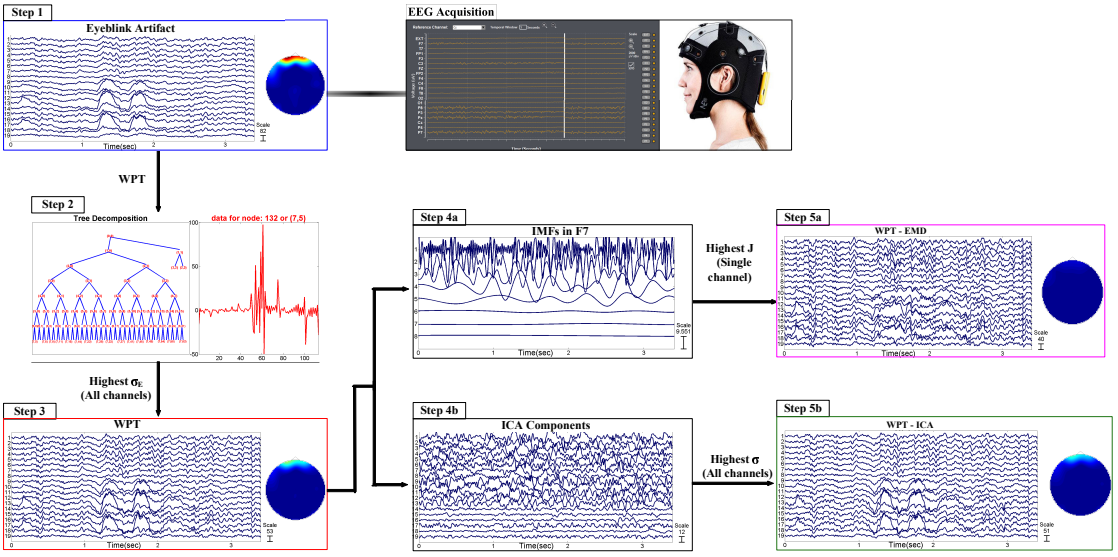

Figure 4.2: Schematic diagram of computation sequence of the two hybrid algorithms WPTEMD and WPTICA. The steps 2 and 3 are common to both algorithms.

Each technique is applied to decompose the signal in its subcomponents; next, various parameters are calculated to identify the artifactual component. Once identified, this component is rejected and the signal is reconstructed and used as input in the subsequent technique. Table 4.1 lists the parameters used to identify the artifactual component for each technique. In both algorithms, EEG data is first decomposed and processed with WPT; next, the WPT-reconstructed signal is used as input to the EMD (in WPTEMD) and ICA (in WPTICA) to be decomposed, processed and reconstructed again.

Algorithm	Technique	Parameters
WPTEMD	WPT	$EGY_{c,node_i}$, $\sigma_{EGY,node_i}$
	EMD	J, S, $S_{resting}$, σ, $\sigma_{resting}$
WPTICA	WPT	$EGY_{c,node_i}$, $\sigma_{EGY,node_i}$
	ICA	σ_c

Table 4.1: List of techniques and parameters for the proposed artefact reduction algorithms.

The next subsections provide details of the proposed algorithms. Since WPT is common to both algorithms: first we describe the WPT processing, next the WPTEMD and WPTICA algorithms.

4.2.1 WPT decomposition in WPTEMD and WPTICA

WPT allows to decompose a signal into several nodes of a tree until the desired decomposition level (see Section 4.1.1). Although it is a single channel technique, we here use it from a multichannel perspective: we build a wavelet tree for each of the 19 EEG signals. Once the 19 trees are obtained, we analyse the nodes of all the trees to identify the node containing the artifactual component common to all channels. To accomplish it, we calculate the energy $EGY_{c,node_i}$ for all the nodes in the last decomposition level of the trees and its standard deviation $\sigma_{EGY,node_i}$ across all channels as:

$$\begin{aligned} \sigma_{EGY,node_i} &= \frac{1}{C-1}\sum_{c=1}^{C}(EGY_{c,node_i} - \overline{EGY}_{node_i})^2, \\ EGY_{c,node_i} &= \sum_{n=1}^{N}(\text{node}_i[n])^2 \end{aligned} \tag{4.10}$$

where i is the number of node ($i \in [1-128]$), N is the number of samples at each node, C is the number of channels. The node characterised by the maximum $\sigma_{EGY,node_i}$ is identified as the one capturing the artefact; it is then rejected while reconstructing the artefact suppressed EEG signal. The obtained WPT-cleaned signal is given as input to the ICA (WPTICA) or EMD (WPTEMD) for further suppression of the artefact, as shown in Figure 4.2.

To obtain the WPT trees the signals are decomposed up to the 7^{th} level, as used in Zima et al. (Zima et al., 2012). In WPT, at each decomposition level the frequency resolution increases and the temporal resolution decreases. A trade-off between frequency and temporal resolution is required to successfully localise the artefact (Akhtar et al., 2012). Since the EEG signal is modified due to the node removal of the WPT (equivalent to a band-stop filtering), rejecting a node of the 7^{th} level ensures that only a narrow-band of its frequency spectrum is filtered and most of the EEG information is retained. For our algorithm Dmey Wavelet of Discrete Meyer family was used as mother wavelet, as in (Wang et al., 2011) for EEG feature extraction.

4.2.2 WPTICA algorithm

The WPTICA algorithm consists of two steps: WPT processing, as described in the previous section, and ICA processing. Once the signal is WPT-reconstructed, Fast-ICA routine (Hyvärinen and Oja, 2000) is applied on the 19-channels EEG with the objective of separating the common component of the artefact traced in all the electrodes. Fast-ICA outputs the 19 independent components of the EEG; their temporal standard deviation σ_c is the criterion used to identify the component containing the artefact. The independent component with the highest σ_c contains the most influential part of the artefact, affecting some/all of the channels. Once identified, the artifactual independent

component is rejected (its coefficient are set to zero) and the "cleaned" 19 channels are reconstructed by applying $X = AS$ (Section 4.1.2).

4.2.3 WPTEMD algorithm

In the WPTEMD algorithm, EMD is applied at each electrode as a second step on the WPT-cleaned signal (Section 4.2.1). For each EEG channel, EMD decomposes the signal in IMFs which are then analysed to capture the irregular oscillations with inconsistently large amplitude (as all the artefacts investigated here). We formulate a criterion J to identify the artifactual IMF. For each IMF extracted from a single EEG channel we calculate the J parameter: the IMF with the highest J is identified as the most accountable for the artefact and rejected during the reconstruction of the cleaned EEG signal. This process is iteratively applied at all the 19 EEG channels.

The J parameter is formulated as a weighted sum of the entropy S and the standard deviation σ normalised with respect to their resting state values:

$$J = w\,(S/S_{resting}) + (1 - w)\,(\sigma/\sigma_{resting}) \tag{4.11}$$

where w is a weight index, S is the entropy and σ the standard deviation of each IMF and of the resting state. The resting state entropy and standard deviation $S_{resting}$ and $\sigma_{resting}$ are extracted from the resting-state EEG (while the subject has the eye-closed and is not performing any task or movement).

The combined use of standard deviation σ and entropy S enables us to take into account different types of artefacts characterised by both higher randomness, like muscle activity (Mammone and Morabito, 2008) and large spikes, like eye-blink or motion artefacts. The *information entropy* S (Gandhi et al., 2011) captures the large amount of randomness introduced by the artefact in the IMFs and is defined as:

$$S(\mathrm{IMF}_i) = \sum_{n=1}^{N} \mathrm{IMF}_i^2[n] \log(\mathrm{IMF}_i^2[n]) \tag{4.12}$$

where N is the number of samples of each IMF. The entropy has already been used to detect unusual activity patterns in EEG data on ICA components (Delorme et al., 2001), since it is a measure of randomness of a signal. The *temporal standard deviation* σ of the IMFs captures the effect of large inconsistent fluctuations due to the artefact compared to that of the EEG (low amplitude high frequency oscillations). The index w weights the normalised S and σ; its value was found to be equal to 0.5, as explained below.

We used eye-blink artefact for different subjects and trials to identify the optimal value of w: the J parameter was calculated on this EEG data by varying the value of w.

Since eye-blink mainly affects the frontal electrodes, our hypothesis is that the optimal J parameter (and its w) should be higher in the frontal electrodes (the most corrupted). Figure 4.3 shows an example of J values obtained by varying w in a single subject-single trial EEG. Highest values of J are found in IMF3 and IMF4, regardless of the value of w, and indicate the presence of the artefact. From this example, it is apparent that the IMF3 which is identified as artefact (with highest J), does not change if a different value of w or any other electrode is chosen. Since both the normalised S and σ identify the same IMF as containing the artefact, a $w = 0.5$ provides equal scaling of the two parts of J.

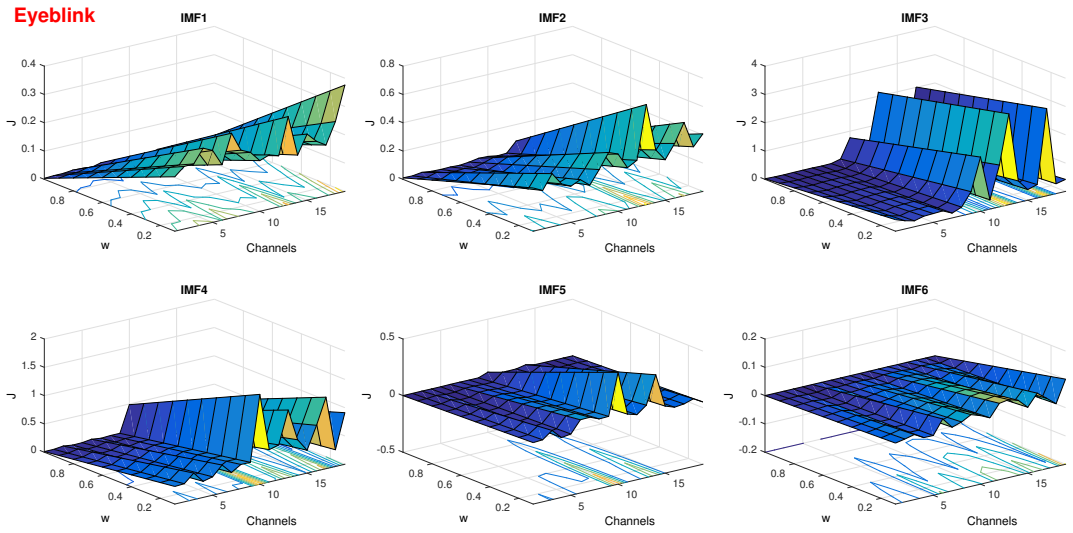

Figure 4.3: Surface plot of the values of the J parameter across channels and IMFs for a single trial eye-blink artefact for different values of w ranging between 0 and 1.

Figure 4.4 shows that J values (with $w = 0.5$) are higher in the frontal channels for the eye-blink artefact across all subjects and all trials, confirming our hypothesis. The performance of the proposed algorithms and the selected benchmarks are evaluated on two EEG datasets with various evaluation metrics, as described in the following section.

4.3 Data generation and performance evaluation metrics

In this section we describe the EEG data generated to analyse the algorithms' performances (Sections 4.3.1 and 4.3.2), the metrics used to evaluate them (Section 4.3.3) and the state-of-the-art algorithms selected as benchmarks (Section 4.3.4). The proposed artefact reduction algorithms are applied on two datasets, (1) a *semi-simulated* and (2) a *real* EEG dataset recorded on healthy subjects. The EEG data in the two datasets are

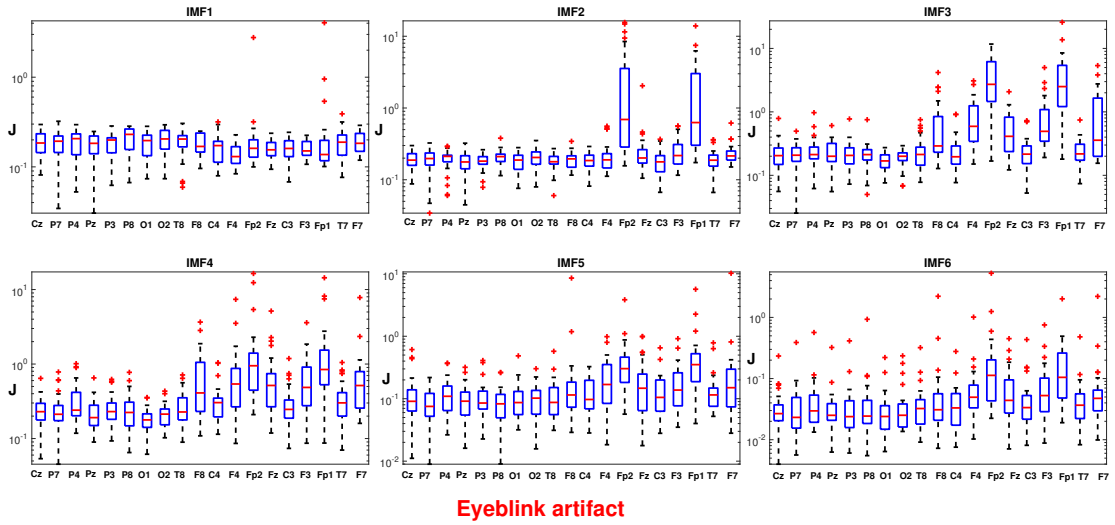

Figure 4.4: J parameter for each IMF and across all trials and subjects for the eye-blink artefact. Consistently with the scalp topography of the eye-blink, the median values of J are higher in the frontal electrodes.

recorded with 19-channel Enobio wireless EEG system[1] from 10 subjects, three females and seven males with mean age of 28.8 years (standard deviation of 3.05).

4.3.1 Semi-simulated EEG Data

Semi-simulated EEG data are generated by combining real artefact-free EEG data and simulated artefacts. The artefact free-EEG epochs are extracted from EEG recorded at-rest from different subjects and selected by careful visual inspection. Synthetic eye-blink artefacts are generated by Matlab functions developed in (Yeung et al., 2004) and multiplied by a typical eye-blink scalp topography (high gain on the frontal electrodes and near zero for the rest), as in (Delorme et al., 2001). The latter was obtained by extracting the ICA unmixing matrix from real 19-channel EEG data corrupted by eye-blink. We generated 32 trials of eye-blink artefact with a sampling rate of 500 Hz and a length of 6 sec. Different levels of artefact contamination were produced by adding the artefact component Artifact(t) to the EEG signals EEG(t) (Chen et al., 2014), as follows:

$$x(t) = \text{EEG(t)} + \lambda \times \text{Artifact(t)} \tag{4.13}$$

where λ represents the contribution of the artefact contamination and it varies between 1 and 15 to estimate the performance of the algorithms for different extent of contamination. Figure 4.5 shows an example of the original resting EEG data (EEG only), corrupted (Corrupted) with simulated eye-blink artefact ($\lambda = 10$) and reconstructed with all the algorithms under investigation.

[1] http://www.neuroelectrics.com/products/enobio/enobio-20/

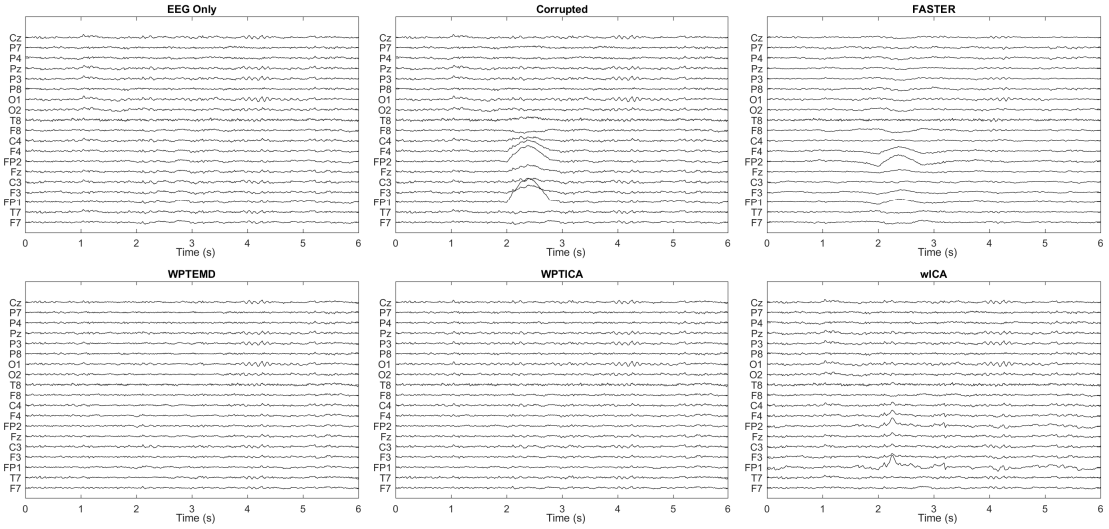

Figure 4.5: Example of semi-simulated EEG data for a single trial with artefact contamination level of $\lambda = 10$. The "EEG Only" is the EEG prior to artefact contamination, Corrupted is the EEG contaminated by the simulated artefact, the rest of the EEG data are obtained by processing the corrupted with the corresponding techniques.

However, since the insertion of simulated artefacts may not correspond to the real contamination of the EEG data and due to the unavailability of existing database containing body motion artefacts, we recorded real EEG data to evaluate the performances of the algorithms on body movement artefacts, as described in the following subsection.

4.3.2 Real EEG Data

Real EEG data was recorded while the subjects were performing body movements that might occur in naturalistic settings. The participants were seated approximately 80 cm from a computer monitor with backrest and armrest and were asked to perform specific movements with the purpose of creating eight different types of artefacts, listed in Table 4.2. Each type of movement was repeated over three trials for each subject. EEG at rest was recorded at the beginning and at the end of the recording session for two minutes. The labelling of the task and the artefacts affecting the EEG recordings was performed with the Enobio software during the recording session. The real EEG data was used to analyse the performances of the two proposed artefact reduction algorithms.

4.3.3 Performance Evaluation Metrics

Results from the proposed and the state-of-the-art algorithms are evaluated and compared by: (a) visual inspection of time domain morphology of the signal, (b) frequency spectrum, (c) spatial scalp topography, (d) Root Mean Squared Error ($RMSE$), (e)

Artefact to Signal Ratio (ASR) and (f) ΔASR, as suggested in (Urigüen and Garcia-Zapirain, 2015). The analysis is carried out at different frequency bands (Table 2.1). The *visual inspection in time domain* helps us to investigate the quality of the recovered brain signals after the artefact removal. The *power spectrum* and the *scalp topography* aid to inspect the distortions of the EEG power spectrum introduced by the artefact suppression algorithms in various EEG bands and at different electrodes (Castellanos and Makarov, 2006).

Artefact type	**Description**
Resting state	Performed in the first and the last minute of the experiment. It is defined when the subject's eyes are closed and no task is being performed (Michel and Murray, 2012)
Eye open	Keeping the eyes open until a specific task was verbally instructed
Eye-blinking	It is a natural blink without eyes and head movement
Head movement (yaw)	Head movement from left to right
Head movement (pitch)	Head movement from up to down
Head movement (roll)	Shanking the head
Hand movement (left-right only)	One hand at a time was moved along the border of a tablet screen
Chewing	It involves most of the facial muscles; it was performed for five seconds per each trial
Hello	The volunteers were asked to say the word "hello" to acquire artefact generated while speaking

Table 4.2: List of artefacts in the real EEG dataset and related body movement.

$RMSE$ quantifies the similarity between the signal z_1 without artefact (called *ground truth*), and the corrupted signal z_2, output from the artefact removal algorithms. $RMSE$ here is used to evaluate the algorithms' performance with semi-simulated data:

$$RMSE = \sqrt{\frac{1}{K}\sum_{k=1}^{K}[z_1(k) - z_2(k)]^2} \tag{4.14}$$

where z_1 is the ground-truth signal before adding the artefact, z_2 is the signal obtained after the artefact removal and K the number of samples.

ASR is a metric proposed in this work to evaluate the algorithms' performance when the ground truth is not available, as in case of real EEG. It is a new formulation of the SNR-like criterion (Bono et al., 2014) to better understand the cleaning performances in each EEG frequency band (i.e. δ, θ, α, β and γ) and for each electrode:

$$ASR = \frac{P_{\text{Artifact}}}{P_{\text{Resting}}} = \frac{P_{\text{Corrupted}} - P_{\text{Clean}}}{P_{\text{Resting}}} \tag{4.15}$$

where $P_{resting}$ is the power of the EEG at rest, $P_{Corrupted}$ the power of the original data with artefact and P_{Clean} the power of the output from the removal algorithms. The resting state and the corrupted EEG are recorded while the subject has the eyes closed (no artefacts) and while he performs a specific type of motion task, respectively. Higher values of ASR indicate better performances: the $P_{Resting}$ and $P_{Corrupted}$ are constant, lower values of P_{Clean} increase the numerator, which results in an increased ASR. Low values of ASR indicate that the power of the clean signal is comparable to the power of the corrupted one, suggesting that the algorithm did not modify the power spectrum of the corrupted signal in that particular frequency band.

ΔASR is a variant of ASR (Equation 4.15) proposed here to evaluate the algorithms' performance with semi-simulated data, since the ground truth of the data is available:

$$\begin{aligned} \Delta ASR &= ASR - ASR_{GT} \\ ASR_{GT} &= \frac{P_{\text{Artifact}}}{P_{\text{EEG}}} \end{aligned} \tag{4.16}$$

where $P_{Artifact}$ and P_{EEG} indicate the power of artefact and EEG respectively. Since ASR_{GT} indicates the ground truth of the artefact to signal power ratio, ΔASR closer to zero indicates the method with the least distortion of the power spectrum of the reconstructed EEG signal.

The evaluation metrics introduced in this section are used for the comparison of the proposed algorithms with the benchmarks described in the next section.

4.3.4 Benchmarks

We consider two benchmarks algorithms (a) wICA (Castellanos and Makarov, 2006) and (b) FASTER (Nolan et al., 2010) to compare the performance of the proposed methods with state-of-the-art algorithms. The *wICA* combines the use of the DWT and ICA to suppress the EEG data contaminated by the artefacts. Each independent component is decomposed by the DWT to identify the wavelet coefficients containing the artefact: those coefficients are identified by a fixed threshold and set to zero. The independent components are then reconstructed to obtain artefact-free EEG data. *FASTER* is an automated artefact removal method based on thresholding criteria to detect and suppress artefacts corrupting EEG data. It is based on different steps, each of which estimates and thresholds various statistical parameters, like variance, mean correlation, Hurst exponent, amplitude range, channel deviation, spatial kurtosis, and median deviation with the aim of: (1) identify the contaminated channels to reject and substitute them with the interpolation of neighbour electrodes; (2) identify and remove the contaminated epochs; (3) detect and subtract the contaminated independent components extracted by ICA and the bad channels within the epochs; (5) remove subject's data heavily contaminated by artefacts. These two benchmarks are applied on semi-simulated data

and compared with the two proposed artefact removal algorithms; results are given in the next section.

4.4 Results and Discussion

Having described our algorithms and the experimental setup, we present our results. In details, we discuss the pre-processing steps applied on the EEG data before the artefact suppression (Section 4.4.1), then compare the performance of the proposed algorithms with the benchmarks in terms of $RMSE$ and ΔASR with the semi-simulated data (Section 4.4.2) and explore the performances of the algorithms under consideration with the real EEG data in terms of ASR, scalp topography and through a qualitative analysis in time domain morphology and frequency spectrum (Section 4.4.3).

4.4.1 Data Preprocessing

The EEG data were pre-processed before the application of the artefact reduction algorithms. A fourth order Butterworth high pass filter was applied with cut-off frequencies of 0.5 Hz and a 15^{th} order low pass filter with cut-off frequency of 45 Hz. Butterworth filters are characterised by a flat magnitude response in the pass band. A 15^{th} order Chebyshev type II Notch filter with a stop band frequency of 50 Hz was applied to the data to ensure the elimination of the power line effect. It is monotonic and free of ripple in pass band, and it provides steeper roll-off characteristics than Butterworth filters.

4.4.2 Performance Evaluation with Semi-Simulated EEG data

Here we present the results obtained with semi-simulated data (Section 4.3.1) to quantitatively analyse the performance of the WPTEMD and WPTICA, in comparison with the benchmarks FASTER[2] (Nolan et al., 2010) and wICA[3] (Castellanos and Makarov, 2006). Figure 4.5 shows the results obtained with the four algorithms in case of semi-simulated artefact ($\lambda = 10$): the frontal electrodes are highly corrupted and the artefact is still present in the EEG reconstructed by wICA and FASTER, while WPTEMD and WPTICA suppress the contamination.

Figure 4.6 compares the performances of the four algorithms in terms of $RMSE$ for the eye-blink artefact for different level of artefact contamination (λ in Equation 4.3.1) in: two of the most affected channels (i.e. Fp1 and Fp2) and in one of the channels (O2) less contaminated by the artefact across the 32 trials. The $RMSE$ in Fp1 and Fp2

[2]The implementation of FASTER algorithm was freely available at http://www.mee.tcd.ie/neuraleng/Research/Faster

[3]The implementation of wICA algorithm was freely available at http://www.mat.ucm.es/~vmakarov/downloads.php

is lower for WPTEMD and WPTICA than wICA for $\lambda > 6$ and becomes higher as λ increases from 6 to 15. Figure 4.6 also shows that for the channel Fp1 the performances of FASTER, WPTEMD and WPTICA are all equivalent over the entire range of λ. In case of channel O2, where the artefact contamination is very low (see the time-domain signal morphology in Figure 4.5), although the $RMSE$ in WPTEMD and WPTICA is lower than FASTER, wICA outperforms all the techniques.

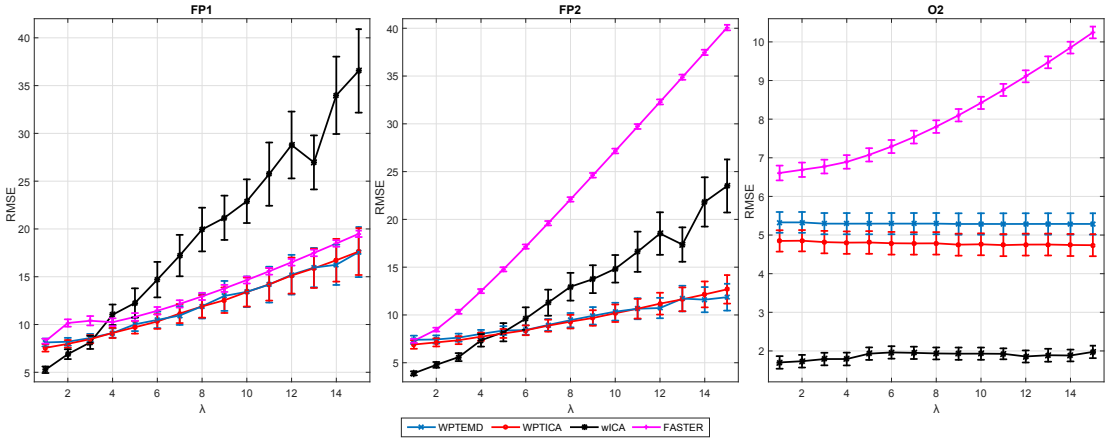

Figure 4.6: $RMSE$ for the semi-simulated EEG data in channels Fp1, Fp2 and O2 across all 32 trials for different strengths (λ) of the artefact. The error bars represent one standard error of the mean ($\mu \pm \sigma$) of $RMSE$.

We performed a two-tailed tailed paired t-test to compare the performance of the algorithms and analyse their statistical significance. Since we target the suppression of highly corrupted data, Table 4.3 shows the difference of $RMSE$ (%) for high level of artefact contamination (λ) in Fp1 and Fp2. Results show that WPTEMD and WPTICA outperform the other techniques in terms of $RMSE$ significantly. The $\Delta RMSE$ values are similar for both WPTEMD and WPTICA, indicating that the performance improvement for these techniques are comparable.

Algorithm	**WPTEMD**		**WPTICA**	
	$\Delta RMSE$ (%)	p	$\Delta RMSE$ (%)	p
wICA-Fp1 ($\lambda = 10$)	41.40%	0.0012	41.50%	9.5620e-04
wICA-Fp1 ($\lambda = 15$)	51.88%	4.2731e-04	51.75%	3.5932e-04
wICA-Fp2 ($\lambda = 15$)	49.53%	3.9978e-04	46.03%	0.0011
FASTER-Fp2 ($\lambda = 15$)	70.40%	$2.18E^{-28}$	68.35%	$2.40E^{-26}$

Table 4.3: $RMSE$ (%) improvements for the proposed artefacts and the correspondent p values.

Figure 4.7 shows the ΔASR (Equation 4.16) in each frequency band for WPTEMD,

WPTICA, FASTER and wICA reconstructed signals. As described in Section 4.3.3, ΔASR closer to zero indicates better performances of the algorithm under investigation. Figure 4.7 shows that ΔASR for WPTEMD remains close to zero and +ve in all the bands and for any value of λ, whereas for the other algorithms ΔASR decreases as the λ increases, in some cases becoming –ve indicating a change in the power spectrum of the reconstructed signal.

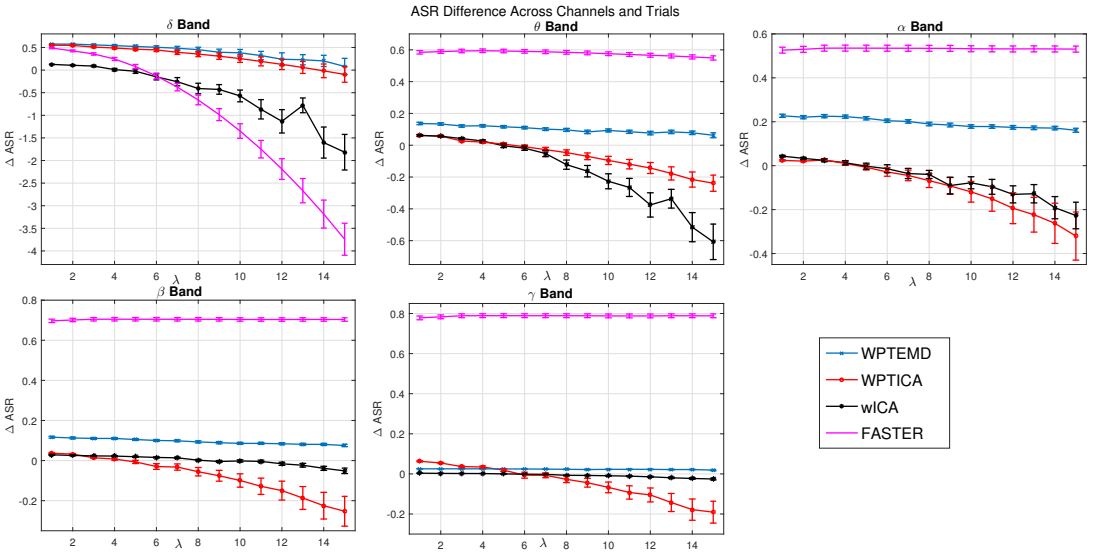

Figure 4.7: ΔASR in each frequency band of the semi-simulated artefact, across different trials and channels for different strengths (λ) of the artefact. The error bars represent one standard error of the mean ($\mu \pm \sigma$) of ΔASR

In δ band, which is the most contaminated band by the artefact, for high λ ($\lambda > 5$) both WPTEMD and WPTICA can be considered the best methods, since the ΔASR is closer to zero (ΔASR is equal to 0.01 for WPTEMD, -0.1 for WPTICA, -1.82 for wICA and -3.74 for FASTER). In case of θ band for high λ ($\lambda > 9$), WPTEMD outperforms all the other methods. In the α band, wICA and WPTICA perform similarly and show ΔASR values closest to zero, although the negative value of ΔASR indicates that these two methods modify the power spectrum of the original signal in this band. In case of β band, wICA performs better than the rest of the methods; while in γ band both wICA and WPTEMD show similar performances. It is worth noting that WPTEMD is designed for heavily contaminated EEG data, in which cases (frontal channels and high λ) has shown the best performances in terms of ASR for semi-simulated eye-blink.

Figure 4.8 shows the performance of the four algorithms on the semi-simulated EEG for a single trial in time domain and in the different frequency bands. Since the eye-blink affects mostly the frontal electrodes, the EEG data in channel Fp1 is shown as an example for $\lambda = 15$. The time domain graph shows that all techniques reduce the large oscillation caused by the artefact, but the visual appearance of the WPTEMD-reconstructed signal is closer to the original artefact-free EEG. In addition, the power spectra in different bands show that, especially above 6 Hz, WPTEMD and wICA give

the closest spectrum to the original one, while WPTICA and FASTER overestimate and underestimate the spectra of the reconstructed signal respectively.

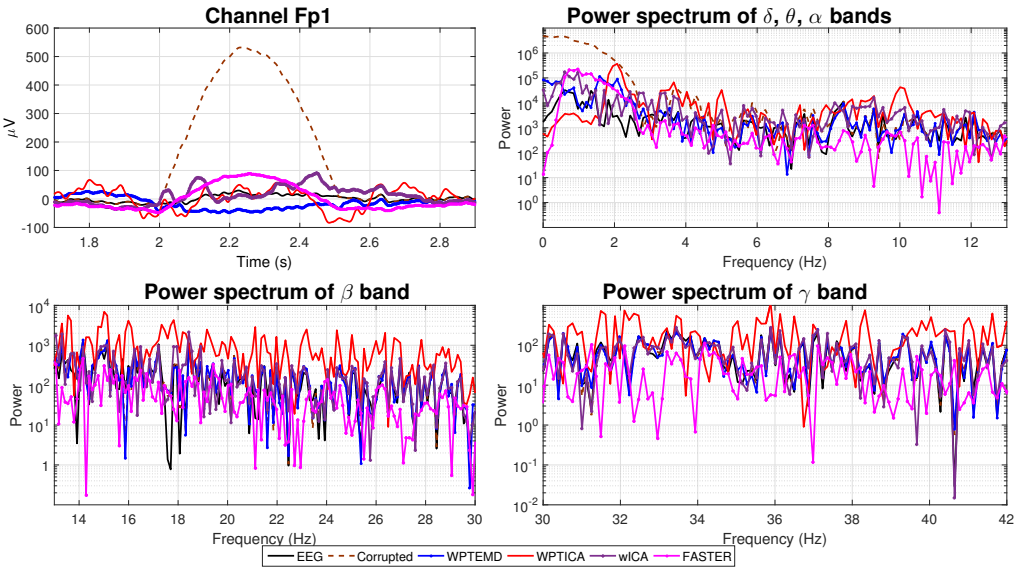

Figure 4.8: Semi-simulated eye-blink artefact in the channel Fp1 in time domain, and in frequency domain in each EEG frequency band (δ, θ, α, β and γ).

Overall, the exploration with the semi-simulated data shows that WPTEMD outperforms the rest of the methods in case of heavily contaminated data (frontal channels and high λ in the lower frequency bands where eye-blink is contaminating the EEG).

4.4.3 Performance Evaluation with Real EEG data

The previous subsection shows the analysis of semi-simulated EEG, here we explore eight types of real artefact examples commonly encountered in pervasive EEG system during natural body movement. Some of the artefacts, like eye-blink or talking, affect only a few of the channels but the stronger artefacts like the yaw, pitch and roll head movement corrupt most of the electrodes at the same time. Due to the unavailability of the ground truth signal (unlike the semi-simulated case), here we analyse the performances of WPTEMD and WPTICA in terms of *ASR* (Section 4.4.3.1), scalp topography (Section 4.4.3.2) and the time and frequency domain (Section 4.4.3.3).

4.4.3.1 Artifact to Signal Ratio (ASR) Analysis

From the exploration with the semi-simulated data it is clear that the *ASR* criterion could be considered as an effective quantitative metric for evaluating the performance of the algorithms for cleaning artefacts. The *ASR* was calculated for real data across multiple subjects and trials and for each type of artefact in each band to investigate:

(a) which channels and (b) bands are mostly modified by each of the algorithms and (c) also to quantify the variability of the artefact suppression performance across multiple trials and subjects. The electrodes with high ASR are the ones which are modified by the algorithms to a higher extent.

Figure 4.9 shows the performance of WPTEMD and WPTICA in terms of ASR and the corresponding power for each electrode. The ASR in α, β and γ bands are in a lower range compared to the δ and θ bands, suggesting that the high frequency bands were not severely modified by the algorithms. In most of the electrodes (apart from the frontals), the median of the ASR is close to zero; indicating that the algorithms did not affect these channels so that the power of the "clean" signal is nearly equal to the corrupted EEG. The power in δ, θ and α bands is higher in the channels Fp1 and Fp2 and the corresponding ASR values for both algorithms are higher than the rest of the electrodes. This indicates that the algorithms modified mainly these two electrodes: in δ and θ bands the performances are similar, whereas in α band the negative ASR indicates that the WPTICA increased the power of the reconstructed signal. In the higher frequency bands (β and γ), although the power is similar in all electrodes of the corrupted EEG, WPTICA increases the power spectrum of the frontal channels ($ASR < 0$).

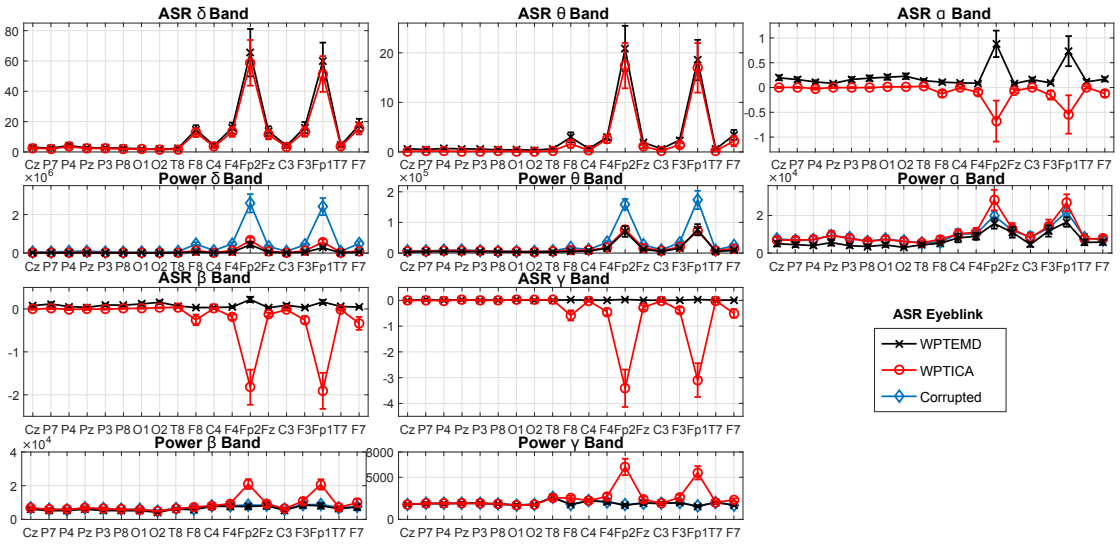

Figure 4.9: ASR and power of real eye-blink EEG data across all subjects and trials for each EEG band (δ, θ, α, β and γ). The error bars represent one standard error of the mean ($\mu \pm \sigma$) of ASR

4.4.3.2 Scalp Topography Analysis

An alternative way to investigate the algorithms' performance is to show how the scalp topography of the EEG varies when the signal is affected by a specific type of artefact and when each of the proposed algorithms is applied. The scalp topography shows the mean power across all subjects for each EEG signal (Resting, Corrupted, WPT, WPTEMD

and WPTICA), for all the frequency ranges and for each band separately (Table 2.1). The power shown at each scalp is normalised within each band and across the different signals (Resting, Corrupted, WPT, WPTEMD and WPTICA). The distribution of the power over the scalp was shown for each band to highlight how the algorithms affect each frequency band. The power at each electrode was estimated through the Fourier Transform magnitude squared and normalised between zero and one for five different cases: Resting, Corrupted, WPT, WPTEMD and WPTICA. The resting EEG is shown here because its entropy and standard deviation are used to calculate the J parameter in the WPTEMD algorithm. However, the resting EEG appears different in each artefact case because of the normalisation across the different signals (Resting, Corrupted, WPT, WPTEMD and WPTICA) for all the frequency range (*All bands*, i.e. from δ to γ) and for each band separately (δ, θ, α, β and γ).

Figure 4.10(a) shows the topographical maps during the eye-blink artefact. From the scalp topography across *All bands* of the corrupted signal it is evident that only the frontal region shows high power. The same pattern is visible in all the frequency bands except β and γ, suggesting that the artefact affects the EEG power in the frequency range up to 13 Hz. The WPT is capable of reducing most of the power in the frontal electrodes only in the δ band, while the WPTEMD technique reduces the power in all the affected frequency bands (δ, θ and α). WPTICA, instead, reduces the power of the frontal electrodes in δ and θ bands, but it increases the power in the rest of the bands.

Figure 4.10(b) shows the topographical maps related to the yaw movement of the head. The corrupted signal is characterised by high power in the left temporal and occipital electrodes, as visible in *All bands* and the same pattern is present in the δ band. This suggests that δ is the most corrupted band and this contamination is fully removed by all the algorithms. The rest of the bands are characterised by a common pattern of high power across the head. Both WPTEMD and WPTICA decrease this power across all the bands (from θ to γ).

The head (pitch) movement causes high power in the occipital electrodes, as visible in *All bands* in Figure 4.10(c). The occipital region shows high power in all the frequency bands (from δ to γ), suggesting that this artefact affects all of them. The WPTEMD algorithm is the most capable of reducing the high power in all the bands, except the β and γ bands which show the same pattern in the signal even after the application of all algorithms. It is worth noting that in case of WPT the overall power (*All bands*) in the occipital channels is reduced due to the reduction of the power in δ band only.

Head (roll) movement affects the temporal lobes, as shown in *All bands* in Figure 4.10(d). A similar topography pattern is visible in the δ band, while the other bands show high power also in the frontal region. All the algorithms are capable of removing the artefact in the δ band, due to the action of the WPT technique. WPTEMD reduces also the power in the θ and α bands, whereas WPTICA increases the power in α and β bands.

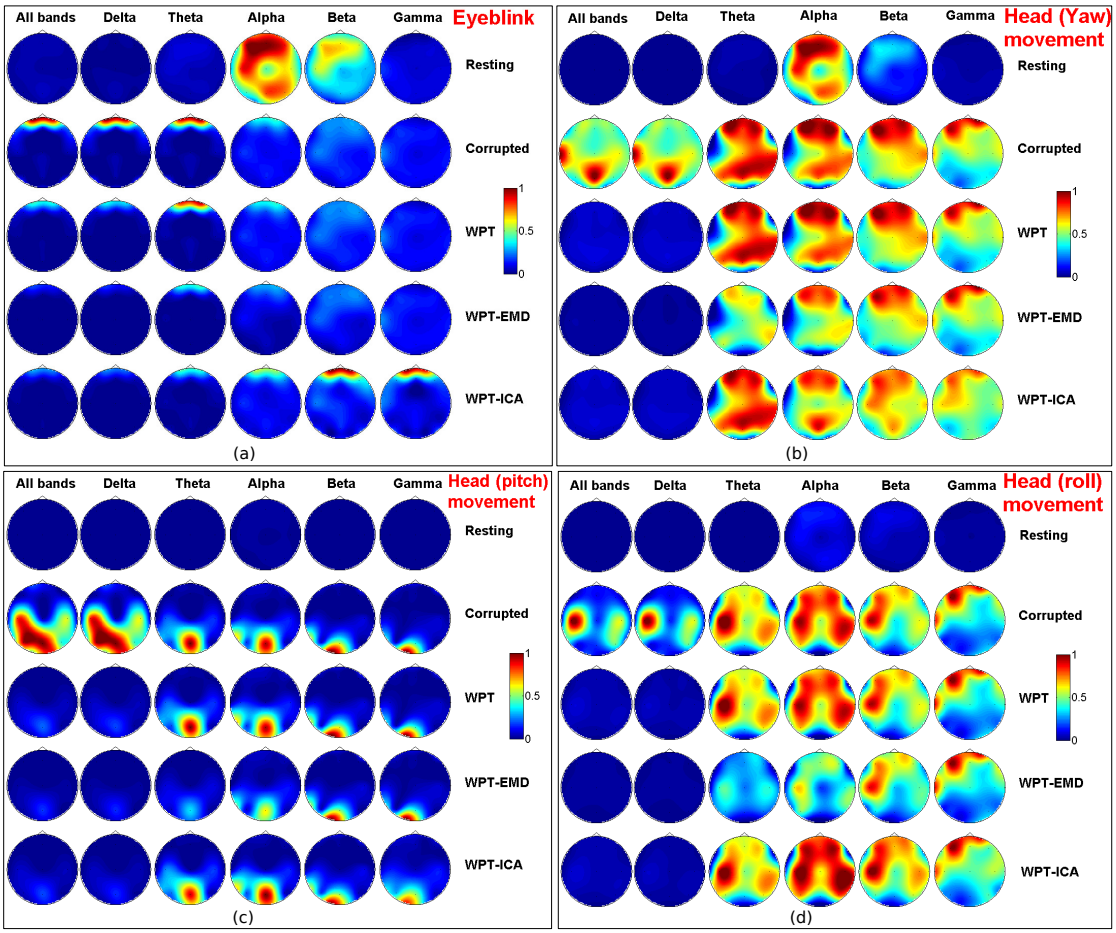

Figure 4.10: Scalp topography of EEG data contaminated by: eye-blink (a), head movement in yaw (b), pitch (c) and roll (d), across different subjects and trials. The power at each scalp is normalised within each band and across the different signals (i.e. Resting, Corrupted, WPT, WPTEMD and WPTICA). The high power in the scalp in All bands is present in δ band, suggesting that it is the most affected band by the artefact.

Figure 4.11(a) shows that the highest power is located in the frontal, left temporal and occipital regions for the left hand movement artefact. The high power in *All bands* is also visible in the δ and θ bands, suggesting that the artefact might affect the power in the frequency range up to 8 Hz, which is mostly suppressed by the WPTEMD. Unlike WPTEMD, the scalp topography in WPT and WPTICA still contains high power in the frontal region in the θ band.

The scalp topography in *All bands* from data recorded while the subject was performing right hand movement shows high power in the frontal region, as can be seen in Figure 4.11(b). A similar pattern is also visible in the δ, θ and β bands. WPT decreases the power in *All bands* and in δ band. Additionally, WPTEMD decreases the power of the frontal electrodes in the θ and β bands. WPTICA decreases the power of θ band but does not modify β and γ bands.

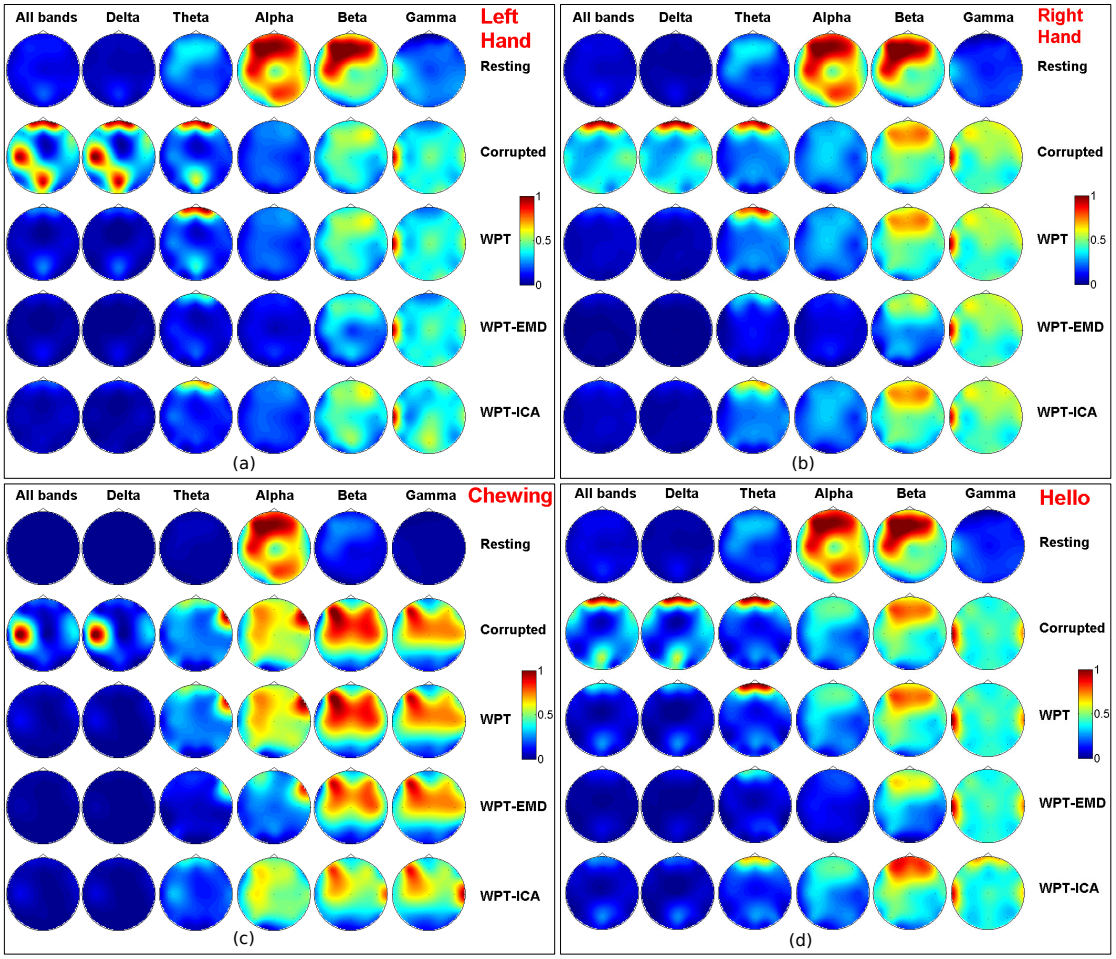

Figure 4.11: Scalp topography of EEG data contaminated by: hand movements (a, b), chewing (c) and talking (d), across different subjects and trials. The power at each scalp is normalised within each band and across the five different signals. The high power in the scalp in All bands is present in δ band, suggesting that it is the most contaminated band.

Figure 4.11(c) shows that the left temporal lobe has the highest power in case of chewing, as visible in *All bands*. The same pattern is detectable in the δ band and it is reduced by all the techniques. The high power of the rest of the bands is reduced in a higher extent by the WPTEMD compared to the other techniques. WPTICA decreases the power in all the bands but it also increases the power of the right temporal lobe in γ band.

Talking affects the frontal and occipital regions, as shown in *All bands* in Figure 4.11(d). These high power patterns are also present in the δ band, in a greater extent, and in all the other bands except the γ band. The highest power suppression is achieved by the WPTEMD in all the bands except the γ, while WPTICA increases the power in the frontal electrodes in β and γ bands.

4.4.3.3 Time and Frequency Domain Analysis

In this section we explore the time and frequency domain characteristics of the single subject-single trial EEG, before and after the application of the artefact suppression algorithms. In order to highlight the specific modifications of the frequency spectrum in the different EEG bands, we show the analysis on lower (δ, θ and α) and higher (β and γ) bands separately. The power spectrum was estimated through Fourier transform magnitude squared and the average power in each band was calculated by integrating the Power Spectral Density curve over the frequency band of interest.

Figure 4.12 shows an example of the eye-blink artefact in time and frequency domain. The spikes related to the artefacts are reduced by the WPTEMD, but not by WPT and WPTICA. In the low frequency bands (δ, θ and α), the power spectrum is modified mostly below 6 Hz, since WPT acts as a band stop filter between 3 and 6 Hz. WPTEMD preserves the power spectrum in the rest of the frequency bands, while WPTICA distorts the power spectrum almost in all the bands and increases the power in β and γ bands.

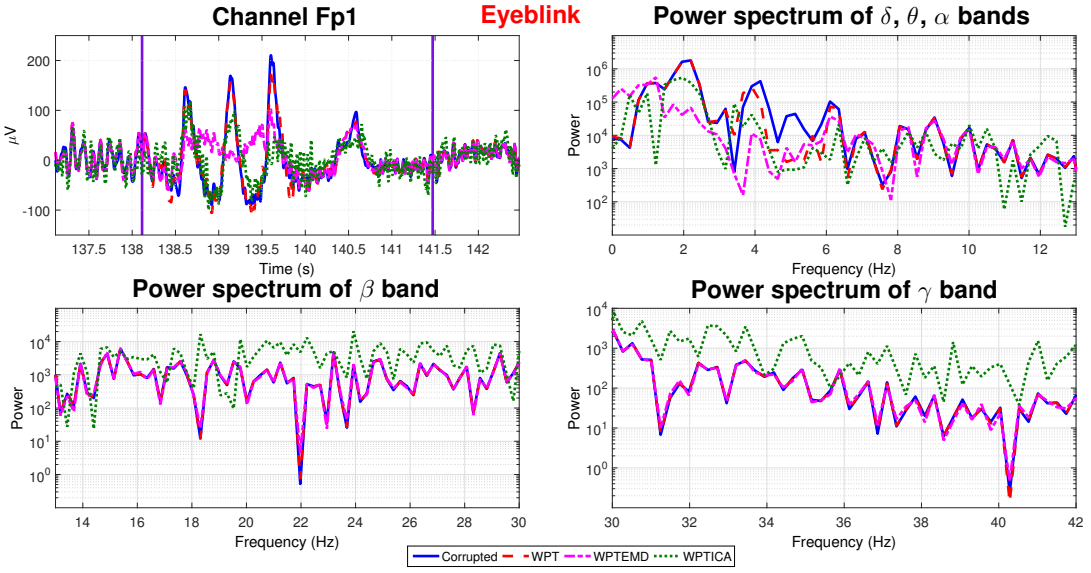

Figure 4.12: EEG data in time and frequency domain in case of eye-blink artefact in channel Fp1. WPTEMD is the most capable of reducing the high amplitude spikes and preserves the power spectrum of the EEG in the higher frequency bands.

Unlike the eye-blink, the head (yaw) movement generates artefacts that affect almost all the channels. Figure 4.13 shows an example of head movement artefact in the frontal electrode Fp2. In time domain, WPT and WPTICA signals overlap, while WPTEMD reduces the spikes in the time intervals $131.5 - 132$s and $134.5 - 135.5$s. Below 2 Hz the power spectrum of the corrupted signal is modified by the WPT, but it is preserved in the rest of the bands. WPTEMD modified the power spectrum up to 10 Hz. The rest of the bands appear not to have been affected by any of the techniques.

Similar results in time and frequency domains were found in the EEG acquired during the head (pitch) movement, as shown in Figure 4.14. In time domain, the spikes are suppressed by all the applied techniques. All the algorithms affect only the power spectrum in the low frequency bands. WPT removes the low frequency components (below 2 Hz) and it is overlapped with the spectrum related to WPTICA, while WPTEMD modified the spectrum up to 6 Hz.

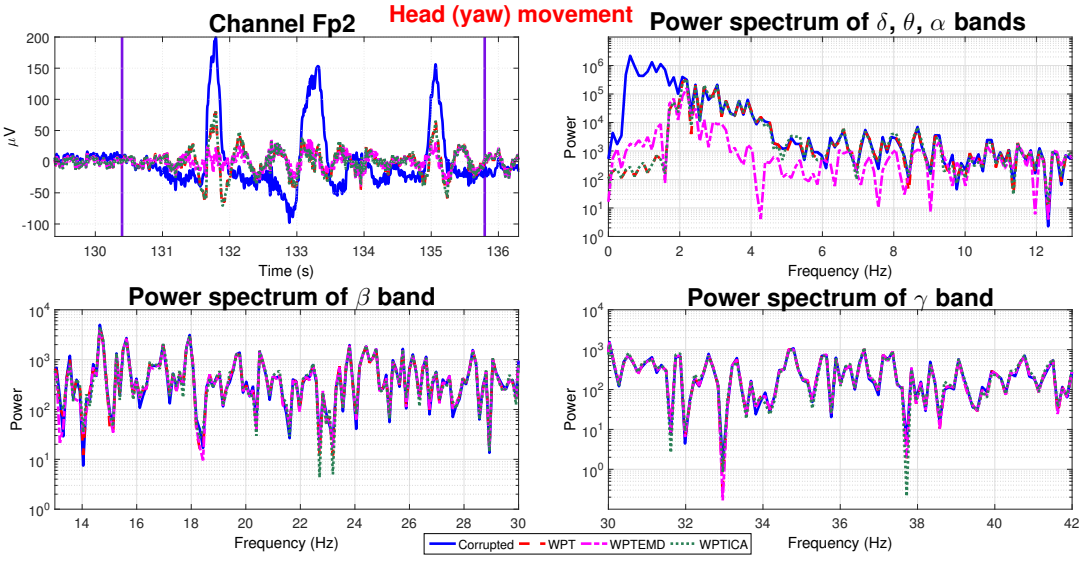

Figure 4.13: EEG data in time and frequency domain for head (yaw) movement in channel Fp2. WPTEMD is the most capable of reducing the high amplitude spikes and reduces the power spectrum of the EEG in the lower frequency bands.

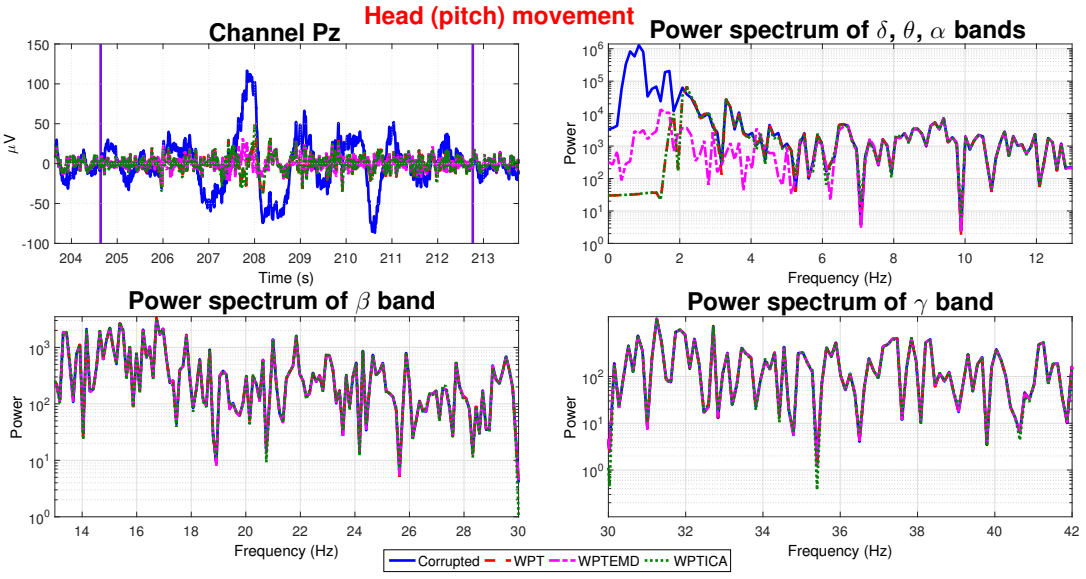

Figure 4.14: EEG in time and frequency domain affected by head (pitch) movement in channel Pz. The high amplitude spikes are reduced in a higher extent by the WPTEMD which modifies the EEG power spectrum up to 7 Hz.

When considering shaking the head sidewise (roll), the amplitude of the EEG is found to be much higher compared to the artefacts previously described (10 times bigger than the clean EEG) as shown in Figure 4.15. The spikes are reduced by all the techniques, but WPTEMD showed the best results, although some slow and big oscillations are still visible. The δ, θ and α bands contain the highest power spectrum, modified below 2 Hz by the WPT and WPTICA and up to 10 Hz by the WPTEMD.

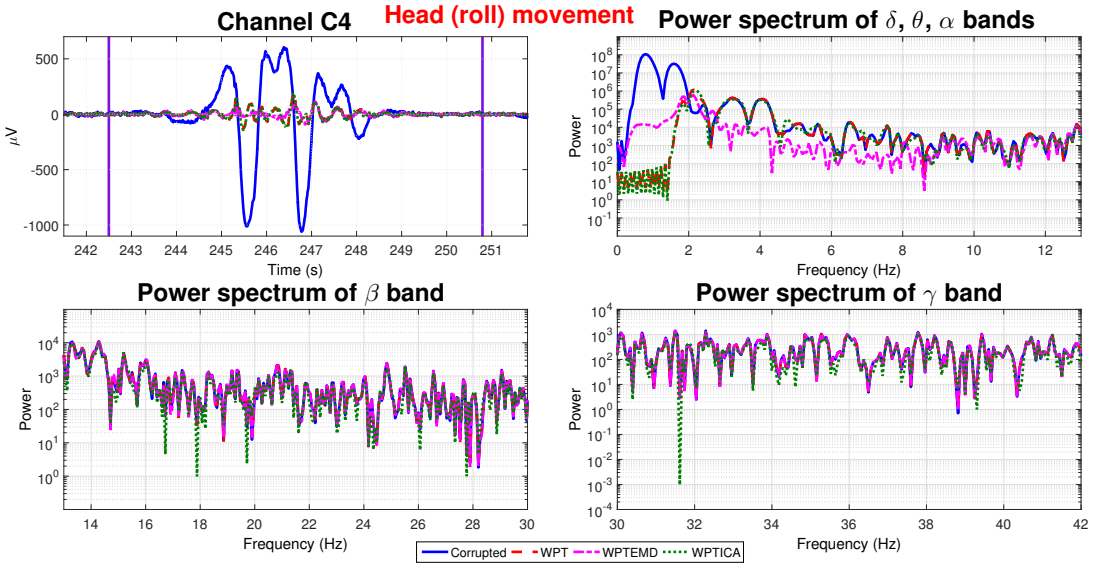

Figure 4.15: EEG data in time and frequency domain for shaking head (roll) movement in channel C4. The high amplitude spikes are reduced in a higher extent by the WPTEMD which modifies the EEG power spectrum up to 9 Hz.

An example of the left hand-movement is shown in Figure 4.16: the high amplitude oscillations in the time interval $322-324$ s are significantly reduced and the best performance is given by WPTEMD. Only the low frequency spectrum is modified: WPT and WPTICA altered the spectrum below 2 Hz, while WPTEMD modified the frequency components of the signal up to 16 Hz.

Figure 4.17 shows that WPTEMD is better capable of reducing the large oscillations caused by the right hand movement. In frequency domain, the spectrum of the corrupted signal is modified only up to 10 Hz in case of WPTEMD and below 3 Hz for the other algorithms.

The frontal and temporal electrodes are affected by the artefacts caused by the muscles activity during chewing. The high amplitude oscillations are better reduced by the WPTEMD as shown in Figure 4.18. The power spectrum is slightly modified by the WPT and WPTICA below 2 Hz, while is reduced up to 6 Hz in the case of WPTEMD.

The last type of artefact investigated here was caused while the subject was asked to pronounce the word "hello" to evaluate the effect of speaking on the acquired EEG. The

frontal electrodes are likely to capture the effect of facial muscle activity. Figure 4.19 shows that the high amplitude oscillations in the signal are better reduced by WPTEMD. WPT acts as a high-pass filter with a cutoff frequency around 2 Hz. The spectrum is modified in all the frequency bands by WPTICA. WPT and WPTEMD techniques alter only the spectrum in the δ, θ and α bands.

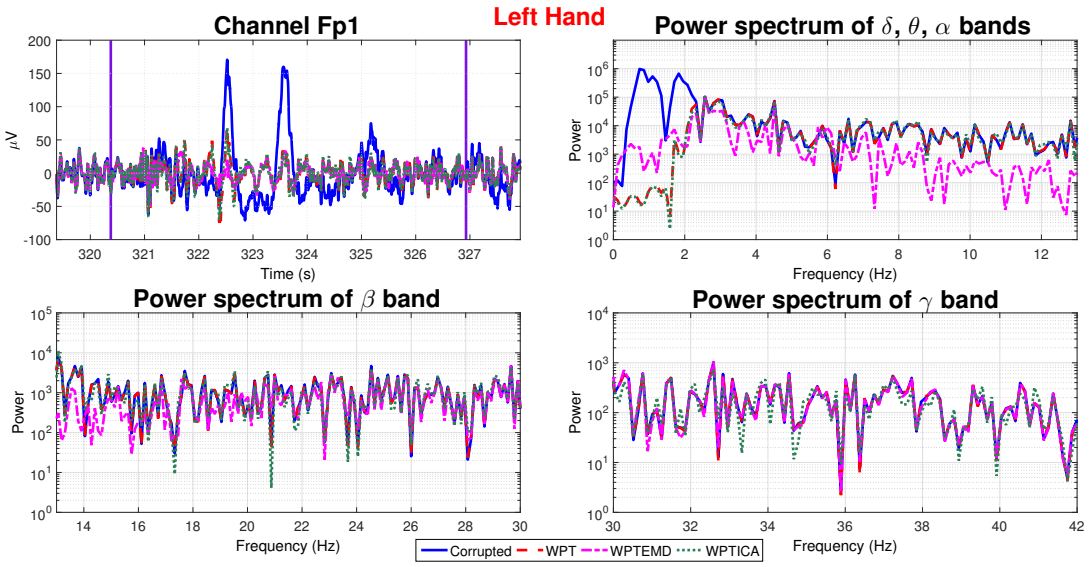

Figure 4.16: EEG (channel Fp1) in time and frequency domain for left hand movement. The high amplitude spikes are reduced in a higher extent by the WPTEMD which modifies the EEG power spectrum up to 17 Hz.

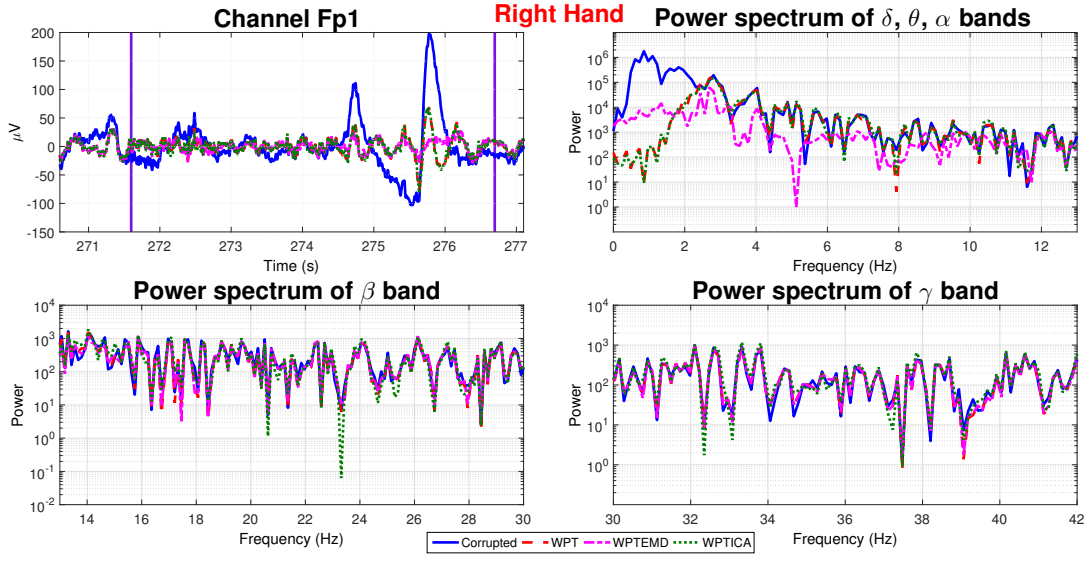

Figure 4.17: EEG (channel Fp1) in time and frequency domain for right hand movement. The high amplitude spikes are reduced in a higher extent by the WPTEMD, as visible around second 276.

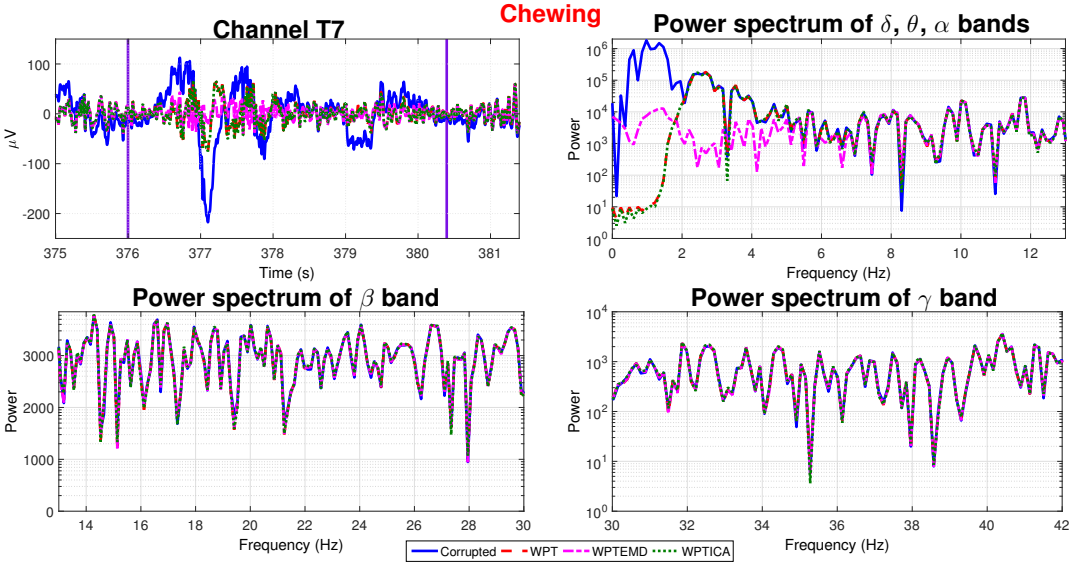

Figure 4.18: EEG (channel T7) in time and frequency domain contaminated by chewing. The high amplitude spikes are reduced in a higher extent by the WPTEMD, as visible around second 377.

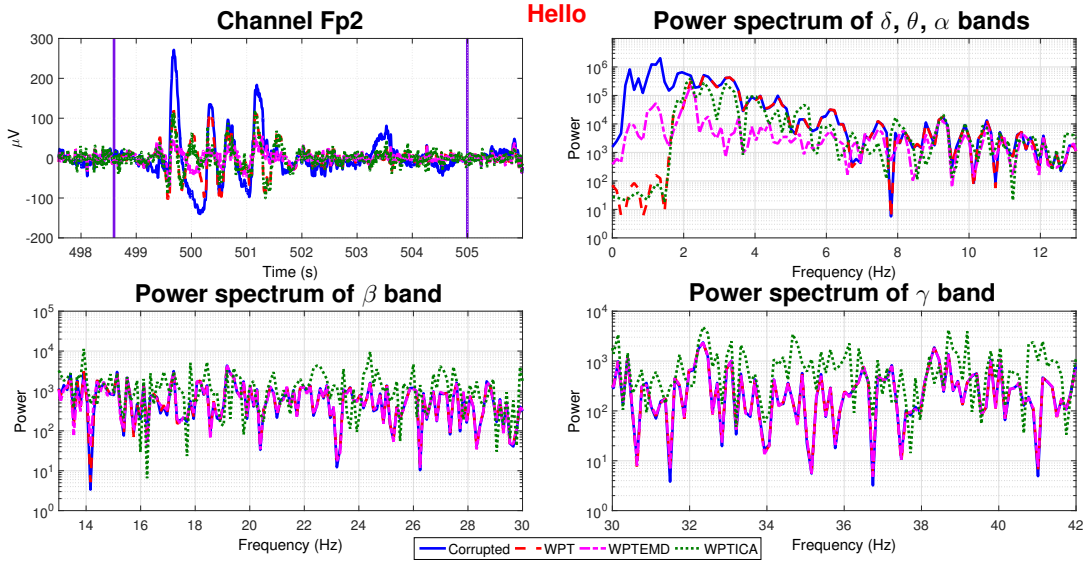

Figure 4.19: EEG (channel Fp2) in time and frequency domain contaminated by talking. The high amplitude spikes are reduced in a higher extent by the WPTEMD, which preserves the EEG power spectrum in the higher frequency bands.

From the above exploration it is evident that the two proposed hybrid algorithms outperform the benchmark algorithms and the basic constituents – WPT, ICA and EMD – for both the semi-simulated and real pervasive EEG. We have validated our results on multiple subjects and multiple trials of each of the eight types of artefacts. Results show that WPTEMD performs better than WPTICA in case of heavily corrupted data when dealing with low number of electrodes (i.e. 19 channels) and motion artefacts. Unlike

WPTICA, WPTEMD requires the availability of the EEG recording with no artefact to calculate the J parameter. However, we do not consider this requirement as a limitation of the method since it is a common practice to include resting EEG with closed and open eyes during a recording session (Hoedlmoser et al., 2011).

4.5 Summary

In this chapter, we propose two hybrid algorithms–WPTEMD and WPTICA–for suppressing motion related artefacts when *a-priori* knowledge about the characteristics of the artefacts is not available; more specifically, in the case of pervasive EEG recording. We tested the two methods with semi-simulated data and compared their performances with state-of-the-art artefact separation algorithms (wICA and FASTER). The performances were analysed by comparing the reconstructed signals after processing the artefacts with the available artefact-free ground truth signal. Later, we tested the algorithms with experimentally acquired data corrupted with eight types of motion artefacts across multiple subjects and trials using a 19-channel wireless EEG system. Results with semi-simulated data showed that WPTEMD algorithm outperforms all the other techniques under investigation, in terms of *RMSE* for highly corrupted channels and maintains the power spectrum of different frequency bands close to the original ground truth signals. When analysed with real EEG data, the algorithms' performance were similar: for highly corrupted channels WPTEMD consistently showed better performance than WPTICA in all the frequency bands and reduced the high-amplitude oscillations in the time-domain signal. This result holds true for all the eight different types of artefacts we explored. Therefore, our exploration indicates that for a naturalistic EEG recording scenario WPTEMD could be the best choice for suppressing unwanted motion artefacts during natural movement of the subject.

Chapter 5

Brain Connectivity analyses on Game-based EEG data in ASD

As discussed earlier in Chapter 1 and 2, interventions in ASD merge the behavioural and developmental treatments, are early intensive (at least 25 hours/week), delivered in naturalistic settings, parent-mediated and personalised (tailored according to the child's skill outlined during his/her characterisation). Monitoring the intervention is crucial to understand the outcome of the treatment. In Chapter 3, we proposed a novel multi-player gaming platform (GOLIAH) for the delivery of early intervention in young ASD children. The GOLIAH game fulfils the intervention's criteria described above and allows to monitor the treatment with the behavioural measures that it generates. However, treatments in ASD and their monitoring should span across multiple disciplines (Lai et al., 2014) to better understand and interpret their outcomes. Their monitoring becomes more difficult in naturalistic settings (outside the hospital) and when implemented by the parents. In this Chapter, we focus on how to augment the objective measures used to monitor the intervention, specifically to include both behavioural and neuro-developmental areas.

We here propose a novel framework to monitor the intervention implemented with GOLIAH game based on two categories of objective measures: (a) *behavioural* from GOLIAH game, and (b) *neuro-developmental* from EEG recordings. The two groups of measures are obtained by using the GOLIAH platform in conjunction with a wireless EEG system. EEG data is recorded during the GOLIAH game sessions. This will allow to monitor both behavioural and neuro-developmental outcomes of the intervention delivered in naturalistic settings (at home and hospital) with both therapists and parents. On one side, GOLIAH behavioural data is extracted to monitor the child's behavioural improvements, as described in Chapter 3. On the other side, EEG recordings are processed to explore how the functional brain connectivity is affected during the GOLIAH-based intervention.

The main goal of the framework is to provide and explore various physiological measurements that capture the information processing in the brain occurring during a behavioural response to a specific task of the GOLIAH game. The brain response and its changes during the intervention are measured by Functional Connectivity (FC) and its complex networks. First, FC measures the synchronisation between the EEG recordings at each pair of electrodes. Then, complex network analysis allows to build brain networks from the FC and extract neurologically meaningful graph indexes. These graph metrics describe the synchronisation at a scalp network level, taking into account the FC values from all the electrode pairs. They are informative of the integration and segregation phenomena occurring when performing a cognitive task. This approach gives insights into how the brain works as a network where segregated regions process different types of information and integrate the results of the processing. Table 5.1 details the different FC and graph theoretic measures applied in this framework. The FC can be formulated by various methods; each technique presents its own advantages and disadvantages and relies on different assumptions. In this chapter, two categories of non linear FC are extracted: Phase Synchronisation (PS) and Generalised Synchronisation (GS). This will allow us to explore and identify the FC-networks that are more appropriate in tracking the progress of the children during the GOLIAH based intervention.

Measure type	**Category**	**List**
Functional Connectivity	Phase Synchronisation (PS)	Phase Locking Value (PLV), Phase Lag Index (PLI), Rho (ρ)
	Generalised Synchronisation (GS)	S, H, N, M, L, Synchronisation Likelihood (SL)
Graph theory		Transitivity, Modularity, Characteristic Path Length, Global Efficiency, Radius, Diameter

Table 5.1: List of functional connectivity and graph theoretic measures used for the neurological monitoring.

Compared to the contemporary approaches, here the brain connectivity is assessed in a game-based routine and over several sessions of the treatment. This may pave the way for a methodology that will allow: (a) the characterisation of the child and (b) the analysis of its progression during the intervention in terms of both behavioural and neuro-developmental means. Current research on brain synchronisation and neuro-developmental disease focuses on the use of control case design where the subjects are divided into a control group and a non-healthy group (Matlis et al., 2015). As opposed to this approach, a longitudinal study can give more insights on the abnormal brain network and its reorganisation over developmental time and during an early intervention in a young population (Vértes and Bullmore, 2015; Hernandez et al., 2015).

The method is validated on a group of five children with ASD recruited for a 3-month open trial of the GOLIAH-based intervention. During this trial, the intervention was

delivered: (a) at *home*, where the GOLIAH game is used on a parent-child interaction; (b) at *hospital*, where the GOLIAH game is used on a therapist-child interaction with simultaneous EEG recording. The analysis presented in this chapter was conducted on the EEG data and on the GOLIAH behavioural metrics recorded at hospital. Although data is scarce we make an attempt to investigate that these FC-network parameters could be indicative to the progress of a child's cognitive states.

The remainder of this chapter is structured as follows. In Section 5.1 we describe the various formulations of the FC employed in the proposed framework and categorised as (a) Phase Synchronisation and (b) Generalised Synchronisation based. In Section 5.2, we explain how the brain networks are constructed from the FC and the neurological meaning of the graph metrics extracted from these FC-networks. The development and application of the framework here proposed are described in section 5.3 and 5.4, respectively. Results obtained during a 3-month open trial of the GOLIAH monitoring are given in Section 5.5. Finally, Section 5.6 concludes the chapter with a summary of the results.

5.1 Formulation of Functional Connectivity

Performing a cognitive task demands segregated brain areas with different functional specialisation to exchange information that they process separately. The information processing within a specialised region and the information flow between various specialised areas is mainly based on neuronal oscillations. In particular, the information processing relies on the synchronised fluctuations within local neuronal groups (Buzsáki and Wang, 2012), while the information flow between brain areas is enabled by synchronised oscillations amongst different local neuronal ensembles (Womelsdorf et al., 2007). This flow of information in the brain is also dynamically modulated by changes of the pattern, strength and frequency of those synchronised neuronal oscillations between different brain areas (Bastos and Schoffelen, 2015). The analysis of these synchronised neuronal oscillations within and between brain areas can reveal quantitative differences between typical and atypical brain functioning. For this purpose, the information brain processing is analysed by performing the following steps: (1) FC is extracted from the EEG recordings, (2) brain complex networks are constructed from the FC and (3) several graph metrics are extracted from these FC-networks. The obtained graph indexes quantitatively describe the integration and segregation phenomena occurring in both task-based and task free experimental conditions.

In this section, we focus on the extraction of FC from the EEG recorded during the GOLIAH-based intervention. Although several FC formulations exist in literature, the selection of the appropriate method for extracting FC is challenging and often their algorithmic implementation has limited accessibility. Therefore, we here perform an

open exploration of various FC measures of two main categories (Table 5.1): PS and GS, based on phase information and non-linear dynamic analysis respectively. Next, we will build a brain network for each FC method and separately explore the corresponding graph metrics in order to identify the most appropriate FC to monitor the brain response to the GOLIAH-based intervention.

The following sections give an insight into the FC metrics employed in this work: Section 5.1.1 describes the FC matrices based on Phase Synchronisation (Phase Locking Value, Phase Lag Index and RHO indexes), while Section 5.1.2 describes the ones based on Generalised Synchronisation (S, H, N, M, L and Synchronisation Likelihood indexes).

5.1.1 Phase Synchronisation

Phase synchronisation describes the situation when the phases of two signals synchronise, indicated by a phase locking condition (Lachaux et al., 1999):

$$\Delta\phi(t) = |\phi_x(t) - \phi_y(t)| \leq cost \tag{5.1}$$

where $\phi_x(t)$ and $\phi_y(t)$ are the instantaneous phases of the signals $x(t)$ and $y(t)$ calculated from the analytical signals $x_{an}(t)$ and $y_{an}(t)$, and $\Delta\phi$ indicates the phase difference between the two signals.

The analytical signal $x_{an}(t)$ of a generic signal $x(t)$, like the EEG recorded at an electrode, is obtained from the Hilbert transform and is defined as:

$$x_{an}(t) = x(t) + ix_H(t) \tag{5.2}$$

where $x_H(t)$ is the Hilbert transform defined as:

$$x_H(t) = \frac{1}{\pi} PV \int_{-\infty}^{\infty} \frac{x(t')}{t - t'} dt' \tag{5.3}$$

where PV denotes the Cauchy principal value.

The analytical signal $x_{an}(t)$ can also be expressed in polar form as:

$$\begin{aligned} x_{an}(t) &= A_x(t)e^{i\phi_x(t)}, \\ A_x(t) &= \sqrt{x_H(t)^2 + x(t)^2}, \\ \phi_x(t) &= \arctan \frac{x_H(t)}{x(t)} \end{aligned} \tag{5.4}$$

where $A_x(t)$ and $\phi_x(t)$ are the instantaneous amplitude and phase, respectively.

When analysing the synchronisation, the relative phase difference between two signals $x(t)$ and $y(t)$ is commonly wrapped between $[0, 2\pi)$. With this procedure, the phase

locking condition is analysed in terms of distribution of the cyclic relative phase.

$$\Delta\phi_{rel}(t) = \Delta\phi(t) \bmod 2\pi = |\phi_x(t) - \phi_y(t)| \bmod 2\pi \tag{5.5}$$

The relative phase difference $\Delta\phi_{rel}(t)$ is used to obtain several FC formulations among which we will employ the following: Phase Locking Value (PLV), Phase Lag Index (PLI) and RHO which are described in the following subsections.

5.1.1.1 Phase Locking Value (PLV)

Phase Locking Value (PLV) is a measure of the distribution of the relative phase difference $\Delta\phi_{rel}$ over the unit circle (Lachaux et al., 1999). It is defined as the average across time of the relative phase difference:

$$PLV = \left|\langle e^{i\Delta\phi_{rel}(t)}\rangle\right| = \left|\frac{1}{N}\sum_{n=1}^{N} e^{i\Delta\phi_{rel}(t_n)}\right| \tag{5.6}$$

where N is the number of samples of the signals $x(t)$ and $y(t)$, $\Delta\phi_{rel}$ is calculated at each time sample t_n and $\langle\ldots\rangle$ indicates the average over time t. Its value ranges between 0 and 1: if there is strong synchronisation between the two signals, their relative phase is concentrated in a small portion of the unit circle and PLV will be close to 1; otherwise, the relative phase occupies all the circle and PLV will be close to 0.

The main drawback of this approach is its vulnerability to field spread and volume conduction. To mitigate this effect, other measures are proposed in literature, which will be described in the following sections.

5.1.1.2 Phase Lag Index (PLI)

Unlike the PLV, PLI discards relative phase differences centred around 0 and π, making it more robust against common sources and volume conduction. PLI measures the asymmetry of the distribution of the relative phase difference $\Delta\phi_{rel}$ over the unit circle. It is defined as:

$$PLI = |\langle sign[\Delta\phi_{rel}(t)]\rangle| = \left|\frac{1}{N}\sum_{n=1}^{N} sign[\Delta\phi_{rel}(t_n)]\right| \tag{5.7}$$

where N is the number of samples of the signals $x(t)$ and $y(t)$, $\Delta\phi_{rel}$ is calculated at each time sample t_n, $\langle\ldots\rangle$ indicates the average over time t and $sign$ indicates the signum function.

PLI is less sensitive to common sources because volume conduction does not generate time delay between two different electrode sites (Nolte et al., 2004). In details, we can divide three cases of synchronisation between two signals:

- *Synchronisation due to volume conduction.* When two electrodes record a common source, their relative phase difference can either be 0 or $\pm\pi$, resulting in a PLI close to 0.
- *No synchronisation.* When two signal are not synchronised, their relative phase difference is uniform over the unit circle; this results in PLI close to 0.
- *Synchronisation due to true interaction.* A consistent phase lag between the signals at two different electrodes reflects the true synchronisation between the two sites and results in a PLI close to 1.

5.1.1.3 RHO (ρ)

RHO (ρ) is another measure to analyse the relative phase difference $\Delta\phi_{rel}(t)$ (see Equation 5.5) between two signals $x(t)$ and $y(t)$. In particular, ρ measures the distribution of $\Delta\phi_{rel}(t)$ on the unit circle based on the entropy of $\Delta\phi_{rel}(t)$ (Tass et al., 1998). It is defined as:

$$\rho = \frac{S_{uniform} - S}{S_{uniform}} \tag{5.8}$$

where S is the entropy of the distribution of the relative phase difference $\Delta\phi_{rel}(t)$ on the unit circle, and $S_{uniform}$ is the entropy in case $\Delta\phi_{rel}(t)$ was uniformly distributed on the unit circle and equal to 1. The entropy S is defined as:

$$S = -\sum_{k=1}^{N} p_k ln(p_k) \tag{5.9}$$

where p_k is the probability to find $\Delta\phi_{rel}(t)$ in the k^{th} bin and N is the number of bins.

The values of ρ range between 0 and 1, indicating no synchronisation and full synchronisation between the two signals respectively. When the two signals are synchronised their relative phase difference $\Delta\phi_{rel}$ will occupy only a small portion of the unit circle and its entropy will be close to 0, leading to a ρ close to 1. On the contrary, when there is no synchronisation between the two signals, the relative phase difference will be distributed along the circle and its entropy will be close to the uniform entropy $S_{uniform}$, leading to a ρ close to 0.

As mentioned above, in the framework proposed here we extract two categories of FC from the EEG recordings. In this section we described the first category of FC, based on the relative phase difference between two signals. The next subsections describe the

second category of FC measures employed in the proposed framework and based on non-linear dynamic approach.

5.1.2 Generalised Synchronisation

The Generalised Synchronisation (GS) quantifies the non linear temporal interdependencies and similarities between EEG signals based on the theory of nonlinear dynamical systems. In fact, the brain behaves in a similar manner to a non linear dynamical system: when a stimulus is given to our brain, this integrates the information processed across neural assemblies activated at different locations (Alba et al., 2015). Such dynamical system, whose internal dynamics are unknown, can be studied through the analysis in the state space of the measurements recorded at different scalp locations (at the different electrodes). From the analysis of the state space, we can extract quantitative information about the system that generates the output signals recorded during an experiment. In our case, it allows to gather information about the brain activity occurring while playing the GOLIAH game and recorded with the EEG device.

The first step for the nonlinear dynamic analysis of our system is the state space reconstruction, performed by employing the delay embedding technique and the Takens' time-delay embedding theorem. According to Takens' time-delay embedding theorem (Takens, 1981), given a time series output of a complex dynamical system, the state space of the system can be reconstructed by using the consecutive values of the time series. When analysing the synchronisation between two variables generated from the same system (in our case the EEG recorded at two different electrodes and produced by the brain activity), we can build the state space of such variables by applying the Takens' theorem. Let us consider two EEG signals $x(t)$ and $y(t)$ recorded at two different electrodes:

$$\begin{aligned} x(t) &= (x_1, x_2, \ldots, x_N) \\ y(t) &= (y_1, y_2, \ldots, y_N) \end{aligned} \tag{5.10}$$

with N being the number of samples of each signal. According to the Takens' theorem, the corresponding *delay vectors* (or phase-space vectors) of the two signals are defined as follows:

$$\begin{aligned} x_n &= (x(n), x(n+\tau), \ldots, x(n+(m-1)\tau)) \\ y_n &= (y(n), y(n+\tau), \ldots, y(n+(m-1)\tau)) \end{aligned} \tag{5.11}$$

where $n = 1, 2, \ldots, N$, m is the *embedding dimension* of the state space and τ is the *time delay*. The embedding dimension m is estimated using the false nearest neighbours approach, while the time delay τ is estimated using the autocorrelation or the auto mutual information function of the data. All the delay vectors constitute the array vectors $X = (x_1, ..., x_N)$ and $Y = (y_1, ..., y_N)$.

Once the state space of the two signals is constructed, through the GS measures we want to find vectors that are close in the state space of both the signals $x(t)$ and $y(t)$. In fact, the existence of synchronisation between the two signals implies that similar states occur in both the signals. In essence, when the vectors $x(t)$ and $y(t)$ are synchronised, if $x(t)$ at time t_i and t_j shows similar patterns, also $y(t)$ at t_i and t_j will be similar. Several measures have been formulated to estimate the similarity of the state space of $x(t)$ and $y(t)$. These GS indexes are based on measures of distance between the states of each state space.

Let us consider the time indices $r_{n,j}$ and $s_{n,j}$ of the k nearest neighbours of x_n and y_n respectively with $j = 1, \ldots, k$ in the state space. For each x_n, the mean squared Euclidean distance $R_n^{(k)}(X)$ to its k nearest neighbours is defined as:

$$R_n^{(k)}(X) = \frac{1}{k} \sum_{j=1}^{k} (x_n - x_{r_{n,j}})^2 \tag{5.12}$$

If we replace the k nearest neighbours by the equal time partners of the closest neighbours of y_n, we obtain the Y-conditioned mean squared Euclidean distance $R_n^{(k)}(X|Y)$:

$$R_n^{(k)}(X|Y) = \frac{1}{k} \sum_{j=1}^{k} (x_n - x_{s_{n,j}})^2 \tag{5.13}$$

Finally, the mean squared Euclidean distance of the delay vector x_n to all other delay vectors of the array vector X is defined as:

$$R_n(X) = \frac{1}{N-1} \sum_{\substack{j=1 \\ j \neq n}}^{N} (x_n - x_j)^2 \tag{5.14}$$

If the dynamics of X is independent of Y, there is no relation between $r_{n,j}$ and $s_{n,j}$ and the following is verified:

$$R_n(X) \approx R_n^{(k)}(X|Y) \gg R_n^{(k)}(X) \tag{5.15}$$

In contrast, if there is a relation between $r_{n,j}$ and $s_{n,j}$, closeness in Y implies closeness in X and the following is verified:

$$R_n(X) \gg R_n^{(k)}(X|Y) \approx R_n^{(k)}(X) \tag{5.16}$$

Various measures of GS can be obtained by using these three distances: S, H, N, M, L and Synchronisation Likelihood indexes; they will be described in the following subsections.

5.1.2.1 S index

The S index (Arnhold et al., 1999) is a measure of the interdependence between the two systems and defined as:

$$S(X|Y) = \frac{1}{N}\sum_{n=1}^{N}\frac{R_n^{(k)}(X)}{R_n^{(k)}(X|Y)} \tag{5.17}$$

If the two time series are independent, the S index will be close to 0, because the Equation 5.15 is verified; otherwise, if the two signals are strongly correlated, the squared Euclidean distances will be similar and the S index will be close to 1.

5.1.2.2 H index

Similar to the S index, the H index (Arnhold et al., 1999) is another nonlinear interdependence measure and defined as:

$$H(X|Y) = \frac{1}{N}\sum_{n=1}^{N}\log\frac{R_n(X)}{R_n^{(k)}(X|Y)} \tag{5.18}$$

This index does not have upper bounds. If positive, the H index indicates that for equal time partners nearness in Y implies nearness in X; when equal to 0, the two time series $x(t)$ and $y(t)$ are independent. The H index would be negative if close pairs in Y corresponds to distant pairs in X. Because the $R_n(X)$ is less dependent on the dimensionality and structure of X than $R_n^{(k)}(X)$, the H index is more robust against noise (Andrzejak et al., 2003), but it is not normalised. To obviate to this drawback, the N index is proposed in literature and described in the next subsection.

Both the S and the H indexes were proposed in (Arnhold et al., 1999) and applied on epileptic EEG data, where showed promising results on the understanding of seizures in epilepsy.

5.1.2.3 N index

Similarly to the previous measures, the N index (Quiroga et al., 2002) describes the interdependence of the two array vectors X and Y starting from the Euclidean distances in the phase space.

$$N(X|Y) = \frac{1}{N}\sum_{n=1}^{N}\frac{R_n^{(k)}(X) - R_n^{(k)}(X|Y)}{R_n(X)} \tag{5.19}$$

The N index ranges between 0 and 1, indicating independence and synchronisation between the two signals $x(t)$ and $y(t)$, respectively. Like the H index, the N index is more robust against noise than the S index. Though, the main drawback of this measure is that it is equal to 1 only in case $R_n(X|Y) = 0$, which occurs only if the two systems are

periodic. In case of perfect synchronisation, the N index is smaller than 1 by a quantity dependent on the value of $R_n^{(k)}(X)$, which is strongly influenced by the autocorrelations and/or finite dimensionality of X. This limitation is corrected in the following measure.

5.1.2.4 M index

As mentioned above, the M index (Andrzejak et al., 2003) is a normalised measure of interdependence, defined as:

$$M(X|Y) = \frac{1}{N}\sum_{n=1}^{N}\frac{R_n(X) - R_n^{(k)}(X|Y)}{R_n(X) - R_n^{(k)}(X)} \tag{5.20}$$

It ranges between 0 and 1, indicating independence and full synchronisation, respectively. In fact, in case of independent X and Y, the Equation 5.15 will hold true, otherwise the Equation 5.16 will be verified.

5.1.2.5 L index

The L index (Chicharro and Andrzejak, 2009) is based on the rank of the distances between the array vectors X and Y. Let consider $g_{n,r_{n,j}}$ the rank that the distance between x_n and x_j occupies in a sorted ascending list containing the distances between x_n and all $x_{j\neq n}$. The rank $g_{n,s_{n,j}}$ is obtained by replacing the nearest neighbours with the equal time partners of the closest neighbours of y_n. The rank $g_{n,s_{n,j}}$ is used to calculate the Y-conditioned mean weighted rank $G_n^k(X|Y)$:

$$G_n^{(k)}(X|Y) = \frac{1}{k}\sum_{j=1}^{k} g_{n,s_{n,j}} \tag{5.21}$$

The L index is defined as:

$$L(X|Y) = \frac{1}{N}\sum_{n=1}^{N}\frac{G_n(X) - G_n^{(k)}(X|Y)}{G_n(X) - G_n^k(X)} \tag{5.22}$$

where $G_n(X) = \frac{N}{2}$ and $G_n^k(X) = \frac{k+1}{2}$ denote the mean and minimal mean rank, respectively.

Like the other GS measures described in the previous sections, the L index ranges between 0 and 1, indicating independence and strong synchronisation between two time series respectively. All the GS measures described above are calculated pairwise by considering only the EEG data recorded at each pair of EEG electrodes. Unlike these measures, the Synchronisation likelihood described in the next section is a multivariate measure of FC.

5.1.2.6 Synchronisation Likelihood (SL) index

The Synchronisation Likelihood (SL) (Stam and Van Dijk, 2002) is the most popular measure among the Generalised Synchronisation indexes described above. Unlike the previous indexes, the SL takes into account the time series recorded at all the electrodes and not only pairwise. For this purpose, the delayed vectors corresponding to the M time series $x_1(t), x_2(t), \ldots, x_M(t)$ (i.e. EEG recorded at M electrodes) are defined as:

$$\begin{aligned} x_{1,n} &= (x_1(n), x_1(n+\tau), \ldots, x_1(n+(m-1)\tau)) \\ x_{2,n} &= (x_2(n), x_2(n+\tau), \ldots, x_2(n+(m-1)\tau)) \\ &\vdots \\ x_{M,n} &= (x_M(n), x_M(n+\tau), \ldots, x_M(n+(m-1)\tau)) \end{aligned} \tag{5.23}$$

First, we consider a delay vector x_m from the signal $x_m(t)$ recorded at the m electrode. Let $P^{\varepsilon}_{m,i}$ denote the probability that two embedded vectors $x_{m,i}$ and $x_{m,j}$ at time instants i and j are closer than a small critical value ε: if this condition is verified they are considered to be in the same state. The probability $P^{\varepsilon}_{m,i}$ that $|x_{m,i} - x_{m,j}| < \varepsilon$ is defined as:

$$P^{\varepsilon}_{m,i} = \frac{1}{2(w_2 - w_1)} \sum_{\substack{j=1 \\ w_1 < |i-j| < w_2}}^{N} \Theta(\varepsilon - |x_{m,i} - x_{m,j}|) \tag{5.24}$$

where w_1 is the Theiler window for autocorrelation effects, w_2 is a window chosen such that $w_1 \ll w_2 \ll N$, where N is the sample of the time series x_m and Θ is the Heaviside step function:

$$\Theta(c) = \begin{cases} 1, & \text{if } c > 0 \\ 0, & \text{otherwise.} \end{cases} \tag{5.25}$$

The critical distance ε is determined such that: $P^{\varepsilon}_{m,i} = p_{ref} \ll 1$, where p_{ref} is the percentage of the reconstructed state vectors in x_m which are close enough to $x_{m,i}$ to be considered in the same state. Its value does not depend on the property of the time series and can be set at an arbitrary low level. While p_{ref} is the same for all the M signals, the critical distance ε can be different for each signal.

For each time pair (i, j) within the time window $w_1 < |i - j| < w_2$, we determine the number of electrodes $H_{i,j}$ where the embedded vectors $x_{m,i}$ and $x_{m,j}$ are closer than the critical distance $\varepsilon_{m,i}$:

$$H_{i,j} = \sum_{m=1}^{M} \Theta(\varepsilon_{m,i} - |x_{m,i} - x_{m,j}|) \tag{5.26}$$

$H_{i,j}$ varies between 0 and M and indicates the number of the embedded signals which are in similar states. It is used to define the synchronisation likelihood for each signal

recorded at the m electrode and at the discrete time pair (i, j):

$$SL_{m,i,j} = \begin{cases} \frac{H_{i,j}-1}{M-1}, & \text{if } |x_{m,i} - x_{m,j}| < \varepsilon_{m,i} \\ 0, & \text{otherwise.} \end{cases} \tag{5.27}$$

The Synchronisation Likelihood $SL_{m,i}$ at time i is obtained by averaging $S_{m,i,j}$ over all time instant j:

$$SL_{m,i} = \frac{1}{2(w_2 - w_1)} \sum_{\substack{j=1 \\ w_1 < |i-j| < w_2}}^{N} S_{m,i,j} \tag{5.28}$$

$SL_{m,i}$ indicates how well the signal $x_m(t)$ at time i is synchronised to all other $M-1$ electrodes. By averaging $SL_{m,i}$ over all time instants we obtain the synchronisation likelihood SL_m of the electrode m with all the other channels. SL_m ranges between p_{ref} and 1 indicating uncorrelation with all the M time series and maximal synchronisation among them respectively.

Rather than optimising the analysis parameters for each of the GS measures, we chose a fixed default setting for all the measures. They are calculated using an embedding dimension $m = 3$, a time delay $\tau = 87$, a number of nearest neighbours of 4. For the calculation of SL, we also used a Theiler correction w_1 of 87 samples and $p_{ref} = 0.05$. The default value of the embedding dimension m is such that the percentage of false nearest neighbours falls below 10%. The default value of the embedding delay τ corresponds to the time at which the envelope of the autocorrelation function is equal to $1/e(0.32)$.

Once obtained the FC measures, we are able to extract information related to the synchronisation of each pair of electrode. Although these measures can indicate how two brain sites are synchronised during a specific cognitive process, we aim at extracting neurological information able to characterise the brain activity as a whole instead of at each site. Graph theory can give insights to fulfil this requirement and is described in the next section.

5.2 Theoretic characterisation of Functional Connectivity Networks

The brain is believed to operate according to the two principles of functional segregation and integration (Tononi and Sporns, 2003). Functional segregation describes the propensity of neural assemblies to combine and form specialised groups of neurones segregated across the cortical brain regions. On the other hand, functional integration refers to the coordinated activation of these segregated neural groups and is responsible for cognitive processes and motor responses. The interaction of these two principles underlies

the complexity of the brain network and can be described in terms of graph measures extracted from the brain functional connectivity. In the following subsections, we first introduce the concept of complex brain network, then we describe the graph metrics (Table 5.1) that are extracted from those networks and provide information about the integration and segregation of these networks and their neurological meaning.

5.2.1 Complex brain network

A network is represented by a graph consisting of nodes and edges. The N individual components (the EEG electrodes) of the network are called *nodes* and the K connections (pairwise correlation or synchronisation measures) are called *edges*. The edges between nodes represent the correlation or synchronisation between the activity at different neural regions, which is recorded by the EEG electrodes.

A graph can be *undirected* or *directed*, and *unweighted* or *weighted*. In an *undirected* graph, the edges describe the relations (synchronisation) between nodes, whereas the edges of a *directed* graph explain the causal relationships (like Granger causality) between nodes. Depending on the type of network, the edges across all networks can have equivalent strength (*unweighted* network) and can be either absent or present, or have different strength (*weighted* network).

The brain functional connectivity networks are weighted and fully connected. Typically, they are thresholded to obtain a binary network, regardless the type of functional connectivity estimates they are representing. During the binarisation, only the connection weights greater than the threshold are retained and used for the extraction of the graph theoretic measures (Bullmore and Bassett, 2011; Bassett and Bullmore, 2006). However, there is no common consensus on the arbitrary threshold to be applied for the binarisation, consequently graph measures are extracted for different values of the threshold. Empirical results showed that such discretisation of the intrinsically continuos edge weights is not capable to analyse the complex nature of the real systems (Boccaletti et al., 2006). Some authors have proposed graph measures that allow to preserve all the available edge weights (Rubinov and Sporns, 2010) and retain additional information to provide more accurate models of the real system under investigation (Stam and Reijneveld, 2007). In this work, we used the graph measures developed for weighted graphs.

Some of the functional connectivity measures retrieve a positive real value of the connection weights (synchronisation) between the brain nodes. Some others, like correlation, describe the correlation with weights that can be either positive or negative. In this case, the absolute value of such weight edges is considered, because we are interested on the presence of a statistical interaction regardless its directionality.

5.2.2 Graph theory measures

The functional connectivity networks built from the FC described in the previous sections are *undirected* and fully connected with weights w_{ij} of N nodes and a number of connections equals to $\frac{1}{2}N(N-1)$. The nodes and their edges are described by several metrics, like the *degree* of the node and the *length* of the connections between nodes.

The *degree* k_i of a node i is the sum of its connection weights with the rest of the nodes; it is defined as $k_i = \sum_{j \in N} w_{ij}$. The *total weight* l of the network is the sum of all connection weights of the graph, defined as: $l = \sum_{ij} w_{ij}$.

The *length* P_{ij} of an edge connecting two nodes is defined as the inverse of its weight, $P_{ij} \approx 1/w_{ij}$, such that shorter lengths correspond to higher weights (Rubinov and Sporns, 2010). In fact, large weights correspond to strong associations and close proximity. When considering the FC measures, the length of the edge is the inverse of the connectivity, since stronger synchronisation implies closer connection between two nodes.

The *path* between any two nodes is a sequence of nodes and edges that must be traversed to directly connect the two nodes of interest. In a weighted connection matrix, the length of a weighted path, *path length*, is defined as the sum of the lengths of edges in this path. An important feature derived from the concept of length and path is the *shortest path length* d_{ij} between any two nodes i and j. It indicates the minimal number of edges that will be crossed to directly connect the two nodes (Watts and Strogatz, 1998) and it is defined as:

$$d_{ij} = \sum_{a_{ij} \in g^w_{i \leftrightarrow j}} P_{ij} \tag{5.29}$$

where $g^w_{i \leftrightarrow j}$ is the shortest weighted path between the nodes i and j.

Various graph theoretic measures can be used to quantify the segregation and integration phenomena, among which we selected: (a) *transitivity*, (b) *modularity*, (c) *characteristic path length*, (d) *global efficiency*, (e) *network radius* and (f) *network diameter*.

5.2.2.1 Transitivity and Modularity

Transitivity and modularity are measures of functional segregation. They quantify how easily the brain network can be divided into subnetworks. They determine the presence of clusters or modules (segregated neural groups) within the network and are based on the concept of triangles.

In social network, *transitivity* T indicates the mean probability that A and C are friends of each other if they have a common friend B. In graph theory, transitivity T indicates the mean probability that two vertices A and C that are neighbours of the same vertex

B will themselves be neighbours. In essence, T measures the fraction of the neighbours of a node which are also neighbours of each other (Watts and Strogatz, 1998). It is defined as:

$$T = \frac{\sum_{i \in N} 2t_i}{\sum_{i \in N} k_i(k_i - 1)} \tag{5.30}$$

where t_i is the weighted geometric mean of triangles around the node i and k_i is the degree of the node i. The geometric mean of triangles t_i around the node i is defined as:

$$t_i = \frac{1}{2} \sum_{j,k \in N} (w_{ij} w_{ih} w_{jk})^{\frac{1}{3}} \tag{5.31}$$

where w_{ij} is the connection weight between nodes i and j. Here we used the transitivity T as a measure of local segregation to identify the density of connections between node's neighbours, hence to measure local connectivity. High values of transitivity T indicates higher number of triangles, thus a higher local connectivity.

Modularity Q is a measure of community structure: it reveals the size and composition of densely interconnected groups of nodes. Modularity refers to the tendency of the brain functional organisation to form segregated neural groups with specialised functional properties (Sporns, 2011). To estimate Q the system is decomposed into a lower level of multiple organised subsystems by dividing the network into groups of nodes with maximum number of interconnections within-group and minimum number of connections between-groups (Rubinov and Sporns, 2010). The modularity Q of a network is defined as:

$$Q = \frac{1}{l} \sum_{i,j \in N} [w_{ij} - \frac{k_i k_j}{l}] \delta_{m_i, m_j} \tag{5.32}$$

where w_{ij} is the connection weight between node i and j, k_i and k_j indicate the node's degree, l is the total weight, m_i is the module containing the node i, and $\delta_{m_i, m_j} = 1$ when i and j are in the same module ($m_i = m_j$) and 0 otherwise.

5.2.2.2 Characteristic path length and Global efficiency

Characteristic path length L and *Global efficiency* E_{Glob} are measures of functional integration. They describe the ability and ease with which the clusters (distributed brain regions) communicate and are based on the concept of path. A path is a sequence of nodes and edges and is given by the number of edges crossed to connect any two nodes: a short path indicates a stronger potential for integration between clusters.

The *characteristic path length CPL* of a network is the average shortest path length of the nodes in the network. It is estimated by averaging the shortest path length L_i for each of the $i = 1, 2, 3, ...N$ nodes and all other nodes:

$$CPL = \frac{1}{N} \sum_{i \in N} L_i = \frac{1}{N} \sum_{i \in N} \frac{\sum_{j \in N, j \neq i} d_{ij}}{N - 1} \tag{5.33}$$

where d_{ij} is the shortest path length between the nodes i and j, defined in Equation 5.29.

Similarly to the characteristic path length, the *global efficiency* E_{Glob} is the average inverse shortest path length in the network $E_{Glob} \approx 1/L$ (Latora and Marchiori, 2001):

$$E_{Glob} = \frac{1}{N}\sum_{i\in N} E_i = \frac{1}{N}\sum_{i\in N}\frac{\sum_{j\in N, j\neq i} d_{ij}^{-1}}{N-1} \tag{5.34}$$

Unlike the characteristic path length, the computation of E_{Glob} is numerically easier when dealing with disconnected graphs, since paths between disconnected nodes are characterised by infinite length, hence zero efficiency. For this reason, the characteristic path length is influenced by long paths, whereas the global efficiency is mainly influenced by short paths. Because of its ease of computation in case of disconnected nodes, global efficiency may be considered a superior measure of integration (Achard and Bullmore, 2007). As mentioned above, both characteristic path length L and global efficiency E_{Glob} are measures of functional integration. Pairs of nodes which, on average, have short communication distances are characterised by high efficiency or low path length.

5.2.2.3 Network radius and diameter

The network diameter and network radius are the other two measures employed to characterise the brain connectivity. Both these measures derive from the eccentricity. The eccentricity $ecc(i)$ of a node i is another measure related to the path between the node i and the rest of the nodes in the network (Harris et al., 2008). It is the greatest distance among the shortest paths from i to the rest of the nodes and defined for each node as:

$$ecc_i = \max_{j\in N}\{d_{ij}\} \tag{5.35}$$

where d_{ij} is the shortest weighted path length between i and j (Equation 5.29). Essentially, the eccentricity of a node is its shortest path length from the farthest node in the graph: if the node i is isolated, its eccentricity value is zero.

The *network radius* R is the minimum eccentricity among all nodes and defined as:

$$R = \min_{i\in N}(ecc_i) \tag{5.36}$$

The *network diameter* D is, instead, the maximum eccentricity among all nodes and defined as:

$$D = \max_{i\in N}(ecc_i) \tag{5.37}$$

The FC and graph theoretic measures can be combined to describe how well the information processed by the segregated neuronal groups is integrated across them. The next section shows how these measures are combined together to build a framework to understand the functional brain connectivity variation in response to the intervention.

5.3 Tool chain and development

The framework proposed in this chapter aims at the behavioural and neuro-developmental monitoring of the GOLIAH-based intervention, by using both the GOLIAH game and a simultaneous recording of EEG with a wireless device. To fulfil this goal, the proposed methodology combines three platforms: (a) the GOLIAH gaming library developed in .NET environment described in Chapter 3, (b) a wireless EEG recording system[1], and (c) the processing of the EEG recordings in Matlab environment.

On one side, the GOLIAH platform implements the ESDM intervention protocol and generates various objective measures that allow the behavioural monitoring of the intervention. It also generates timestamp events that support the monitoring of the GOLIAH objective measures together with the correspondent $FC - network$ measures from the EEG recordings.

On the other side, EEG data processing is enabled by various tools implemented in Matlab environment. Specifically, first a preprocessing step is implemented by performing the artefact reduction of the EEG recordings with the WPTEMD algorithm proposed in Chapter 4. Once the EEG recordings are preprocessed, 1 second-EEG epochs are extracted by combining the timestamps of the GOLIAH game (Bono et al., 2016b) with the EEG timestamps generated by the EEG recording system. All the identified epochs are then employed for the $FC - network$ extraction. For this purpose, we used the following Matlab toolboxes: (1) the WPTEMD algorithm for the artefact suppression (Bono et al., 2016a), (2) the HERMES toolbox (Niso et al., 2013) for calculating the FC, and (3) the Brain Connectivity Toolbox (Rubinov and Sporns, 2010) for the construction of the $FC - networks$ and their related graph metrics. The entire framework and its application are detailed in the following section.

5.4 Proposed behavioural and neuro-developmental monitoring of GOLIAH-based intervention

The framework proposed in this chapter allows the behavioural and neuro-developmental monitoring of the GOLIAH-based intervention, by employing both the GOLIAH game and EEG recorded with the wireless EEG system. Figure 5.1 shows the flowchart for extracting the functional connectivity networks and the behavioural objective measures in a typical session of the intervention. Although the proposed framework is employable in naturalistic settings, we here conceptually prove the methodology during the sessions at hospital.

[1] http://www.neuroelectrics.com/products/enobio/enobio-20/

For each session at hospital (a), the intervention monitoring is performed by analysing: the *behavioural* metrics from the GOLIAH game (Figure 5.1 (b)-(d)), and the *FC − networks* from the EEG recordings (Figure 5.1 (e)-(l)). Among the GOLIAH metrics, we select the average time response for each session as the objective behavioural measure, although other metrics are available (Section 4.3.3). For monitoring the neurodevelopmental metrics various EEG processing steps are performed to obtain various *average FC-network* features for each session, described below.

To obtain both the average time response and the *average FC-network* features, all categories of stimuli given by any game of the GOLIAH platform were considered. A more rigorous investigation would require the averaging of the time response for a single category of stimuli, in order to analyse the progression of the graph metrics and the time response related to each game. However, because the main aim of this work was to assess the feasibility of the combined platform and due to the short open trial and the limited number of subjects, the number of stimuli of each game was not sufficient to conduct a game-specific investigation.

First, the EEG recordings are processed with the WPTEMD artefact suppression algorithm (Figure 5.1-(f)), described in Chapter 4, to suppress the artefacts corrupting the data due to the body movement and physiological activity. Once the EEG recordings are pre-processed, the next step is the extraction of the epochs (Figure 5.1-(g)). An *epoch* here is identified as 1 sec post-stimulus given by the GOLIAH game; an example of stimulus is the picture of a dog shown to the child, who then has to mimic the animal call. Since the EEG epochs might contain residual artefacts, even after the artefact suppression, the epochs were thresholded at $\pm 200\mu V$ (Righi et al., 2014) and only the epochs within this voltage range are considered for further analysis. Once obtained, the "clean" epochs are used for the FC extraction (Figure 5.1-(h)). The FC in its various formulations is calculated for each stimulus (each epoch) presented in the GOLIAH game and in various frequency bands, as explained later in the section.

In order to construct the FC-networks, we here consider the FC averaged across all the stimuli given in a session. The FC averaging across stimuli is performed to neglect possible spurious connectivity (Fallani et al., 2014). Hardmeier et al. (2014) showed that the graph theoretic measures extracted from averaged FC are more reliable than graph measures extracted from single epoch FC. In essence, all the FC extracted from the "clean" epochs are averaged to construct a functional connectivity network (Figure 5.1-(i)). Finally, the FC-networks obtained are described in terms of the six graph features (Figure 5.1-(l)) detailed in section 5.2 which are informative of the brain processing during the game. In the following sections we will refer to these six graph features as *average FC-graph* features.

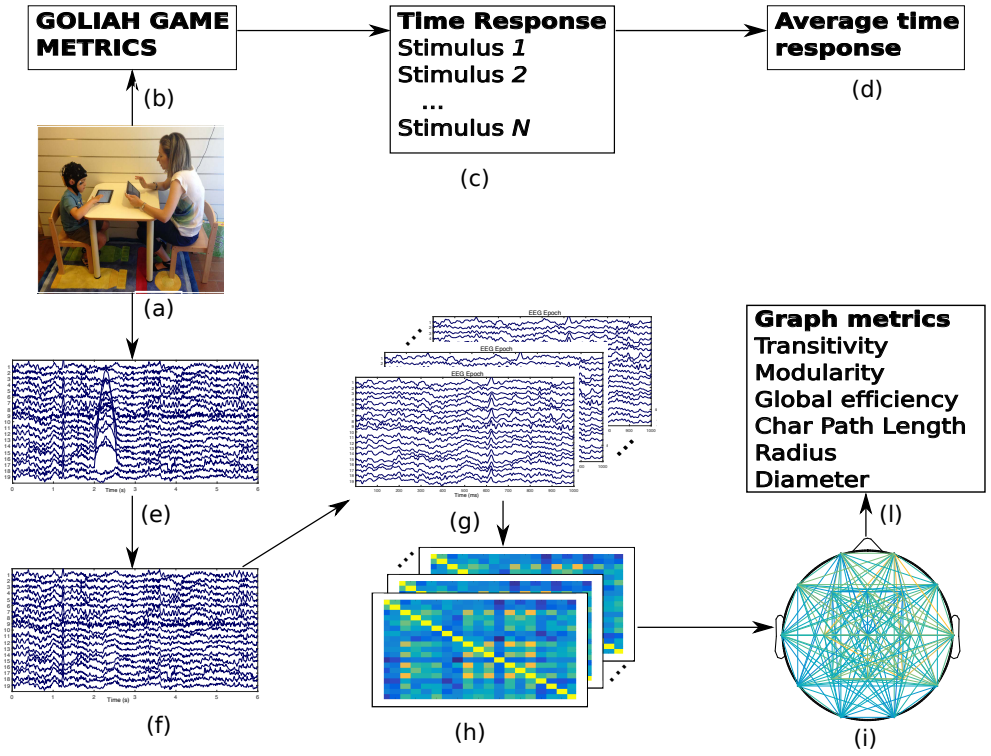

Figure 5.1: Monitoring of the GOLIAH-based intervention. For a given session (a) at hospital, both behavioural measures from the GOLAH game (c-d) and neuro-developmental measures from EEG recordings (e-l) are used in conjunction to analyse the performance of a child.

The FC for each epoch in its various formulations (Section 5.1) is calculated for each band (θ, α, β and γ) and across bands (*AllBands–4-42 Hz*), since it is useful to investigate the FC synchronisation in a band-specific routine. The synchronous activity of neural assemblies takes place in different bands according to the different cognitive processes demanded by the different nature of the stimuli and can be indicative of different pathologies (Başar et al., 2001). Since the GOLIAH-based stimuli have different nature, from visual to sound or a combination of the two types, we here investigate the FC measures in each band.

The FC measures extracted from the EEG epochs are the following:

- Phase Locking Value (PLV) in θ, α, β, γ and *AllBands*
- Phase Lag Index (PLI) in θ, α, β, γ and *AllBands*
- RHO (ρ) in θ, α, β, γ and *AllBands*
- Generalised Synchronisation indexes: *GS*, *H*, *L*, *M*, *N*, *S*.

In a given session, a *FC-network* is constructed for each of the above FC and for each band and six graph measures are obtained to describe the network organisation (Table 5.1). In total, we obtain 126 *average FC-graph* features to describe the brain connectivity related to the stimuli given by the GOLIAH game in each session. This set of features is analysed to monitor the effect of the GOLIAH-based intervention during a 3-month open trial at hospital and results are given in the next section.

5.5 Results and Discussion

In this chapter, we present a proof of concept of the GOLIAH-based intervention to favour: (a) intensive, (b) parent-mediated intervention, (3) systematically monitored in (4) multiple areas (behavioural and neuro-developmental). The main aim of this work is to assess the feasibility of the combined platform during three 3-month open trial. In order to do so, in this section we describe the participants recruited in the open trial, the sessions of the intervention and the outcomes in terms of functional brain connectivity and behavioural response during the intervention.

5.5.1 Participants and sessions

The GOLIAH-based intervention was carried out at the Department of Developmental Neuroscience, IRCCS Stella Maris Foundation, Pisa, Italy. Five children were recruited for a 3-month open trial. Table 5.2 describes the five children recruited in the study, in terms of their age and diagnosis. All children were assessed with two diagnostic tools (DSM IV and ADOS), administered at T_s and at T_e, before and after the three months of the GOLIAH-based intervention, respectively. The ADOS module 2 (for non verbally fluent subjects) was administered only to the Child 02, while the rest of the children were assessed with ADOS module 3. A diagnosis of *autism* indicates more severe symptoms than the *ASD* diagnosis. The diagnosis based on the DSM IV and ADOS at T_s differs for

ID	**Gender**	**Age (Year)**	**DSM IV** (T_s, T_e)	**ADOS** (T_s) [M, C, S]	**ADOS** (T_e) [M, C, S]
02	Male	5	ASD	ASD: [2, 4, 4]	ASD: [2, 2, 5]
03	Male	7	ASD	ASD [3, 2, 5]	No spectrum [3, 2, 4]
07	Male	6	ASD	ASD [3, 2, 7]	ASD [3, 2, 5]
08	Male	6	ASD	ASD [3, 3, 6]	ASD [3, 2, 5]
09	Male	6	ASD	Autism [3, 4, 7]	Autism [3, 4, 7]

Table 5.2: Children recruited for the GOLIAH-based intervention. The diagnostic tools DSM IV and ADOS are administered before and after the 3-month open trial (T_s and T_e). The ADOS module M can be administered in its version 3 or 2, depending if a subject is verbally fluent or not respectively. The ADOS comprises of a Communication score C and a Social interaction score S.

the child 09. This mismatch can be explained by two main reasons. First, although DSM IV and ADOS are both based on clinical observations, the second is a scoring method while the first is a categorical method and it only diagnoses the subject as affected or not by the ASD. Second, the ADOS does not analyse some of the ASD criteria listed in the DSM IV, such as relationships with others and peers. According to the ADOS score, only the Child 03 changed its diagnosis at T_e and was observed to be outside the ASD spectrum.

In a typical GOLIAH-based session, first the therapist and the subject sit on a table, then the child wears the EEG cap to record the electrical brain activity for the entire duration of the session. For the first few minutes of the session, EEG at rest with closed eyes is recorded to ensure the recording of the EEG baseline (EEG-resting state) for the EEG pre-processing stage.

A GOLIAH game session lasts 20 minutes, during which a variable number of games can be played according to the plan outlined by the therapist. Various stimuli are given for each of the games played and, consequently, several EEG epochs are extracted during a GOLIAH session. As described in Section 5.4, the EEG data and the respective epochs are pre-processed before obtaining the $FC-network$ measures. Table 5.3 describes the number of epochs obtained after the artefact reduction and employed for the FC and graph measures extraction for each child. The number of sessions used for the $FC-network$ extraction varies substantially across children, especially for the children 08 and 09. It is worth mentioning that the 3-month open trial included the setup phase of the platform composed by the simultaneous use of the GOLIAH game, the EEG recordings and numerous cameras used for the analysis of eye contact. Due to the low number of sessions available, the data from children 08 and 09 were discarded and only three children were considered for further EEG analysis. The epochs listed in Table 5.3

	Child 02	**Child 03**	**Child 07**	**Child 08**	**Child 09**
No. Sessions	9	6	8	4	3
No. Stimuli					
Session 1	63	5	33	45	54
Session 2	53	3	40	27	15
Session 3	49	17	13	43	27
Session 4	17	7	4	28	x
Session 5	18	11	22	x	x
Session 6	38	11	24	x	x
Session 7	26	x	20	x	x
Session 8	31	x	6	x	x
Session 9	20	x	x	x	x

Table 5.3: Number of sessions and corresponding number of stimuli from GOLIAH game employed from the FC-network extraction from EEG recordings.

are used to extract the 126 *average FC-graph* features (Section 5.4). In essence, the

brain response to the GOLIAH-based intervention for each session can be quantified by these 126 *average FC-graph* features, while the behavioural response is quantified by the average time response detailed in the next section.

5.5.2 Performance monitoring

The aim of this monitoring framework is to (a) analyse the progress of a child across the sessions of the intervention, (b) whether behavioural improvements correspond to functional brain connectivity alterations and (c) which *average FC-graph features* is more appropriate to describe these brain connectivity modifications. To fulfil these objectives, we conducted two different analyses.

- To address aims (a) and (c), we analyse if any *average FC-graph* features changes monotonically across the different sessions of the intervention (Section 5.5.2.1).
- To address aim (b), we investigate weather any of the 126 *average FC-graph* correlate with the *average time response* to the stimuli given during each session (Section 5.5.2.2).

We also attempted to investigate any correlation between the average FC graph measures and the clinical ADOS scores assessed before and after the trial (at T_s and T_e), in a similar approach to (Barttfeld et al., 2011) but no significant correlation was found. The next subsections describe the results obtained by performing the analyses listed above: among the 126 *average FC-graph* features, we will detail only those features showing changes along with the intervention and correlation with the behavioural outcomes.

5.5.2.1 Average FC-Graph measures

The neuro-developmental monitoring of a subject during the GOLIAH-based intervention is here performed by analysing the 126 *average FC-graph* features extracted from the EEG epochs described in Table 5.3. To identify any brain connectivity change induced by the intervention and which *average FC-graph* feature is more appropriate for this identification, we investigate possible monotonic increase or decrease of the *average FC-graph* measures. In order to identify those features showing monotonic trend across sessions, we generate a variable $y_{sessions}$ monotonically increasing defined as: $y_{sessions} = [1, 2, \ldots, n]$ with n being the number of the GOLIAH-based sessions. Pearson correlation coefficient between the variable $y_{sessions}$ and each *average FC-graph* features is calculated here. A positive correlation between the two variables would indicate a monotonic increase of the brain connectivity of the child during the intervention. On the contrary, a negative correlation would indicate a monotonic decrease in the brain connectivity across the sessions.

Table 5.4 shows the *average FC-graph* features that are found to be correlated with the variable $y_{sessions}$ for each child and the respective correlation coefficient. Among the children considered for this analysis (children 02, 03 and 07), the Child 02 did not show any monotonic change across the GOLIAH sessions of any of the *average FC-graph* measures. Both the diameter of the PLI in the γ band and the radius of the ρ measure in the α band decreased across the sessions for the children 03 and 07, respectively. The efficiency of the PLI in the θ band increased across the different sessions for the child 07.

Child	**FC-graph measure**	**Correlation**
02	None	
03	PLI-γ Radius	-0.72
07	ρ-α Diameter	-0.72
	PLI-θ Efficiency	0.78

Table 5.4: FC-networks measures monotonically decreasing and increasing across the GOLIAH game sessions.

Figure 5.2 shows the three *average FC-graph* features (Table 5.4) across the different sessions of the intervention period for the children 03 and 07. The *radius* and *diameter* indicate how strongly a graph is connected. Both features are calculated from the eccentricity, which measures the shortest path length of each node with its most distant node. The radius and the diameter measure the minimum and maximum of such distances among all the connections, respectively. A decrease in any of the two measures indicate that the connections in the graph become stronger. This implies that the ability of integrating the information among brain areas is enhanced along with the GOLIAH-based intervention in the children 03 and 07, as suggested from the radius of the PLI in the γ band and from the diameter of the ρ in the α band.

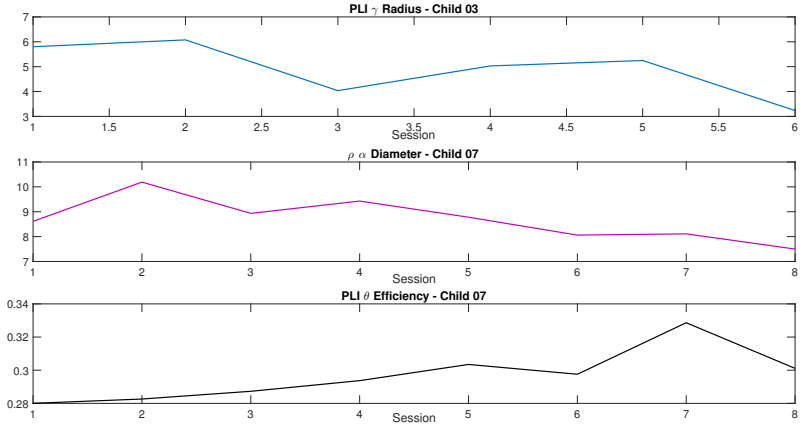

Figure 5.2: FC graph metrics extracted from the GOLIAH-based intervention showing a decrease (radius and diameter) and an increase (efficiency) across the sessions of the treatment for different children.

Figure 5.3 shows an example of *average-FC-graph* built from the PLI in the γ band across the sessions of the intervention. Each scalp is an *average-FC-graph* extracted from the stimuli in a session of the intervention. The coloured connections between electrodes on the scalp indicate their synchronisation values (PLI). As the number of session increases, the overall synchronisation between the different electrodes increases leading to a lower shortest path length, hence to a decrease in their radius.

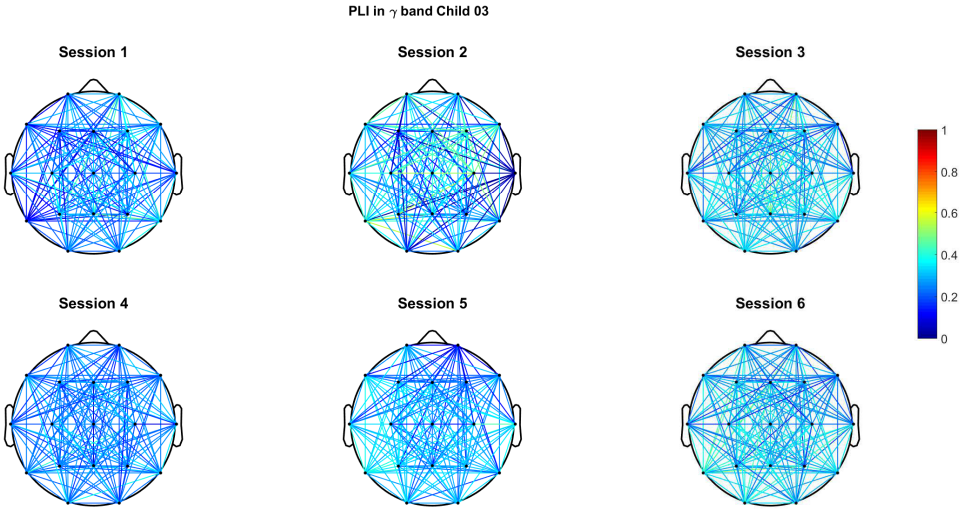

Figure 5.3: PLI connectivity in the γ band for child 03 across different sessions of the GOLIAH-based intervention.

Table 5.4 and Figure 5.2 also show that the *efficiency* of the network corresponding to the PLI in the θ band increases during the GOLIAH-based intervention in the Child 07. Higher global efficiency implies more efficient information transfer between brain regions. In fact, those pairs of electrodes with short communication distances are characterised by high efficiency.

Figure 5.4 shows the scalp networks across different sessions of the PLI in θ band for the Child 07. According to the increase of global efficiency in Figure 5.2, the synchronisation values increase along the sessions, reaching their maximum at the session 7. In fact, an increase of the synchronisation between electrodes corresponds to a shorter communication between the respective nodes, leading to their higher efficiency. While the results in this subsection were focused only on the neuro-developmental outcomes of the intervention, in the next subsection we provide the results obtained when using both behavioural and neural measures to track the children improvements during the GOLIAH-based intervention.

5.5.2.2 Average FC-Graph measures and Time Response analysis

The purpose of this exploration is to investigate whether the behavioural changes occurring during the intervention correspond to underlying brain connectivity and if the

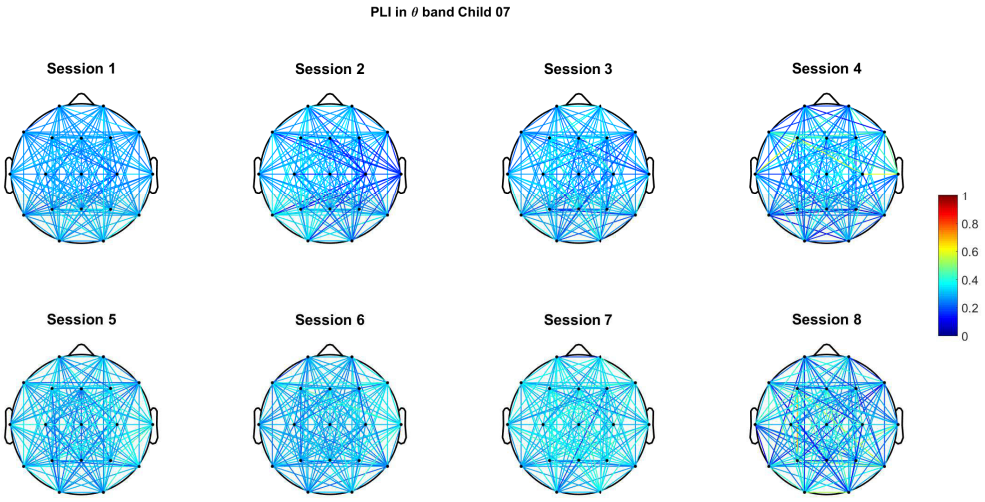

Figure 5.4: PLI connectivity in the θ band for Child 07 across different sessions of the GOLIAH-based intervention.

average FC-graph features are capable to capture them. On one side, the behavioural performance of a child in a given session can be described in terms of *average time response*. On the other side, the *average FC-graph* features in the same session quantify the corresponding neural performance. The *average FC-graph* features are extracted as described in Section 5.4. Similarly, the *average time response* is calculated by averaging the time response to the stimuli given by GOLIAH during a session and correspondent to the EEG epochs considered for extracting the FC-graph features.

Figure 5.5 shows the average time response related to all the stimuli considered for the EEG epochs extracted during the GOLIAH sessions at hospital (Table 5.3). Since the average time response is extracted from the stimuli of the games played in a session, it does not increase or decrease across the GOLIAH sessions for any child. The variation of the time response to the stimuli in a game-specific approach is presented in Chapter 3. Instead, the objective of the current analysis is to investigate the possible correlation between the graph theoretic metrics and the average time response.

Pearson's correlation coefficient was calculated between the average time response and each of the 132 average FC graph measures across the GOLIAH game sessions. Among all the *average FC-graph* measures extracted for all the three children, the features in Table 5.5 showed high correlation with the average time response. Among all the FC measures, only the Phase Synchronisation based measures (ρ and PLV) showed correlation with the average time response. In particular, only the efficiency and the transitivity of the FC networks show high correlation with the average time response.

Figure 5.6 shows the average time response and its correlated *FC-graph* measures for each child. All the variables in the figure are standardised ($x_{std} = (x - \mu)/\sigma$) to facilitate their comparison: they are transformed to have zero mean and unit variance.

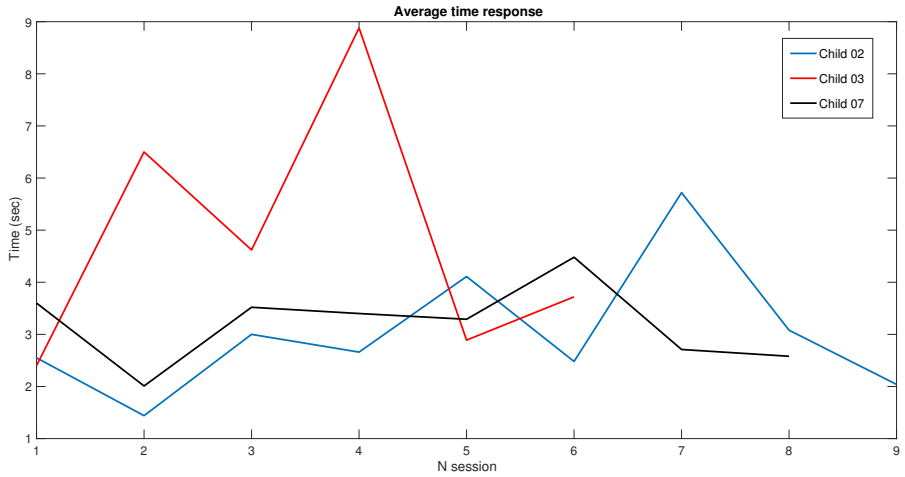

Figure 5.5: Average time response of the stimuli considered for the extraction of the FC-graph metrics across the different sessions for the three children considered.

FC-graph measure	**Child 02**	**Child 03**	**Child 07**
ρ-θ Efficiency	0.77	-0.91	-0.76
PLV-θ Efficiency	0.80	-0.90	-0.74
ρ-α Efficiency	0.81	-0.88	-0.73
ρ-α Transitivity	0.92	-0.86	-0.71
ρ Efficiency	0.92	-0.74	-0.71

Table 5.5: Correlation between the FC-network measures and the time response to the GOLIAH stimuli.

The efficiency indicates the ability of the network to transfer the information between different brain regions. Its negative correlation with the average time response indicates that an increase in efficiency corresponds to a quicker response to the stimulus. This occurs in the children 03 and 07, but it is not verified in child 02. In fact, for the child 02 the average time response is positively correlated with all the average FC-graph measures listed in the Table 5.5.

Transitivity is another graph feature correlated with the average time response and provides a different type of information compared to the efficiency. The latter is only based on path length estimation: it relies on the hypothesis that short paths lead to more direct transfer of neural signals between nodes (Goñi et al., 2014). Unlike the efficiency, the transitivity estimates how the communication paths are embedded in the network. If along a given path, the nodes constitute a loop, these loops could contribute in amplifying the neural signals being transported and prevent the potential signal dispersion. On the contrary, in absence of closed loop, the path would lead to signal dispersion and attenuation of the measured FC feature. A higher value of transitivity indicates the presence of such loops within the network. According to the

Table 5.5 and the Figure 5.6, the transitivity of the ρ network in the α band is higher when the average time response decreases for children 03 and 07.

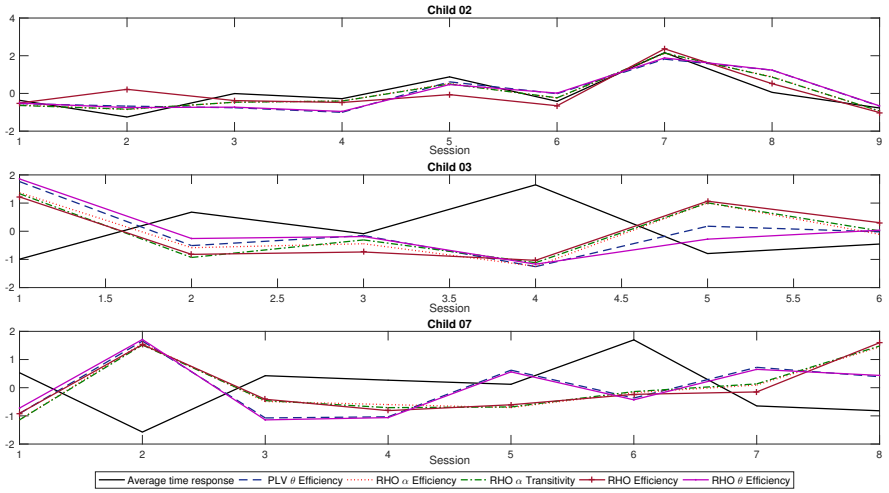

Figure 5.6: Average time response and FC-graph measures relative to the GOLIAH stimuli across different sessions for each child.

5.6 Summary

Complex network analysis on functional connectivity is a potential tool in objectively measuring the segregation and integration phenomena underlying the brain activity. These measures can be used to identify the key issues on the ongoing brain processing responsible for neurological diseases affecting in a lifespan from Autism Spectrum Disorder to Alzheimer disease. Therefore, they can be used to assess the neurological changes due to brain plasticity or due to an intervention, whether it is a behavioural or a pharmaceutical treatment. In case of a behavioural intervention, complex network would be useful for monitoring the progress of a subject undergoing the treatment in terms of neurological and related behavioural outcomes.

In recent studies, various functional connectivity and network measures have been applied for investigating the altered brain connectivity in ASD. In (Orekhova et al., 2014; Boersma et al., 2013; Matlis et al., 2015; Peters et al., 2013; Barttfeld et al., 2011) the characteristic path length, network modularity and clustering coefficient were found to differ in ASD population compared to the typical subjects, indicating a less efficient brain network. However, these studies were conducted on subjects with different ages, from childhood to adulthood, making the comparison of their results impractical. Nevertheless, each study focuses on different EEG bands and is based on different types of functional connectivity network, from coherence to synchronisation likelihood.

These limitations motivated us to investigate the brain connectivity in different EEG bands and using various functional connectivity measures. Moreover, these studies are conducted either on a resting condition or on a task-dependent condition, like the presentation of repetitive stimuli. Unlike the previous studies, we use engaging stimuli that are based on pivotal skills to assess the child's brain connectivity across the intervention along with the correspondent behavioural metrics.

The analysis following this approach showed that only the networks based on the phase synchronisation in almost all the bands (except the γ band) are indicative of the child progression. Among the network metrics, the transitivity and the path-based features, like radius and diameter, change across the intervention. However, there are several limitations which prevent us from drawing any significant conclusion. The present study has several limitations, mainly related to the sample size and the absence of a control group and due to the setup-phase of the framework.

First, a control group with age-matched children would have lead to a comparison of neurobiological features in children with ASD versus a typical population. This comparison is needed both for the characterisation of the two populations as well as for the assessment of the GOLIAH-based intervention in a longitudinal approach.

Second, given the ample set of stimuli and games, the framework has high potentials for a longitudinal analysis assessing the changes in brain connectivity along the intervention. With a longer period of intervention, the games and stimuli can be selected to ensure the analysis of EEG features in a stimulus and game specific approach. Since each game addresses different crucial skills in ASD, the correspondent game specific-neurobiological features could indicate the progress of the child in each skill during the intervention. Furthermore, this progress could be then analysed from a behavioural perspective by comparison with the GOLIAH features, as attempted in this analysis.

Third, the 3-month open trial included the setup phase of the framework which reduced additionally the sample size available for the analysis presented in this chapter.

Nonetheless, this framework can be used with a greater population size including typical and autistic children in a prolonged longitudinal study to lead to neurological biomarkers for further analysis of developmental trajectories.

Chapter 6

Brain Connectivity analysis in predicting cognitive outcomes in HIE classification

Chapter 5 demonstrated how to monitor intervention in ASD with behavioural and neuro-developmental features. Specifically, we performed the neuro-developmental monitoring by using the *FC-networks* extracted from EEG recorded during the GOLIAH game activity. The graph theoretical measures extracted from the *FC-networks* were used to analyse the changes in cognitive efficiency during the behavioural intervention. Different network measures reflected the variation of the degree of local and global brain connectivity.

This *FC-networks* analysis can be assessed from the EEG recorded not only in children or adults, but also during early postnatal period (Tokariev et al., 2015), allowing the analysis of the neuro-cognitive functions in newborns at-risk (who can develop neurological pathologies later in life). In essence, the *FC-network* features could be used to predict the development of neuro-congnitive pathologies in newborns. We identified the neonates affected by HIE at birth as an at-risk population for neuro-cognitive and neuromotor impairments, as described in Section 2.7.

In this Chapter, we employ *FC-networks* to predict neuromotor and cognitive outcomes in newborns affected by HIE at birth and recruited for a two-year follow-up. The subjects were assessed at two years old with a standardised clinical examination. EEG data recorded at birth are used for the extraction of the *FC-networks*. The graph properties of the *FC-networks* are used in a classification approach to distinguish the group of individuals who will later develop atypical brain functioning from those who will not. The main goal of this approach is to investigate whether it is possible to predict cognitive outcomes within two years of life by using the *FC-networks* constructed from EEG recorded at birth.

Chapter 2 presented the traditional methods employed in the analysis of the EEG recordings for HIE disease to predict neuro-developmental outcomes at an older age. They are based on the visual inspection by expert clinicians and the use of thresholds of the EEG amplitude values (Awal et al., 2016). Although used for predicting neuro-developmental outcomes, these methods are not informative on the type of brain functioning alterations. In contrast to the typical approach, *FC-network* features from EEG data are informative of the brain connectivity efficiency and can be used to identify the type of brain connectivity alterations, concerning the integration and segregation phenomena within and between brain areas.

The remainder of this chapter is structured as follows. In Section 6.1 we describe the methodology proposed to predict cognitive outcomes in newborns at-risk. In Section 6.2, we describe the classifiers employed to perform the outcome predictions together with details on the feature ranking and reduction. Next, we provide details of the selected population at risk recruited in a two-year follow-up in 6.3. The classification results obtained on this population are given in Section 6.4. Finally, Section 6.5 concludes the chapter with a summary of the results.

6.1 Classification of Hypoxic Ischemic Encephalopathy using Brain Connectivity Measures Extracted from Resting State EEG

The purpose of this work is to investigate whether the EEG recorded at birth after a HIE episode is informative to predict neuro-motor outcomes assessed with a neurological evaluation at two years old. To fulfil this objective we propose a methodology which combines: (a) the *FC-networks* constructed from the EEG recorded at birth and (b) the results of a neurological assessment at two years old. In essence, we consider newborns affected by HIE at birth as a population at risk of developing cognitive impairments.

Figure 6.1 shows the methodology applied for the outcome prediction in children affected by HIE. After the episode of HIE at birth, during the first two weeks of their life EEG data was recorded from the newborns during sleep (Figure 6.1(a)). The EEG recordings are then pre-processed with the WPTEMD artefact suppression algorithm (Chapter 4) to suppress the presence of artefacts due to physiological activity and body movement (Figure 6.1(b)). The processed EEG data are then divided into epochs of eight seconds (Figure 6.1(c)). For each subject six epochs are obtained and used for the extraction of various FC (Figure 6.1(d)). To neglect spurious connectivity (Fallani et al., 2014), the FC are averaged across the six epochs (Figure 6.1(e)). The average-FC is then used to extract the corresponding *FC-networks* (Figure 6.1(e)) and the related *FC-graph* features (Figure 6.1(f)) through the application of graph theoretic measures. Feature ranking and selection are performed on the obtained *FC-graph* features (Figure 6.1(g))

to identify the most discriminative features used as input to the classifiers. Both feature ranking and selection together with the classification are performed iteratively for several runs during the Leave-One-Out Crossvalidation. A follow-up of two years is performed at hospital on the newborns (Figure 6.1(h)). The results of a standardised neurological assessment conducted at two years old are used as class labels during the training of the classifiers (Figure 6.1(i)).

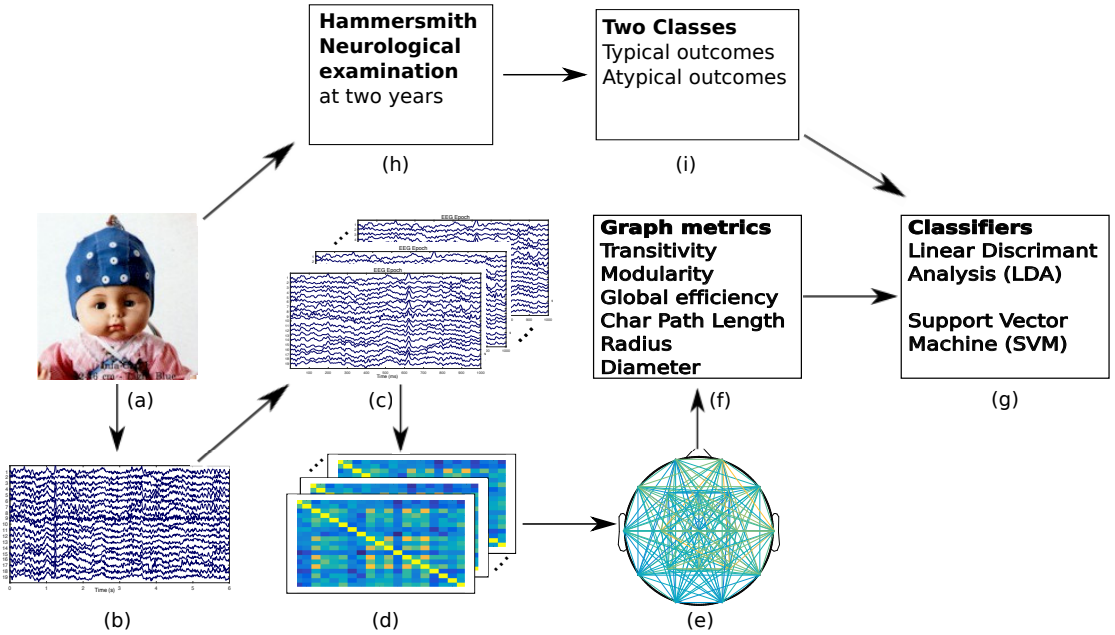

Figure 6.1: Workflow of the classification of the HIE neuromotor outcomes based on resting-state EEG recordings. For each newborn (a) the EEG recordings are used to extract functional connectivity network features (b-f) describing the functional connectivity during the first two weeks of life. These features, together with (h-i) a neurological assessment tool, are used to (g) train the classifiers for the prediction of atypical cognitive functionalities at two years.

While in Chapter 5 the *FC-graph* features are extracted from stimulus-based EEG data, here we use eight seconds resting-state EEG data. The resting state condition encompasses spontaneous brain activity that occurs according to a complex network which can reveal information about the brain organisation in neurodevelopment disorders (Birn et al., 2013). During the eight seconds epoch, the neural activity of interest takes place recurrently and hence can be sufficiently represented by the recordings (Fallani et al., 2014). Eight seconds EEG resting epochs were used in (Van Diessen et al., 2013) to extract brain networks based on Synchronisation Likelihood to classify between children diagnosed with partial epilepsies from the typical children. van der Molen et al. (2014) found altered FC and network topology from resting EEG in individuals affected by Fragile X syndrome, showing increased path length of the PLI indicating impaired information transfer between brain regions in θ band.

Among the Functional Connectivity measures introduced in Section 1.2, undirected FC measures are selected in this work listed in Table 5.1. The Phase Synchronisation based measures are extracted in specific frequency bands: *theta* $(4-7.5$ Hz), α $(8-13$ Hz), β $(13-30$ Hz), γ $(30-42$ Hz), *AllBands* $(4-42$ Hz). Different bands are informative of different mind states (see Section 2.4.2). Various studies on different brain pathologies showed altered complex networks in these bands (Heunis et al., 2016; Alba et al., 2015), although there is no consensus on a single band. Thus, we here select all these bands to identify any alteration in the brain connectivity that could be caused by HIE at birth.

As shown in Figure 6.1(e), various graph measures were extracted from the average FC to describe these variables in terms of complex networks. Table 6.1 lists the graph networks applied on the *average FC-networks* along with a brief description. More details on these measures are given in Section 5.2.1. In general, given a FC measure the graph features of the corresponding complex network describe the interactions among the EEG at different electrodes, in terms of communication paths, segregated community and integration among those communities (Rubinov and Sporns, 2010).

Complex network measure	**Description**
Transitivity	Measure of segregation; it measures how many node's neighbours are connected among themselves
Modularity	Measure of segregation; it measures how much the network can be divided into subgroups with dense links within-groups and few links between-group
Characteristic path length	Measure of integration; measures the average distance between nodes across the entire network
Global efficiency	Measure of integration; it is the inverse of the distance between nodes
Radius	Measure of shape of network- minimum eccentricity
Diameter	Measure of shape of network- maximum eccentricity

Table 6.1: Graph theoretic measures extracted from the FC variables.

The combination of the FC measures and the graph matrices generate a total of N features that can be given as input to the classifier:

$$N = [6\,GS + (3\,PS * 5\,Bands)] \times 6\,Complex\ Network = 126 \tag{6.1}$$

These 126 *FC-graph* features are ranked based on their discriminative ability to identify those features that can be informative of future atypical cognitive and motor disabilities. Details on how to perform the feature ranking and reduction will be given in Section 6.2.4. The next section shows the classification techniques employed for the identification of the children with typical and atypical outcomes.

6.2 Classification techniques

Numerous classification algorithms have been applied on EEG features to distinguish between healthy population and individuals affected by various mental disorders. Among the various classification techniques, discriminant analysis, K-Nearest Neighbour (KNN), Support Vector Machine (SVM) and Naive Bayesian have been applied to classify between healthy subjects and individuals with a diagnosis or defined at high risk of ASD (Matlis et al., 2015; Khosrowabadi et al., 2015; Bosl et al., 2011). Binary decision tree was used to identify epileptic children (Van Diessen et al., 2013). To the best of our knowledge, there are no previous studies on the classification of neuro-motor outcomes on individuals affected by HIE at birth based on EEG recordings. Cognitive outcomes on individuals with neonatal encephalopathy (an umbrella term including HIE disease) were predicted using a SVM classifier based on the network features extracted from Diffusion Tractography Imaging (Ziv et al., 2013).

Among the various techniques cited above, in this study we restricted the classification problem to two supervised learning algorithms: Linear Discriminant Analysis (LDA) and Support Vector Machine (SVM). A probabilistic classification based approach is here avoided due to the limited number of subjects, as it is not reliable to build multi-dimensional probability density functions from the features for Bayesian classifier (Rogers and Girolami, 2015). In a common two class classification problem (typical and atypical condition, commonly indicated as normal vs diseased), the LDA and SVM construct a decision boundary to separate the two classes. While the LDA utilises all the training samples to build the decision boundary, the SVM considers those points that are critical between the two classes. More details about these classifiers and the decision boundary construction are given in the next sections.

6.2.1 Linear Discriminant Analysis (LDA)

Linear classifiers separate two classes by finding a single linear boundary between the two classes: they use decision boundaries which are straight lines, planes or hyperplanes in case of two, three or four or more features respectively. The class in a linear discriminant classifier is defined as:

$$y = \sum_{i=1}^{N} x_i w_i + b = \sum_{i=1}^{N+1} x_i w_i = \mathbf{Xw} \tag{6.2}$$

where the output y indicates the class label ($y \in [0, 1]$) depending if it is greater or less than 0.5, N is the number of input features, x_i is the i^{th} input feature, w_i and b are the free parameters of the classifier termed weight and offset respectively. The classifier is built by constructed the values of the free parameters that best separate the data.

During the training of the classifier, the vector d containing the class labels is specified: it consists of 0 and 1 depending of the class of each sample data. A Least Squared Estimation (LSE) approach is commonly applied to the training set to determine the values of the free parameters of the classifier. In this approach, the squared error between the predicted class d and the output class y is minimised. The squared error is defined as:

$$\varepsilon^2(w) = \sum_{i=1}^{N+1}(d_i - x_i^T w)^2 = (\mathbf{d} - \mathbf{Xw})^T(\mathbf{d} - \mathbf{Xw}) \tag{6.3}$$

The optimal weights w_{opt} of the classifier are obtained as following:

$$\mathbf{w} = (\mathbf{X^T X})^{-1}\mathbf{X^T d} \tag{6.4}$$

where T indicates the transpose of the input matrix $\mathbf{X}$.

Many biomedical datasets contain data which are not separable by a linear boundary; in this cases it is possible to apply a kernel function to transform the data into a higher dimensional space which will be linearly separable. The kernel function $k(x_i)$ applies a non linear transformation to the original data generating a new set of data. An example is a quadratic kernel function on a 2D dataset (consisting of two variables x_1 and x_2) that produces a 5D dataset with variables $x_1, x_2, x_1x_2, x_1^2, x_2^2$. These increased number of variables will then be used for the least squared error approach to find the new optimal free parameters. Since the number of weights in the classifier is bound to the number of input variables, the use of a kernel increases the number of free parameters used for the classification. On the other hand, working with a higher dimensional dataset requires a large number of samples in the training set to generalise well and increases the training time.

6.2.2 Support vector machine (SVM)

The SVM is another type of classifier which is based on decision boundaries. Unlike the LDA, giving emphasis to all data points of the training set, the SVM considers the most critical points (samples of the two classes that are closest to each other) during the search of the optimal free parameters. These points are called *support vectors* and the distance between these critical support vectors is referred as the margin M. The objective of the SVM classifier is to maximise this distance M between the two classes of support vectors employing an optimisation routine. In the maximisation of this distance, it is considered that all the data points lie on the appropriate side of the decision boundary. We here explain the value of the distance M to be maximised in the search of the optimum classification. In the SVM classifier, the class labels y are assumed to be ± 1, so that the

decision boundary is at $y = 0$ and defined as:

$$y = \sum_{i=1}^{N} x_i w_i + b = 0 \tag{6.5}$$

where y is the class label, x_i are the input data, w_i and b are the weights and bias of the classifier respectively. The line vectors at the critical points are defined as:

$$\begin{aligned} x_i w_i + b \geq 1 \text{ if } y = +1 \\ x_i w_i + b \leq 1 \text{ if } y = -1 \end{aligned} \tag{6.6}$$

The distance from these line vectors to the origin is defined as:

$$\begin{aligned} d_{0,1} &= \frac{1-b}{\|w\|} \\ d_{0,-1} &= \frac{-1-b}{\|w\|} \end{aligned} \tag{6.7}$$

which indicates that the free parameters w and b are chosen such that the samples of the two classes lie in the corresponding side of the support vector lines. According to the Equation 6.8, the distance M between the two vectors is defined as:

$$M = \frac{-1-b}{\|w\|} - \frac{-1-b}{\|w\|} = \frac{2}{\|w\|} \tag{6.8}$$

where $\|w\|$ is the norm of the weights and is equal to $\sqrt{w_1^2 + w_2^2 + w_3^2 + \cdots + w_N^2}$. This equation indicates that the maximum margin between the support vectors is obtained by minimising the weights w. The minimisation of the weights w is performed with the Sequential Minimal Optimisation (SMO) routine (Platt, 1998), although the Quadratic Programming (QP) can also be employed.

The SVM classifier described above separates the classes by using linear decision boundaries. When dealing with more complex datasets, the SVM classifier is applied on higher dimensional data obtained via a kernel transformation to separate the data. This allows to obtain non-linear decision boundaries to separate the classes. Common kernels used to increase the dimensionality of the dataset are the polynomial and spline.

The evaluation of the performance of a classifier is typically performed on separate datasets, named validation and test sets. A typical approach to validate the performance of the classifier is the cross-validation technique, explained in the following section.

6.2.3 LOOCV Cross-validation scheme

A good classifier should correctly classify the training examples and generalise its model to accurately predict on unseen data without overfitting the training data. Typically,

the supervised learning process is divided in three steps. First, the classifier is trained on a *training set*, where the examples are given to the classifier with the respective labels (indicating the class to which they belong to, like healthy vs. unhealthy). During this phase, the parameters of the classifier are modified in order to minimise the classification errors. Once the classifier's model is obtained, it is then tested on a *validation set* (composed by unseen data) to identify the classification model that gives the best performances. This validation phase is used to measure how well the classifier generalises. These two stages (training and validation) are repeated to determine the best model that will be then used on a *test set* to predict the unknown outcomes.

When dealing with a small sample size, as in our case, this three-stage procedure is slightly different. The generalisation performance is influenced by the choice of the validation data. In this case, a Leave One Out Cross Validation (LOOCV) approach reduces this problem by making a more efficient use of the limited sample size. In the LOOCV, the entire dataset containing N observations, is divided in turn into a training set of $N-1$ examples, and a validation set comprised of the remaining single observation. This held out sample will be used to test the model trained with the $N-1$ observations. This procedure is repeated N times, so that all data will be used for validating the trained classifier. The final average accuracy is obtained by averaging over the accuracies of the multiple independent runs. The LOOCV is more computationally expensive than the well known N-fold cross-validation technique, but it is suitable in case of small sample size, as in our case. The datasets used as input to the classifiers both for the training and the validation of the models consist of several features which describe each sample belonging to one class or the other. The next section will introduce the selection and reduction of the features composing the datasets.

6.2.4 Preprocessing of Features, Feature Ranking and Reduction

In a classification problem, the data are described in terms of features which are preprocessed before modelling the classifier. The features extracted from the data are standardised according to the following:

$$z = \frac{x - \mu}{\sigma} \tag{6.9}$$

where z is the standardised feature with zero mean and unit standard deviation, μ is the mean value and σ the standard deviation of the original feature x. The standardisation of the features eliminates bias from features with high range of values and features with different units.

Once the features are standardised, they are used as input to the classifier to distinguish between two or more classes. The classification performance will depend on several factors: the discriminative power of the features, the suboptimal number of features, the

type of classifier and its parameters. The number of observations required to represent each class increases with the number of features given as input to the classifier (Lotte et al., 2007). A reduced dimensionality of the feature space leads to a lower computational complexity which could favour improved classification performance (Tanaka et al., 2006). Feature reduction is a common technique performed to reduce the dimensionality of the feature space, so that only the most discriminative features are employed. In order to do so, Fisher's Discriminant Ratio (FDR) is used to rank the features according to their discriminative ability. The FDR of an individual feature is calculated by the following:

$$FDR = \frac{\mu_1 - \mu_2}{\sigma_1^2 - \sigma_2^2} \tag{6.10}$$

where μ is the mean and σ^2 is the variance of the feature in class 1 and 2. The FDR allows to analyse each feature individually, with low computational cost compared to other approaches, like sequential forward selection. According to the Equation 6.10, the features with a large between-classes distance and a small within-class variance will be the most discriminative. The feature reduction is achieved by ranking the original k features in terms of FDR in ascending order and selecting the highest ranked l features.

Once the features are selected, the training set will be built and given as input to the classifier. The training and validation phases will allow to identify the best classifier model capable of separating the classes. The ability of this classifier of performing the class separation is then evaluated with different measures described in the next section.

6.2.5 Classification Performance Measures

The performance of a classifier is evaluated by the conventional measures of sensitivity, specificity and accuracy, described in Equation 6.11. These measures are calculated by assessing the amount of correct and wrong classification. In a binary classification problem, the two classes are defined as positive P (diseased class) and negative N (healthy class). The sensitivity of the classifier, also known as True Positive Rate (TPR), indicates the ratio of atypical subjects correctly classified. The specificity, also known as True Negative Rate (TNR), indicates the ratio of healthy individuals correctly classified with respect to all the subjects affected by the disease. The accuracy is the ratio of correctly classified individuals among all the classified samples.

$$\begin{aligned} Sensitivity &= \frac{\mathrm{TP}}{\mathrm{TP} + \mathrm{FN}} \\ Specificity &= \frac{\mathrm{TN}}{\mathrm{TN} + \mathrm{FP}} \\ Accuracy &= \frac{\mathrm{TP} + \mathrm{TN}}{\mathrm{TP} + \mathrm{TN} + \mathrm{FP} + \mathrm{FN}} \end{aligned} \tag{6.11}$$

An ideal classifier would have both Sensitivity and Specificity equal to 1. However, real classifiers require a trade-off between sensitivity and specificity: the higher the sensitivity, the lower the specificity.

6.3 Participants and sessions

The methodology described in Figure 6.1 was tested on 16 subjects affected by HIE at birth at the University Hospital Southampton, Department of Clinical Neurophysiology. 19-channel EEG data was recorded during sleep for 20 minutes during the first two weeks of life with Xltek (Natus Medical Incorporated) and Nihon Kohden EEG systems with a sampling frequency of 512 Hz. The EEG electrodes were placed according to the international 10-20 system. A segment of EEG of 1-minute duration was selected for the EEG analysis and epoch extraction. At a mean age of 24 months, the standardised Hammersmith Infant Neurological Examination tool was performed by expert clinicians for the assessment of posture, muscle and reflexes. The findings were categorised into three groups: *typical*, *unspecific signs* and *atypical outcomes*. The unspecific signs indicate mild, hypo- or hypertonia, mild asymmetry in tone without functional impairment and not meeting criteria for the diagnosis of cerebral palsy. Atypical outcomes are identified when meeting the criteria for the diagnosis of Cerebral Palsy (CP) as defined by the Surveillance of Cerebral Palsy in Europe, SCPE, 2000. For the purpose of this study, based on the assessment outcomes, the subjects were divided in two categories: *typical* and *atypical*, as shown in Table 6.2. The typical group consists of nine newborns categorised as normal with the Hammersmith Infant Neurological Examination at the age of two. The atypical class groups seven neonates classified as having unspecific signs (four subjects) and abnormal outcomes (three subjects). One subject was not considered in this analysis because he was deceased before the assessment planned at two years. The age of the newborns at the time of EEG recording is variable, and some of the children have been cooled at the time of EEG recordings.

Groups	**Neonates**	**Age (days) at EEG (mean ± std)**	**Cooled at time of EEG**
Typical outcome	9	3 ± 3.11	6
Atypical outcome	7	3 ± 2.07	5

Table 6.2: Clinical data for neonates in the two groups used to predict clinical outcomes from EEG-based features and assessed at two years old.

The classification task between the two groups is based on 126 *FC-graph* features extracted from the EEG recordings, as defined in Equation 6.1. Although the Phase Synchronisation and the Generalised Synchronisation are measures based on different approaches (the first is in frequency domain, the latter in time domain), they both determine the statistical dependency between the electrophysiological signals at different

electrode sites. Therefore, it might be of interest to investigate which feature or which combination of them can best discriminate between the two health conditions. For this purpose, we apply feature ranking, as described in the next section.

The techniques introduced in the previous sections related to the features reduction and selection and the classifiers are used as described in Section 6.1. The results obtained by employing such approach are described in the following section.

6.4 Results and Discussion

In this chapter, we investigate whether the *FC-graph* features extracted from EEG data recorded from newborns in the first two weeks of life can predict altered neuromotor and cognitive outcomes assessed at hospital at two years old. To do so, we extracted 126 *FC-graph* features and used them as input to two classifiers. In this section, first we show the various features obtained with the ranking and selection across different training runs, along with their occurrence of selection. Later, we show the performances obtained with the two classifiers.

6.4.1 Feature ranking and reduction of the Functional Connectivity Network

The most discriminative features are here identified with the FDR criterion (Equation 6.10). At each run of the LOOCV, the standardised dataset (with M samples) is divided into training (with $M-1$ samples) and test set (with 1 sample). Next, the training set is used to rank the features according to the FDR criterion. For its calculation, each feature is considered individually to identify its class separability strength. Once the FDR is obtained for all the *FC-graph* features, the features are then ranked according to their decreasing order of importance. Among the N number of original features, only the K most discriminative features (with the highest FDR-based ranking) are further analysed. The Pearson's correlation coefficient is calculated for the K features to identify the most discriminative variables containing singular (non-redundant) information. As a results of this approach, a reduced set of Q features is obtained from the original feature set with N variables. The reduced dataset consists of Q informative discriminant variables that could address the presence of atypical functional connectivity in subjects who will later develop cognitive impairments. The ensemble of FDR and Pearson's correlation coefficient allows to perform feature reduction while preserving the physical significance of each variables, as opposed to other feature reduction techniques. In fact, feature reduction is typically accomplished by the Principal Component Analysis: it applies a transformation on the original features to provide a reduced number of

uncorrelated features. However, this technique provides new features which are difficult to interpret, being a combination of the original variables.

Figure 6.2 shows the 20 features characterised by the highest rank in terms of FDR, where the x-axis denotes the *FC-graph* features and the y-axis indicates the relative weightage (FDR). This is the result obtained with the generated training set for a single run of the LOOCV. The ranking changes at each iteration. Both categories of functional connectivity measures, (the Phase Synchronisation and the Generalised Synchronisation based measures) show high ranking. Within the Phase Synchronisation, all the measures extracted (PLI, PLV and RHO ρ) are within the 20 highest ranked features, although the PLI is characterised by the highest FDR. As mentioned above, these measures are extracted in different frequency bands. Among these bands, only the measures in the α band did not show any discrimination between the two groups. Among the Generalised Synchronisation, only the S measure is within the 20 highest ranked. While some of the functional connectivity measures are not within the best ranking, all the graph theoretic features are informative of the difference between the two classes.

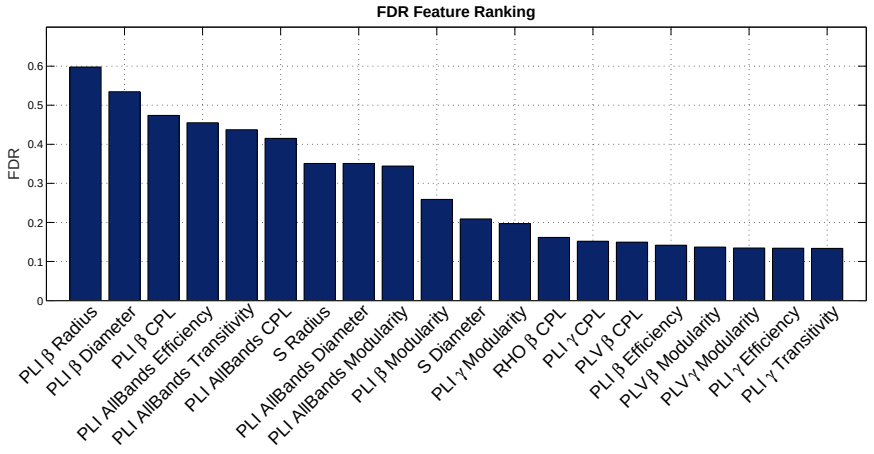

Figure 6.2: FDR score of the 20 features with the highest score in one of the 16 runs of the LOOCV.

The FDR ranking is informative on the discriminative nature of the features and it yields to a substantial reduction of the number of variables. Figure 6.2 shows that the FDR decreases to less than 0.2 around the 10^{th} features (PLI β Modularity).

Despite substantial feature space reduction, the FDR does not reveal the possible correlation among these 20 features. This implies that different variables could provide redundant information. Since the highest ranked features could convey similar information, we proceed to analyse the correlation among these highest FDR ranked based features. To identify a reduced number of measures that can give us unique information,

we calculate the Pearson's correlation coefficient to select those variables containing different information. Again this process is applied for the different training set generated at each iteration of the LOOCV.

Figure 6.3 shows the matrix of correlations among pairs of features. For ease of visualisation, only the 10 features with the highest FDR rank are shown. Each graph off the diagonal of Figure 6.3 is a scatterplot between two variables. The slope of the least-squares reference line is indicated in black and corresponds to the Pearson's correlation coefficient. The graphs in the diagonal of Figure 6.3 show the histogram of each variable which indicates the distribution of the values of each feature. As instance, Figure 6.4 shows that the variable 1 (PLI-Radius in β band) is highly correlated with the variables PLI-Diameter and Characteristic Path Length in β band. This analysis is performed for all the 20 features characterised by the highest FDR. This approach allows us to identify those variables containing redundant information for the purpose of the classification between the two class conditions. A threshold of 0.7 was set for the selection of the correlated features: those variables showing a correlation coefficient greater than the threshold are considered redundant and are discarded for the subsequent analysis.

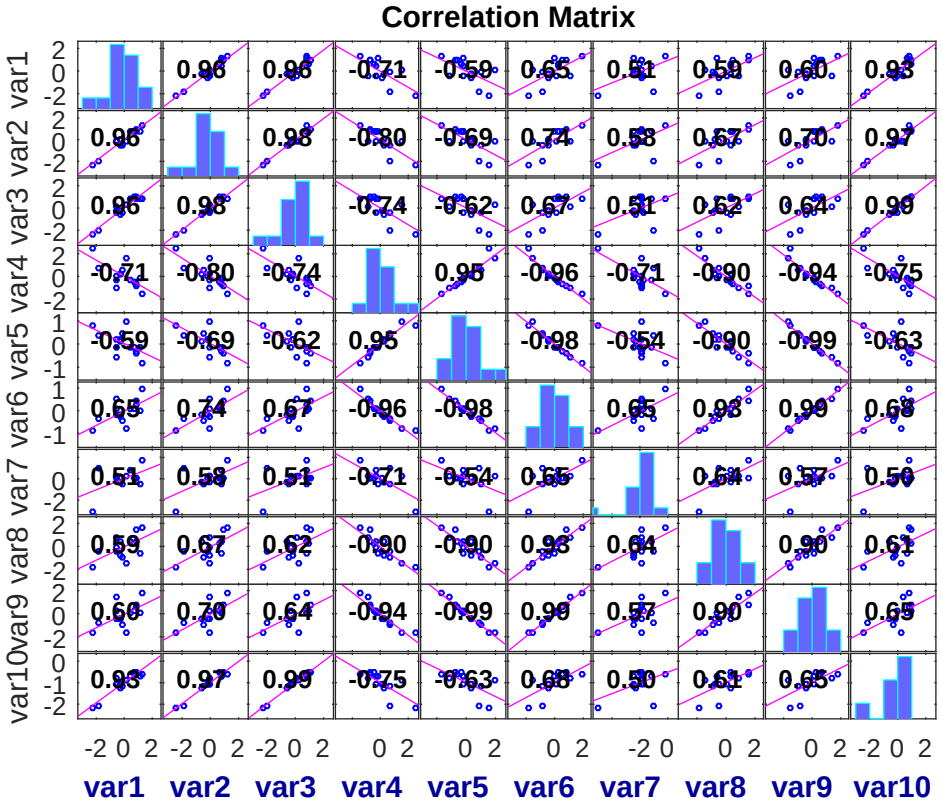

Figure 6.3: Pearson's correlation coefficient among the 10 features with the best ranking in terms of FDR.

This approach of feature selection and reduction using the FDR and the Pearson's correlation coefficient has yielded to ten total features for each iteration of the LOOCV.

Figure 6.4 shows the final ten features selected in the first iteration of the LOOCV, ranked in decreasing order of FDR value, where a high rank indicates a small within-class variance and a large between-class distance among the data points in the respective feature space. The ranked and least correlated features are then used as input to the classifiers to separate the newborns who were assessed as atypical (with unspecific signs or with cerebral palsy) from those who were assessed as typical at two years old.

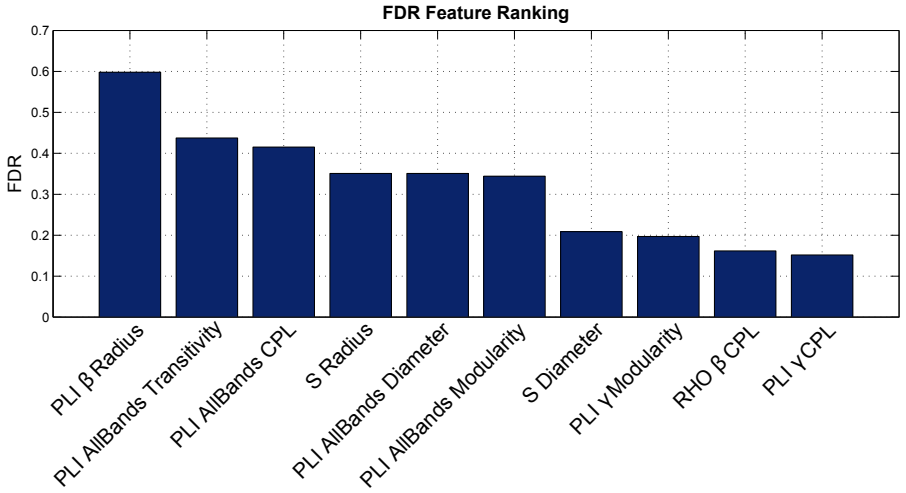

Figure 6.4: The ten features selected for the classification stage for a single iteration of the LOOCV.

The method described above was repeated at each run of the LOOCV: different features where obtained at each run. Figure 6.5 shows all the features that were included across all the runs, along with their selection occurrence. Among them, the PLI in *All Bands* ($[4-42]$Hz) and β band was the most selected.

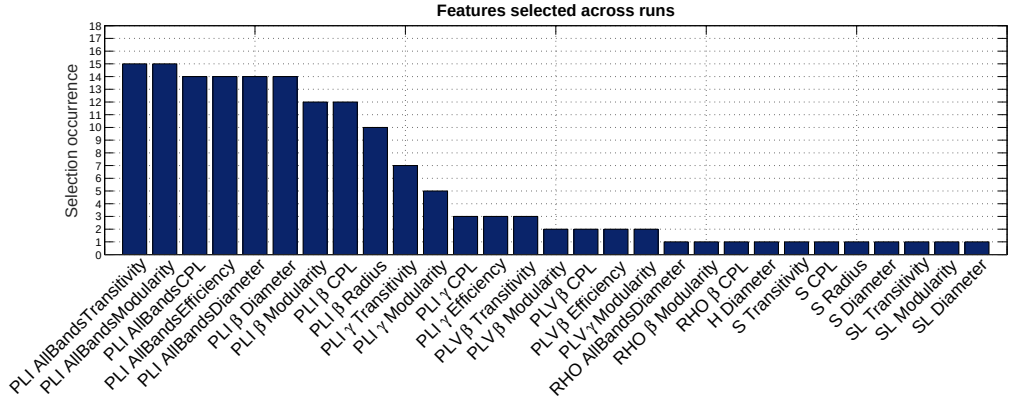

Figure 6.5: The selection occurrence indicates the number of runs in which each feature was selected.

The next section will show the performance obtained when classifying the HIE outcomes using the features selected with the method described above.

6.4.2 Classification performances

The classification of the neonates is performed using LOOCV on an increasing number of features among the ten best ranked and uncorrelated found at each single iteration, as shown in Figure 6.4. The approach used in this case is similar to the sequential forward algorithm: the classifiers are trained iteratively with two, three , four features and so on. The performance of the classifiers using different number of features are shown in Figure 6.6. The SVM classifier is used in its linear form and in combination with two polynomial kernels with order two and three respectively.

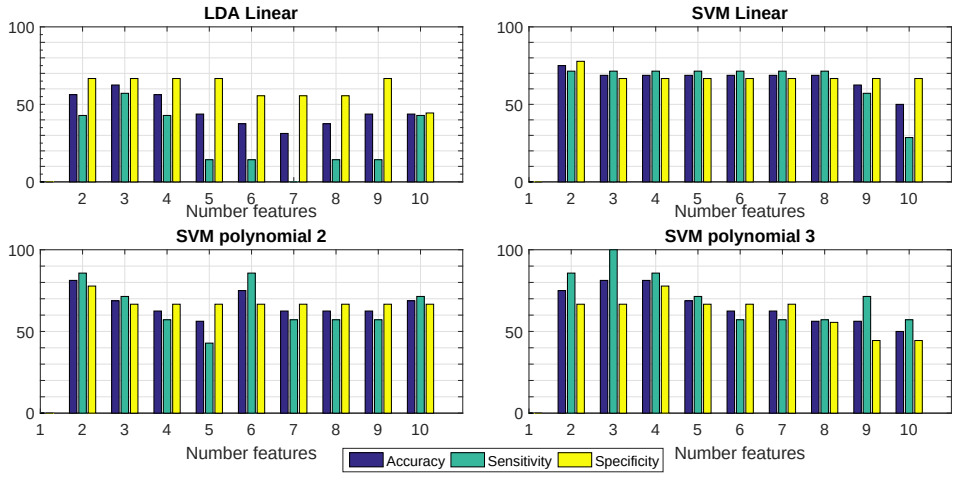

Figure 6.6: Performance of different classifiers with varying number of features. The performance is calculated in terms of accuracy, specificity and sensitivity.

Overall the best performances are provided by the SVM with the polynomial kernels of order two when using two features by the SVM with the polynomial kernels of order two when using three and four features. In the first case, the accuracy rate reaches the 81.3%, with a sensitivity of 85.7% and a specificity of 77.8%. This indicates that some of the healthy subjects were misclassified as atypical newborns and vice versa. In case of SVM with polynomial kernel of order two with three and four features, the accuracy obtained is the same, but the sensitivity and specificity reach 100% and 66.7% respectively in the first case, and 85.7% and 77.8% in the latter. The specificity at 100% indicates that all the subjects belonging to the atypical class were correctly classified, while some of the healthy subjects were misclassified as atypical newborns. The discriminant analysis performs poorly and does not provide significant classification rate. It is worth noting that, due to the small sample size, the chance level of classification is lower than 50%. Assuming that the classification errors obey a binomial cumulative distribution, the chance level of classification with a significance level of 0.05 with 17 samples and 2 classes is of 70.59%. For more details on the empirical chance level refer to Combrisson and Jerbi (2015).

6.5 Summary

The purpose of this study was to explore the possibility of using functional brain connectivity measures derived from resting-EEG recordings to classify newborns affected by HIE at birth who will later show atypical neuro-developmental tracts. The aim was also to identify those functional connectivity measures that yield to the best classification. The summary of the key findings of the present work for the prediction of neuro-developmental outcomes are as follow:

- The Phase Lag Index combined with various graph measures is the most selected index extracted from the EEG at rest to predict cognitive disabilities that are currently assessed at a later age.
- The SVM combined with polynomial kernels provides significant classification accuracy.
- Existing studies on the prediction of HIE outcomes are based on EEG based features describing the morphology of the recordings (amplitude and background EEG). However, these studies make use of thresholds for the classification of neurocognitive impairments. Nonetheless, there is no consensus on the threshold to be used. In contrast with the existing approaches, the work here described performs the classification without requiring any threshold.
- The misclassification of the SVM with polynomial kernel of order three affects the specificity, which implies that some of the healthy subjects are recognised as having atypical neuro-developmental outcomes. In a hospital scenario such classification method could be thought as a screening tool, for which a misclassification of the false positive would be less harmful than a misclassification on the false negative, as commonly accepted from the medical community.

Overall, these promising results suggest that the functional connectivity extracted on neonates can provide information on cognitive functioning which can be only assessed at a later age. Hence, further extensions of this work can lead to a longer follow-up with greater amount of subjects to both train and assess the classification on a larger pool of data.

Chapter 7

Conclusions

In this dissertation, we are concerned about developing strategy for treating cognitively impaired young children, more specifically ASD. Three things are extremely important for combating autism: early diagnosis, intensive intervention and monitoring. We contribute to each of these three strands throughout the work done in the dissertation in the following manner.

7.1 Summary of Results

Research has proved that at least 25 hours/week intensive intervention is needed for treating autistic children. However, such intervention hour is difficult to achieve in clinical settings. Therefore, in Chapter 3 we developed the multi-payer gaming platform GOLIAH to enable delivering computer-based intervention at-home settings to maximise the intervention hour.

The key feature of our game library is to implement a naturalistic treatment by targeting two cognitive skills impaired in autism (i.e. imitation and joint attention) fundamental for the learning process. We created various games with multiple difficulty levels and tasks, to allow the intervention to be tailored according to the child's cognitive skills. The platform was piloted in a 3-month open trial at two different hospital sites, mainly to assess its seamless operation and the appropriateness in extracting behavioural measures. The game platform was positively accepted by the therapists and parent during this longitudinal study. It also showed a rapid performance amelioration on cognitive tasks based on Imitation and joint attention skills and an amelioration in the child's abilities that were not directly targeted in the game. This also opens up the possibility of delivering tailored intervention in naturalistic settings and in a parent-mediated scenario.

Although the GOLIAH platform will generate the behavioural measures, it is more important to monitor the neurological bases of the behavioural outcome in this intervention scenario. For this purpose, we developed an EEG-based monitoring strategy. However, in naturalist environment EEG signal is highly corrupted by artefacts. Therefore, in Chapter 4, we proposed two novel automated artefact reduction algorithms for EEG recordings corrupted by body movements in naturalistic setting. Specifically, we designed two algorithms that do not require *a-priori* information of the nature of the artefact. We designed experiments to record eight types of artefacts and tested the two algorithms on semi-simulated and real EEG data. We also compared the two novel approaches with two *state-of-the-art* artefact reduction techniques. Results with semi-simulated data showed that WPTEMD algorithm outperforms all the other techniques, with an improved RMSE equal to 49.53% and 70.4% compared to wICA and FASTER respectively for highly corrupted data. WPTEMD also preserves the power spectrum of the EEG data in various frequency bands close to the original ground truth recordings. Similar results are shown with highly corrupted real data: WPTEMD performs consistently better than WPTICA in all the frequency bands and reduced the high-amplitude oscillations in the time-domain signal. WPTEMD outperforms the other technique for all the eight types of artifactual EEG recordings, thus it is selected for artefact suppression of the EEG recordings analysed in the next chapters of this dissertation.

In Chapter 5, we addressed the problem of analysing the ensemble of behavioural and neurological outcomes of the computer based intervention for five children recruited during the 3-month open trial. For these children, from the EEG recorded we first formulated the complex functional brain connectivity networks representing the functional brain connectivity underlying the cognitive tasks performed during the intervention. We then extracted the characteristic features of these complex networks and analysed their correlation with the behavioural measures generated by the game library. The exploration of these measures showed that the radius and diameter of the functional brain connectivity networks change along with the intervention together with the response time to the cognitive tasks that the children perform. However, the results should be considered as an exploratory step as the total number of samples was small to draw any statistical conclusion. However, this initial result shows the potential of the connectivity measures in monitoring cognitive development which needs to be validated using bigger sample size.

Finally, in Chapter 6, we further explored the possibility of using the functional brain connectivity networks derived from EEG data recorded from newborns affected by HIE at birth, identified as a population at-risk of developing ASD, as markers for early detection of cognitive impairments. In particular, we explored the problem of predicting the cognitive and neuromotor outcomes of the HIE assessed at a later age. Our objective was to test whether the functional connectivity networks extracted during the first two weeks of life are informative of the cognitive condition of the children at two years

age. We used the diagnosis obtained with a standardised assessment tool from expert clinicians to label the cognitive condition of the children at two years old. These labels were then used in a classification scenario to distinguish between the newborns who later manifested cognitive impairments from those who did not. Results showed that we were able to correctly classify between typical and atypical cognitive outcomes with a single brain connectivity feature (i.e. PLI-Radius in β band) with an accuracy of 87.5%.

When taken together, these results make a significant contribution to implementing a computer-based parent-mediated early intensive intervention combining behavioural and neuro-developmental analysis.

7.2 Future Work

The work described in this thesis provides a novel approach and framework that can further be exploited and expanded to study functional brain dynamics in a vast array of neuro-developmental disorders affecting young populations. In particular, the novelty relies on the fact that it allows to analyse the children's trajectories from a dual perspective: behavioural and neurological. The future prospects of this work are outlined as follows.

- **Longitudinal study with ample sample size**
  The framework proposed and described in this thesis was tested on a three month-open trial at two hospital sites and at home settings on ten children with ASD. Results assessed positively the feasibility of such methodology and were promising. It would be interesting to further exploit this framework in a longer period, as typically done with the conventional interventions. Moreover, a bigger sample size would allow to perform a variety of investigations. Since the ASD is a spectrum with different degrees of impairments, the children could be divided into subgroups based on their characteristics. In this scenario, it would be possible to assess the efficacy of the computer-based intervention for different subgroups of the spectrum.

- **Different neuro-developmental disorders**
  The framework proposed here can be employed to investigate the behavioural and neurological characteristics of other neuro-developmental disorder, as the ADHD. In fact, the game library could be expanded to implement games traditionally performed to treat other disorder. By doing so, it would allow to first investigate on the characteristics of those disorder, and possibly to identify the commonalities and differences between them.

- **Neurofeedback**
  The functional brain networks employed in this study provide a deeper understanding of the brain organisation during cognitive tasks. They could help therapists to

assess the improvement of the children during the intervention and could be used in a neuro-feedback scenario. Essentially, the games along with their different difficulty levels could be selected by therapist, based on the behavioural scores, with the help of neurophysiologist, based on the functional connectivity results.

References

Achard, S. and Bullmore, E. (2007). Efficiency and cost of economical brain functional networks. *PLoS Computational Biology*, 3(2):1–10.

Adam, I. (2010). *Complex Wavelet Transform: application to denoising*. PhD thesis, Politehnica University of Timisoara and Université de Rennes 1.

Adeli, H., Zhou, Z., and Dadmehr, N. (2003). Analysis of eeg records in an epileptic patient using wavelet transform. *Journal of neuroscience methods*, 123(1):69–87.

Adrian, E. D. and Matthews, B. H. (1934). The interpretation of potential waves in the cortex. *The Journal of Physiology*, 81(4):440–471.

Akhtar, M. T., Mitsuhashi, W., and James, C. J. (2012). Employing spatially constrained ica and wavelet denoising, for automatic removal of artifacts from multichannel eeg data. *Signal Processing*, 92(2):401–416.

Alaerts, K., Geerlings, F., Herremans, L., Swinnen, S. P., Verhoeven, J., Sunaert, S., and Wenderoth, N. (2015). Functional organization of the action observation network in autism: A graph theory approach. *PloS one*, 10(8):e0137020.

Alba, G., Pereda, E., Mañas, S., Méndez, L. D., González, A., and González, J. J. (2015). electroencephalography signatures of attention-deficit/hyperactivity disorder: clinical utility. *Neuropsychiatric disease and treatment*, 11:2755.

Altemeier, W. A. and Altemeier, L. E. (2009). How can early, intensive training help a genetic disorder? *Pediatric annals*, 38(3):167–70.

Ameis, S. H. and Catani, M. (2015). Altered white matter connectivity as a neural substrate for social impairment in autism spectrum disorder. *Cortex*, 62:158–181.

American Psychiatric Association (2013). *Diagnostic and Statistical Manual of Mental Disorders (DSM-5®)*. American Psychiatric Pub.

Andrzejak, R. G., Kraskov, A., Stögbauer, H., Mormann, F., and Kreuz, T. (2003). Bivariate surrogate techniques: necessity, strengths, and caveats. *Physical review E*, 68(6):066202–1–066202–15.

Arnhold, J., Grassberger, P., Lehnertz, K., and Elger, C. E. (1999). A robust method for detecting interdependences: application to intracranially recorded eeg. *Physica D: Nonlinear Phenomena*, 134(4):419–430.

Assaf, M., Jagannathan, K., Calhoun, V. D., Miller, L., Stevens, M. C., Sahl, R., O'Boyle, J. G., Schultz, R. T., and Pearlson, G. D. (2010). Abnormal functional connectivity of default mode sub-networks in autism spectrum disorder patients. *Neuroimage*, 53(1):247–256.

Awal, M. A., Lai, M. M., Azemi, G., Boashash, B., and Colditz, P. B. (2016). Eeg background features that predict outcome in term neonates with hypoxic ischaemic encephalopathy: A structured review. *Clinical Neurophysiology*, 127(1):285–296.

Babiloni, C., Pizzella, V., Gratta, C. D., Ferretti, A., and Romani, G. L. (2009). Fundamentals of electroencefalography, magnetoencefalography, and functional magnetic resonance imaging. *International review of neurobiology*, 86:67–80.

Bailey, D. L., Townsend, D. W., Valk, P. E., and Maisey, M. N. (2005). *Positron emission tomography*. Springer.

Baoi, J. (2014). Prevalence of autism spectrum disorder among children aged 8 years. *MMWR Morb. Mortal. Wkly. Rep*, 63:1–21.

Barbaro, J. and Halder, S. (2016). Early identification of autism spectrum disorder: Current challenges and future global directions. *Current Developmental Disorders Reports*, 3(1):67–74.

Barger, B. D., Campbell, J. M., and McDonough, J. D. (2013). Prevalence and onset of regression within autism spectrum disorders: a meta-analytic review. *Journal of autism and developmental disorders*, 43(4):817–828.

Barnea-Goraly, N., Kwon, H., Menon, V., Eliez, S., Lotspeich, L., and Reiss, A. L. (2004). White matter structure in autism: preliminary evidence from diffusion tensor imaging. *Biological psychiatry*, 55(3):323–326.

Barttfeld, P., Wicker, B., Cukier, S., Navarta, S., Lew, S., and Sigman, M. (2011). A big-world network in asd: dynamical connectivity analysis reflects a deficit in long-range connections and an excess of short-range connections. *Neuropsychologia*, 49(2):254–263.

Başar, E., Başar-Eroglu, C., Karakaş, S., and Schürmann, M. (2001). Gamma, alpha, delta, and theta oscillations govern cognitive processes. *International journal of psychophysiology*, 39(2):241–248.

Bassett, D. S. and Bullmore, E. (2006). Small-world brain networks. *The neuroscientist*, 12(6):512–523.

Bassett, D. S., Wymbs, N. F., Porter, M. A., Mucha, P. J., Carlson, J. M., and Grafton, S. T. (2011). Dynamic reconfiguration of human brain networks during learning. *Proceedings of the National Academy of Sciences*, 108(18):7641–7646.

Bastos, A. M. and Schoffelen, J.-M. (2015). A tutorial review of functional connectivity analysis methods and their interpretational pitfalls. *Frontiers in systems neuroscience*, 9.

Battocchi, A., Pianesi, F., Tomasini, D., Zancanaro, M., Esposito, G., Venuti, P., Ben Sasson, A., Gal, E., and Weiss, P. L. (2009). Collaborative puzzle game: a tabletop interactive game for fostering collaboration in children with autism spectrum disorders (asd). In *Proceedings of the ACM International Conference on Interactive Tabletops and Surfaces*, pages 197–204. ACM.

Belmonte, M. K., Allen, G., Beckel-Mitchener, A., Boulanger, L. M., Carper, R. A., and Webb, S. J. (2004). Autism and abnormal development of brain connectivity. *The Journal of Neuroscience*, 24(42):9228–9231.

Belmonte, M. K., Gomot, M., and Baron-Cohen, S. (2010). Visual attention in autism families:unaffectedsibs share atypical frontal activation. *Journal of Child Psychology and Psychiatry*, 51(3):259–276.

Berger, R. and Garnier, Y. (1999). Pathophysiology of perinatal brain damage. *Brain Research Reviews*, 30(2):107–134.

Bernardini, S., Porayska-Pomsta, K., and Smith, T. J. (2014). Echoes: An intelligent serious game for fostering social communication in children with autism. *Information Sciences*, 264:41–60.

Birn, R. M., Molloy, E. K., Patriat, R., Parker, T., Meier, T. B., Kirk, G. R., Nair, V. A., Meyerand, M. E., and Prabhakaran, V. (2013). The effect of scan length on the reliability of resting-state fmri connectivity estimates. *Neuroimage*, 83:550–558.

Blumberg, S. J., Zablotsky, B., Avila, R. M., Colpe, L. J., Pringle, B. A., and Kogan, M. D. (2015). Diagnosis lost: Differences between children who had and who currently have an autism spectrum disorder diagnosis. *Autism*, page 1362361315607724.

Boccaletti, S., Latora, V., Moreno, Y., Chavez, M., and Hwang, D.-U. (2006). Complex networks: Structure and dynamics. *Physics reports*, 424(4):175–308.

Boersma, M., Kemner, C., de Reus, M. A., Collin, G., Snijders, T. M., Hofman, D., Buitelaar, J. K., Stam, C. J., and van den Heuvel, M. P. (2013). Disrupted functional brain networks in autistic toddlers. *Brain connectivity*, 3(1):41–49.

Bono, V., Das, S., Jamal, W., and Maharatna, K. (2016a). Hybrid wavelet and emd/ica approach for artifact suppression in pervasive eeg. *Journal of neuroscience methods*, 267:89–107.

Bono, V., Jamal, W., Das, S., and Maharatna, K. (2014). Artifact reduction in multichannel pervasive eeg using hybrid wpt-ica and wpt-emd signal decomposition techniques. In *Acoustics, Speech and Signal Processing (ICASSP), 2014 IEEE International Conference on*, pages 5864 – 5868. IEEE.

Bono, V., Narzisi, A., Jouen, A.-L., Tilmont, E., Hommel, S., Jamal, W., Xavier, J., Billeci, L., Maharatna, K., Wald, M., et al. (2016b). Goliah: A gaming platform for home-based intervention in autism–principles and design. *Frontiers in psychiatry*, 7.

Bosl, W., Tierney, A., Tager-Flusberg, H., and Nelson, C. (2011). Eeg complexity as a biomarker for autism spectrum disorder risk. *BMC medicine*, 9(1):1.

Boucher, J. (2012). Research review: structural language in autistic spectrum disorder–characteristics and causes. *Journal of Child Psychology and Psychiatry*, 53(3):219–233.

Bressler, S. L. and Kelso, J. (2001). Cortical coordination dynamics and cognition. *Trends in cognitive sciences*, 5(1):26–36.

Buescher, A. V., Cidav, Z., Knapp, M., and Mandell, D. S. (2014). Costs of autism spectrum disorders in the united kingdom and the united states. *JAMA pediatrics*, 168(8):721–728.

Bullmore, E. T. and Bassett, D. S. (2011). Brain graphs: graphical models of the human brain connectome. *Annual review of clinical psychology*, 7:113–140.

Bunce, S. C., Izzetoglu, M., Izzetoglu, K., Onaral, B., and Pourrezaei, K. (2006). Functional near-infrared spectroscopy. *Engineering in Medicine and Biology Magazine, IEEE*, 25(4):54–62.

Bush, R. A., Stahmer, A. C., and Connelly, C. D. (2015). Exploring perceptions and use of the electronic health record by parents of children with autism spectrum disorder: A qualitative study. *Health informatics journal*, page 1460458215581911.

Bushberg, J. T. and Boone, J. M. (2011). *The essential physics of medical imaging*. Lippincott Williams & Wilkins.

Buzsáki, G. and Wang, X.-J. (2012). Mechanisms of gamma oscillations. *Annual review of neuroscience*, 35:203.

Carpenter, M., Nagell, K., Tomasello, M., Butterworth, G., and Moore, C. (1998). Social cognition, joint attention, and communicative competence from 9 to 15 months of age. *Monographs of the society for research in child development*, pages i–174.

Carter, A. R., Shulman, G. L., and Corbetta, M. (2012). Why use a connectivity-based approach to study stroke and recovery of function? *Neuroimage*, 62(4):2271–2280.

Castellanos, N. P. and Makarov, V. A. (2006). Recovering eeg brain signals: artifact suppression with wavelet enhanced independent component analysis. *Journal of neuroscience methods*, 158(2):300–312.

Catani, M., DellAcqua, F., and De Schotten, M. T. (2013). A revised limbic system model for memory, emotion and behaviour. *Neuroscience & Biobehavioral Reviews*, 37(8):1724–1737.

Chen, X., Liu, A., Peng, H., and Ward, R. K. (2014). A preliminary study of muscular artifact cancellation in single-channel eeg. *Sensors*, 14(10):18370–18389.

Cheng, L., Kimberly, G., and Orlich, F. (2003). Kidtalk: online therapy for aspergers syndrome. Technical report, Technical Report, Social Computing Group, Microsoft Research.

Chi, Y. M., Jung, T.-P., and Cauwenberghs, G. (2010). Dry-contact and noncontact biopotential electrodes: methodological review. *Biomedical Engineering, IEEE Reviews in*, 3:106–119.

Chicharro, D. and Andrzejak, R. G. (2009). Reliable detection of directional couplings using rank statistics. *Physical Review E*, 80(2):026217.

Chien, M.-E., Jheng, C.-M., Lin, N.-M., Tang, H.-H., Taele, P., Tseng, W.-S., and Chen, M. Y. (2015). ican: A tablet-based pedagogical system for improving communication skills of children with autism. *International Journal of Human-Computer Studies*, 73:79–90.

Cobb, W., Guiloff, R., and Cast, J. (1979). Breach rhythm: the eeg related to skull defects. *Electroencephalography and clinical neurophysiology*, 47(3):251–271.

Coben, R., Mohammad-Rezazadeh, I., and Cannon, R. L. (2014). Using quantitative and analytic eeg methods in the understanding of connectivity in autism spectrum disorders: a theory of mixed over-and under-connectivity. *Frontiers in human neuroscience*, 8:45.

Collado-Mateo, D., Adsuar, J. C., Olivares, P. R., Cano-Plasencia, R., and Gusi, N. (2015). Using a dry electrode eeg device during balance tasks in healthy young-adult males: Test–retest reliability analysis. *Somatosensory & Motor Research*, 32(4):219–226.

Combrisson, E. and Jerbi, K. (2015). Exceeding chance level by chance: The caveat of theoretical chance levels in brain signal classification and statistical assessment of decoding accuracy. *Journal of neuroscience methods*, 250:126–136.

Costanzo, V., Chericoni, N., Amendola, F. A., Casula, L., Muratori, F., Scattoni, M. L., and Apicella, F. (2015). Early detection of autism spectrum disorders: From retrospective home video studies to prospective high risksibling studies. *Neuroscience & Biobehavioral Reviews*, 55:627–635.

Courchesne, E., Carper, R., and Akshoomoff, N. (2003). Evidence of brain overgrowth in the first year of life in autism. *Jama*, 290(3):337–344.

Courchesne, E., Karns, C., Davis, H., Ziccardi, R., Carper, R., Tigue, Z., Chisum, H., Moses, P., Pierce, K., Lord, C., et al. (2001). Unusual brain growth patterns in early life in patients with autistic disorder an mri study. *Neurology*, 57(2):245–254.

Courchesne, E. and Pierce, K. (2005a). Brain overgrowth in autism during a critical time in development: implications for frontal pyramidal neuron and interneuron development and connectivity. *International journal of developmental neuroscience*, 23(2):153–170.

Courchesne, E. and Pierce, K. (2005b). Why the frontal cortex in autism might be talking only to itself: local over-connectivity but long-distance disconnection. *Current opinion in neurobiology*, 15(2):225–230.

Crespo-Garcia, M., Atienza, M., and Cantero, J. L. (2008). Muscle artifact removal from human sleep eeg by using independent component analysis. *Annals of biomedical engineering*, 36(3):467–475.

Da Silva, F. L. (2009). Eeg: Origin and measurement. In *EEG-fMRI*, pages 19–38. Springer.

Darvas, F., Scherer, R., Ojemann, J. G., Rao, R., Miller, K. J., and Sorensen, L. B. (2010). High gamma mapping using eeg. *Neuroimage*, 49(1):930–938.

Dawson, G. (2008). Early behavioral intervention, brain plasticity, and the prevention of autism spectrum disorder. *Development and psychopathology*, 20(03):775–803.

Dawson, G., Jones, E. J., Merkle, K., Venema, K., Lowy, R., Faja, S., Kamara, D., Murias, M., Greenson, J., Winter, J., et al. (2012). Early behavioral intervention is associated with normalized brain activity in young children with autism. *Journal of the American Academy of Child & Adolescent Psychiatry*, 51(11):1150–1159.

Dawson, G. and Osterling, J. (1997). Early intervention in autism. *The effectiveness of early intervention*, pages 307–326.

Dawson, G., Rogers, S., Munson, J., Smith, M., Winter, J., Greenson, J., Donaldson, A., and Varley, J. (2010). Randomized, controlled trial of an intervention for toddlers with autism: the early start denver model. *Pediatrics*, 125(1):e17–e23.

De Clercq, W., Vergult, A., Vanrumste, B., Van Paesschen, W., and Van Huffel, S. (2006). Canonical correlation analysis applied to remove muscle artifacts from the electroencephalogram. *Biomedical Engineering, IEEE Transactions on*, 53(12):2583–2587.

de Lissa, P., Sörensen, S., Badcock, N., Thie, J., and McArthur, G. (2015). Measuring the face-sensitive n170 with a gaming eeg system: A validation study. *Journal of neuroscience methods*, 253:47–54.

Delorme, A., Makeig, S., and Sejnowski, T. (2001). Automatic artifact rejection for eeg data using high-order statistics and independent component analysis. In *International workshop on ICA (San Diego, CA)*.

Dominey, P. F. and Dodane, C. (2004). Indeterminacy in language acquisition: the role of child directed speech and joint attention. *Journal of Neurolinguistics*, 17(2):121–145.

Dworzynski, K., Ronald, A., Bolton, P., and Happé, F. (2012). How different are girls and boys above and below the diagnostic threshold for autism spectrum disorders? *Journal of the American Academy of Child & Adolescent Psychiatry*, 51(8):788–797.

Eisenberger, N. I., Lieberman, M. D., and Williams, K. D. (2003). Does rejection hurt? an fmri study of social exclusion. *Science*, 302(5643):290–292.

Elliott, R. (2003). Executive functions and their disorders imaging in clinical neuroscience. *British medical bulletin*, 65(1):49–59.

Elsabbagh, M., Divan, G., Koh, Y.-J., Kim, Y. S., Kauchali, S., Marcín, C., Montiel-Nava, C., Patel, V., Paula, C. S., Wang, C., et al. (2012). Global prevalence of autism and other pervasive developmental disorders. *Autism Research*, 5(3):160–179.

Emery, N. (2000). The eyes have it: the neuroethology, function and evolution of social gaze. *Neuroscience & Biobehavioral Reviews*, 24(6):581–604.

Fallani, F. D. V., Richiardi, J., Chavez, M., and Achard, S. (2014). Graph analysis of functional brain networks: practical issues in translational neuroscience. *Phil. Trans. R. Soc. B*, 369(1653):20130521.

Fein, D., Barton, M., Eigsti, I.-M., Kelley, E., Naigles, L., Schultz, R. T., Stevens, M., Helt, M., Orinstein, A., Rosenthal, M., et al. (2013). Optimal outcome in individuals with a history of autism. *Journal of Child Psychology and Psychiatry*, 54(2):195–205.

Fombonne, E. (2009). Epidemiology of pervasive developmental disorders. *Pediatric research*, 65(6):591–598.

Friston, K. J. (1994). Functional and effective connectivity in neuroimaging: a synthesis. *Human brain mapping*, 2(1-2):56–78.

Frith, C. (2003). What do imaging studies tell us about the neural basis of autism. *Autism: Neural basis and treatment possibilities*, pages 149–176.

Funahashi, S. (2001). Neuronal mechanisms of executive control by the prefrontal cortex. *Neuroscience research*, 39(2):147–165.

Gandhi, T., Panigrahi, B. K., and Anand, S. (2011). A comparative study of wavelet families for eeg signal classification. *Neurocomputing*, 74(17):3051–3057.

García-Primo, P., Hellendoorn, A., Charman, T., Roeyers, H., Dereu, M., Roge, B., Baduel, S., Muratori, F., Narzisi, A., Van Daalen, E., et al. (2014). Screening for autism spectrum disorders: state of the art in europe. *European child & adolescent psychiatry*, 23(11):1005–1021.

Goñi, J., van den Heuvel, M. P., Avena-Koenigsberger, A., de Mendizabal, N. V., Betzel, R. F., Griffa, A., Hagmann, P., Corominas-Murtra, B., Thiran, J.-P., and Sporns, O. (2014). Resting-brain functional connectivity predicted by analytic measures of network communication. *Proceedings of the National Academy of Sciences*, 111(2):833–838.

Greenspan, S. I. and Wieder, S. (2009). *Engaging autism: Using the floortime approach to help children relate, communicate, and think*. Da Capo Press.

Grummett, T., Leibbrandt, R., Lewis, T., DeLosAngeles, D., Powers, D., Willoughby, J., Pope, K., and Fitzgibbon, S. (2015). Measurement of neural signals from inexpensive, wireless and dry eeg systems. *Physiological measurement*, 36(7):1469.

Gutstein, S. and Sheely, R. K. (2002). *Relationship development intervention with children, adolescents and adults: Social and emotional development activities for Asperger syndrome, autism, PDD and NLD*. Jessica Kingsley Publishers.

Haacke, E. M., Brown, R. W., Thompson, M. R., Venkatesan, R., et al. (1999). *Magnetic resonance imaging: physical principles and sequence design*. Wiley-Liss New York.

Hall, H. R. (2012). Families of children with autism: behaviors of children, community support and coping. *Issues in comprehensive pediatric nursing*, 35(2):111–132.

Hallez, H., De Vos, M., Vanrumste, B., Van Hese, P., Assecondi, S., Van Laere, K., Dupont, P., Van Paesschen, W., Van Huffel, S., and Lemahieu, I. (2009). Removing muscle and eye artifacts using blind source separation techniques in ictal eeg source imaging. *Clinical Neurophysiology*, 120(7):1262–1272.

Handayani, N., Akbar, Y., Khotimah, S., Haryanto, F., Arif, I., and Taruno, W. (2016). Preliminary study of alzheimer's disease diagnosis based on brain electrical signals using wireless eeg. In *Journal of Physics: Conference Series*, volume 694, page 012068. IOP Publishing.

Happé, F. and Frith, U. (2006). The weak coherence account: Detail-focused cognitive style in autism spectrum disorders. *Journal of autism and developmental disorders*, 36(1):5–25.

Hardmeier, M., Hatz, F., Bousleiman, H., Schindler, C., Stam, C. J., and Fuhr, P. (2014). Reproducibility of functional connectivity and graph measures based on the

phase lag index (pli) and weighted phase lag index (wpli) derived from high resolution eeg. *PloS one*, 9(10):e108648.

Harris, J. M., Hirst, J. L., and Mossinghoff, M. J. (2008). *Combinatorics and graph theory*, volume 2. Springer.

Helt, M., Kelley, E., Kinsbourne, M., Pandey, J., Boorstein, H., Herbert, M., and Fein, D. (2008). Can children with autism recover? if so, how? *Neuropsychology review*, 18(4):339–366.

Hernandez, L. M., Rudie, J. D., Green, S. A., Bookheimer, S., and Dapretto, M. (2015). Neural signatures of autism spectrum disorders: insights into brain network dynamics. *Neuropsychopharmacology*, 40(1):171–189.

Herwig, U., Satrapi, P., and Schönfeldt-Lecuona, C. (2003). Using the international 10-20 eeg system for positioning of transcranial magnetic stimulation. *Brain topography*, 16(2):95–99.

Hesse, C. W. and James, C. J. (2006). On semi-blind source separation using spatial constraints with applications in eeg analysis. *Biomedical Engineering, IEEE Transactions on*, 53(12):2525–2534.

Heunis, T.-M., Aldrich, C., and de Vries, P. J. (2016). Recent advances in resting-state electroencephalography biomarkers for autism spectrum disordera review of methodological and clinical challenges. *Pediatric neurology*, 61:28–37.

Hill, E. L. and Frith, U. (2003). Understanding autism: insights from mind and brain. *Philosophical Transactions of the Royal Society B: Biological Sciences*, 358(1430):281–289.

Hoedlmoser, K., Birklbauer, J., Rigler, S., Mueller, E., and Schabus, M. (2011). Eeg recorded during gross-motor behavior. *Brain Products Press Release*, 40:11–12.

Horwitz, B. (2003). The elusive concept of brain connectivity. *Neuroimage*, 19(2):466–470.

Hourcade, J. P., Bullock-Rest, N. E., and Hansen, T. E. (2012). Multitouch tablet applications and activities to enhance the social skills of children with autism spectrum disorders. *Personal and ubiquitous computing*, 16(2):157–168.

Howard, J. S., Sparkman, C. R., Cohen, H. G., Green, G., and Stanislaw, H. (2005). A comparison of intensive behavior analytic and eclectic treatments for young children with autism. *Research in developmental disabilities*, 26(4):359–383.

Howlin, P., Moss, P., Savage, S., and Rutter, M. (2013). Social outcomes in mid-to later adulthood among individuals diagnosed with autism and average nonverbal iq as children. *Journal of the American Academy of Child & Adolescent Psychiatry*, 52(6):572–581.

Hu, B., Mao, C., Campbell, W., Moore, P., Liu, L., and Zhao, G. (2011). A pervasive eeg-based biometric system. In *Proceedings of 2011 international workshop on Ubiquitous affective awareness and intelligent interaction*, pages 17–24. ACM.

Huang, N. E., Shen, Z., Long, S. R., Wu, M. C., Shih, H. H., Zheng, Q., Yen, N.-C., Tung, C. C., and Liu, H. H. (1998). The empirical mode decomposition and the hilbert spectrum for nonlinear and non-stationary time series analysis. In *Proceedings of the Royal Society of London A: Mathematical, Physical and Engineering Sciences*, volume 454, pages 903–995. The Royal Society.

Huettel, S. A., Song, A. W., and McCarthy, G. (2004). *Functional magnetic resonance imaging*, volume 1. Sinauer Associates Sunderland, MA.

Huppert, T. J., Diamond, S. G., Franceschini, M. A., and Boas, D. A. (2009). Homer: a review of time-series analysis methods for near-infrared spectroscopy of the brain. *Applied optics*, 48(10):D280–D298.

Hyvarinen, A. (1999). Fast and robust fixed-point algorithms for independent component analysis. *Neural Networks, IEEE Transactions on*, 10(3):626–634.

Hyvärinen, A. and Oja, E. (2000). Independent component analysis: algorithms and applications. *Neural Networks*, 13(4):411–430.

Iacoboni, M. and Dapretto, M. (2006). The mirror neuron system and the consequences of its dysfunction. *Nature Reviews Neuroscience*, 7(12):942–951.

Iovannone, R., Dunlap, G., Huber, H., and Kincaid, D. (2003). Effective educational practices for students with autism spectrum disorders. *Focus on Autism and Other Developmental Disabilities*, 18(3):150–165.

Isler, J., Martien, K., Grieve, P., Stark, R., and Herbert, M. (2010). Reduced functional connectivity in visual evoked potentials in children with autism spectrum disorder. *Clinical Neurophysiology*, 121(12):2035–2043.

Johnson, N. L., Burkett, K., Reinhold, J., and Bultas, M. W. (2016). Translating research to practice for children with autism spectrum disorder: Part i: Definition, associated behaviors, prevalence, diagnostic process, and interventions. *Journal of Pediatric Health Care*, 30(1):15–26.

Jones, P., Wilcox, C., and Simon, J. (2016). Evidence-based instruction for students with autism spectrum disorder: Teachtown basics. In *Technology and the Treatment of Children with Autism Spectrum Disorder*, pages 113–129. Springer.

Jones, R. M. and Lord, C. (2013). Diagnosing autism in neurobiological research studies. *Behavioural brain research*, 251:113–124.

Joyce, C. A., Gorodnitsky, I. F., and Kutas, M. (2004). Automatic removal of eye movement and blink artifacts from eeg data using blind component separation. *Psychophysiology*, 41(2):313–325.

Just, M. A., Cherkassky, V. L., Keller, T. A., and Minshew, N. J. (2004). Cortical activation and synchronization during sentence comprehension in high-functioning autism: evidence of underconnectivity. *Brain*, 127(8):1811–1821.

Kak, A. C. and Slaney, M. (2001). *Principles of computerized tomographic imaging*. Society for Industrial and Applied Mathematics.

Khosrowabadi, R., Quek, C., Ang, K. K., Wahab, A., and Chen, S.-H. A. (2015). Dynamic screening of autistic children in various mental states using pattern of connectivity between brain regions. *Applied Soft Computing*, 32:335–346.

Klinger, L., OKelley, S., Mussey, J., Goldstein, S., and DeVries, M. (2009). Assessment of intellectual functioning in autism spectrum disorders. *Assessment of autism spectrum disorders*, pages 209–252.

Kurinczuk, J. J., White-Koning, M., and Badawi, N. (2010). Epidemiology of neonatal encephalopathy and hypoxic–ischaemic encephalopathy. *Early human development*, 86(6):329–338.

Lachaux, J.-P., Rodriguez, E., Martinerie, J., Varela, F. J., et al. (1999). Measuring phase synchrony in brain signals. *Human brain mapping*, 8(4):194–208.

Lai, M.-C., Lombardo, M. V., and Baron-Cohen, S. (2014). Autism. *Lancet*, 383(9920):896–910.

Lai, M.-C. and Yang, S.-N. (2010). Perinatal hypoxic-ischemic encephalopathy. *BioMed Research International*, 2011:609813–1–609813–6.

Lainhart, J. E., Piven, J., Wzorek, M., Landa, R., Santangelo, S. L., Coon, H., and Folstein, S. E. (1997). Macrocephaly in children and adults with autism. *Journal of the American Academy of Child & Adolescent Psychiatry*, 36(2):282–290.

Landa, R. J. (2008). Diagnosis of autism spectrum disorders in the first 3 years of life. *Nature Clinical Practice Neurology*, 4(3):138–147.

Latora, V. and Marchiori, M. (2001). Efficient behavior of small-world networks. *Physical review letters*, 87(19):198701.

Lawn, J. E., Kerber, K., Enweronu-Laryea, C., and Cousens, S. (2010). 3.6 million neonatal deathswhat is progressing and what is not? In *Seminars in perinatology*, volume 34, pages 371–386. Elsevier.

Lehnertz, K., Elger, C., Arnhold, J., and Grassberger, P. (2000). *Chaos in brain?* World Scientific.

Léveillé, C., Barbeau, E. B., Bolduc, C., Limoges, É., Berthiaume, C., Chevrier, É., Mottron, L., and Godbout, R. (2010). Enhanced connectivity between visual cortex and other regions of the brain in autism: a rem sleep eeg coherence study. *Autism Research*, 3(5):280–285.

Li, H., Xue, Z., Ellmore, T. M., Frye, R. E., and Wong, S. T. (2014). Network-based analysis reveals stronger local diffusion-based connectivity and different correlations with oral language skills in brains of children with high functioning autism spectrum disorders. *Human brain mapping*, 35(2):396–413.

Li, Y., Ma, Z., Lu, W., and Li, Y. (2006). Automatic removal of the eye blink artifact from eeg using an ica-based template matching approach. *Physiological Measurement*, 27(4):425.

Lofland, K. B. (2016). The use of technology in the treatment of autism. In *Technology and the Treatment of Children with Autism Spectrum Disorder*, pages 27–35. Springer.

Lord, C. (2000). Commentary: achievements and future directions for intervention research in communication and autism spectrum disorders. *Journal of Autism and Developmental Disorders*, 30(5):393–398.

Lord, C., Rutter, M., DiLavore, P., Risi, S., Gotham, K., and Bishop, S. (2012). Autism diagnostic observation schedule second edition (ados-2) manual (part 1): Modules 1–4. *Torrance, CA: Western Psychological Services.*

Lord, C., Rutter, M., and Le Couteur, A. (1994). Autism diagnostic interview-revised: a revised version of a diagnostic interview for caregivers of individuals with possible pervasive developmental disorders. *Journal of autism and developmental disorders*, 24(5):659–685.

Lotte, F., Congedo, M., Lécuyer, A., Lamarche, F., and Arnaldi, B. (2007). A review of classification algorithms for eeg-based brain–computer interfaces. *Journal of neural engineering*, 4(2):R1.

Lotter, V. (1966). Epidemiology of autistic conditions in young children. *Social psychiatry*, 1(3):124–135.

Macpherson, K., Charlop, M. H., and Miltenberger, C. A. (2015). Using portable video modeling technology to increase the compliment behaviors of children with autism during athletic group play. *Journal of autism and developmental disorders*, 45(12):3836–3845.

Maglione, M. A., Gans, D., Das, L., Timbie, J., Kasari, C., et al. (2012). Nonmedical interventions for children with asd: Recommended guidelines and further research needs. *Pediatrics*, 130(Supplement 2):S169–S178.

Malinverni, L., Mora-Guiard, J., Padillo, V., Valero, L., Hervás, A., and Pares, N. (2016). An inclusive design approach for developing video games for children with autism spectrum disorder. *Computers in Human Behavior*.

Mammone, N. and Morabito, F. C. (2008). Enhanced automatic artifact detection based on independent component analysis and renyis entropy. *Neural networks*, 21(7):1029–1040.

Mandell, D. S., Listerud, J., Levy, S. E., and Pinto-Martin, J. A. (2002). Race differences in the age at diagnosis among medicaid-eligible children with autism. *Journal of the American Academy of Child & Adolescent Psychiatry*, 41(12):1447–1453.

Manning-Courtney, P., Murray, D., Currans, K., Johnson, H., Bing, N., Kroeger-Geoppinger, K., Sorensen, R., Bass, J., Reinhold, J., Johnson, A., et al. (2013). Autism spectrum disorders. *Current problems in pediatric and adolescent health care*, 43(1):2–11.

Mathewson, K. J., Jetha, M. K., Drmic, I. E., Bryson, S. E., Goldberg, J. O., and Schmidt, L. A. (2012). Regional eeg alpha power, coherence, and behavioral symptomatology in autism spectrum disorder. *Clinical Neurophysiology*, 123(9):1798–1809.

Matlis, S., Boric, K., Chu, C. J., and Kramer, M. A. (2015). Robust disruptions in electroencephalogram cortical oscillations and large-scale functional networks in autism. *BMC neurology*, 15(1):1.

Matsumoto, K. and Tsuda, I. (1988). Calculation of information flow rate from mutual information. *Journal of Physics A: Mathematical and General*, 21(6):1405.

Mazurek, M. O. and Engelhardt, C. R. (2013). Video game use in boys with autism spectrum disorder, adhd, or typical development. *Pediatrics*, 132(2):260–266.

McMenamin, B. W., Shackman, A. J., Greischar, L. L., and Davidson, R. J. (2011). Electromyogenic artifacts and electroencephalographic inferences revisited. *Neuroimage*, 54(1):4–9.

McPheeters, M. L., Warren, Z., Sathe, N., Bruzek, J. L., Krishnaswami, S., Jerome, R. N., and Veenstra-VanderWeele, J. (2011). A systematic review of medical treatments for children with autism spectrum disorders. *Pediatrics*, 127(5):e1312–e1321.

Menshawy, M. E., Benharref, A., and Serhani, M. (2015). An automatic mobile-health based approach for eeg epileptic seizures detection. *Expert Systems with Applications*, 42(20):7157–7174.

Mevarech, Z. R., Silber, O., and Fine, D. (1991). Learning with computers in small groups: Cognitive and affective outcomes. *Journal of Educational Computing Research*, 7(2):233–243.

Michel, C. M. and Murray, M. M. (2012). Towards the utilization of eeg as a brain imaging tool. *Neuroimage*, 61(2):371–385.

Mijovic, B., De Vos, M., Gligorijevic, I., Taelman, J., and Van Huffel, S. (2010). Source separation from single-channel recordings by combining empirical-mode decomposition and independent component analysis. *Biomedical Engineering, IEEE Transactions on*, 57(9):2188–2196.

Moore, D. (1998). Computers and people with autism. *Asperger Syndrome*, pages 20–21.

Moore, M. and Calvert, S. (2000). Brief report: Vocabulary acquisition for children with autism: Teacher or computer instruction. *Journal of autism and developmental disorders*, 30(4):359–362.

Moseley, R., Ypma, R., Holt, R., Floris, D., Chura, L., Spencer, M., Baron-Cohen, S., Suckling, J., Bullmore, E., and Rubinov, M. (2015). Whole-brain functional hypoconnectivity as an endophenotype of autism in adolescents. *NeuroImage: Clinical*, 9:140–152.

Nadel, J. (2006). Does imitation matter to children with autism. *Imitation and the social mind*, pages 118–134.

Narasimhan, S. and Dutt, D. N. (1996). Application of lms adaptive predictive filtering for muscle artifact (noise) cancellation from eeg signals. *Computers & electrical engineering*, 22(1):13–30.

Narzisi, A., Muratori, F., Calderoni, S., Fabbro, F., and Urgesi, C. (2013). Neuropsychological profile in high functioning autism spectrum disorders. *Journal of autism and developmental disorders*, 43(8):1895–1909.

National Academy of Sciences-National Research Council, Washington, D. (2001). *Educating children with autism*. ERIC Clearinghouse.

Niedermeyer, E. (2005). *Electroencephalography: Basic principles, clinical applications, and related fields*, chapter The Normal EEG of the Waking Adult, page 167. Lippincott Williams & Wilkins.

Niedermeyer, E. and da Silva, F. L. (2005). *Electroencephalography: basic principles, clinical applications, and related fields*. Lippincott Williams & Wilkins.

Niso, G., Bruña, R., Pereda, E., Gutiérrez, R., Bajo, R., Maestú, F., and del Pozo, F. (2013). Hermes: towards an integrated toolbox to characterize functional and effective brain connectivity. *Neuroinformatics*, 11(4):405–434.

Nolan, H., Whelan, R., and Reilly, R. (2010). Faster: fully automated statistical thresholding for eeg artifact rejection. *Journal of neuroscience methods*, 192(1):152–162.

Nolte, G., Bai, O., Wheaton, L., Mari, Z., Vorbach, S., and Hallett, M. (2004). Identifying true brain interaction from eeg data using the imaginary part of coherency. *Clinical neurophysiology*, 115(10):2292–2307.

Nunez, P. L. and Srinivasan, R. (2006). *Electric fields of the brain: the neurophysics of EEG*. Oxford University Press, USA.

Omidvarnia, A., Metsäranta, M., Lano, A., and Vanhatalo, S. (2015). Structural damage in early preterm brain changes the electric resting state networks. *NeuroImage*, 120:266–273.

Orekhova, E. V., Elsabbagh, M., Jones, E. J., Dawson, G., Charman, T., and Johnson, M. H. (2014). Eeg hyper-connectivity in high-risk infants is associated with later autism. *Journal of neurodevelopmental disorders*, 6(1):1.

Ospina, M. B., Seida, J. K., Clark, B., Karkhaneh, M., Hartling, L., Tjosvold, L., Vandermeer, B., and Smith, V. (2008). Behavioural and developmental interventions for autism spectrum disorder: a clinical systematic review. *PloS one*, 3(11):e3755.

Ozonoff, S., Goodlin-Jones, B. L., and Solomon, M. (2005). Evidence-based assessment of autism spectrum disorders in children and adolescents. *Journal of Clinical Child and Adolescent Psychology*, 34(3):523–540.

Pascualvaca, D. M., Fantie, B. D., Papageorgiou, M., and Mirsky, A. F. (1998). Attentional capacities in children with autism: Is there a general deficit in shifting focus? *Journal of Autism and Developmental Disorders*, 28(6):467–478.

Pellicano, E., Maybery, M., Durkin, K., and Maley, A. (2006). Multiple cognitive capabilities/deficits in children with an autism spectrum disorder:weak central coherence and its relationship to theory of mind and executive control. *Development and psychopathology*, 18(01):77–98.

Pereda, E., Quiroga, R. Q., and Bhattacharya, J. (2005). Nonlinear multivariate analysis of neurophysiological signals. *Progress in neurobiology*, 77(1):1–37.

Peters, J. M., Taquet, M., Vega, C., Jeste, S. S., Fernández, I. S., Tan, J., Nelson, C. A., Sahin, M., and Warfield, S. K. (2013). Brain functional networks in syndromic and non-syndromic autism: a graph theoretical study of eeg connectivity. *BMC medicine*, 11(1):54.

Picard, R. and Goodwin, M. (2008). Developing innovative technology for future personalized autism research and treatment. *Autism Advocate*, 50(1):32–39.

Pikovsky, A., Rosenblum, M., and Kurths, J. (2003). *Synchronization: a universal concept in nonlinear sciences*, volume 12. Cambridge university press.

Pilling, S., Baron-Cohen, S., Megnin-Viggars, O., Lee, R., Taylor, C., Group, G. D., et al. (2012). Recognition, referral, diagnosis, and management of adults with autism: summary of nice guidance. *BMJ*, 344:e4082.

Piper, A. M., O'Brien, E., Morris, M. R., and Winograd, T. (2006). Sides: a cooperative tabletop computer game for social skills development. In *Proceedings of the 2006 20th anniversary conference on Computer supported cooperative work*, pages 1–10. ACM.

Platt, J. (1998). Sequential minimal optimization: A fast algorithm for training support vector machines. Technical report.

Ploog, B. O., Scharf, A., Nelson, D., and Brooks, P. J. (2013). Use of computer-assisted technologies (cat) to enhance social, communicative, and language development in children with autism spectrum disorders. *Journal of autism and developmental disorders*, 43(2):301–322.

Polanczyk, G. V., Salum, G. A., Sugaya, L. S., Caye, A., and Rohde, L. A. (2015). Annual research review: A meta-analysis of the worldwide prevalence of mental disorders in children and adolescents. *Journal of Child Psychology and Psychiatry*, 56(3):345–365.

Porro, C. A., Francescato, M. P., Cettolo, V., Diamond, M. E., Baraldi, P., Zuiani, C., Bazzocchi, M., and Di Prampero, P. E. (1996). Primary motor and sensory cortex activation during motor performance and motor imagery: a functional magnetic resonance imaging study. *The Journal of neuroscience*, 16(23):7688–7698.

Quiroga, R. Q., Kraskov, A., Kreuz, T., and Grassberger, P. (2002). Performance of different synchronization measures in real data: a case study on electroencephalographic signals. *Physical Review E*, 65(4):041903.

Reichow, B. and Wolery, M. (2009). Comprehensive synthesis of early intensive behavioral interventions for young children with autism based on the ucla young autism project model. *Journal of autism and developmental disorders*, 39(1):23–41.

Remington, B., Hastings, R. P., Kovshoff, H., degli Espinosa, F., Jahr, E., Brown, T., Alsford, P., Lemaic, M., Ward, N., and MacLean, Jr, W. E. (2007). Early intensive behavioral intervention: outcomes for children with autism and their parents after two years. *American Journal on Mental Retardation*, 112(6):418–438.

Righi, G., Tierney, A. L., Tager-Flusberg, H., and Nelson, C. A. (2014). Functional connectivity in the first year of life in infants at risk for autism spectrum disorder: an eeg study. *PloS one*, 9(8):e105176.

Rilling, G., Flandrin, P., Goncalves, P., et al. (2003). On empirical mode decomposition and its algorithms. In *IEEE-EURASIP Workshop on Nonlinear Signal and Image Processing NSIP*, volume 3, pages 8–11.

Robertson, F. C., Douglas, T. S., and Meintjes, E. M. (2010). Motion artifact removal for functional near infrared spectroscopy: a comparison of methods. *Biomedical Engineering, IEEE Transactions on*, 57(6):1377–1387.

Robins, D. L., Casagrande, K., Barton, M., Chen, C.-M. A., Dumont-Mathieu, T., and Fein, D. (2014). Validation of the modified checklist for autism in toddlers, revised with follow-up (m-chat-r/f). *Pediatrics*, 133(1):37–45.

Roelfsema, P. R., Engel, A. K., Konig, P., and Singer, W. (1997). Visuomotor integration is associated with zero time-lag synchronization among cortical areas. *Nature*, 385:157–161.

Rogers, S. and Girolami, M. (2015). *A first course in machine learning*. CRC Press.

Rogers, S. J. (1996). Brief report: Early intervention in autism. *Journal of autism and developmental disorders*, 26(2):243–246.

Rogers, S. J. and Dawson, G. (2009). *Early Start Denver Model Curriculum Checklist for Young Children with Autism*. Guilford Press.

Rogers, S. J. and Vismara, L. A. (2008). Evidence-based comprehensive treatments for early autism. *Journal of Clinical Child & Adolescent Psychology*, 37(1):8–38.

Roux, A. M., Shattuck, P. T., Cooper, B. P., Anderson, K. A., Wagner, M., and Narendorf, S. C. (2013). Postsecondary employment experiences among young adults with an autism spectrum disorder. *Journal of the American Academy of Child and Adolescent Psychiatry*, 52(9):931–939.

Rubinov, M. and Sporns, O. (2010). Complex network measures of brain connectivity: uses and interpretations. *Neuroimage*, 52(3):1059–1069.

Rudie, J. D., Brown, J., Beck-Pancer, D., Hernandez, L., Dennis, E., Thompson, P., Bookheimer, S., and Dapretto, M. (2013). Altered functional and structural brain network organization in autism. *NeuroImage: clinical*, 2:79–94.

Rutkove, S. B. and Blum, A. S. (2007). *The clinical neurophysiology primer*. Springer.

Sacrey, L.-A. R., Bennett, J. A., and Zwaigenbaum, L. (2015). Early infant development and intervention for autism spectrum disorder. *Journal of child neurology*, 30(14):1921–1929.

Safieddine, D., Kachenoura, A., Albera, L., Birot, G., Karfoul, A., Pasnicu, A., Biraben, A., Wendling, F., Senhadji, L., and Merlet, I. (2012). Removal of muscle artifact from eeg data: comparison between stochastic (ica and cca) and deterministic (emd and wavelet-based) approaches. *EURASIP Journal on Advances in Signal Processing*, 2012(1):1–15.

Saint-Georges, C., Cassel, R. S., Cohen, D., Chetouani, M., Laznik, M.-C., Maestro, S., and Muratori, F. (2010). What studies of family home movies can teach us about autistic infants: A literature review. *Research in Autism Spectrum Disorders*, 4(3):355–366.

Sakkalis, V. (2011). Review of advanced techniques for the estimation of brain connectivity measured with eeg/meg. *Computers in biology and medicine*, 41(12):1110–1117.

Sallows, G. O. and Graupner, T. D. (2005). Intensive behavioral treatment for children with autism: Four-year outcome and predictors. *Journal Information*, 110(6).

Sanei, S. and Chambers, J. A. (2008). *EEG signal processing*. John Wiley & Sons.

Schnitzler, A. and Gross, J. (2005). Normal and pathological oscillatory communication in the brain. *Nature reviews neuroscience*, 6(4):285–296.

Schreglmann, M., Helps, S., Hart, D., and Vollmer, B. (2016). Are 2-year old children who underwent therapeutic hypothermia for neonatal hypoxic-ischemic encephalopathy at risk for behavioral problems? *Neuropediatrics*, 47(S 01):FV04–09.

Schreibman, L. (2000). Intensive behavioral/psychoeducational treatments for autism: Research needs and future directions. *Journal of autism and developmental disorders*, 30(5):373–378.

Schreibman, L., Dawson, G., Stahmer, A. C., Landa, R., Rogers, S. J., McGee, G. G., Kasari, C., Ingersoll, B., Kaiser, A. P., Bruinsma, Y., et al. (2015). Naturalistic developmental behavioral interventions: Empirically validated treatments for autism spectrum disorder. *Journal of autism and developmental disorders*, 45:2411–2428.

Serret, S., Hun, S., Iakimova, G., Lozada, J., Anastassova, M., Santos, A., Vesperini, S., and Askenazy, F. (2014). Facing the challenge of teaching emotions to individuals with low-and high-functioning autism using a new serious game: a pilot study. *Molecular autism*, 5(1):1.

Sherer, M. R. and Schreibman, L. (2005). Individual behavioral profiles and predictors of treatment effectiveness for children with autism. *Journal of consulting and clinical psychology*, 73(3):525.

Sinha, S., McGovern, R. A., and Sheth, S. A. (2015). Deep brain stimulation for severe autism: from pathophysiology to procedure. *Neurosurgical focus*, 38(6):E3.

Sörnmo, L. and Laguna, P. (2005). *Bioelectrical signal processing in cardiac and neurological applications*. Academic Press.

Sporns, O. (2011). *Networks of the Brain*. MIT press.

Stam, C. and Van Dijk, B. (2002). Synchronization likelihood: an unbiased measure of generalized synchronization in multivariate data sets. *Physica D: Nonlinear Phenomena*, 163(3):236–251.

Stam, C. J., Nolte, G., and Daffertshofer, A. (2007). Phase lag index: assessment of functional connectivity from multi channel eeg and meg with diminished bias from common sources. *Human brain mapping*, 28(11):1178–1193.

Stam, C. J. and Reijneveld, J. C. (2007). Graph theoretical analysis of complex networks in the brain. *Nonlinear biomedical physics*, 1(1):1.

Sterman, M., Macdonald, L., and Stone, R. K. (1974). Biofeedback training of the sensorimotor electroencephalogram rhythm in man: effects on epilepsy. *Epilepsia*, 15(3):395–416.

Stone, W. L. and Yoder, P. J. (2001). Predicting spoken language level in children with autism spectrum disorders. *Autism*, 5(4):341–361.

Supekar, K., Menon, V., Rubin, D., Musen, M., and Greicius, M. D. (2008). Network analysis of intrinsic functional brain connectivity in alzheimer's disease. *PLoS Comput Biol*, 4(6):e1000100.

Sweeney, K. T., Ayaz, H., Ward, T. E., Izzetoglu, M., McLoone, S. F., and Onaral, B. (2012a). A methodology for validating artifact removal techniques for physiological signals. *Information Technology in Biomedicine, IEEE Transactions on*, 16(5):918–926.

Sweeney, K. T., McLoone, S. F., and Ward, T. E. (2013). The use of ensemble empirical mode decomposition with canonical correlation analysis as a novel artifact removal technique. *Biomedical Engineering, IEEE Transactions on*, 60(1):97–105.

Sweeney, K. T., Ward, T. E., and McLoone, S. F. (2012b). Artifact removal in physiological signalspractices and possibilities. *Information Technology in Biomedicine, IEEE Transactions on*, 16(3):488–500.

Szatmari, P., Bryson, S., Boyle, M., Streiner, D., and Duku, E. (2003). Predictors of outcome among high functioning children with autism and asperger syndrome. *Journal of Child Psychology and Psychiatry*, 44(4):520–528.

Takens, F. (1981). Detecting strange attractors in turbulence. In *Dynamical systems and turbulence, Warwick 1980*, pages 366–381. Springer.

Tanaka, J., Klaiman, C., Koenig, K., and Schultz, R. (2005). Plasticity of the neural mechanisms underlying face processing in children with asd: Behavioral improvements following perceptual training on faces. In *Poster presented at the International Meeting for Autism Research, Boston, MA*.

Tanaka, J. W., Wolf, J. M., Klaiman, C., Koenig, K., Cockburn, J., Herlihy, L., Brown, C., Stahl, S., Kaiser, M. D., and Schultz, R. T. (2010). Using computerized games to teach face recognition skills to children with autism spectrum disorder: The lets face it! program. *Journal of Child Psychology and Psychiatry*, 51(8):944–952.

Tanaka, K., Kurita, T., Meyer, F., Berthouze, L., and Kawabe, T. (2006). Stepwise feature selection by cross validation for eeg-based brain computer interface. In *The 2006 IEEE International Joint Conference on Neural Network Proceedings*, pages 4672–4677. IEEE.

Tass, P., Rosenblum, M., Weule, J., Kurths, J., Pikovsky, A., Volkmann, J., Schnitzler, A., and Freund, H.-J. (1998). Detection of n: m phase locking from noisy data: application to magnetoencephalography. *Physical review letters*, 81(15):3291.

Thorndike, E. L. (1898). Animal intelligence: An experimental study of the associative processes in animals. *Psychological Monographs: General and Applied*, 2(4):i–109.

Ting, K., Fung, P., Chang, C., and Chan, F. (2006). Automatic correction of artifact from single-trial event-related potentials by blind source separation using second order statistics only. *Medical engineering & physics*, 28(8):780–794.

Tokariev, A., Videman, M., Palva, J. M., and Vanhatalo, S. (2015). Functional brain connectivity develops rapidly around term age and changes between vigilance states in the human newborn. *Cerebral Cortex*, page bhv219.

Tomasello, M. (1995). Joint attention as social cognition. *Joint attention: Its origins and role in development*, pages 103–130.

Tononi, G. and Sporns, O. (2003). Measuring information integration. *BMC neuroscience*, 4(1):31.

Tononi, G., Sporns, O., and Edelman, G. M. (1994). A measure for brain complexity: relating functional segregation and integration in the nervous system. *Proceedings of the National Academy of Sciences*, 91(11):5033–5037.

Tymofiyeva, O., Hess, C. P., Ziv, E., Tian, N., Bonifacio, S. L., McQuillen, P. S., Ferriero, D. M., Barkovich, A. J., and Xu, D. (2012). Towards the baby connectome: mapping the structural connectivity of the newborn brain. *PloS one*, 7(2):e31029.

Urigüen, J. A. and Garcia-Zapirain, B. (2015). Eeg artifact removalstate-of-the-art and guidelines. *Journal of neural engineering*, 12(3):031001.

van der Molen, M. J., Stam, C. J., and van der Molen, M. W. (2014). Resting-state eeg oscillatory dynamics in fragile x syndrome: Abnormal functional connectivity and brain network organization. *PloS one*, 9(2):e88451.

Van Diessen, E., Otte, W. M., Braun, K. P., Stam, C. J., and Jansen, F. E. (2013). Improved diagnosis in children with partial epilepsy using a multivariable prediction model based on eeg network characteristics. *PloS one*, 8(4):e59764.

van Schie, P. E., Schijns, J., Becher, J. G., Barkhof, F., van Weissenbruch, M. M., and Vermeulen, R. J. (2015). Long-term motor and behavioral outcome after perinatal hypoxic-ischemic encephalopathy. *European Journal of Paediatric Neurology*, 19(3):354–359.

Varela, F., Lachaux, J.-P., Rodriguez, E., and Martinerie, J. (2001). The brainweb: phase synchronization and large-scale integration. *Nature reviews neuroscience*, 2(4):229–239.

Venkatesh, S., Phung, D., Duong, T., Greenhill, S., and Adams, B. (2013). Toby: early intervention in autism through technology. In *Proceedings of the SIGCHI Conference on Human Factors in Computing Systems*, pages 3187–3196. ACM.

Vergult, A., De Clercq, W., Palmini, A., Vanrumste, B., Dupont, P., Van Huffel, S., and Van Paesschen, W. (2007). Improving the interpretation of ictal scalp eeg: Bss–cca algorithm for muscle artifact removal. *Epilepsia*, 48(5):950–958.

Vértes, P. E. and Bullmore, E. T. (2015). Annual research review: Growth connectomics–the organization and reorganization of brain networks during normal and abnormal development. *Journal of Child Psychology and Psychiatry*, 56(3):299–320.

Vialatte, F.-B., Solé-Casals, J., and Cichocki, A. (2008). Eeg windowed statistical wavelet scoring for evaluation and discrimination of muscular artifacts. *Physiological measurement*, 29(12):1435.

Vinck, M., Oostenveld, R., van Wingerden, M., Battaglia, F., and Pennartz, C. M. (2011). An improved index of phase-synchronization for electrophysiological data in the presence of volume-conduction, noise and sample-size bias. *Neuroimage*, 55(4):1548–1565.

Vismara, L. A., McCormick, C., Young, G. S., Nadhan, A., and Monlux, K. (2013). Preliminary findings of a telehealth approach to parent training in autism. *Journal of autism and developmental disorders*, 43(12):2953–2969.

Vuilleumier, P., Armony, J. L., Driver, J., and Dolan, R. J. (2001). Effects of attention and emotion on face processing in the human brain: an event-related fmri study. *Neuron*, 30(3):829–841.

Wainer, A. L. and Ingersoll, B. R. (2015). Increasing access to an asd imitation intervention via a telehealth parent training program. *Journal of autism and developmental disorders*, 45(12):3877–3890.

Walczak, B. and Massart, D. (1997). Noise suppression and signal compression using the wavelet packet transform. *Chemometrics and Intelligent Laboratory Systems*, 36(2):81–94.

Wallon, H. (1942). *De l'acte à la pensée.* Flammarion.

Walsh, B., Murray, D., and Boylan, G. (2011). The use of conventional eeg for the assessment of hypoxic ischaemic encephalopathy in the newborn: a review. *Clinical neurophysiology*, 122(7):1284–1294.

Wang, D., Miao, D., and Xie, C. (2011). Best basis-based wavelet packet entropy feature extraction and hierarchical eeg classification for epileptic detection. *Expert Systems with Applications*, 38(11):14314–14320.

Wang, H. E., Bénar, C. G., Quilichini, P. P., Friston, K. J., Jirsa, V. K., and Bernard, C. (2014). A systematic framework for functional connectivity measures. *Front Neurosci*, 8.

Wang, L., Metzak, P. D., Honer, W. G., and Woodward, T. S. (2010a). Impaired efficiency of functional networks underlying episodic memory-for-context in schizophrenia. *The Journal of Neuroscience*, 30(39):13171–13179.

Wang, L., Yu, C., Chen, H., Qin, W., He, Y., Fan, F., Zhang, Y., Wang, M., Li, K., Zang, Y., et al. (2010b). Dynamic functional reorganization of the motor execution network after stroke. *Brain*, 133(4):1224–1238.

Watts, D. J. and Strogatz, S. H. (1998). Collective dynamics of small-worldnetworks. *nature*, 393(6684):440–442.

Welchew, D. E., Ashwin, C., Berkouk, K., Salvador, R., Suckling, J., Baron-Cohen, S., and Bullmore, E. (2005). Functional disconnectivity of the medial temporal lobe in aspergers syndrome. *Biological psychiatry*, 57(9):991–998.

Wen, D., Zhou, Y., and Li, X. (2015). A critical review: coupling and synchronization analysis methods of eeg signal with mild cognitive impairment. *Frontiers in aging neuroscience*, 7.

Whiten, A. and Ham, R. (1992). On the nature and evolution of imitation in the animal kingdom: reappraisal of a century of research. *Advances in the Study of Behavior*, 21:239–283.

Whyte, E. M., Smyth, J. M., and Scherf, K. S. (2015). Designing serious game interventions for individuals with autism. *Journal of autism and developmental disorders*, 45(12):3820–3831.

Wolpaw, J. R., Birbaumer, N., McFarland, D. J., Pfurtscheller, G., and Vaughan, T. M. (2002). Brain–computer interfaces for communication and control. *Clinical neurophysiology*, 113(6):767–791.

Womelsdorf, T., Schoffelen, J.-M., Oostenveld, R., Singer, W., Desimone, R., Engel, A. K., and Fries, P. (2007). Modulation of neuronal interactions through neuronal synchronization. *science*, 316(5831):1609–1612.

World Health Organization (2011). *International Statistical Classification of Diseases and Related Health Problems. 10th revision (2010 ed.)*.

Wu, J., Zhang, J., Liu, C., Liu, D., Ding, X., and Zhou, C. (2012). Graph theoretical analysis of eeg functional connectivity during music perception. *Brain research*, 1483:71–81.

Wyckoff, S. N., Sherlin, L. H., Ford, N. L., and Dalke, D. (2015). Validation of a wireless dry electrode system for electroencephalography. *Journal of neuroengineering and rehabilitation*, 12(1):1.

Yeung, N., Bogacz, R., Holroyd, C. B., and Cohen, J. D. (2004). Detection of synchronized oscillations in the electroencephalogram: an evaluation of methods. *Psychophysiology*, 41(6):822–832.

Yoder, K. J. and Belmonte, M. K. (2010). Combining computer game-based behavioural experiments with high-density eeg and infrared gaze tracking. *Journal of visualized experiments: JoVE*, (46).

Yoder, P. and Compton, D. (2004). Identifying predictors of treatment response. *Mental retardation and developmental disabilities research reviews*, 10(3):162–168.

Zaroff, C. M. and Uhm, S. Y. (2012). Prevalence of autism spectrum disorders and influence of country of measurement and ethnicity. *Social psychiatry and psychiatric epidemiology*, 47(3):395–398.

Zima, M., Tichavskỳ, P., Paul, K., and Krajča, V. (2012). Robust removal of short-duration artifacts in long neonatal eeg recordings using wavelet-enhanced ica and adaptive combining of tentative reconstructions. *Physiological measurement*, 33(8):N39.

Ziv, E., Tymofiyeva, O., Ferriero, D. M., Barkovich, A. J., Hess, C. P., and Xu, D. (2013). A machine learning approach to automated structural network analysis: application to neonatal encephalopathy. *PloS one*, 8(11):e78824.

Zou, L., Xu, S., Ma, Z., Lu, J., and Su, W. (2013). Automatic removal of artifacts from attention deficit hyperactivity disorder electroencephalograms based on independent component analysis. *Cognitive Computation*, 5(2):225–233.

Zwaigenbaum, L., Bryson, S., and Garon, N. (2013). Early identification of autism spectrum disorders. *Behavioural Brain Research*, 251:133–146.